L-Amino acid Based Poly(ester-urethane) Nano-assemblies and Their Drug Delivery Applications

A Thesis

**Submitted in Partial Fulfillment of the Requirements
Of the Degree of
Doctor of Philosophy**

By

Rajendra Aluri

Reg. No. 20113141

Department of Chemistry

INDIAN INSTITUTE OF SCIENCE EDUCATION AND RESEARCH, PUNE

Pune 411008, Maharashtra, India

May 2017

Dedicated to.....

My Grandfather

Prof. M. Jayakannan

Professor and Chair
Department of Chemistry

CERTIFICATE

Certified that the work incorporated in the thesis entitled "*L-Amino acid Based Poly(ester-urethane) Nano-assemblies and Their Drug Delivery Applications*" Submitted by **Mr. Rajendra Aluri** was carried out by the candidate under my supervision. The work presented here or any part of it has not been included in any other thesis submitted previously for the award of any degree or diploma from any other University or Institution.

Date:
Pune (MH) India

Prof. M. Jayakannan
(Thesis Supervisor)

2/6/2017

DECLARATION

I declare that this written submission represents my ideas in my own words and where others' ideas have been included; I have adequately cited and referenced the original sources. I also declare that I have adhered to all principles of scientific honesty and integrity and have not misrepresented or fabricated or falsified any idea/data/fact/source in my submission. I understand that violation of the above will be cause for disciplinary action by the institute and can also evoke penal action from the sources which have thus not been properly cited or from whom proper permission has not been taken when needed.

Date: 02|06|17

Pune (MH) India

Rajendra Aluri

Roll No: 20113141

Synopsis

Name of the Candidate: Rajendra Aluri
Thesis Title: *L-Amino acid Based Poly(ester-urethane) Nano-assemblies and Their Drug Delivery Applications*

L-Amino acid based polymer nano-carriers are emerging as excellent platform for drug delivery in cancer therapy. Significant advances have been made on L-amino acid based synthetic polypeptides and their di- and tri-block copolymers in biomedical field. Alternatively, non-peptide synthetic polymers from L-amino acid resources are relatively less studied and this is partially associated with the lack of the unavailability of synthetic methodologies to make biodegradable polymer structures. Thus, the development of new synthetic methodologies for the large abundant of natural L-amino acid resources is one of the emerging area in biomedical research especially in drug delivery applications. The thesis work is aimed to develop new eco-friendly melt polycondensation approach for multi-functional L-amino acid resources such as L-tyrosine, L-serine and L-threonine. Further, these new polymers were self-assembled into enzyme-responsive and thermo-responsive nano-carriers for multiple drug delivery in cancer treatment. The thesis has been divided into following four chapters:

(i) Chapter 1: The introduction chapter provides literature survey on the synthetic polymers in drug delivery and L-amino acid based polymer nano-carriers in drug delivery, and describe the aim of the thesis work.

(ii) Chapter 2: A classes of ***enzyme-responsive L-tyrosine based amphiphilic poly(ester-urethane)s*** were developed based on ***dual ester-urethane melt polycondensation*** approach. The self-assembled nano-scaffold was employed as multiple drug vectors and the proof-of-concept was demonstrated in cancer cells.

(iii) Chapter 3: ***Thermo and Enzyme dual-responsive polymer nano-carriers*** were designed and developed for enriching the drug concentration at the cancer tissue and also biodegrade them at the intracellular compartments. The self-assembly of the thermo-responsive polymer was studied in detail and structure-properly correlation was established.

*(iv) C*hapter 4: ***One-pot two polymers:*** First examples of synthetic hyperbranched poly(ester-urethane)s and their linear polyester counterparts in one-pot via temperature selective polymerization approach from a single monomer source was demonstrated. The topologies of the new polymers were found to drive their molecular self-assembly with respect to their diverse polymer backbones.

The last chapter summarized the thesis work with future perspectives.

In chapter 2, new classes of enzymatic-biodegradable amphiphilic poly(ester-urethane)s were designed and developed from L-tyrosine amino acid resources and their self-assembled nanoparticles were employed as multiple drug delivery vehicles in cancer therapy. L-tyrosine was converted into dual functional ester-urethane monomers and they were subjected to solvent free melt polycondensation with hydrophilic polyethylene glycols to produce

comb-type poly(ester-urethane)s. The topology of the polymer was found to play major role on the glass transition, crystallinity and visco-elastic rheological properties of L-tyrosine poly(ester-urethane)s. The amphiphilic polymers were self-assembled as 200 ±10 nm nanoparticles and they exhibited excellent encapsulation capabilities for anticancer drugs such as doxorubicin (DOX) and camptothecin (CPT). *In-vitro* drug release studies revealed that the drug loaded L-tyrosine nanoparticles were stable at extracellular conditions and they underwent enzymatic-biodegradation exclusively at the intracellular level to release the drugs. Cytotoxicity studies in the cervical cancer (HeLa) and normal WT-MEFs cell lines revealed that the nascent L-tyrosine nanoparticles were non-toxic whereas the CPT and DOX drug loaded polymer nanoparticles exhibited excellent cell killing in cancer cells. Confocal microscopic imaging confirmed the cellular internalization of drug loaded nanoparticles. The drugs were taken up by the cells much higher quantity while delivering them from L-tyrosine nanoparticle platform compare to their free state. Flow cytometry analysis showed that the DOX loaded polymer nano-scaffolds were internalized the drugs 8-10 times higher compare to free DOX. Both the synthesis of new classes of poly(ester-urethane)s via melt polycondensation approach and the enzyme-responsive drug delivery concept were accomplished for the first time.

In chapter 3, new thermo and enzyme-responsive poly(ester-urethane)s from L-tyrosine amino acid were developed and their aqueous self-assembled nanostructures were employed as multiple-drug nano-carriers to cancer cells. L-Tyrosine amino acid was tailor-made into multifunctional monomer by carefully substituting long PEG-chain at the phenolic position and it was subjected to melt dual ester-urethane polycondensation with different linear and cyclic aliphatic diols to yield amphiphilic poly(ester-urethane)s. The amphiphilic polymer design with appropriate hydrophilic-hydrophobic balance was self-assembled into 100 ± 10 nm nanoparticles in the aqueous medium. Interestingly, these polymers were completely soluble or dispersible in water at ambient temperature and they become turned into turbid solution at higher temperature with respect to lower critical solution temperature (LCST) behaviours. This thermo-responsive LCST phase transition of the poly(ester-urethane)s were extensively inves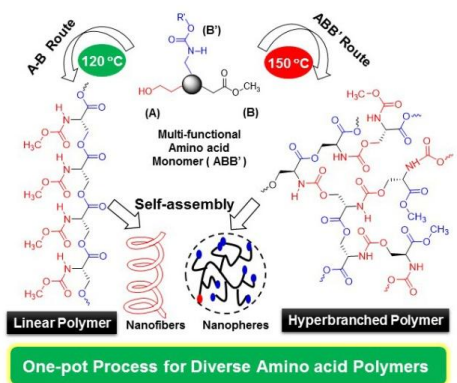tigated by variable temperature transmittance, DLS and ^{1}H-NMR studies. Polymers with C_{12} main chain in the backbone and PEG-350 side chain showed LCST at 44 °C which was very near to cancer

tissue temperature for drug delivery applications. The self-assembled polymer nanoparticles were found to be capable of encapsulating wide ranges of anticancer drugs such as DOX and CPT. *In vitro* drug release studies revealed that the polymer nanoparticles were stable at physiological conditions and they underwent to disassembly at temperature near to cancer tissue temperature. Further, the polyester-urethane linkages in the polymer nanoparticles were found to be responsive to biodegrade in the presence of lysosomal esterase enzyme at the intracellular level. Cytotoxic of these poly(ester-urethane)s were investigated in tumor tissue (MCF 7 and HeLa) and normal cell lines (WT-MEFs). Drug loaded polymer nanoparticles showed better cytotoxic effects than their free drugs. Confocal images and Flow cytometry confirmed the cellular internalisation of the drug loaded nanoparticles.

In chapter 4, one-pot ABB' synthetic approach for linear polyester and hyperbranched poly(ester-urethane)s based on multi functional L-amino acid monomers through temperature selective melt polycondensation approach. L-Serine, D-serine and L-threonine amino acids have carboxylic acid, amine and hydroxyl functional groups that enabled us to make multi functional ABB' monomer (A= hydroxyl, B= ester and B' = urethane). At 120 °C, the ABB' monomer underwent thermo-selective transesterification polycondenstaion (only B is active towards A) to produce linear polyesters with B' functionality as pendent in each repeating unit. At 150 °C, the ABB' monomer underwent dual ester-urethane polycondensation to produce new classes of hyperbranched poly(ester-urethane)s. Interestingly, the secondary hydroxyl group in the L-threonine monomer did not react at 120

°C, but at 150 °C exclusively produced linear polyester. The temperature selective polycondenstaion process was confirmed by appropriate model reactions and also by ^{1}H-NMR, ^{13}C-NMR spectroscopic analysis. The role of the macrocyclic formation in the polycondensation process was also investigated by MALDI-TOF technique. The diverse topologies of the new amino acid polymers were found to drive their molecular self-assembly. The linear polyesters were found to adapt expanded β-sheet chain conformation that produced exclusively helical nano-fibrous morphology. The hyperbranched polymers adapted globular coil-like conformation that produced spherical nano-particle assemblies. Both the secondary structures formations as well as their morphological features were confirmed by Circular dichroism spectroscopy and electron microscopic analysis.

The work described in the thesis opens up new synthetic pathways for diverse linear and hyperbranched polymer structures based on natural L-amino acids such as L-tyrosine, L-serine and L-threonine. L-Tyrosine based enzyme and thermo-responsive nano-assemblies were demonstrated for drug delivery. The entire polymer reported in the thesis work is new generation biodegradable polymers; thus they have find wide range applications in biomedical and thermoplastic industry.

TABLE OF CONTENTS

Chapter 1

Introduction

1.1. Introduction to Cancer Drug delivery

Cancer is one of the deadliest diseases of all times affecting millions of people globally and every year the number of cancer cases growing at an alarming rate.[1] To eradicate the growth of cancer tissues several anticancer drugs has been formulated till date.[2] The typical profile of drug concentration in plasma as a function of time in oral or intravenous administration is depicted in figure 1.1.[3] The concentration of drug rises in the blood plasma followed by peak and then subsequently declining in the drug profile.[4] The higher plasma level of each drug characterizes toxicity and lower is ineffective. Thus, the patient requires multiple administrations to maintain drug concentration at a particular time to be in the therapeutic window or at therapeutic dose level.[5] Mostly low molecular weight therapeutic agents employed in cancer treatment; As a result rapid renal clearance undergone by these drug molecules. Furthermore, diffusion mechanism compelled the absorption of the drug molecules after systemic administration. Thus, there is an even distribution of drug molecules throughout the entire body thereby, lacking tumour selectivity and causing damage to healthy tissues.[6]
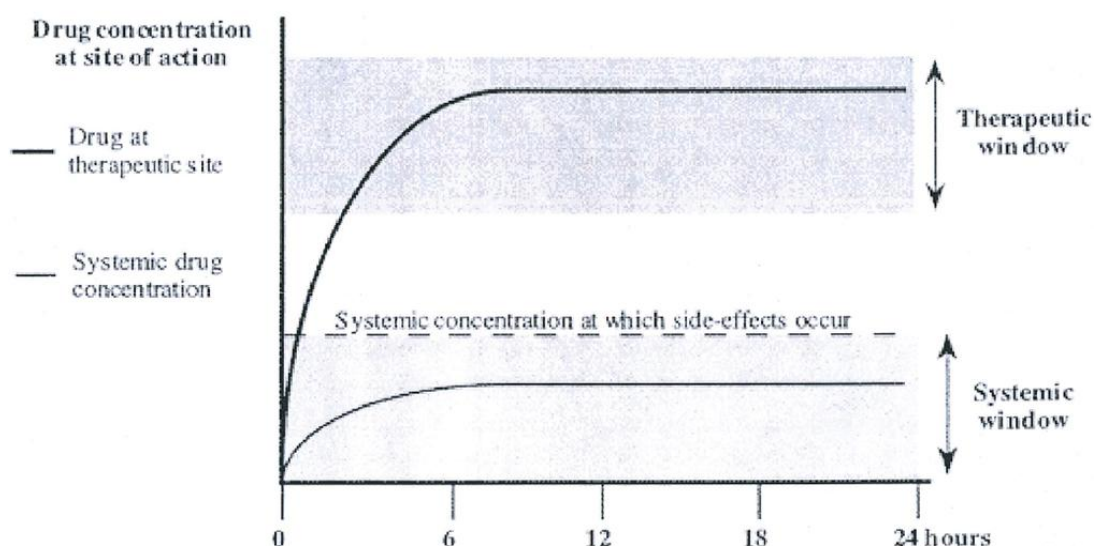
Figure 1.1. Comparison of conventional and controlled drug delivery system (adopted from Uhrich et al. *Chem. Rev*. **1999**, *99*, 3181-3198).

Paul Ehrlich, the founder of chemotherapy, proposed the presence of receptors in cells or in blood stream capable of specifically binding to antigens, toxins and nutritive substances. His postulates influenced the area of drug delivery and were adapted for polymeric scaffold for targeted drug delivery. He predicted that antibodies were like magic bullets as these were capable of identifying their target receptors and causes no harm to the organism.[7] Various nano-drug carriers were developed aiming for (a) controlled drug release, and (b) site-specific drug delivery. Drug is generally delivered at a pre-determined rate for an absolute time period in controlled release system (see figure 1.1).[8] In these systems, the rate of drug release completely depends on the design but is independent of the surrounding environmental conditions. On the other hand, targeting ligands incorporation attains the site specific drug delivery which elaborates the drug efficacy at the desired site of therapeutic need by increasing the local drug concentration.[9] Thus, a controlled delivered system retained the drug concentration for longer time in the therapeutic window(see figure 1.1). Therefore, there is a sustained release of drug is accomplished in controlled release system over oscillating drug plasma level in conventional delivery. These controlled drug release systems provides various other advantages over the conventional drug therapies such as: (a) enhanced bioavailability of drug, (b) preventing premature degradation of therapeutic agents, (c) avoiding rapid renal clearance, (d) reducing the dose level, (e) minimized side effects (local/systemic) and (f) improved patient compliance etc.[10]

Different types of small molecular amphiphiles have been employed as delivery agents owing to their biocompatibility and biodegradability characters. Self-assembly of these amphiphilic small molecules designs broad range of nano-carriers[11] such as liposomes, micelles, nanoparticles etc. The drug molecules are physically entrapped in these nano- carriers via non-covalent interactions which further deliberates stealth character to the drug molecule.[12] Since then it minimizes the binding of plasma proteins to the drug molecules followed by reduced uptake by reticulo-endothelial system (RES) or macrophages. In other words, these delivery agents increase the blood circulation time or half-life of the drug molecule.[13] These nano- carriers encapsulate both hydrophobic and hydrophilic therapeutic agents. For instance, hydrophobic drugs can sequestered through small molecule based micelle in their inner hydrophobic pocket; while encapsulation of both hydrophilic and

hydrophobic drug molecules facilitated over presence of outer hydrophobic layer and inner aqueous interior in liposomes.

1.2 Polymers in drug delivery applications

Polymers are macromolecules with variety of functional groups and can be blended with other low and/or high molecular weight materials for using in different applications. Natural polymers such agar, insulin, cellulose and chitin etc have been used as components of herbal medicines for wound dressing, emulsifying agent etc. Polymers are the backbone for pharmaceutical drug delivery systems; they have been found extensive applications in drug delivery because they offer unique advantages which have not been attained by any other materials. Based on the source polymers can be divided in to two main categories: (i) natural polymers such as chitosan, alginate, gelatin, albumin, collagen and dextran, and (ii) synthetic polymers includes polyethylene, polylactic acid, polypropylene, polyacrylates etc. Synthetic polymers are of increasing interest in drug delivery as therapeutic agent, polymers show usually an improved pharmacokinetics compared to small molecule drugs with longer circulation time and better tumour accumulation this can be explained by enhanced permeability and retention effect.

1.2.1. Enhanced Permeability and Retention Effect

Nano-scale drug carriers achieve tumour targeting mainly through two mechanisms namely active targeting and passive targeting. Usually, passive targeting is attained due to presence of defective, leaky vasculature of the tumour blood vessels.[14,15] The disorganized endothelial cells forms the large fenestrations on the inner lining of tumour blood vessels leads to enhanced vascular permeability, thereby facilitating in better penetration of the nano-carriers in tumour tissue (see figure 1.2). Due to this, the local drug concentration maximises 10-50 fold times in tumour tissues as compared to normal tissue.[16] Likewise, these nano drug carriers has capability to be retained for prolonged period in the dysfunctional lymphatic drainage of tumour tissues thereby allowing them to release drug in tumour vicinity. This phenomenon of higher accumulation and retention of drug carrier in tumour tissues was termed as "enhanced permeability and retention (EPR) effect".[17] In 1990, Maeda and

Matsumura discovered this efficient strategy for anticancer drug design having high selectivity towards tumour tissues.[18] Interestingly, this EPR effect is not associable to
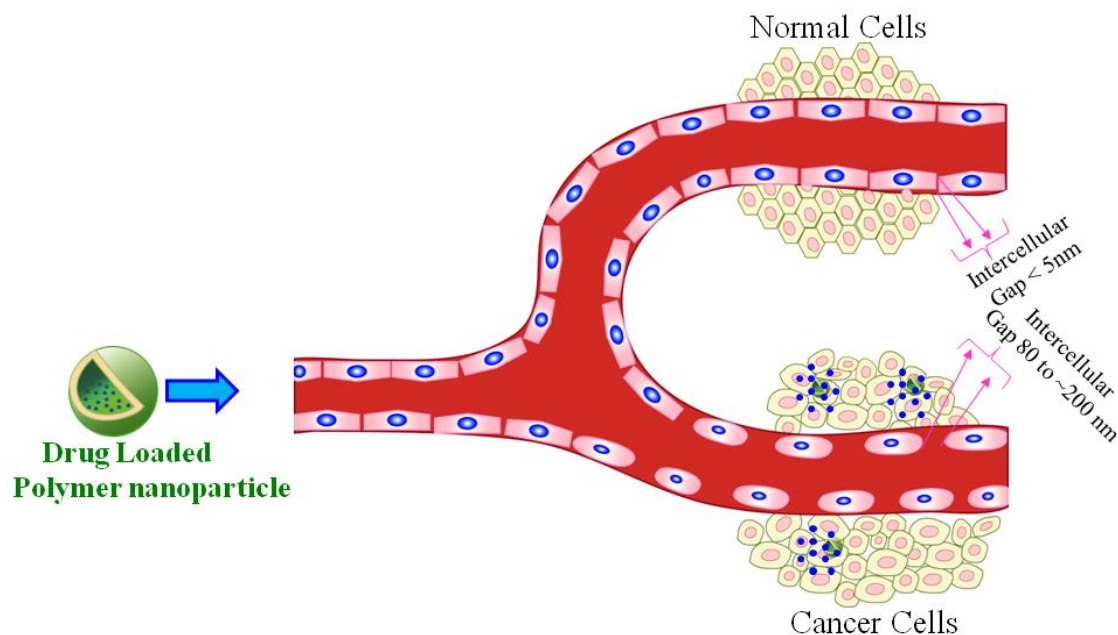
free drugs with low molecular weights or conventional chemotherapeutic agent (see figure 1.2). Though, the concept of EPR is widely accepted for selective solid tumour targeting of nano drug carriers and is a key mechanism for novel drug carrier design.[19,20]

Figure 1.2. The enhanced permeability and retention effect of nano-carriers as compared to conventional therapeutic agents.

Passive targeting approach suffered from several limitations such as: (a) accumulation and penetration of drug carriers in tumour non-specifically, (b) release of drug molecules before reaching the target site, and (c) low level of drug concentration in tumour tissues.[21] In other words, low therapeutic efficacy and undesirable systemic side effects executed through delivery of fraction of drug molecule at the diseased.[22,23] Furthermore, Drug carriers surface were modified with various molecules which has capability of binding to receptors that are over expressed on cancer cells in order to circumvent the limitation of passive targeting with respect to its specificity.[24,25] In contrast, "active targeting" or "ligand-mediated targeting" requires surface modification of the nano-carrier to incorporate conjugating ligands having affinity for cancer specific receptors for delivering drug at desired site.[26] Conjugating ligands generally used for tumour therapy are folate, antibodies, aptamers, transferring, proteins, peptides, nucleic acids and sugar molecules.[27] By

linking targeting ligand with receptor expressing cancer cells leads to drug carrier accumulation in tumour tissue followed by cellular internalization and release of the therapeutic agent in intracellular compartment.[28,29] Thus, active targeting moieties significantly enhances the intracellular drug concentration and minimizes the toxicity to non-cancerous cells adjacent to tumour tissues.[27] In other words, actively targeted nanosystems in combination with EPR effect have the potential to revolutionize cancer therapy and improves the efficacy of nanomedicines for cancer treatment.

1.3. Biodegradable synthetic polymers:

Synthetic biodegradable polymers are versatile polymeric materials that have a high potential in biomedical applications avoiding subsequent surgeries to remove. Biodegradable polymeric materials are preferable candidates for their unique physical, chemical and mechanical properties which can be easily varied by the material composition and polymer architecture and their degradation rates can be adjusted as required for an efficient therapeutical treatment. Biodegradable polymers also have versatile applications as implants, biodegradable polymers containing entrapped drug can be placed in the body and are used for localised drug delivery and/or the controlled release of a drug over a period of time, for example small polymer rods (goserelin (Zoladex)) and polymer microparticles (Leuprolide (Leupron Depot)) made from poly lactide-co-glycolide-entrapping leutinizing hormone releasing hormone (LHRH) analogues are common treatments for prostate cancer. As the polymer slowly degrade therapeutic levels of the anti-tumor peptide are maintained upto 3 months, making the therapy very convenient for the patient use (Figure 1.3).[30]
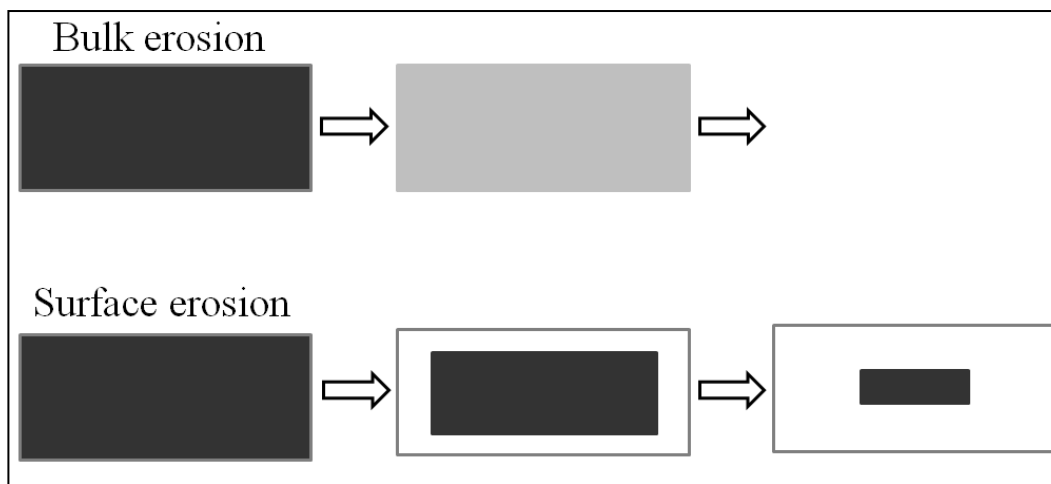
Figure 1.3. Schematic representation for bulk erosion and surface erosion (adopted from Chang-Sik et al. *Chem. Rev.* **2005**, *105*, 4205-4232).

Another biodegradable polymeric implant, carmustine (Gliadel) is used to treat brain cancer. In this case a biodegradable polyanhydride polymer is made into small polymer discs containing the alkylating agent bis(2-chloroethyl)nitrosourea (BCNU). These discs are placed into the brain following the surgical removal of the tumor, and thereafter they slowly degrade to deliver the drug locally, therefore preventing tumor re-growth. In the last decades synthetic biodegradable polymers such as poly(lactide acid) (PLA), poly(ε-caprolactone) and its copolymers or blends approved by the US Food and Drug administration (FDA) have been widely used in biomedical applications.

Degradation of the polymer material can occur either in the bulk or at the surface of the material, depending on the pH conditions external and internal to a polymer either mechanism can dominate. In the case of bulk erosion degradation proceeds throughout the polymer matrix and an immediate drop of molecular weight is observed, whereas the mass loss is retarded. In the case of surface erosion the biodegradation proceeds exclusively at the surface. Bulk degradation is useful for
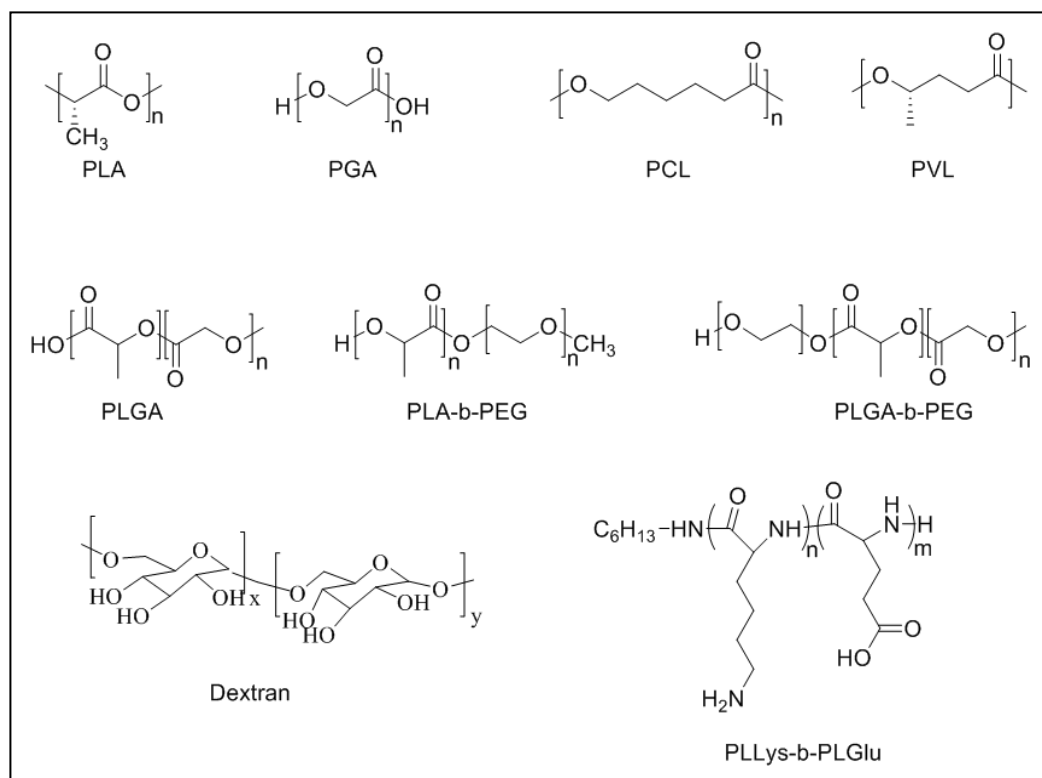
Figure 1.4. Chemical structures of Biodegradable polymers

applications such as degradable plastics for packaging, surface degradation is desirable in applications such as drug delivery systems. To maximise control over drug release, it is desirable for a system to degrade only from its surface. In systems with surface erosion the drug release rate is proportional to the rate of erosion of the polymer.

Polylactide (PLA), polyglycolide (PGA), poly(ε-caprolactone) (PCL), poly(γ-valerolactone) (PVL), poly(lactide-co-glycolide) (PLGA), PLA-b-PEG, PLGA-b-PEG, polysacaharides, (Chitosan, Cyclodextrin, Dextran), poly(aminoacids) and polypeptides are some of the extensively studied biodegradable polymer materials in

drug/gene delivery applications (Figure 1.4). Among these Poly(aminoacids) or Polypeptides are naturally occur biodegradable polymers, they often employed for the design of targeted drug delivery systems because they are made of hydrolysable peptidic bonds and can form electrolyte complexes with DNA. In addition they can form micelles, nanoparticles or polymersomes by copolymerising with PEG. Synthetic PAA are usually obtained from the polymerization of N-carboxyanhydride initiated by primary amino compounds. The complete details of the synthesis and applications of the synthetic poly aminoacids and their subclasses has described in the following section.

1.4. Introduction to amino acids

Amino acids are the most essential biomolecules constitutesin the human body and play major roles in various biochemical functions.[31] These are the mostabundant organic compounds or building blocks, of proteins joined by a specific type of covalent linkage. Its basic structure consists both amino groups ($-NH_3^+$), carboxylate groups (COO^-), and a side chain (-R).Thus, the α-carbon atom is linked to four substituent groups. Based upon the side chain functional group, amino acids are classified as, acidic, basic, aliphatic, aromatic, thiol, alcohol and amidic (see figure 1.5).[32] These amino acids either directly or in their modified form, concur in numerous metabolic functions. They comprise neurotransmitter function (gamma-aminobutyric acid), and as precursor for the synthesis of non-protein nitrogen containing metabolites (e.g., heme, creatine, purines and pyrimidines). Some amino acids are called as essential amino acids because they are not synthesized in the body and are supplied in the diet to maintain normal growth and metabolism.[33]
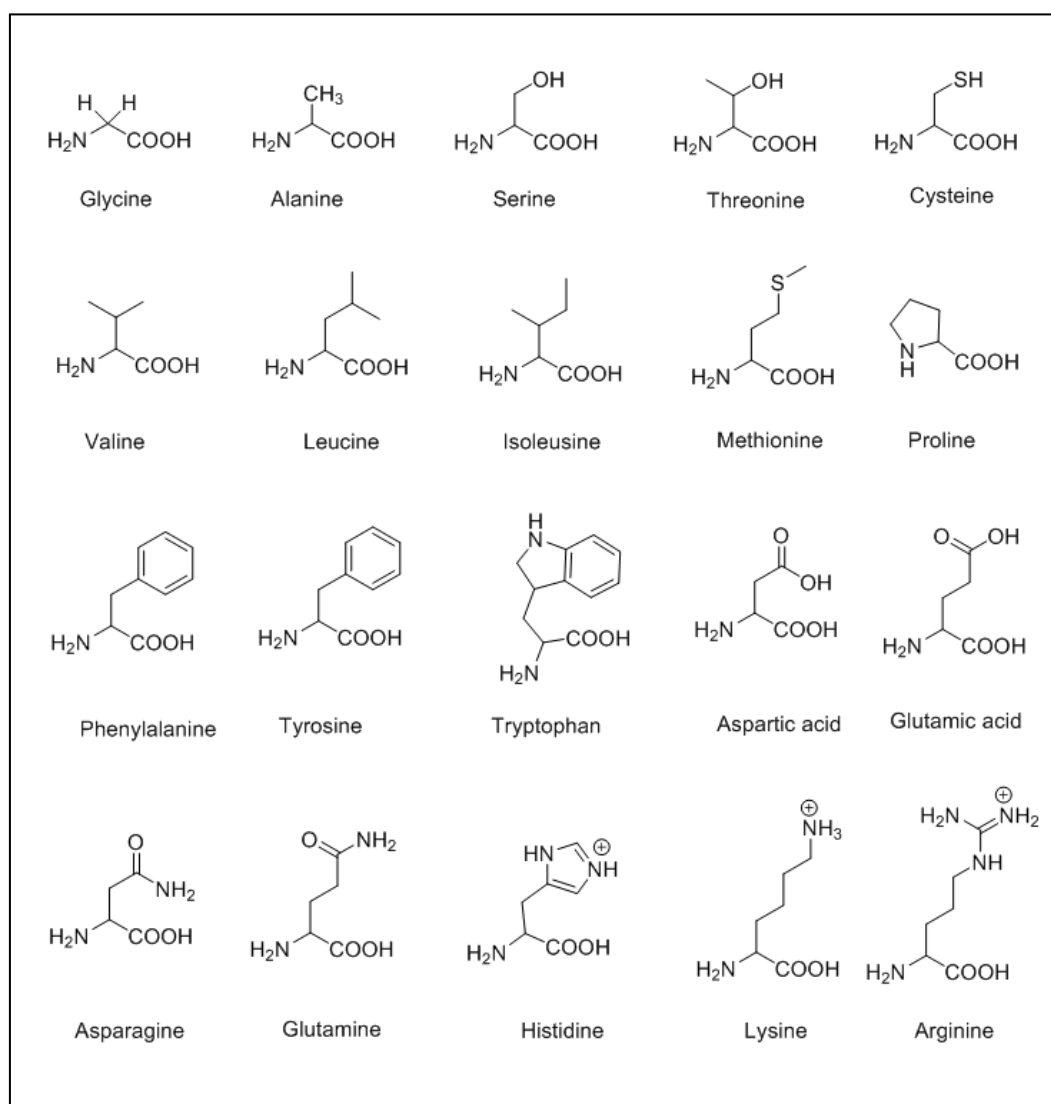
Figure 1.5. Chemical structures of natural α-amino acids.

Due to the rapid development of the aminoacid market, many companies and academic associations has enthusiastically started research and development to produce amino acids more efficiently. The main amino acid market is in food, which absorbs about 50% of global market (see figure 1.6).[34] The major amino acids consumed in food and flavour enhancers are Glutamic acid, which accounted for 34% of the total US amino acid market size in 2011.[35] Also, phenylalanine and aspartic acid are highly standard amino acids as these are the feedstock for producing aspartame (an artificial sweetener). In 2012, methionine, lysine, threonine and tryptophan are the prominent products, accounting to over 31% of total market value in the feed sector.[36] The amino acids market is estimated to grow with 26% over the period 2012-2016.[37] Furthermore, four ways of production have been developed to

meet the amino acids demand; extraction, chemical synthesis, fermentation and enzymatic catalysis.
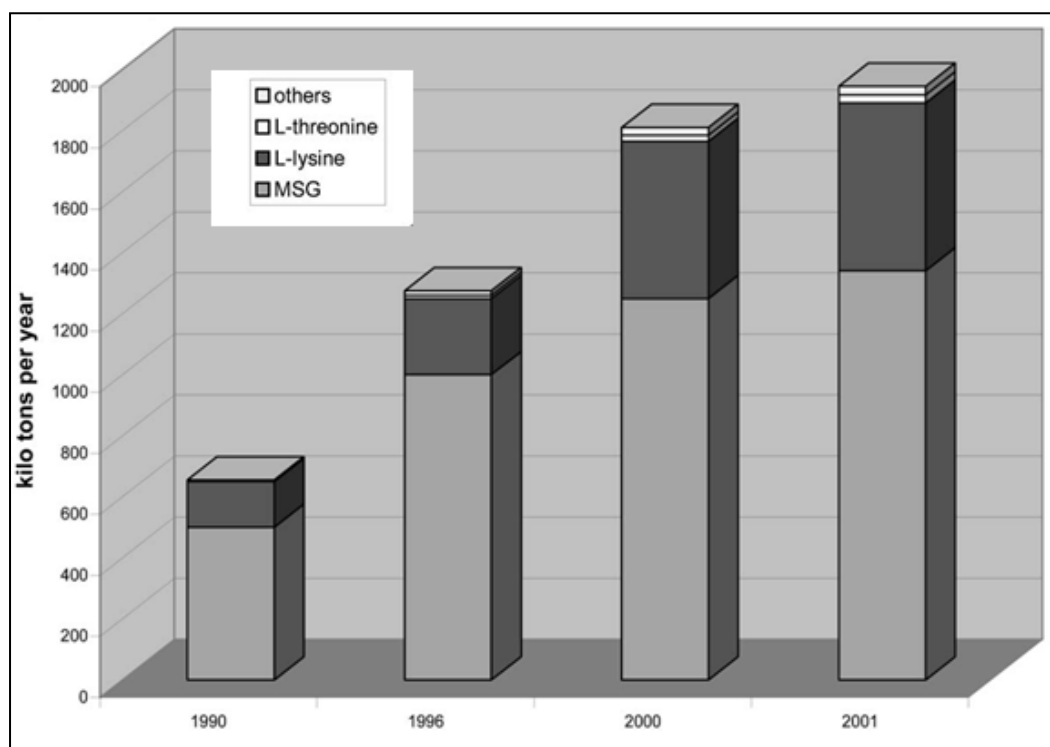
Figure 1.6. Global production of selected amino acids with the total amount of 1.5 million tonnes (adopted from Shahid, M. et.al. *European Journal of Lipid Sci. and Tech.,* **2011,** *113*, 1012-1018).

Historically, extraction method was used for the industrial production of amino acids. In 1908, Kikunae Ikeda isolated the unique flavour of seaweed that later became monosodium glutamate (MSG) known as the first original industrial application of an amino acid. Soon after this innovation, extraction of MSG was also accomplished from other biomass such as wheat gluten and soyabean.[33] In addition to glutamic acid, some other amino acids are also extracted for food namely, cysteine (as dough conditioner), leucine (as flavour enhancer), and valine (as dietary supplement). All these amino acids can be extracted from feather and hair.[38,39] To meet the current industrial needs for amino acids, extraction confides on the availability of biomass and the effectiveness of extraction process. However, amino acids may once again be extracted from various agricultural residues to meet future biorefinery concepts. In chemical synthesis method, confined number of amino acids has been produced such as i) Glutamic acid synthesised through oxo reaction from acrylonitrile[40] and a reduction reaction from di-ester-alpha-nitroglutaric acid,[41] ii) Glycine from

11

formaldehyde or monochloroacetic acid and ammonia,[42] iii) Methionine through a complex chemical synthesis involving mercaptan, propylene, and hydrogen cyanide.[43] This method can only produce a mixture of D and L-form of amino acids. On the other hand, living organisms are used as catalyst for the production of amino acids in enzyme catalysis process.[44] Based on these approaches, L-phenylalanine was synthesised from (*E*)-cinnamic acid by utilising phenylalanine ammonia lyase enzyme as the catalyst. Similarly, L-aspartic acid was synthesised from fumaric acid and ammonia using L-aspartate ammonia lyase enzyme as catalyst.[45] Currently, the development of microbial process for producing glutamic acid from soil bacterium, Cornyebacterium glutamicum, using sugar and ammonia, paved the way for the progress of fermentive production of amino acids.[46,47] Now a days, fermentation method has commonly been used to produce L-lysine, L-phenylalanine, L-threonine, L-glutamine, L-arginine, L-tryptophan, L-valine, L-leucine, L-isoleucine, L-histidine, L-proline, and L-serine.[48]

1.5. Oligo-peptide amphiphiles

Oligo-peptides congregate into an array of structures mediated by electrostatic attractions between charged amino acids, hydrogen bonding, π–π stacking interactions and hydrophobic associations.[49] The evident separation between hydrophobic and hydrophilic parts of the molecule in amphiphilic peptides are able to form spherical, membrane and fibrous aggregates as well as peptide nanofibre based hydrogels (Figure 1.7).[50-52] Amphiphilic peptides are synthesized using solid or solution phase techniques followed by conjugation with hydrophobic units.[53] The most appealing self-assemblies are peptide spheres, peptide hydrogels and peptide fibres with respect to drug delivery.[51] Peptide spheres commenced as 20-30nm micellar arrangements and peptide nanofibres have an internal diameter of 10-20nm and length periodically exceeds to micron.[54] Furthermore, peptide nanofibres consist of a central hydrophobic core surrounded by a β-sheet of peptides.[55] As the alkyl chains concord, it is possible to envisage the β-sheet formation that astonish the self-assembly and prevents the assembling molecules from accomplishing a prominent radius of curvature and spherical shape, instead giving rise to a hydrophobic cylindrical assembly surrounded by a β-sheet. Although, literature presents the rules for the formation of peptide nanofibres i.e. peptide sequence forms by the presence of a β-sheet, a charged amino acid and an alkyl chain linked to one end of the peptide.[54] In the literature, nanofibres

assembled from acyl derivatised therapeutic peptides, namely from O-palmitoyl tyrosinate ester1-leucine5-enkephalin[56] which is devoid of a charged peptide residue and O-palmitoyl tyrosinate ester1-dalargin.[50] Additionally, other molecules such as dipeptide, diphenyl Alanine also self-assemble into nanofibres.[57,58] It is clear that peptide nanofibres are also able to aggregate to form gels by virtue of the peptides's intrinsic chemical composition. Self assembly for short peptides has been determined by chemical coupling of a variety of aromatic groups, such as carboxybenzoyloxy, naphthalene or fluorenylmethyl-1oxycarbonyl (Fmoc) on the N-terminal end of di- and tri-peptides, with the resultant formation of stable hydrogels.[59]
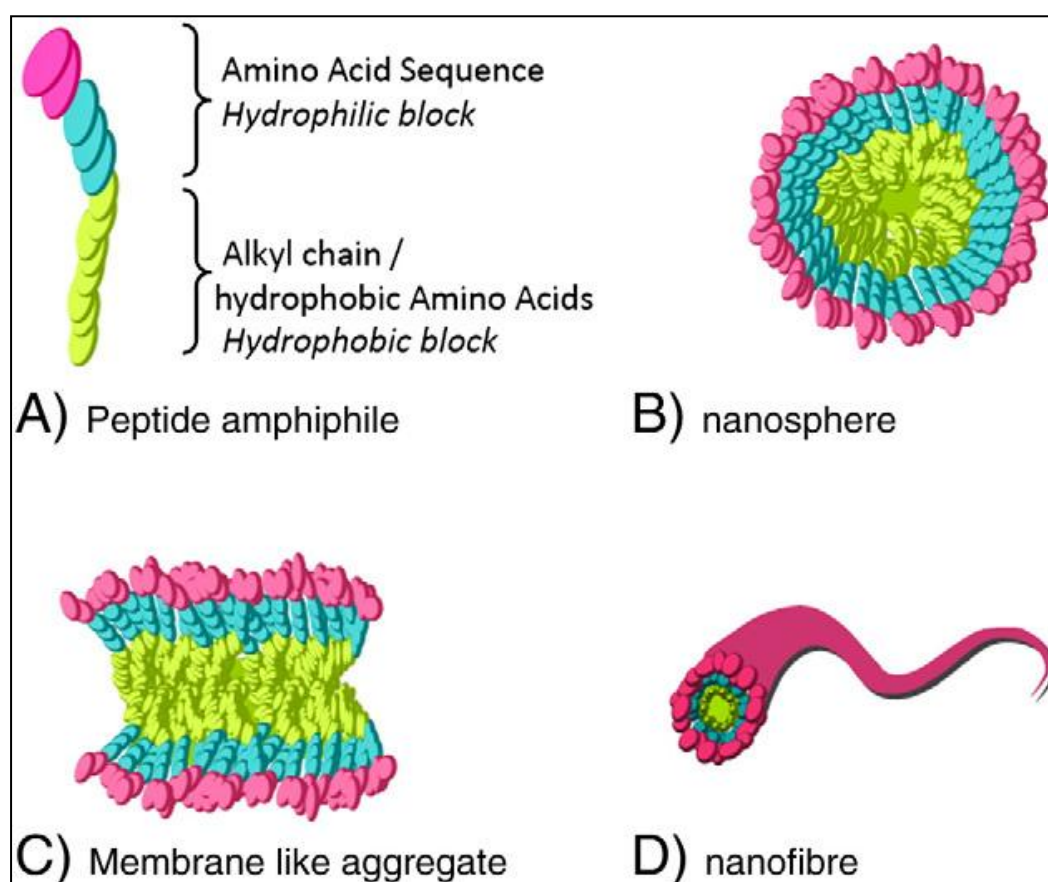
Figure 1.7. Self assembly of peptide amphiphiles into: nanospheres, membranes and nanofibres. (adopted from A. *Lalatsa et.al. Journal of Controlled release*, **2012,** *161,* 523-536).

Self-assembled peptide amphiphiles have been applied as a drug delivery agents and tissue engineering scaffolds.[53,60] Several in vitro experiments have been performed to illustrates the utility of self assembling peptides as possible drug delivery agents such as i) in vitro cell uptake and cytotoxic activity for a peptide

nanofibre by bearing a bioactive epitope attached to the peptide amphiphile,[61] ii) in vitro cell uptake for peptide amphiphiles by bearing electrostatically bound DNA, loaded with hydrophobic drugs or recurrently loaded with both drugs (e.g. doxorubicin) and therapeutic (e.g. p53 genes) plasmids.[62-64] Pivotal in vivo data has been generated to support that peptide amphiphiles may use as a new class of medicines. Further, two peptides, YGAA[KKAAKAA]2 (AKK), and KLFKRHLKWKII (SC4), conjugated to lauric acid exemplifies that cationic peptide amphiphiles employ their anti-microbial activity by disrupting bacterial cell walls.[65] Likely, there is a evidence of anti-microbial activity from the spherical self-assemblies which was prepared from the TAT peptide amphiphiles, in that the cationic TAT peptide (YGRKKRRQRRR) is conjugated to cholesterol via a spacer unit comprising three glycines followed by six arginines (cholesterolG3R6-TAT). These spherical nanoparticles were active via the intravenous route against a staphylococcus aureus infection in mice and a S. aureus infected meningitis rabbit model.[53]

1.10. L-Amino acid based Polymers in drug delivery

Natural L-amino acids are rotinely employed as one of the constituenets in the polymer backbone or as side chain units for bio-degradation, inroduction of functionality and employed as self-organizing tools. Natural amino acids, i.e. glutamic acid (Glu), phenylalanine (Phe), arginine (Arg), and lysine (Lys), have merits such as biodegradability, good biocompatibility, and the physical and chemical characteristics of side-chain functional groups, were employed to develop amphiphilic polymers.[66] Two families of amino-acid-based poly(esteramide) (AA-PEA) and poly(ester urea urethane) (AA-PEUU) biomaterials with good biocompatibility and biodegradibilty have been developed. These amino-acid containing polymers (AA-PEA and AA-PEUU) illustrates useful pendant reactive sites, tunable hydrophilicity, anionic/cationic charge, degradation rates, and a wide range of chemical, mechanical, thermal, physical, and biological properties compared to conventional biodegradable aliphatic polyester biomaterials, e.g., poly(lactic acid) (PLA), poly-(caprolactone) (PCL), poly(glycolic acid) (PGA) and their copolymers.[67] In recent years, cationic amino acids, such as Arg or Lys synthesizes amino acid based PEA or PEUU materials are of particular interest. Arginine (Arg) shows an important role in macrophage-induced TNF-α and nitric oxide (NO) production due to their strong

cationic nature which allows for better cell uptake. Leucine (Leu), a neutral and hydrophobic amino acid interdependent to hydrophilic Arg due to the presence of hydrophobic moiety appropriate for the self-assembly and stability of the resulting self-assembled nanoparticles. Chu et al. reported that the supramolecular structure formed and stabilized by the presence of Leu moiety in the protein, peptide and synthetic polymers (Figure 1.8).[68]
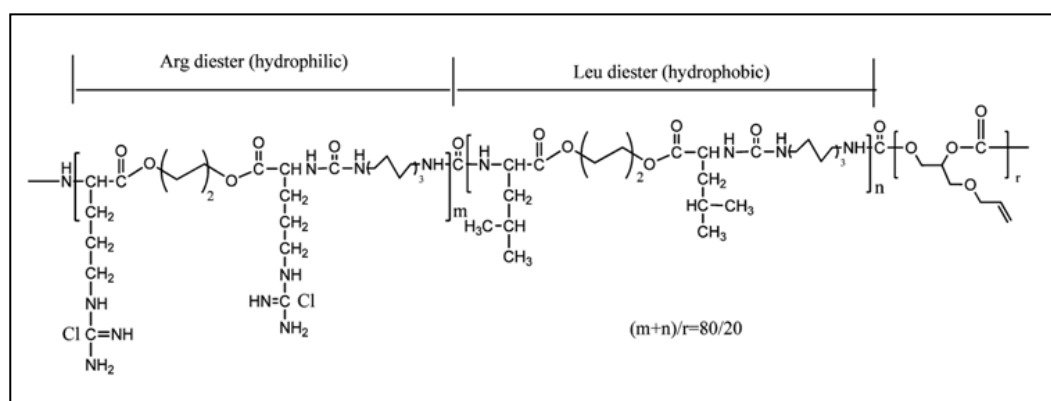
Figure1.8. Chemical structure of Arg-Leu PEUUs (adopted from Chu et al. *Biomacromolecules*, **2016**, *17,* 523-537).

Further, controlled and targeted drug delivery systems have been studied through biodegradable polymers. Based on poly(LLA-co-Lys)-g-Lys (Figure 1.9 A), Langer et al. described the use of large porous particles (d =8.2 μm and F = 0.1 g/cm3) for pulmonary drug delivery.[69] The encapsulation and in vitro release of model drugs, such as diclofenac (acidic), nicardipine (basic) and dicumarol (neutral) from microspheres prepared from degradable PEEA based on dihydroxy-terminated oligomeric PCL, sebacoyl chloride, and 1,13-di(L-phenylalaninamido)-4,7,10-trioxatridecane was studied from Rotonda et al. (Figure 1.9 B). In vitro release experiments (pH 7.8, tris buffer) concludes that dicumarol loaded PEEA microspheres exhibits a slow drug release (10% after 50d) while diclofenac loaded PCL and PEEA microspheres show rapid and complete release in 2h. Also, Nicardipine-loaded PEEA and PCL microspheres released about 70 and 30% drug, respectively, after 8 h. [70]

Zhuo et al. designed the encapsulation and in vitro release of prednisone acetate (PA) from microspheres prepared from poly-R,β-[N-(2-hydroxyethyl)-L-aspartamide]-g-PLLA (PHEAg-PLLA) graft copolymers (Figure 1.9 C).[71] Likewise, the antimicrobial efficacy in vitro and in vivo were studied with L-tyrosine

polyphosphate loaded (Figure 1.9D) with silver N-heterocyclic carbine complex (SCC 10).[72]
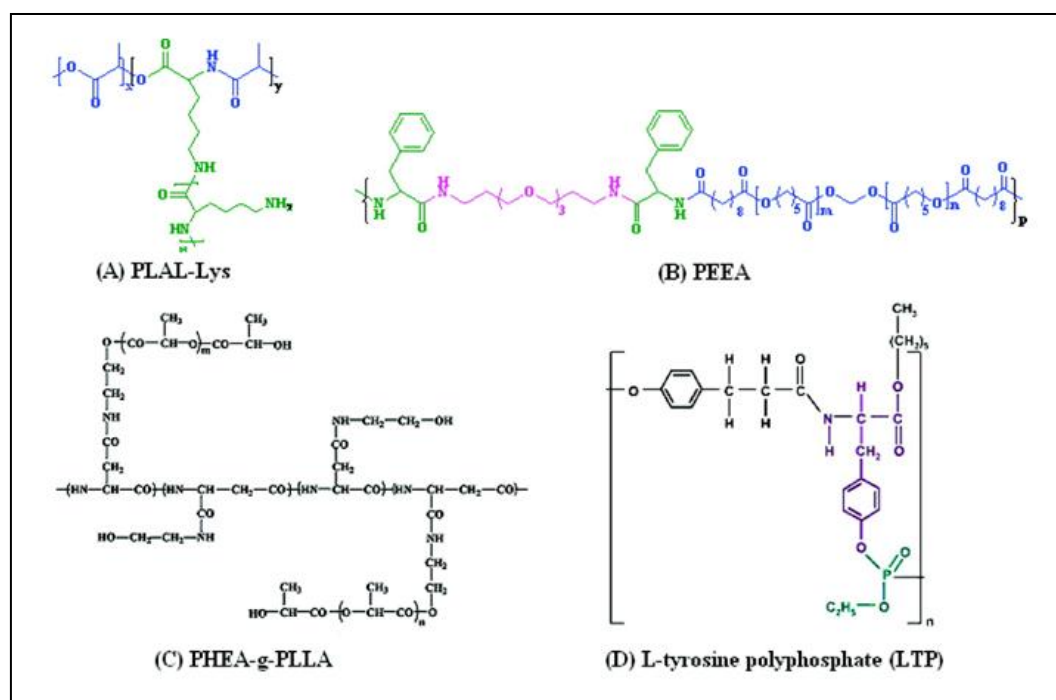
Figure 1.9. Chemical Structures of Amino Acid Containing Degradable Polymers Investigated for Drug Delivery Applications (adopted from Feijen et al. *Biomacromolecules*, **2011**, *12*, 1937-1955.

Polyurethanes are a unique class of biomaterials that are widely used in various medical devices including heart valves, catheters, vascular grafts, and prostheses.[73] The integration of acetal bonds in polyurethane is appealing due to its high pH sensitivity. In addition to, pH sensitive degradable micelles and polymerosomes adapted by incorporating pendant acetal groups at the side chain of polycarbonate or polyacrylate. The studies reveals that pendant acetal groups alter the hydrophobic block into hydrophilic, concludes an accelerated drug release.[74] Gu et al. commenced that acetal linked PTX prodrug micellar nanoparticles presented potent growth inhibition of human cancer cells in vitro.[75]
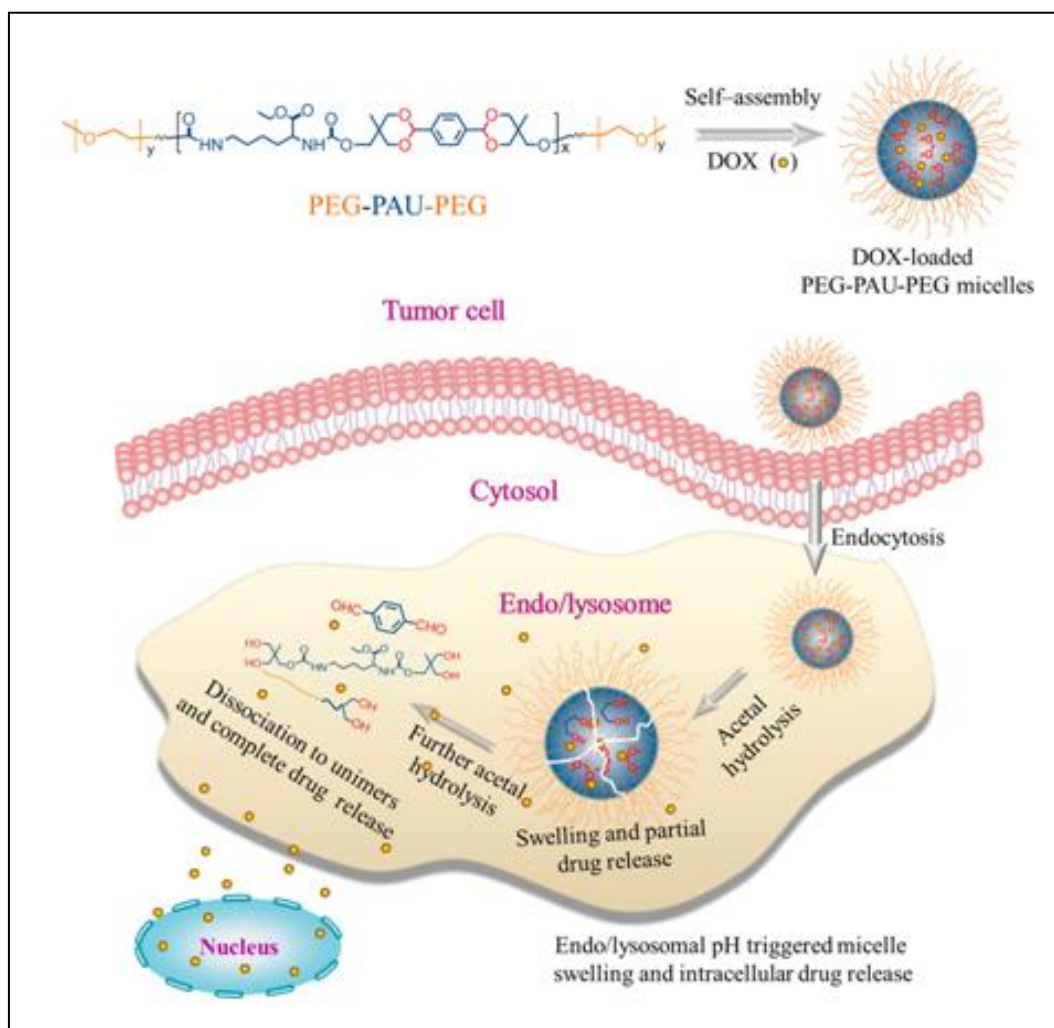
Figure 1.10. Acid-Degradable PEG-PAU-PEG Triblock Copolymer Micelles for pH-Triggered Intracellular DOX Delivery (adopted from Huang et al.B*iomacromolecules*, **2015**, *16*, 2228-2236).

The Figure 1.10 defines that acid degradable PEG-PAU-PEG triblock copolymer micelles are showing potent anticancer effects and arbitrates efficient pH triggered intracellular DOX delivery. This triblock copolymer has various advantages including, i) easy to prepare and noncytotoxic in nature, (ii) have good stability with a low critical micelle concentration at physiological pH while undergoing fast degradation under a mild acidic environment, and (iii) endo/lysosomal pH triggers drug release resulting in effective reversal of drug resistance.[76]

1.7. Polypeptides

Preparation of polypeptides are mainly via ring opening polymerization (ROP) of α - amino acid *N*-carboxyanhydrides (NCAs) by utilizing amine based initiators.[77] The typical mechanisms of amine-initiated ROP of NCAs comprise "amine mechanism (AM)" which is accomplished by attacking CO-5 of the NCAs using 1^0amines or some highly nucleophilic 2^0amines (Scheme 1a) and "activated monomer mechanism (AMM), attained by deprotonation of NH-3 of the NCAs using 3^0 amines or some 2^0 amines with bulky substitution groups (Scheme 1.1.).[78,79] Different kinds of polypeptides and polypeptide-based copolymers with desired molecular weights and architectures are successfully prepared by the ROP of NCAs initiated by primary amines. Although some side reactions causes contamination of polypeptide products during the primary amine-initiate-polymerization, Recently, noticeable approaches have been developed to prepare polypeptides with controlled molecular weight (MW) and polydispersities (PDIs) as well as distinct topological structures. Deming and co-workers have used a series of transition metal complexes as initiators to attain explicit polypeptides and block copolypeptides.[77] Schlaad et al. and Lutz et al. have described that ammonium chloride-functionalized macro-initiators can effectively suppress side reactions, leading to the formation of distinct polypeptide-based block copolymers.[80,81] Further, by using organosilicon, controlled ROP of NCAs has been produced.[82] Subsequently, amphiphilic polypeptide-based block copolymers have been synthesized for biomedical applications including, i) the ROP of NCAs by using polymeric macro-initiators, ii) highly effective coupling reactions, such as click chemistry and carbondiimide chemistry, between functionalized polypeptide blocks and other polymer blocks. Comparatively, Deming and co-workers have synthesized different amphiphilic diblock copolypeptides containing a charged block and a hydrophobic block by using transition metal complexes as initiators.[83] Poly(ethylene glycol) (PEG)/polypeptide diblock copolymers by using amino-functionalized methoxypoly(ethylene glycol)s (mPEG) as macro-initiators have been adapted by Kataoka and coworkers.[84] Chen and co-workers have developed a series of polyester/polypeptide block copolymers by employing amino-terminated polyester blocks as macro-initiators.[85-90] In addition, Bae and co-workers have developed a class of poly(L-histidine) (PLHis)-based block copolymers by coupling PLHis with other synthetic polymers.[91]
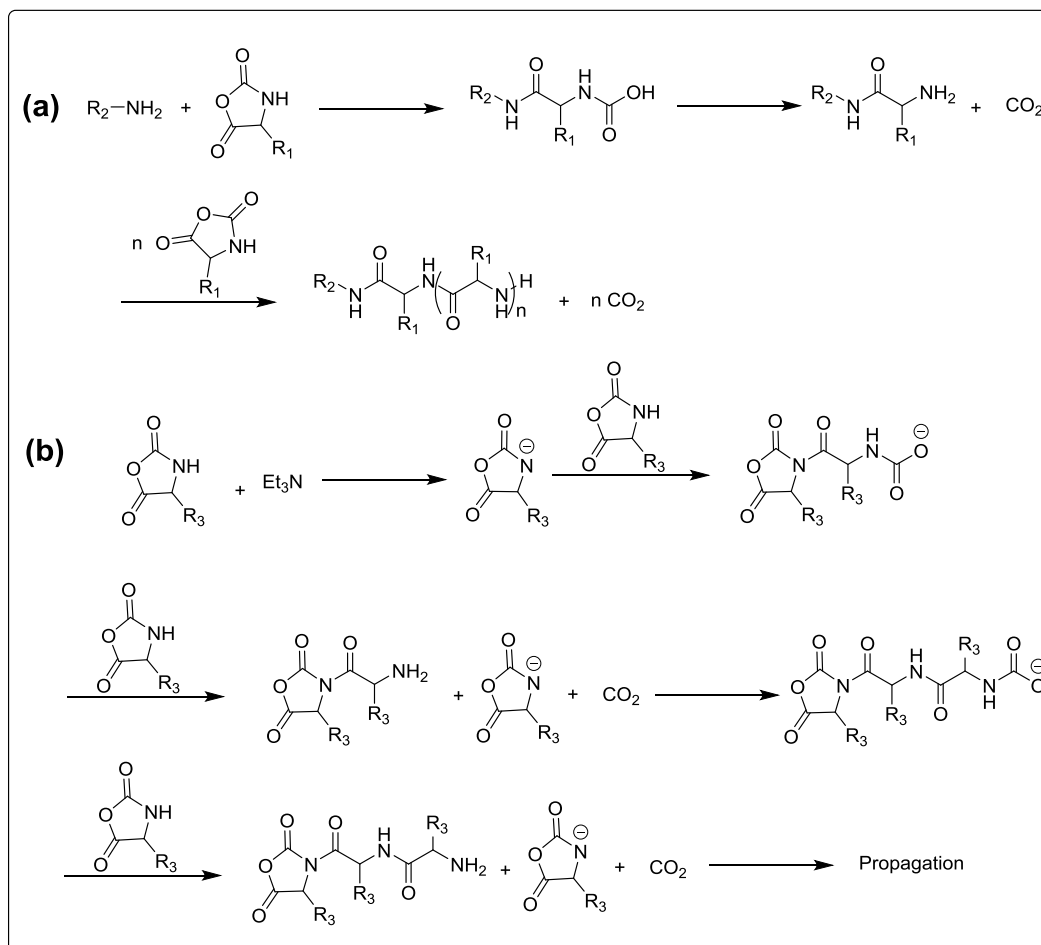
Scheme1.1. The ring opening polymerization of NCAs via "amine mechanism"(a) and "activated monomer mechanism"(b). (adopted from H. R. Kricheldorf , *Angew. Chem. Int. Ed.* **2006** , *45* , 5752-5784).

Additionally, different polypeptide-based materials have been accomplished and determined based on the polymers with different structures for drug- and gene-delivery applications including micelles, vesicles, nanogels, and hydrogels. The self-assembly of amphiphilic polymers in aqueous solution form polymeric micelles.[92] They have a hydrophobic inner core and a hydrophilic outer shell. The micellar cores resides of hydrophilic shells, such as an antifouling PEG shell, which shields and stabilizes the hydrophobic segments or complexes of oppositely charged polyelectrolytes. The hydrophobic cores of micelles facilitate the loading of hydrophobic drugs or ionic biopharmaceuticals, such as DNAs, RNAs, and proteins, while the hydrophilic antifouling shells reform the biocompatibility and stability of the micelles in circulation system in vivo.[93,94] Additionally, micelles based on stimuli-sensitive synthetic polypeptides are emerged as the most popular methods for cancer
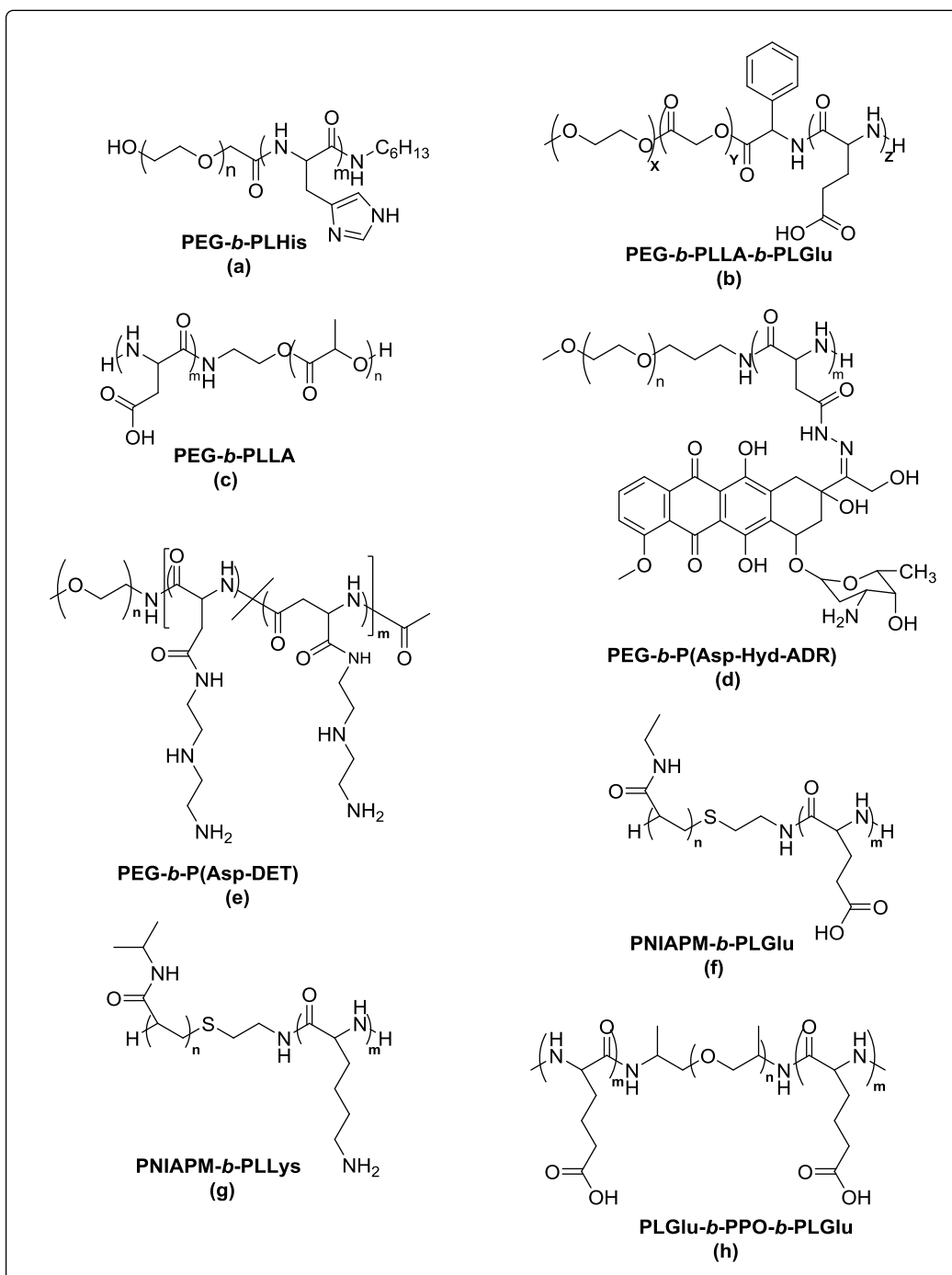
Scheme 1.2. Chemical structures of some representative polypeptide-based block copolymers that form stimuli-sensitive micelles (adopted from Chen, et.al. *Adv. Healthcare Mater.* **2012**, *1*, 48-78).

therapy due to their stimuli-responsive self-assembly behaviours and conformation transitions as well as good biocompatibility and biodegradability. Recently, polypeptide-based micelles comprising pH-sensitive polypeptide blocks, acid-labile

polypeptide–drug conjugates, polypeptide containing ion complexes and dual stimuli-sensitive segments have been developed for controlled drug and gene delivery (Scheme 1.2.).[95,96]

Polymer vesicles have hydrophobic bilayer or interdigitated layer and hydrophilic internal and external shells.[97-99] These are nanometer or micrometer sized hollow spheres. In contrast to polymer micelles, polymer vesicles can load the hydrophobic drugs within hydrophobic domain of the vesicle membrane and form these materials as an ideal candidate for delivery of hydrophilic drugs and bioactive molecules.[98] By adapting the composition and chain length of the amphiphilic polymer, the size and permeability of the vesicle membrane can be tuned. Therefore, stimuli-sensitive vesicles developed and approved for drug delivery applications based on different polypeptide block copolymers (Scheme 1.3).
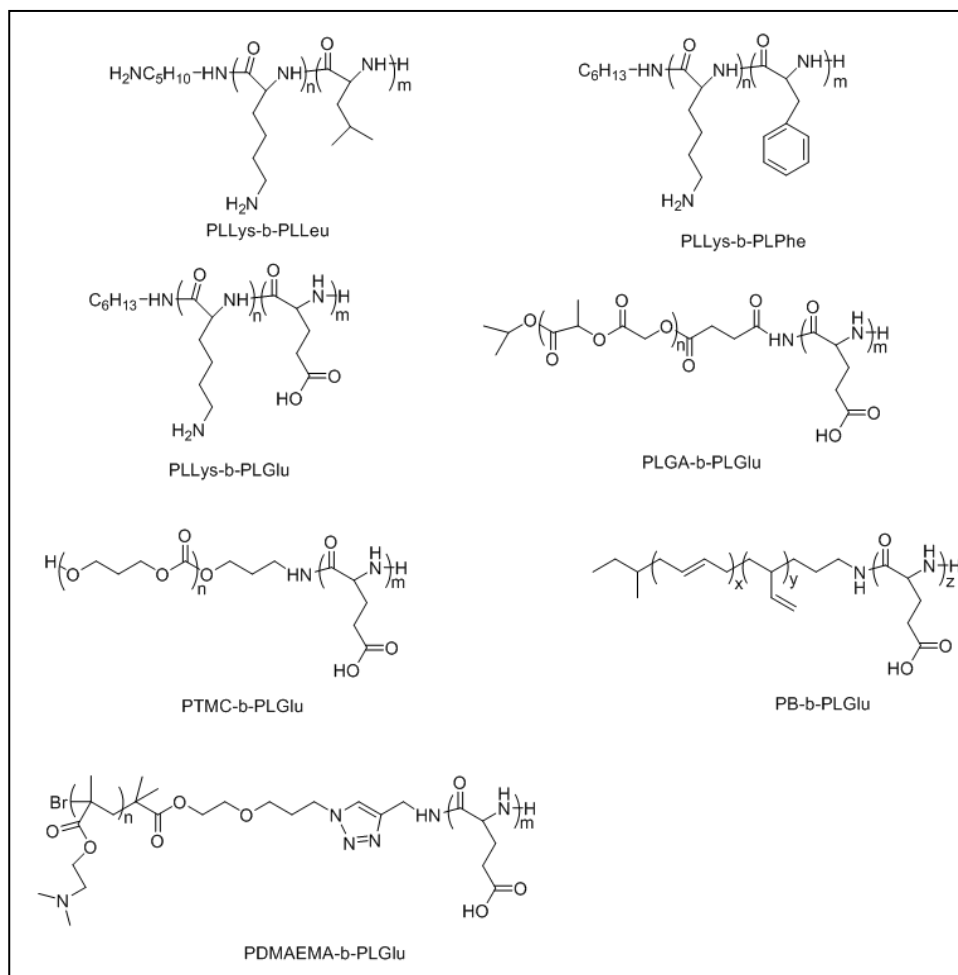
Scheme 1.3. Chemical structures of some typical polypeptide-based block copolymers that form stimuli-sensitive vesicles(adopted from Chen, et.al. *Adv. Healthcare Mater.* **2012**, *1,* 48-78).

Hydrogel nanoparticles, i.e., nanogels, are swollen nanometer-sized networks comprises of hydrophilic or amphiphilic polymers.[100,101] It has a polymeric network or a core-shell structure with a hydrogel core or shell (Scheme 1.4).[101] Due to their smart swelling–deswelling transitions and refined biocompatibility, stimuli-sensitive nanogels with an hydrophilic and biocompatible shell, have earned much consideration. In the past decade, polypeptide-based crosslinked nanoparticles, such as crosslinked micelles and nanogels, have been utilised for different drug delivery applications, since, it responds to external stimuli, such as pH, reducing environment, and dual stimuli. These systems have been assembled through various methods including precipitation polymerization, crosslinking of preformed polymer chains or selfassembled nanoaggregates and one-step ring-opening polymerization.
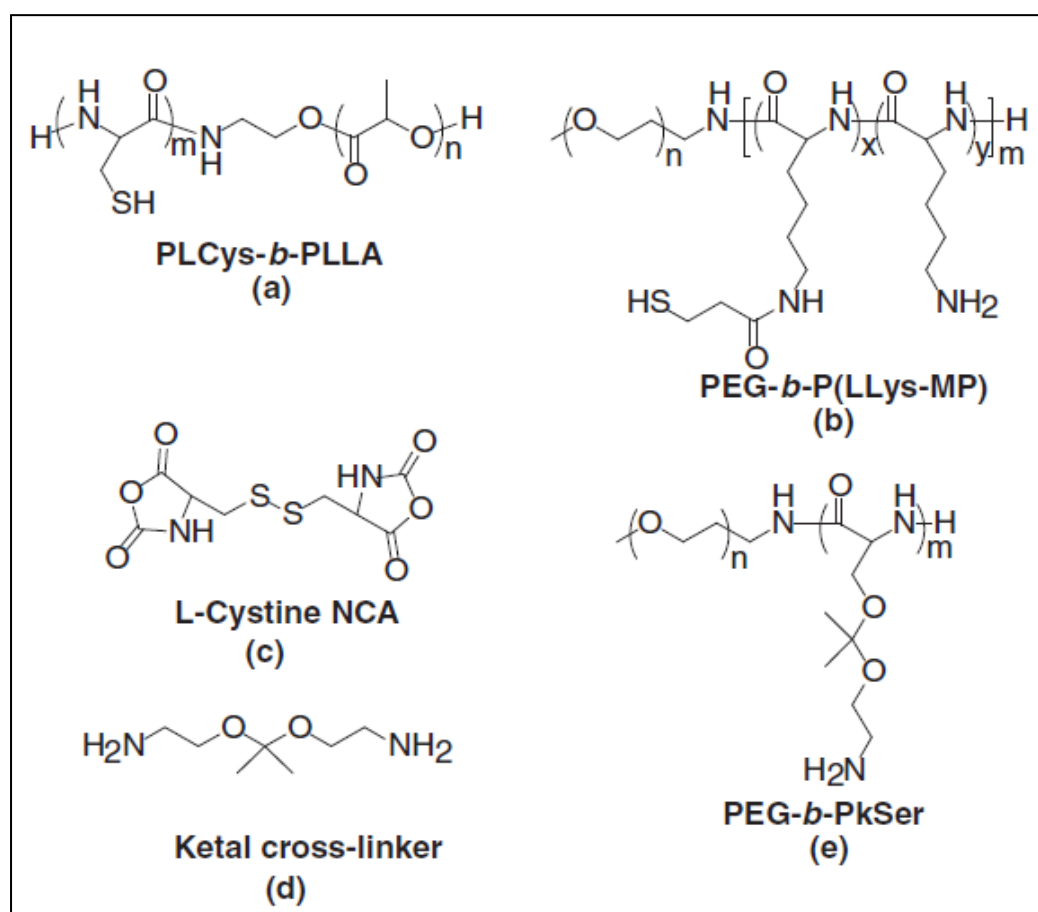
Scheme 1.4. Chemical structures of polypeptide based block copolymers and crosslinkers that are used for the preparation of crosslinked micelles and nanogels. (adopted from Hendrickson et al. *Adv.Funct. Mater*. **2010**, 1697-1712).

Hydrogels are three-dimensional polymer networks made of hydrophilic polymer chains that are cross-linked chemically or physically.[102] Hydrogels exhibited various biomedical, environmental applications due to their unique biocompatibility, chelating nature, desirable physical and physiological characteristics. They can deliver the physiologically important entities in a controlled manner and serve as carriers for drug, protein, and genes. Presently, polypeptide-based chemically crosslinked hydrogels and in situ gelling hydrogels have been fabricated and applied for different drug-delivery applications (Scheme 1.5).[103-106]
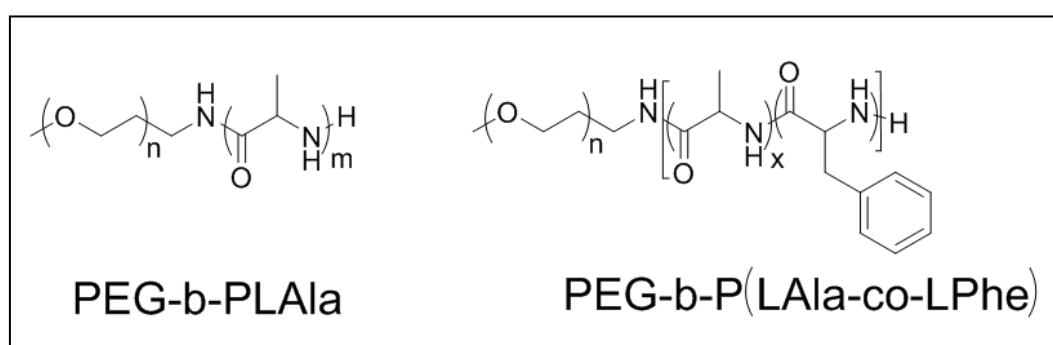
Scheme 1.5. Chemical structures of representative thermo-gelling polypeptide-based block copolymers (adopted from Slaughter et al. *Advanced Materials*, **2009**, *21*, 3307-3329).

1.8. Poly(ester-amide)s

In the past decades, α-amino acid containing degradable polymers have drew much interest and suggest several features including, i) imparting chemical functionality, such as hydroxyl, amine, carboxyl, and thiol groups, which maintains hydrophilicity and possible interactions with proteins and genes, also facilitates further modification with bioactive molecules (e.g.,drugs or biological cues); (ii) improving biological properties of materials including cell-materials interactions (e.g.,cell-adhesion, migration) and enzymatic degradability. (iii) by improving thermal and mechanical properties of degradable polymers; and (iv) providing metabolizable building units/ blocks (Figure 1.11).[107]
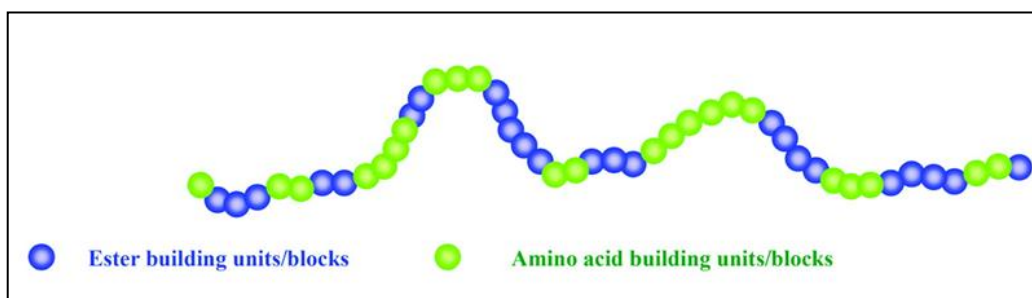
Figure 1.11. Schematic representation of α-amino acid containing degradable polymers (adopted from Feijen et al. *Biomacromolecules*, **2011**, *12*, 1937-1955).

Polydepsipeptides i.e. copolymers of α-hydroxy acids and α-amino acids, are mainly prepared by the ring opening polymerization of morpholine-2,5-dione derivatives. There are three main procedures describes the synthesis of the derivatives of the 6-membered ring of morpholine-2,5-dione (Scheme 1.6) such as (a) Cyclization of *N*-(α-haloacyl)-α-amino acid salts, (b) Intramolecular transesterification of *N*-(α-hydroxyacyl)-α-amino acid esters, and (c) Cyclization of *O*-(α- aminoacyl)-α-hydroxycarboxylic acids.[108-110]
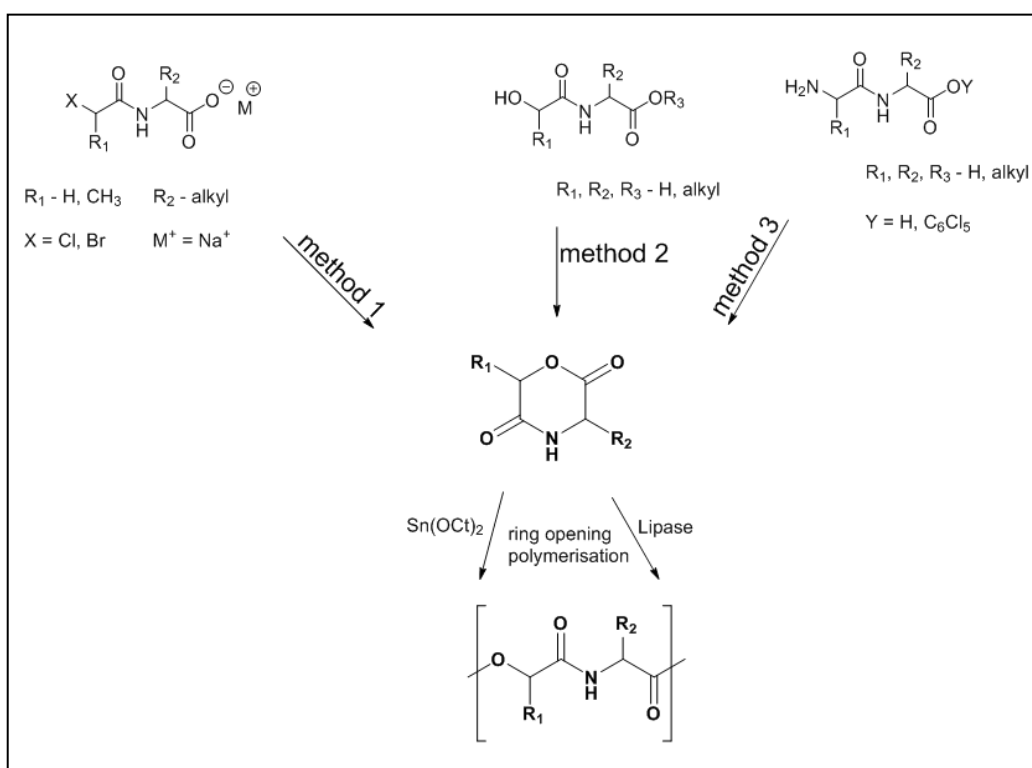
Scheme 1. 6. Synthesis of morpholine-2,5-dione derivatives and polymerization reaction (adopted from Puiggali et al. Polymers **2011**, *3*, 65-99).

Melt condensation method is carried out under reduced pressure and temperature to favour the elimination of condensation products and using transesterification catalysts. After the polymerization reaction, no post treatment is needed which makes this method advantageous for industrial production. The synthesis is usually driven in two temperature steps: i) progress under milder conditions to give rise to a prepolymer, ii) temperature is significantly raised to favour the condensation process and to get a high molecular weight sample. Poly(ester amide)s containing α-amino acid units successfully formed by reaction of a diol with a diamide-diester previously obtained by condensation of a diacid chloride with an α-amino acid methyl ester (Scheme 1.7.).[111,112]
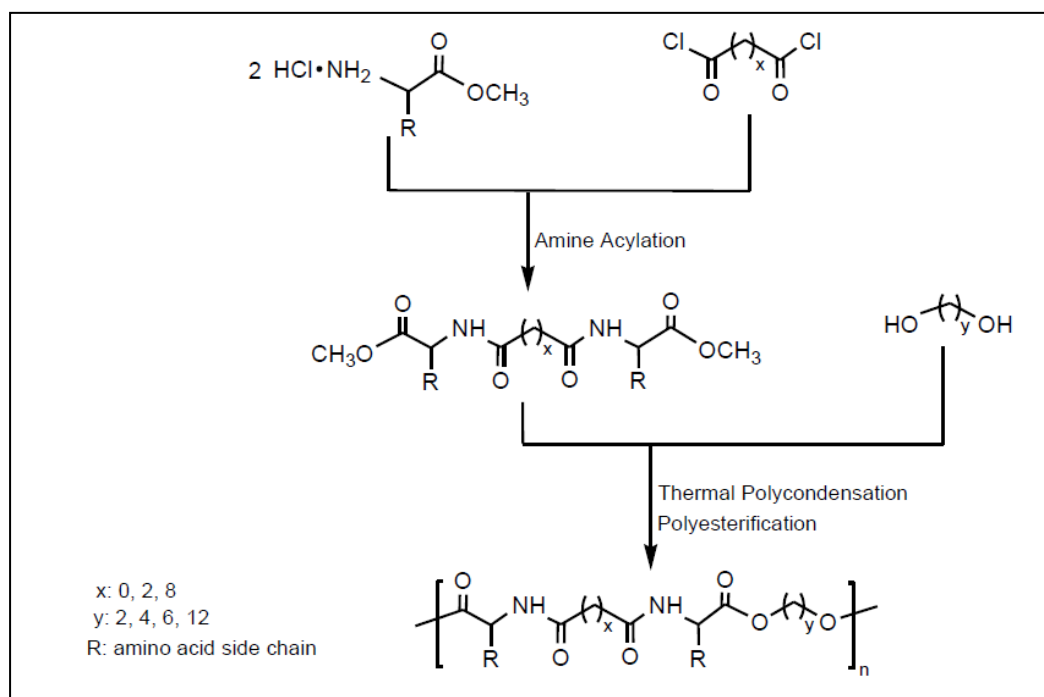
Scheme 1.7: Poly(ester amide)s preparation by melt condensation approach by incorporating α-amino acids of a diamide-diester monomer (Puiggalí et al. *J. J. Appl. Polym. Sci.* **2002**, *85*, 1815-1824).

Solution polycondensation reactions make use of condensing agents or activation groups for the carboxylic acid in order to expedite aminolysis reactions. High polymerization rates, mild reaction conditions, high molecular weights and minimal side reactions are expected characterstics of these reactions. Solution

polycondensation of disulphide containing di-p-toluenesulfonic acid salts of bis-Lphenylalanine diesters (SS-Phe-2TsOH) with di-p-nitrophenyl adipate (NA) in N,N-dimethylformaamide (DMF) in the presence of Et$_3$N under mild conditions readily synthesized α-amino acid based poly(ester-amide)s (SS-PEAs) (Scheme 1.8).[113] In the past decades, α-amino acid-based poly(ester amide)s (PEAs), which acquires the favourable properties of both polyesters and polypeptides, such as enzymatic degradability and bioactivity, have been developed as a versatile class of biodegradable polymers. A series if α-amino acid based PEAs were synthesized mentioned above and studied for various biomedical applications.[114-116]
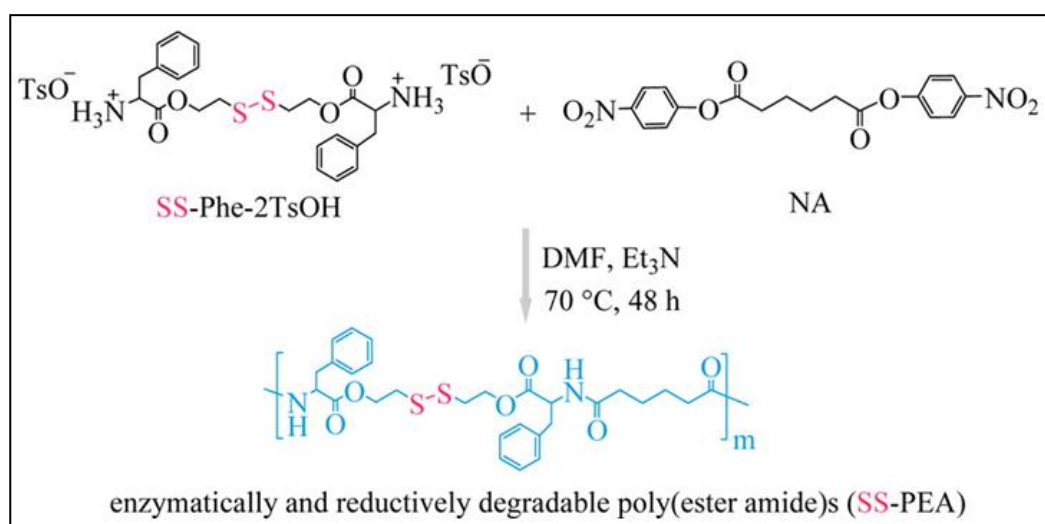
Scheme 1.8: Synthesis of Reduction-Sensitive L-Phenylalanine-based Poly(ester-amide)s (SS-PEA) (adopted from Sun et al. *Biomacromolecules*, **2015**, *16*, 597-605).

Chu et al. synthesised PEAs bearing pendant or embedding carbon-carbon double bonds, which could provide additional functional PEA derivatives via conjugation of thiol containing molecules or bioactive agents.[117] Further, electroactive tetraaniline grafted PEA shown good electroactivity, mechanical properties as well as affirmative cell adhesion and growth behavior of mouse preosteoblastic MC3T3-E1 cells reported by Chen et al.[118] Recently, tremendous attempts have been conducted to the formation of reduction-sensitive biodegradable polymers containing disulfide bonds for efficient intracellular drug and gene delivery. In addition to, during circulation and in the extracellular environment, the stable di-sulphide bonds cleaved

rapidly in the cytosol due to the presence of 2−3 orders higher level of glutathione tripeptide (GSH; about 2−10 mM) than in the extracellular fluids (about 2−20 μM). The therapeutic effect of anticancer drugs in vitro and in vivo distinctly enhanced by intracellular drug release triggered by cytoplasmic GSH.[119] Notably, di-sulphide based poly(ester-amide)s results in effective reversal of drug resistance (ADR) in cancer cells because it exhibits exemplary cell compatibility and effective intracellular drug release (Scheme 1.9).[113]
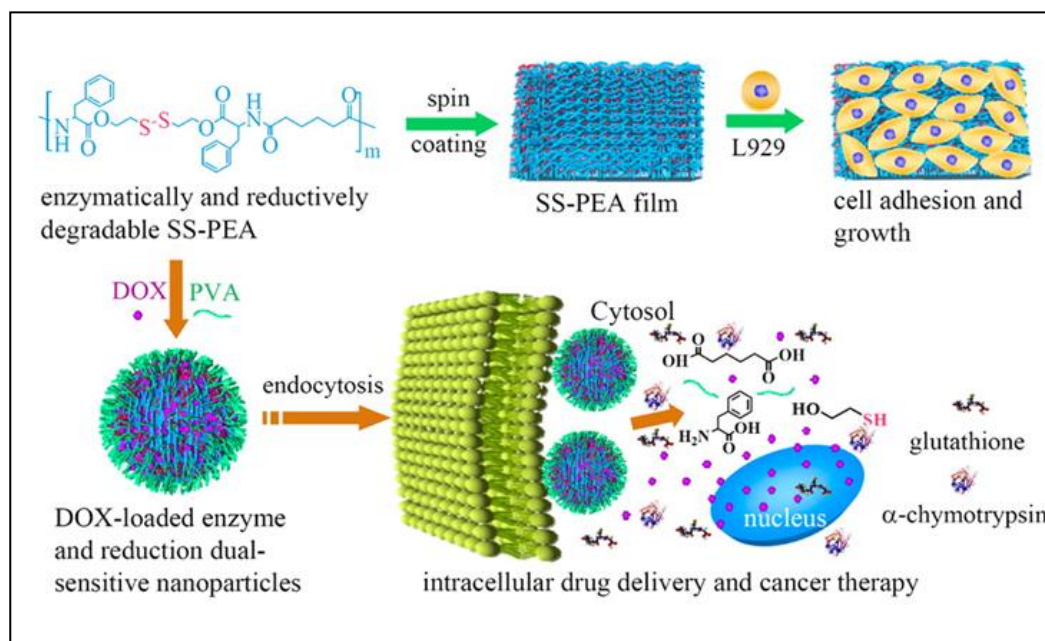
Figure 1.9. Enzymatically and Reductively Degradable SS-PEA Polymer for Cell Culture and Active Intracellular Anticancer Drug Delivery (adopted from Sun et al. *Biomacromolecules,* **2015,** 16, 597-605).

1.8. Polyurethanes and poly(ester-urea)
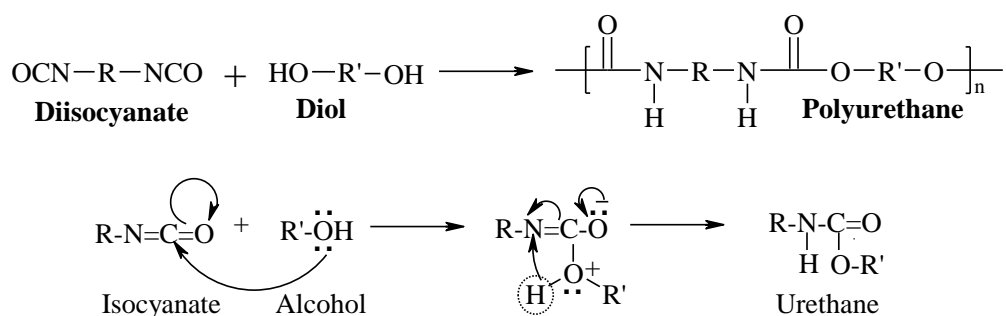
Scheme 1.10. Conventional synthesis of polyurethanes and mechanism of urethane formation (adopted from Bayer et al. *Angew Chem*. **1947**, *59,* 257-272).

Polyurethanes are an essential class of synthetic polymers with major industrial applications constitute flexible and rigid foams, thermoplastic elastomers, adhesives and surface coatings. In 1937, Otto Bayer synthesized polyurethanes and its like polyureas using the most common polyaddition reaction between di-isocyanates and diols (Scheme 1.10) which made a remarkable year in the polyurethane (PU) chemistry.[120] Commonly, Poly(hydroxyl-urethane)s was synthesized by the reaction between bifunctional cyclic carbonates and a diamine (Scheme 1.11).
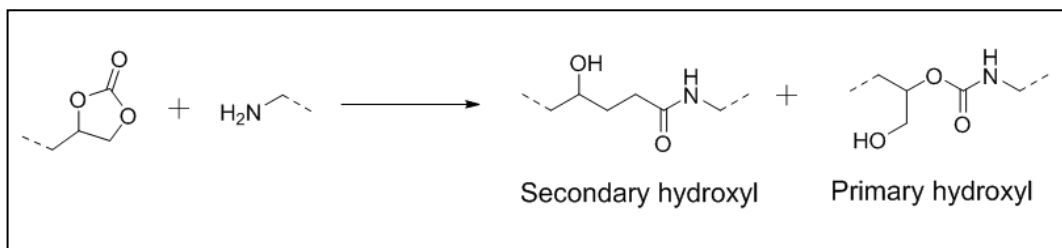
Scheme 1.11. Formation of primary and secondary hydroxyl groups in poly(hydroxyl-urethane)s(adopted from Tomita et al. *Pol. Sci. Part A: Poly. Chem.* **2001**, *39*, 851-859)

Additionally, polyaddition of difunctional alicyclic carbonate (DCHC) and m-xylenediamine(*m*XDA), forms poly(hydroxyl-urethane) (Scheme 1.12).[121]
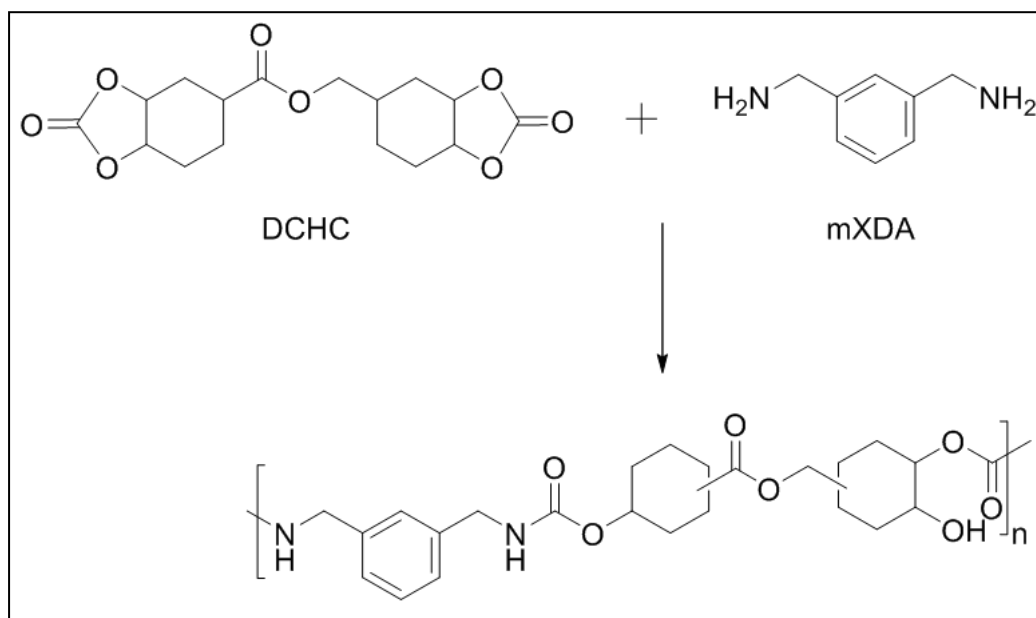
Scheme 1.12. Synthesis of poly(hydroxyl-urethane) (adopted from Takeshi et al. *Polymer bulletin*, **2016**, *73*, 677-685).

Zhong et.al. illustrated synthesis of copolymer of poly(acetal-urethane) i.e. PEG-PAU-PEG triblock copolymers by polycondensation reaction between lysine diisocyanate (LDI) and a diacetal-containing diol, terephthalilidene-bis(trimethylolethane) (TPABTME) followed by thiol-ene click conjugation with thiolated PEG at both ends (Scheme 1.13).[122]
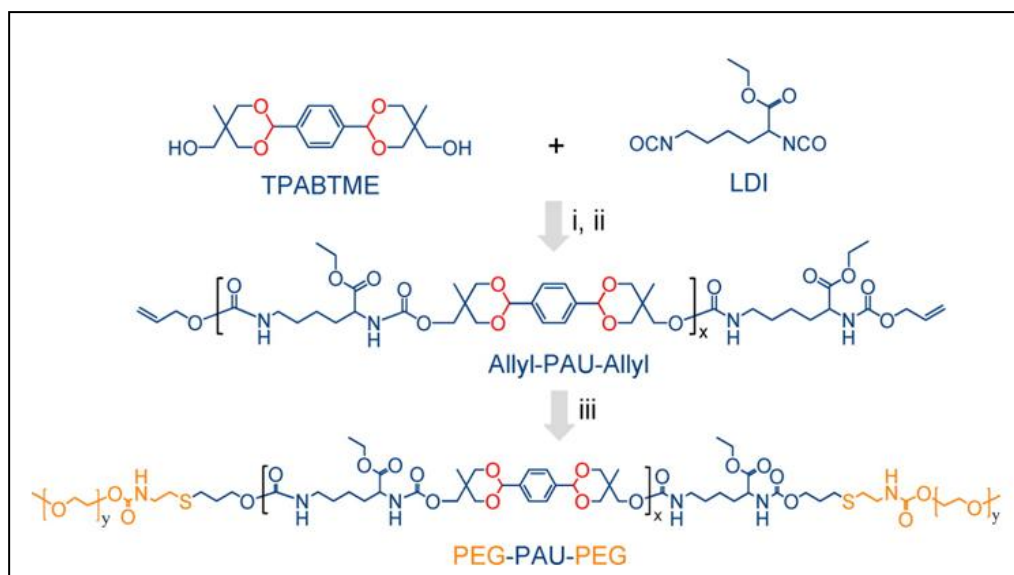
Scheme 1.13. Synthesis of PEG-PAU-PEG (adopted from Zhong et al. *Biomacromolecules*, **2015**, *16,* 2228-2236).

The conditions maintained in the above reaction are i) DBTDL, DMF, 65^0C, 48h;

ii) allyl alcohol, DBTDL, DMF, 65^0C, 12h; iii) PEG-SH, AIBN, 1,4 dioxane, 90^0C, 48h.
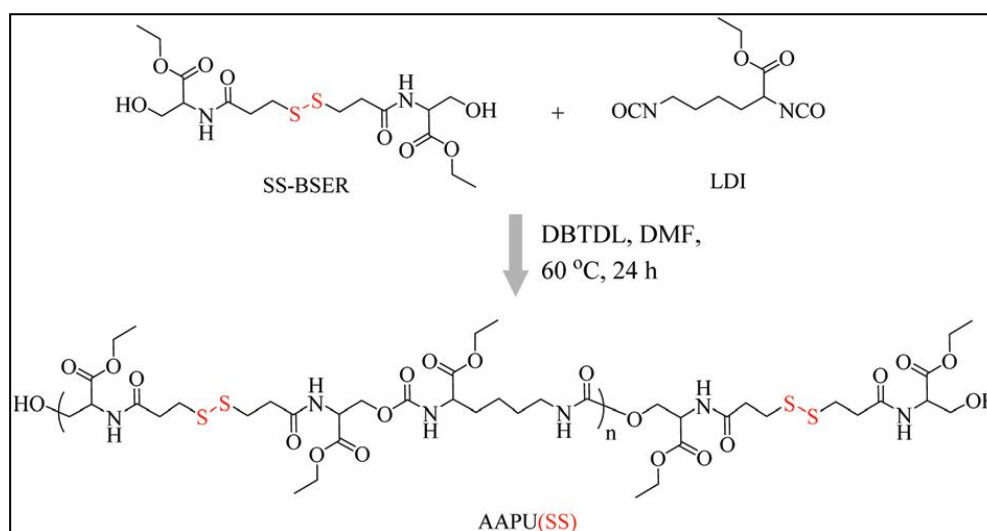
Scheme 1.14. Synthesis of poly(disulphide-urethane)s (adopted from Lu et al. *Polymer Chem.* **2015,** *6*, 6001-6010).

Further, biocompatible and bioreducible poly(disulphide urethane)s denoted as AAPU(SS)s were synthesised by the polycondensation reaction between (SS-BSER) disulphide-linked bis(ethyl L-serinate) and LDI (L-lysine ethyl ester disocyanate) in DMF using DBTDL (di-butyltin dilaurate) as a catalyst (Scheme 1.14).[123] Poly(ester urea)s with α-amino acid is an efficient materials for biomedical applications due to their distinct blood, tissue compatibility, and nontoxic hydrolysis byproducts. Becker et. Al defines the synthesis of L-phenylalanine-based poly(ester urea)s that are strong and biodegradable in nature through two step synthetic interfacial polycondensation approach. During the monomer synthesis, the respective diols (1,6-Hexanediol, 1,8-octanediol, 1,10-decanediol, 1,12-dodecanediol) are reacted with an α-amino acid that is protonated by p-toluenesulfonic acid to prevent amidation and exchange reactions. Afterwards, the diamine synthesis with triphosgene yields the homopolymers followed by polymerization reaction either by interfacial or solution polycondensation to obtain high molecular weight polymers (Scheme 1.15).[124]
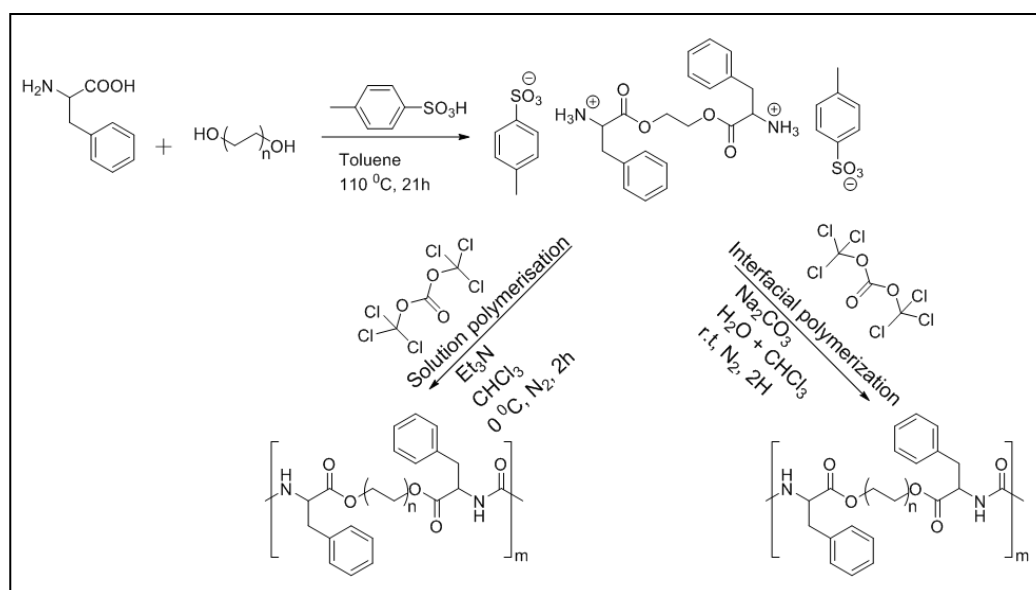
Scheme 1.15. Synthetic route of the L-phenylalanine-based poly(ester urea)s with different chain length of diol (adopted from Becker et al. *Macromolecules*, **2014,** *47,* 121-129).

Polycondensation reaction of AB_2 or A_2B monomers synthesized hyperbranched polyurethane (Scheme 1.16). Also, it can be prepared through in-situ generation of a dihydroxyphenyl isocyanate monomer, by the thermal decomposition of the corresponding carbonyl azide. The synthesized hyperbranched polyurethanes

demonstrates complete solubility in common organic solvents like Tetrahydrofuran (THF), acetone, and dimethylsulfoxide (DMSO).[125]
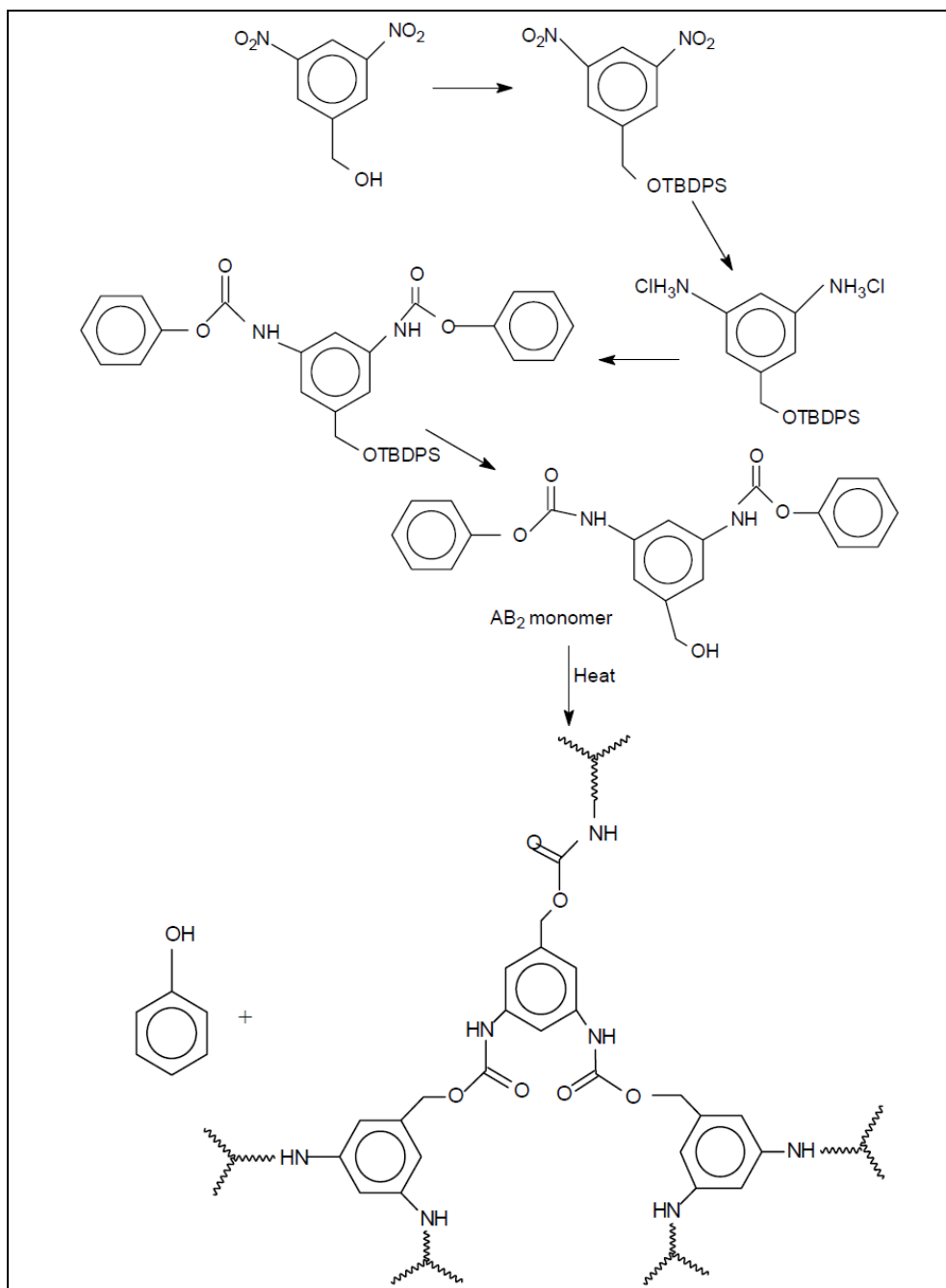
Scheme 1.16. Hyperbranched polyurethane based on AB_2 (adopted from Frechet et al. *Macromolecules*, **1993**, *26*, 4809).

1.9 Polycarbonates based on L-tyrosine

Kohn and co-workers had designed L-tyrosine diphenolic monomers and these monomers were subjected to phosgene assisted solution condensation to make unique classes of L-tyrosine based polycarbonates.[126] Tyrosine derived poly(carbonate)s represent a specific example of pseudo-poly(amino acids). These degradable polymers are derived from the polymerisation of desaminotyrosyl-tyrosine alkyl esters and have significantly improved engineering properties as compared with most conventional poly(amino acids). The monomeric unit for all tyrosine-derived polycarbonates is desaminotyrosyl-tyrosine alkyl ester (DTR), a derivative of naturally occurring tyrosine dipeptide. This Poly(DTE carbonate) has been explored in several biomedical applications, such as sutures, deployable cardiovascular stents, tissue engineering scaffolds for orthopaedic applications, nanospheres for drug delivery, thin film coatings, low or minimally load-bearing orthopaedic implants and also as substrates for the attachment and growth of mammalian cells in tissue culture.[127] Poly(DTE) pins were found to degrade at about the same rate as high molecular weight PLLA pins. To accelerate the degradation rates of the tyrosine derived polycarbonates efforts were made to synthesise the copolymers of DTE with polyethylene glycols such as poly(DTE-co-PEG carbonates) and these polymers were undergone to biodegradation in much higher rate. The hydrophilic PEG provides stable dispersion in aqueous medium and also protects the nanoparticles from protein adsorption and subsequent biological attack.
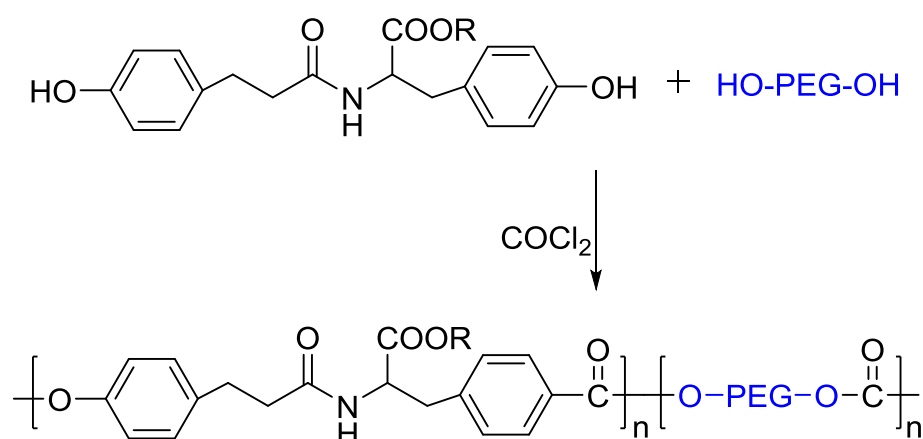
Scheme 1.17. Schematic representation for L-tyrosine polycarbonate copolymerize with PEG (adopted from Chun et al. *Biomaterials*, **1999**, *20*, 253-264).

Tyrosine PEG-derived Poly(ether carbonate) polymer scaffolds also has applications in tissue reconstruction, development of artificial organs, degradable membranes for the prevention of surgical adhesions, and intra arterial coatings for the prevention of thrombosis or restenosis.[128] These advanced applications require biodegradable materials whose physiochemical, chemical, and biological properties can be closely matched to a wide range of narrowly defined, application-specific requirements. So far only polyesters derived from poly(glycolic acid), poly(lactic acid), polydioxanone or various copolymers of these esters were used for the above particular applications because of their synthetic ease and biodegradability. But these polyester materials have some disadvantages such as releasing of acidic degradation products, and they are relatively rigid, inflexible materials. This can be a definite disadvantage when mechanical compliance with soft tissue or blood vessels are required. To overcome this difficulty Kohn and co-workers has developed a Turosine-PEG –derived poly(ether carbonate) by polymerising the tyrosine-derived diphenolic monomers with polyethylene glycols. These polycarbonates have been found to be tissue compatible, strong, tough, and degrade slowly under physiological conditions. These materials are most suitable for use in orthopaedic implants.
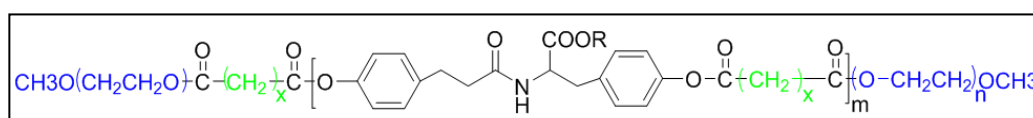
Scheme 1.18. Schematic representation for L-tyrosine triblock polycarbonates copolymerize with PEG and aliphatic diols. (adopted from Sheihet et al. *Biomacromolecules*, 2007, *8*, 998-1003).

These tyrosine derived polycarbonates also explo9red for hydrophobic drug delivery applications by making the triblock copolymers with desaminotyrosyl-tyrosine alkyl ester and PEG and various hydrophodic diols.[129] These polymeric nanoparticles can overcome the obstacle of poor bioavailability of the drug. These nanoparticles can be designed to provide stable dispersions of hydrophobic drugs with low cytotoxicity, thus making them attractive alternatives to less mechanically stable liposomes or more cytotoxic surfactant dispersant systems.

1.10 Poly (α-hydroxy acids)

Poly (α-hydroxy acids) (PAHAs) include poly(lactide), poly(glycolide), and poly(lactide-co-glycolide) are a class of biocompatible and biodegradable polymers. It has been extensively consumed for a variety of biomedical and pharmaceutical applications like restorable sutures and implants, drug delivery, and tissue engineering.[130] Preparations of PAHAs are commonly through two synthetic approaches; one is direct polycondensation of the α-hydroxy acids (Scheme 1.19). This methodology leads to low molecular weight (MW) PAHAs due to the cyclization side reactions. Moreover, for the polymer synthesis, long reaction times and high temperatures are usually recommended which prior to various undesired side reactions.[131]
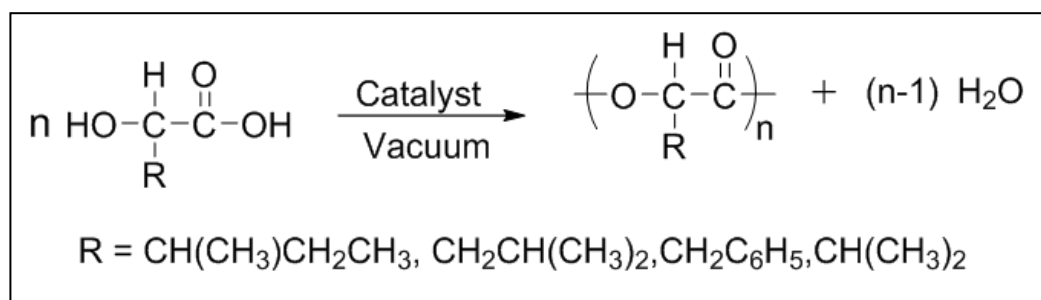
Scheme 1.19. Direct condensation of the α-hydroxy acids (adopted from Naomi et al. *Polymers,* **2010**, *2*, 418-439).

The other approach is ROP of cyclic polymerizable monomers derived from α-hydroxy acids. In this method, diazotisation of functional α-amino acids with sodium nitrite leads to functional α-hydroxy acids (AHAs). Following this, the addition of diphosgene with AHAs results in the synthesis of functional O-carboxyanhydrides (OCAs) which further subjected to controlled ring opening polymerization (ROP) to develop poly(α-hydroxy acids). This mode leads to high MW PAHAs with low dispersity, and well controlled molecular and structural characterstics under mild conditions (Scheme 1.20).[132] Additionally, various catalytic systems have been prepared, such as metal complexes, organic catalysts, and enzymes, to determine controlled ROP of α-hydroxy acid derived cyclic monomers. In 1980s, Kricheldorf prepare homo and co-polymers of lactic acid by employing L-lactic acid O-

carboxyanhydride (L-lac-OCA) as a readily available and highly polymerizable monomer.[133]
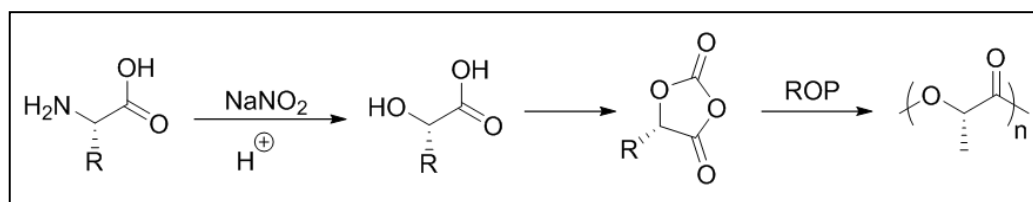
Scheme 1.20. Synthesis of PAHAs via controlled ROP of OCAs (adopted from Cheng et al. *Acc. Chem. Res.* **2015**, *48,* 1777-1787).

Furthermore, Bourissou group attains great improvement to prepare PLA with organocatalytic ROP of Lac-OCA having controlled MW and narrow polydispersity under comparatively mild polymerization conditions.[134]
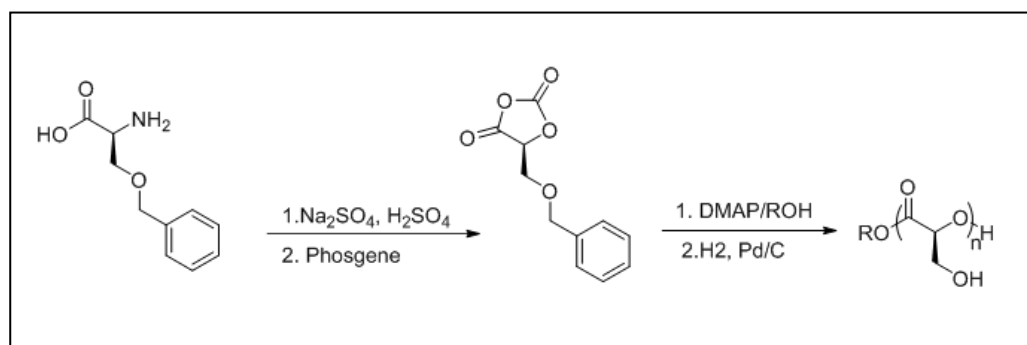
Scheme 1.21. Synthesis of water soluble Poly (α-hydroxy acids) from ROP of O-benzyl-L-serine carboxyanhydrides (adopted from Cheng et al. *ACS Macro Lett.* **2017**, *4,* 441-444).

Recently, Cheng et al. described the design and synthesis of O-benzyl-L-serine carboxyanhydride (Ser(Bn)-OCA) derived from serine (Scheme 1.21). In this report, diazotisation of O-benzyl-L-serine with sodium nitrite in aqueous sulfuric acid solution followed by cyclization of the resulting serine-based α-hydroxy acid with phosgene synthesizes *O*-benzyl-L-serine carboxyanhydrides, which further undergo living ring-opening polymerization, followed by removal of the benzyl group under mild conditions to prepare serine-poly(α-hydroxy acids) (Ser-PAHA). The degradable, water soluble poly (α-hydroxy acids) demonstrates excellent cell compatibility and applicable as novel materials in constructing drug delivery systems and as hydrogel scaffolds for tissue engineering applications.[135]

1.11. Melt Polycondensation Approach for L-Amino acid Polymers:

From our laboratory Anantharaj et al. had developed a new solvent free melt polycondensation approach for the synthesis of aminoacid based poly(ester-urethane)s. In this new process, amino acids were readily converted into dual ester-urethane monomers and polycondensed with diols under melt conditions to produce high molecular weight polymers[136] (see figure 1.12). The novelty of this new process lies in a fact that the aromatic polyurethanes do not have sufficient thermal stability and undergo degradation below 130 °C, due to this restriction the catalyst assisted melt polycondensation reactions reported for polyester synthesis cannot be expanded to polyurethanes. As a result there is no melt polycondensation synthetic methodology reported to create ester and urethane linkages simultaneously in one-pot to make new classes of poly(ester-urethane)s.
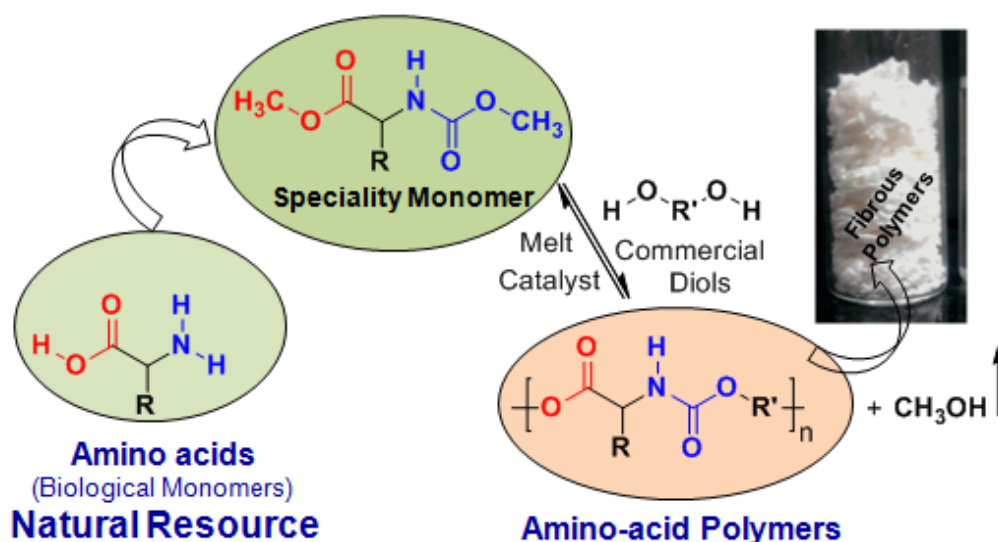
Figure 1.12. Schematic representation of trans ester-urethne melt polycondensation polymerisation process (adopted from Anantharaj et al. *Biomacromolecules*, **2012**, *13,* 2446-2455).

From our group earlier deepa et al. has reported solvent free melt trans urethane polycondensation[137] process for fully aliphatic polyurethanes that were thermally stable up to 250 °C. in this process a diurethane monomer (made from commercial diamine) was polycondensed with diols in presence of 1 mol % Ti-catalyst to yield high molecular weight polyurethanes. This provided new opportunities to make new classes of poly(ester-urethane)s in a single polycondensation process by merging the melt trans esterification process (known for polyester) with melt trans urethane process (from our laboratory). For this purpose

natural L-amino acids were choosen as raw materials and the dual ester-urethane polycondensation chemistry was developed to make amino acid based poly(ester-urethane)s. The effect of the catalyst, polymerization temperature and repeating unit structure on the molecular weight of the polymers and their thermal properties were also investigated. The self organization behaviors of these polymers were studied by CD spectroscopy in organic solvents and the role of amino acid structure on polymer thermal properties were studied by differential scanning calorimetry.

Further the role of temperature and catalyst on chemoselective polymerization was investigated for amino acid monomers to produce diverse macromolecular structures such as linear poly(ester-urethane)s, functional polyesters, A-B diblocks and A-B-A triblocks[138] (figure 1.13). Amino acids were converted into carboxylic ester and urethane dual functional monomers in which the ester part acted as low temperature site for chemoselective reaction towards alcohols. Under this reaction condition; the urethane (or carbamate) part of the monomer unit was completley inert towards alcohol whereas at higher temperature both ester and urethane reacts with alcohol. The influence of catalyst on the process was investigated by choosing wide ranges of catalysis from alkali, alkali earth metal, transition metal and lanthanide series belonging to oxides, nitrates, chloride, acetates, acetylacetonate and alkoxides.
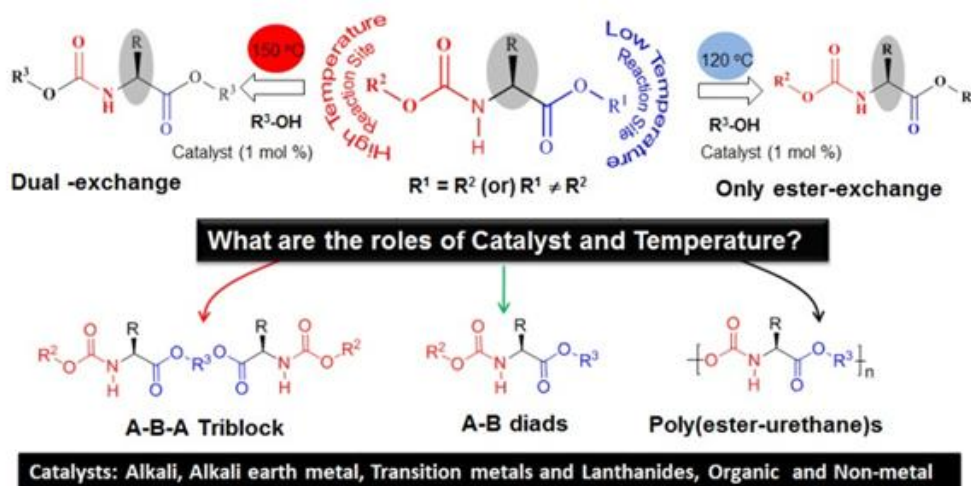
Figure 1.13. Development of poly(ester-urethane)s using various catalysts via melt polycondensation process (adopted from Anantharaj et al. *J. Polym. Sci. Part A: Polym. Chem.* **2016**, *54,* 1065-1077).

Functional polyesters form L-Aspartic acid and L-Glutamic acid was developed by melt condensation process and their self organisation studies has carried out. These L-amino acid polymers underwent reversible self-organization from

amyloid-like fibrils to collapsed coil-like spherical structures. The newly designed synthetic polyester self-assembled through β-sheet hydrogen bonding interactions to produce amyloid-like fibrils consisting of hierarchical double helical structures.
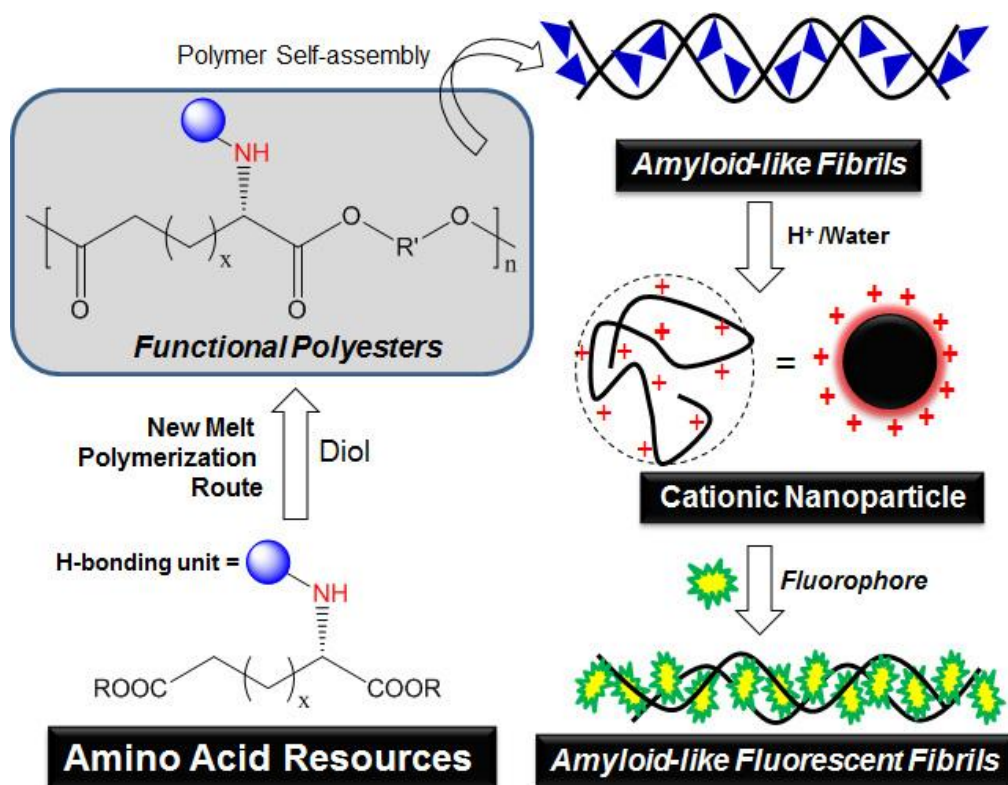
Figure 1.14. Schematic representation for the synthesis of functional poly esters and their self-assembly characteristics. (adopted from Anantharaj et al. *Biomacromolecules*, **2015**, *16,* 1009-10020).

Upon de-protection, the amyloid fibrils underwent coil-like conformational change to produce cationic spherical nano-particles in aqueous medium[139](figure 1.14). Reversible conformational change from the spherical species to expanded fibril structures was achieved via fluorophore substitution. The size and shape of the amyloid fibrils and spherical assemblies were studied by dynamic light scattering, water contact angle measurements, Zeta potential, electron and atomic force microscopes, etc.

This methodology was further explored to synthesize disulfide linkage containing redox degradable polymeric materials. For this purpose, L-cystine was chosen and it was suitably converted into multi-purpose monomer. The amine functionality in L-cystine was converted into Boc urethane which act as β-sheet

hydrogen bonding vector for seeding amyloid-fibril and also as cationic resources upon de-protection into $-NH_3^+X^-$ polymeric salts[140] (figure 1.15).
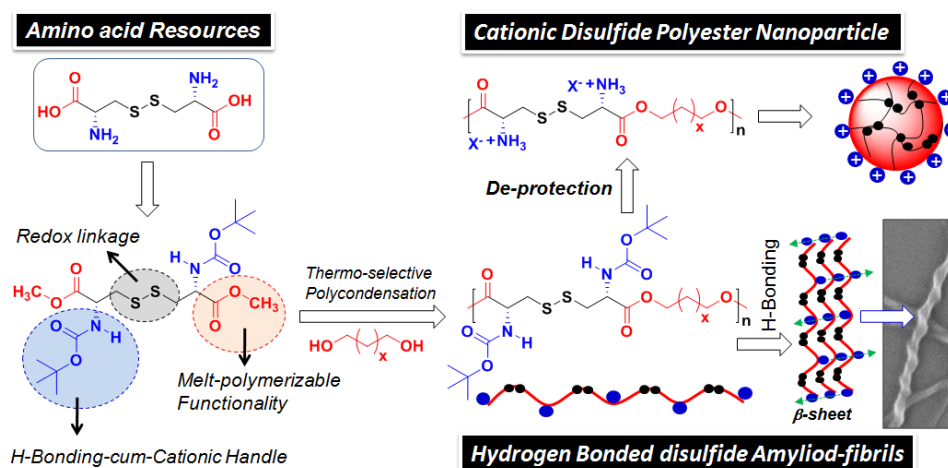
Figure 1.15. Redox-degradable amyloid-like disulfide polyesters and cationic polyester nanoparticles based on L-cystine via melt polycondensation (adopted from Anantharaj et al. *J. Polym. Sci. Part A: Polym. Chem.* **2016**, *54*, 2864-2875).

The dicarboxylic acids were converted into methyl esters which have capabilities to undergo thermo-selective melt polymerization to produce disulfide linkage containing linear polyesters. The disulfide linkage in the polyester backbone is redox degradable; thus, the polymers can be degraded into their monomer species.
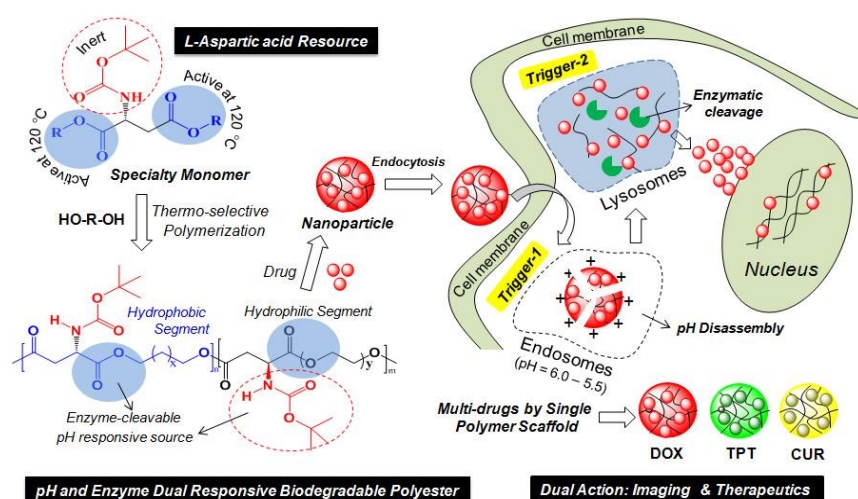
Figure 1.16. Schematic representation of pH and enzyme responsive polymer nano-assemblies from L-aspartic acid (adopted from Sonashree et al. *J. Polym. Sci. Part A: Polym. Chem.* **2016**, *54,* 3279-3296).

Recently Sonashree et al. from our laboratory has developed new pH and enzyme responsive nanocarriers based on L-Aspartic acid was developed for multiple

anticancer drug delivery to cancer cells. L-Aspartic acid monomer was copolymerized with hydrophilic triethylene glycol to produce amphiphilic polyesters. Self-assembly characteristics of these amphiphilic polyesters were investigated in aqueous medium, characterized by DLS and microscopic techniques. These nanoparticles were capable of loading anticancer drugs such as Camptothecin, Doxorubicin and Curcumin. Cytotoxicity and cellular internalization of these drug loaded nanoparticles were investigated in cervical cancer cell lines (HeLa) and breast cancer cell lines (MCF 7) and the results were showed that these polymer nanoparticles could deliver the drugs into intracellular environments[141] (figure 1.16).

This new melt polycondensation polymerization process is not utilized to multifunctional amino acids. In this thesis we have explored this new methodology to multifunctional amino acids such as L and D-Serine, L-Threonine and L-Tyrosine. By using this methodology we have developed new classes of linear polyesters and hyperbranched poly(ester-urethane)s in a one-pot reaction by altering the temperature of the polymerization. Further this methodology also explored to synthesize amphiphilic poly(ester-urethane)s with stimuli responsiveness for Drug delivery applications. These amphiphilic poly(ester-urethane)s were synthesized by polymerizing L-amino acid monomers with hydrophilic polyethylene glycols. These polymers could self-assembled in to polymeric nanoparticles in the aqueous medium and they able to load the anti cancer drugs such as CPT and DOX. Further enzyme and thermal dual responsive poly(ester-urethane)s were also developed and their self-assembly characteristics and anti cancer drug loading, releasing capabilities has studied. Cytotoxicity and cellular internalization of these drug loaded polymer nanoparticles was studied in normal cell lines (WT-MEFs), and cancer cell lines (MCF 7, and HeLa).

Thus the design and development of new polymer architectures, and stimuli responsive polymer nano-carriers by solvent free melt polycondensation is a significant outcome in the class of synthetic biodegradable polymeric materials. The polymers prepared via melt polycondensation approach are particularly important since they are devoid of solvent impurities and directly processed for thermoplastic engineering as well as biomedical devices in high purity. Further, these new classes of polymers were not explored in drug delivery applications (other than the one reports from our laboratory by Sonashree et al.). Hence, the exploration new synthetic polymers based on multi-functional L-amino acids would bring appropriate solubility

and functionality for drug/genre delivery applications of melt polycondensation polymers for applications in cancer treatment.

1.11. Aim of the Thesis work

L-Amino acid based synthetic linear polymers, block and graft copolymers are typically achieved through N-carboxylanhydride mediated ring opening polymerization (ROP) methodology. Polycondensation approaches are versatile to make wide ranges of polymers such as polyesters, polyurethanes and polyesters, etc. Unfortunately, the polycondensation routes are very rarely employed to natural resources such as L-amino acids to explore their full potential for biomedical as well as thermoplastics industry. Thus, the large abundant of natural L-amino acid resources are still one of the un-tapped area in biomedical research especially in drug delivery applications. For the past few years, our group are engaged in developing new melt polycondensation approach for L-amino acid resources to look at new functional
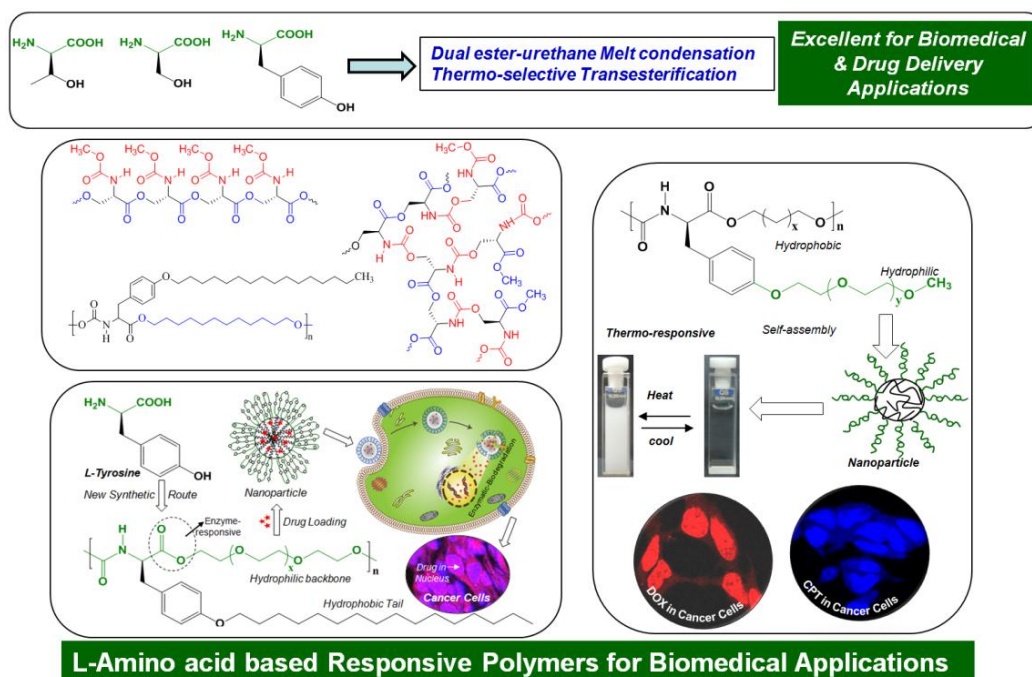
Figure 1.17. Designing new classes of Poly(ester-urethane)s and employ their enzyme responsive, enzyme and thermal dual responsive nanoparticles as multiple anticancer drug delivery vehicles in cancer cells.

polyesters and poly(ester-urethane)s[136-141]. This methodology is required to be expanded to multi-functional L-amino acids so that their structure can be optimized to self-assemble them in aqueous medium for drug delivery applications.

To accomplish this goal, the thesis work is aimed to develop new classes of L-tyrosine amphiphilic poly(ester-urethanes)s under solvent free melt polycondensation process and employed their self-assembled nanoparticles as enzyme-responsive nano-carriers for multiple drug delivery in cancer treatment. L-Tyrosine is very unique an amino acid having phenolic functionality in addition to amine and carboxylic units at the α-carbon. Further, the synthetic approach is also expanded to other amino acids such as L-serine and L-threonine to make new classes of linear and hyperbranched polymers. L-Tyrosine based polymer nano-carriers were developed for drug delivery in cancer cells for the first time. Both the synthetic methodology and the polymer structures are new entities in the literature and they are useful for many applications in biomedical and thermoplastic industries. The polymers were made through solvent free melt polycondensation process; thus, both the drug delivery concept and the new L-tyrosine polymers are new entries for biomaterial applications. This research contribution and outcome of the investigation in the thesis is urgently required for the long-term application for biodegradable and sustainable polymer scaffolds based on L-amino acids in cancer treatment.

References

1. Vidyasagar, A.; *ACS Global Cancer facts and figures* (2ndedn) **2011.**

2. Rothenberg, M. L.; Carbone, D.P.; Johnson, D. H. *Nat. Rev. Cancer* **2003**, *3*, 303-309.

3. Uhrich, K. E.; Cannizzaro, S. M.; Langer, R.; Shakesheff, K. M. *Chem. Rev.* **1999**, *99*, 3181-3198.

4. Kost, J.; Langer, R. S. *Adv. Drug Deliv. Rev.* **2012**, *64,* 327-341.

5. Kim, S.; Kim, J.-H.; Jeon, O.; Kwon, I. C.; Park, K. *Eur. J. Pharm. Biopharm.* **2009**, *71*, 420-430.

6. Cho, K.; Wang, X.; Nie, S.; Chen, Z.; Shin, D. M. *Clin. Cancer Res.* **2008**, *14,* 1310-1316.

7. Strebhardt, K; Ulrich, A. *Nat. Rev. Cancer.* **2008**, *8*, 473-480.

8. Sun, T.; Zhang, Y. S.; Pang, P.; Hyun, D. C.; Yang, M.; Xia, Y. *Angew. Chem. Int. Ed.***2014**, *53*, 12320-12364.

9. Maruyama, K.; Ishida, O.; Takizawa, T.;Moribe, K.*Adv. Drug Deliv. Rev.***1999**, *40*, 89-102.

10. Peer, D.; Karp, J. M.; Hong, S.; Farokhzad, O. C.; Margalit, R.; Langer, R. *Nat. Nanotechnol.***2007**, *2*, 751-760.

11. Haag, R.; Kratz, F. *Angew. Chem. Int. Ed.***2006**, *45*, 1198-1215.

12. Singh, R.; Lillard Jr, J. W. *Exp. Mol. Pathol.* **2009**, *86*, 215-223.

13. Adair, J. H.; Parette, M. P.; Altınoglu, E. I.; Kester, M. *ACS Nano* **2010**, *4*, 4967-4970.

14. Fang, J.; Nakamura, H.; Maeda, H. *Adv. Drug Deliv. Rev.***2011**, *63*, 136-151.

15. Hobbs, S. K.; Monsky, W. L.; Yuan, F.; Roberts, W. G.; Griffith, L.; Torchilin, V. P.; Jain, R. K. *Proc. Natl. Acad. Sci.***1998**, *95*, 4607-4612.

16. Gu,F. X.; Karnik, R.; Wang, A. Z.; Alexis, F.; Levy-Nissenbaum, E.; Hong, S.; Langer, R. S. *Nano Today,* **2007**, *2*, 14-21.

17. Maeda, H. *Bioconjugate Chem.***2010**, *21*, 797-802.

18. Matsumura, Y.; Maeda, H. *Cancer Res.***1986**, *46,* 6387-6392.

19. Wang, Y.; Gao, S.; Ye, W.H.; Yoon, H.S.; Yang, Y.Y., *Nature Mat.***2006**, *5*, 791-796.

20. Kuma, R.; Chen, M.H.; Parmer, V.S.; Samuelson, L.A.; Kumar, J.; Nicolosi, R.; Yoganathan, S.; Watterson, A.C., *Journal of Am. Chem. Soc.***2004**, *126*, 10640-10644.

21. Bertrand, N.; Wu, J.; Xu, X.; Kamaly, N.; Farokhzad, O. C. *Adv. Drug Deliv. Rev.***2014**, *66*, 2-25.

22. Brigger, I. Dubernet, C.; Couvreur, P. *Adv. Drug Deliv. Rev.* **2002**, *54*, 631-651.

23. Ferrari, M. J. *Nat. Rev. Cancer,* **2005**, *5*, 161-171.

24. Sykes, E. A.; Chen, J.; Zheng, G.; Chan, W. C. W. *ACS Nano***2014**, *8*, 5696-5706.

25. Marcucci, F.; Lefoulon, F. *Drug Discov. Today***2004**, *9*, 219-228.

26. Moghimi, M. S.; Hunter, A. C.; Murray, J. C. *Pharmocol. Rev.***2001**, *53*, 283-318.

27. Choi, K. Y.; Chung, H.; Min, K. H.; Yoon, H. Y.; Kim, K.; Park, J. H.; Kwon, I. C.; Jeong, S. Y.*Biomaterials,* **2010**, *31*, 106-114.

28. Torchilin, V. P. *Nat. Rev.DrugDiscov.***2005**, *4*, 145-160.

29. Byrne, J. D.; Betancourt, T.; Brannon-Peppas, L.*Adv. Drug Deliv. Rev.***2008**, 60, 1615-1626.

30. Chang, S.H; Gardella, J.A. *Chem. Rev*. **2005**, *105*, 4205-4232.

31. Deming, T. J. *ProgPolym Sci.,* **2007**, *32*, 858–875.

32. Gomes, S.; Leonor, I. B; Mano, J. F.; Reis, R. L.; Kaplan, D. L. *ProgPolym Sci.,* **2012**, *37*, 1-17.

33. Ikeda, M. *AdvBiochemEngBiotechnol***2003**, *79*, 1-35.

34. Latif, S; Anwar, F; Hussain, A. I; Shahid, M. *European Journal of Lipid Science and Technology*, **2011,***113*, 1012-1018.

35. Hanmoungjai, P; Pyle, D.L; Niranjan, K. *Journal of Chemical Technology andBiotechnology,* **2002,***77*, 771-776.

36. Wang, M; Hettiarachchy, N.S; Qi, M; Burks, W; Siebenmorgen, T. *Journal of Agricultural and Food Chemistry,* **1999**, *47*, 411-416.

37. Hamada, J.S. *Journal of Food Biochemistry*, **1999**, *23*, 307-321.

38. Yacoubou J. Information about L-cysteine. http://www.vrg.org/blog/2013/04/22/information-about-l-cysteine/ [Accessed May 11, 2017].

39. Yacoubou, J. http://www.vrg.org/blog/?s=leucine [Accessed May 11, 2017].

40. Ault, A. *J Chem Educ*. **2004**, *81*, 347-355.

41. Le Nôtre, J; Scott, E.L; Franssen, M.C.R; Sanders, J.P.M. *Green Chem*. **2011,** *13*, 807-809.

42. Ajinomoto. Glycine. http://www.ajiaminoscience.com/products/manufactured_products/lamino_acids/glycine.aspx [Accessed May 11, 2017]

43. Adisseo. The complex process of manufacturing methionine. http://www.allaboutfeed.net/Processing/General/2011/10/The-complex-process-ofmanufacturing-methionine-AAF012677W/ [Accessed May 11, 2017]

44. Breuer, M.; Ditrich, K.; Habicher, T.; Hauer, B.; Kebeler, M.; Sturmer, R.; Zelinski, T. *Angew. Chem. Int. Ed.* **2004**, *43*, 788-824.

45. Yamada, S.; Nabe, K.; Izuo, N. *Appl. Environ. Microbiol*. **1981**, *42*, 773-778.

46. Kinoshita, S; Udaka, S; Shimono, M. *J Gen ApplMicrobiol.***2004**, *50*, 331-343.

47. Leuchtenberger, W; Huthmacher, K; Drauz, K. *ApplMicrobiolBiotechnol.* **2005,** *69*, 1-8.

48. Sugimoto, M, Flickinger, M.C. *John Wiley & Sons, Inc*. **2009**.

49. Ulijn, R.V; Smith, A.M. *Chem. Soc. Rev*. **2008**, *37*, 664-675.

50. Mazza, M; Gaisford, S; Mccarthy, D; Schatzein, A.G; Uchegbau, I.F. *Polymer and Soft nanotechnology*, **2011**, *6*, 650-653.

51. Zhang, S.G; Marini, D.M; Hwang, W; Santoso, S. *Curr. Opin. Chem. Biol*. **2002**, *6,* 865-871.

52. Zhang, S; Holmes, T; Lockshin, C; Rich, A. *Proc. Nat. Acad. Sci*. U.S.A. **1993**, *90*, 3334-3338.

53. Liu, L; Xu, K; Wang, H; Tan, P.K; Fan, W; Venkatraman, S.S; Li, L; Yang, Y.Y. *Nature Nanotechnol*. **2009**, *4*, 457-463.

54. Cui, H; Webber, M.J; Stupp, S.I. *Biopolymers*, **2010**, *94*, 1-8.

55. Paramonov, S.E; Jun, H.W; Hartgerink, J.D. *J. Am. Chem. Soc.,* **2006**, *128*, 7291-7298.

56. Lalatsa, A; Lee, V; Zloh, M; Schatzlein, A; Uchegbu, I. Mol. Pharm. 2012, Mol. Pharm. 2012, 6, 1665- 1680.

57. Reches, M; Gazit, E. *Science*, **2003**, *300*, 625-627.

58. Reches, M; Gazit, E. *Nat. Nanotechnol*. **2006**, *1*, 195-200.

59. Jayawarna, V; Smith, A; Gough, J.E; Ulijn, R.V. *Biochem. Soc. Trans*. **2007**, *35*, 535-537.

60. Webber, M.J; Kessler, J.A; Stupp, S.I. *J. Intern. Med*. **2010**, *267*, 71-88.

61. Standley, S.M; Toft, D.J; Cheng, H; Soukasene, S; Chen, J; Raja, S.M; Band, V; Band, H; Cryns, V.L; Stupp, S.I. *Cancer Res*. **2010**, *70*, 3020-3026.

62. Von Maltzahn, G; Vauthey, S; Santoso, S; Zhang, S. *Langmuir*, **2003**, *19*, 4332-4337.

63. Keller, S; Sauer, I; Strauss, H; Gast, K; Dathe, M; Bienert, M. Angew. Chem. Int. Ed. 2005, 44, 5252-5255.

64. Wiradharma, N; Tong, Y.W; Yang, Y.Y. *Biomaterials*, **2009**, *30*, 3100-3109.

65. Chu-Kung, A.F; Bozzelli, K.N; Lockwood, N.A; Haseman, J.R; Mayo, K.H; Tirrell, M.V. *Bioconjug. Chem*. **2004**, *15*, 530-535.

66. Guo, K.; Chu, C. C. *Biomaterials* **2007**, *28*, 3284−3294.

67. Wu, J.; Wu, D.; Mutschler, M. A.; Chu, C. C. *Adv. Funct. Mater*.**2012**, 22, 3815−3823.

68. He, M; Potuck, A; Kohn, J.C; Fung, K; Reinhart-King, C.A; Chu, C. C. *Biomacromolecules* **2016**, *17*, 523-537.

69. Edwards, D. A.; Hanes, J.; Caponetti, G.; Hrkach, J.; Ben-Jebria, A.; Eskew, M. L.; Mintzes, J.; Deaver, D.; Lotan, N.; Langer, R. *Science* **1997**, *276,* 1868–1872.

70. Barbato, F.; Rotonda, M. I. L.; Maglio, G.; Palumbo, R.; Quaglia, F. *Biomaterials* **2001**, *22*, 1371–1378.

71. Zhou, Y. X.; Li, S. L.; Fu, H. L.; Cheng, S. X.; Zhang, X. Z.; Zhuo, R. X. *Colloids Surf., B* **2008**, *61*, 164–169.

72. Hindi, K. M.; Ditto, A. J.; Panzner, M. J.; Medvetz, D. A.; Han, D. S.; Hovis, C. E.; Hilliard, J. K.; Taylor, J. B.; Yun, Y. H.; Cannon, C. L.;Youngs, W. J. *Biomaterials* **2009**, *30,* 3771–3779.

73. Pascual-Gil, S.; Garbayo, E.; Díaz-Herráez, P.; Prosper, F.; Blanco-Prieto, M. J. *J. Controlled Release* **2015**, *203*, 23−38.

74. Du, Y. F.; Chen, W.; Zheng, M.; Meng, F. H.; Zhong, Z. Y. *Biomaterials* **2012,** *33*, 7291−7299.

75. Gu, Y. D.; Zhong, Y. N.; Meng, F. H.; Cheng, R.; Deng, C.; Zhong, Z. Y. *Biomacromolecules* **2013,** *14*, 2772−2780.

76. Huang, F; Cheng, R; Meng, F; Deng, C; Zhong, Z. *Biomacromolecules* **2015**, *16,* 2228-2236.

77. Deming, T. J. *Prog. Polym. Sci.* **2007**, *32*, 858-875.

78. Kricheldorf, H. R. *Angew. Chem. Int. Ed.* **2006**, *45*, 5752-5784.

79. Hadjichristidis, N; Iatrou, H; Pitsikalis, M; Sakellariou, G. *Chem.Rev.* **2009**, *109*, 5528-5578.

80. Dimitrov, I; Schlaad, H. *Chem. Commun.* **2003**, 2944-2945.

81. Lutz, J. F; Schutt, D; Kubowicz, S. *Macromol. Rapid Commun.* **2005**, *26*, 23-28.

82. Lu, H; Cheng, J. *J. Am. Chem. Soc.* **2007**, *129*, 14114-14115.

83. Deming, T. J. *Nature* **1997**, *390*, 386-389.

84. Bae, Y; Kataoka, K. *Adv. Drug Delivery Rev.* **2009**, *61*, 768-784.

85. Deng, C; Rong, G; Tian, H; Tang, Z; Chen, X; Jing, X. *Polymer* **2005**, *46*, 653-659.

86. Deng, C; Tian, H; Zhang, P; Sun, J; Chen, X; Jing, X. *Biomacromolecules,* **2006**, *7* , 590-596.

87. Deng, C; Chen, X; Yu, H; Sun, J; Lu, T; Jing, X. *Polymer* **2007**, *48*, 139.

88. Deng, C; Chen, X; Sun, J; Lu, T; Wang, W; Jing, X. *J. Polym. Sci. Part A: Polym. Chem.* **2007**, *45*, 3218-3230.

89. Rong, G; Deng, M; Deng, C; Tang, Z; Piao, L; Chen, X; Jing X. *Biomacromolecules* **2003**, *4*, 1800-1804.

90. Deng, M; Wang, R; Rong, G; Sun, J; Zhang, X; Chen, X; Jing, X. *Biomaterials* **2004**, *25*, 3553-3558.

91. Lee, E.S; Shin, H.J; Na, K; Bae, Y.H. *J. Controlled Release* **2003**, *90*, 363-374.

92. Aliabadi, H.M; Lavasanifar, A. *Expert Opin. Drug Delivery* **2006**, *3*,139.

93. Wang, Y; Brown, P; Xia, Y. *Nat. Mater.* **2011**, *10*, 482-483.

94. Xia, Y. *Nat. Mater.* **2008**, *7*, 758-760.

95. Carlsen, A; Lecommandoux, S. *Curr. Opin. Colloid Interface Sci.* **2009**, *14*, 329-339.

96. Schlaad, H. *Adv. Polym. Sci.* **2006**, *202*, 53-73.

97. Disher, D.E; Eisenberg, A. *Science* **2002**, *297*, 967-973.

98. Du, J; O'Reilly, R.K. *Soft Mater* **2009**, *5*, 3544-3561.

99. Disher, B.M; Won, Y; Ege, D.S; Lee, J.C; Bates, F.S; Disher, D.E; Hammer, D.A. *Science* **1999**, *284*, 1143-1146.

100. Kabanov, A.V; Vinogradov, S.V. *Angew. Chem. Int. Ed.* **2009**, *48,* 5418 -5429.

101. Hendrickson, G.R; Smith, M.H; South, A.B; Lyon, L.A. *Adv. Funct. Mater.* **2010**, *20*, 1697-1712.

102. Qiu, Y; Park, K. *Advanced Drug Delivery Reviews*, **2001**, 53, 321-339.

103. Ma, G. *Journal of Controlled Release,* **2014**, *193*, 324-340.

104. Kobsa, S; Saltzman, W.M. *Pediatric Research*, **2008**, *63*, 513-519.

105. Drury, J.L; Mooney, D.J. (2003) *Biomaterials*, **2003**, *24,* 4337-4351.

106. Slaughter, B.V; Khurshid, S.S; Fisher, O.Z; Khademhosseini, A; Peppas, N.A. *Advanced Materials,* **2009,** *21,* 3307-3329.

107. Barrera, D. A.; Zylstra, E.; Lansbury, P. T.; Langer, R. *J. Am.Chem. Soc.* **1993,** *115*, 11010–11011.

108. Feng, Y.; Guo, J. *Int. J. Mol. Sci. Mol. Sci.* **2009**, *10*, 589-615.

109. Hartwig, W.; Schoellkopf, U. *Liebigs Ann. Chem.* **1982**, *1982*, 1952-1970.

110. Kardassis, G.; Brungs, P.; Nothhelfer, C.; Steckhan, E. *Tetrahedron* **1998**, *54*, 3479-3488.

111. Montané, J.; Armelin, E.; Asín, L.; Rodríguez-Galán, A.; Puiggalí, J. *J. Appl. Polym. Sci.* **2002**, *85*, 1815-1824.

112. Asín, L.; Armelin, E.; Montané, J.; Rodríguez-Galán, A.; Puiggalí, J. *J. Polym. Sci. A Polym. Chem.* **2001**, *39*, 4283-4293.

113. Sun, H; Cheng, R; Deng, C; Meng, F; Dias, A.A; Hendriks, M; Feijen, J; Zhong, Z. *Biomacromolecules,* **2015**, *16*, 597-605.

114. Fonseca, A.C.; Gil, M.H.; Simões, P.N. *Prog. Polym. Sci*. **2014**, *39*, 1291−1311.

115. Sun, H.; Meng, F.; Dias, A.A.; Hendriks, M.; Feijen, J.; Zhong, *Biomacromolecules* **2011**, *12*, 1937−1955.

116. Soleimani, A.; Drappel, S.; Carlini, R.; Goredema, A.; Gillies, E. R. *Ind. Eng. Chem. Res.* **2014**, *53*, 1452−1460.

117. Pang, X.; Chu, C. C. *Biomaterials* **2010**, *31*, 3745−3754.

118. Guo, K.; Chu, C. C. J. *Biomed. Mater. Res., Part B* **2009**, *89*, 491−500.

119. Schafer, F. Q.; Buettner, G. R. *Free Radic. Biol. Med.* **2001**, *30,* 1191−1212.

120. Bayer, O. *Angew. Chem.* **1947**, *59*, 257-272.

121. Matsumoto, K; Kokai, A; Endo, T. *Polymer bulletin* **2016**, *73*, 677-685.

122. Huang, F; Cheng, R; Meng, F; Deng, C; Zhong, Z. *Biomacromolecules* **2015**, *16,* 2228-2236.

123. Lu, W; Wang, X; Cheng, R; Deng, C; Meng, F; Zhong, Z. *Polymer Chem.* **2015**, *6*, 6001-6010.

124. Yu, J; Lin, F; Lin, R; Gao, Y; Becker, M.L. *Macromolecules*, **2014**, *47,* 121-129.

125. Spindler, R; Frechet, J.M.J. *Macromolecules,* **1993,** *26*, 4809.

126. New

127. New

128. New

129. New

130. Albertsson, A. C.; Varma, I. K. *Adv. Polym. Sci.* **2002**, *157*, 1−40.

131. Cohen-Arazi, N; Domb, J.A; Katzhendler, J. *Polymers* **2010**, *2*, 418-439.

132. Yin, Q; Yin, L; Wang, H; Cheng, J. *Acc. Chem. Res*. **2015**, *48*, 1777-1787.

133. Kricheldorf, H. R.; Jonte, J. M. *Polym. Bull.* **1983**, *9*, 276−283.

134. du Boullay, O. T.; Marchal, E.; Martin-Vaca, B.; Cossio, F. P.; Bourissou, D. *J. Am. Chem. Soc.* **2006**, 128, 16442−16443.

135. Lu, Y; Yin, L; Zhang, Y; Zhonghai, Z; Xu, Y; Tong, R; Cheng, J. *ACS Macro Lett.* **2017,** *4,* 441-444.

136. Anantharaj S.; Jayakannan, M. *Biomacromolecules,* **2012**, *13*, 2446-2455.

137. Deepa, P: Jayakannan. M. *J. Polym. Sci., Polym Chem.* 2008, 46, 5897-5915.

138. Anantharaj S.; Jayakannan, M. *J. Polym. Sci., Polym Chem.* **2016**, *54*, 1065-1077.

139. Anantharaj S.; Jayakannan, M. *Biomacromolecules,* **2015**, *16*, 1009-1020.

140. Anantharaj S.; Jayakannan, M. *J. Polym. Sci., Polym Chem.* **2016**, *54*, 2864-2875.

141. Saxena, S.; Jayakannan, M. *J. Polym. Sci., Polym Chem.* **2016**, *54*, 3279-3293.

Chapter 2

Development of L-Tyrosine Based Enzyme-responsive Amphiphilic Poly(ester-urethane) Nano-carriers for Multiple Drug Delivery to Cancer Cells

Abstract

New classes of enzymatic-biodegradable amphiphilic poly(ester-urethane)s were designed and developed from L-tyrosine amino acid resources and their self-assembled nanoparticles were employed as multiple drug delivery vehicles in cancer therapy. The amine and carboxylic acid functional groups in L-tyrosine were converted into dual functional ester-urethane monomers and they were subjected to solvent free melt polycondensation with hydrophilic polyethylene glycols to produce comb-type poly(ester-urethane)s. The phenolic unit in the L-tyrosine was anchored with hydrophobic alkyl side chain to bring appropriate amphiphilicity in the polymer geometry to self-assemble them as stable nano-scaffolds in aqueous medium. The topology of the polymer was found to play major role on the glass transition, crystallinity and visco-elastic rheological properties of L-tyrosine poly(ester-urethane)s. The amphiphilic polymers were self-assembled as 200 ±10 nm nanoparticles and they exhibited excellent encapsulation capabilities for anticancer drugs such as doxorubicin (DOX) and camptothecin (CPT). *In-vitro* drug release studies revealed that the drug loaded L-tyrosine nanoparticles were stable at extracellular conditions and they underwent enzymatic-biodegradation exclusively at the intracellular level to release the drugs. Cytotoxicity studies in the cervical cancer (HeLa) and normal WT-MEFs cell lines revealed that the nascent L-tyrosine nanoparticles were non-toxic whereas the CPT and DOX drug loaded polymer nanoparticles exhibited excellent cell killing in cancer cells. Confocal microscopic imaging confirmed the cellular internalization of drug loaded nanoparticles. The drugs were taken up by the cells much higher quantity while delivering them from L-tyrosine nanoparticle platform compare to their free state. Flow cytometry analysis showed that the DOX loaded polymer nano-scaffolds were internalized the drugs 8-10 times higher compare to free DOX. Both the synthesis of new classes of poly(ester-urethane)s via melt polycondensation approach and the enzyme-responsive drug delivery concept were accomplished.

2.1. Introduction

L-Amino acid based synthetic polymers are emerging as important classes of biomaterials[1] in tissue engineering,[2] bone repair,[3] biomineralization,[4] drug and gene delivery in cancer therapy,[5] etc. L-Amino acids were often converted into N-carboxyanhydride cyclic monomers and subjected to ring opening polymerization to make di- and tri-block synthetic polypeptides[6] for biomedical applications.[7-9] L-Amino acids and oligopeptides were used as self-organization building blocks in non-biodegradable polymers such as polyacrylates, etc.[10-13] In the last one decade, non-peptide synthetic polymers from L-amino acid resources have attained significant importance due to their excellent biocompatibility and structural diversity.[14] Poly(ester-amide)s,[15-17] poly(α-hydroxy urethane)s,[18] poly(β-amino esters),[19] poly(ester-urea),[20] poly(ester-urea-urethane),[21] and poly(acetal-urethane)[22] are some of the important non-peptide polymers that were reported in the literature. L-Cysteine based disulfide containing poly(ester-amide)s[23] and poly(disulfide-urethane)s[15,17] were developed for redox-responsive (GSH) delivery of doxorubicin and docetexal.
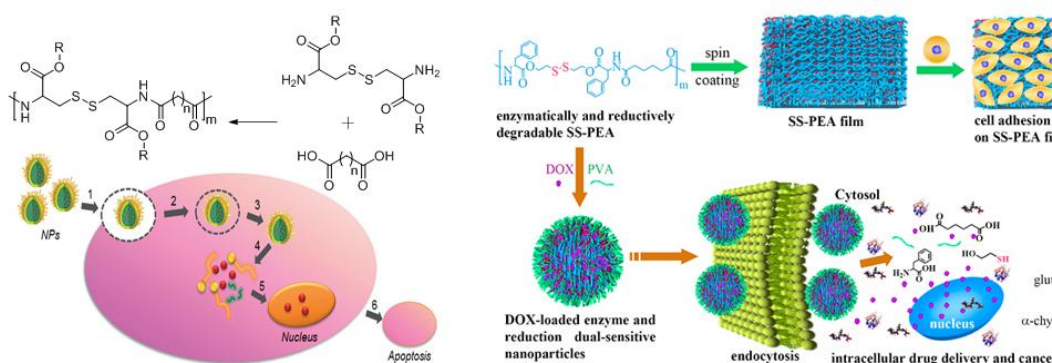
Figure 2.1. L-Cysteine based disulfide containing poly(ester-amide)s (adopted from Jun Wu et al. *Biomacromolecules*, **2015,***16*, 597. and Huanli et al. *Angew. Chem. Int. Ed*. **2015,** *54,* 9218).

From our research group, anantharaj et al. have reported novel ester-urethane melt polycondensation approach for L-amino acid resources to make new classes of poly(ester-urethane)s.[24] This melt process was optimized into catalysis and thermo-selective transesterification for multi-functional L-amino acid resources to make functional polyesters,[25-26] redox-degradable L-cysteine helical polyesters[27] and hyperbranched poly(ester urethanes),[28] etc. Very recently, enzyme and pH dual responsive amphiphilic polyesters based on L-aspartic acid were achieved by this methodology and their self-assembled nanoparticles were successfully demonstrated in drug delivery applications.[29]
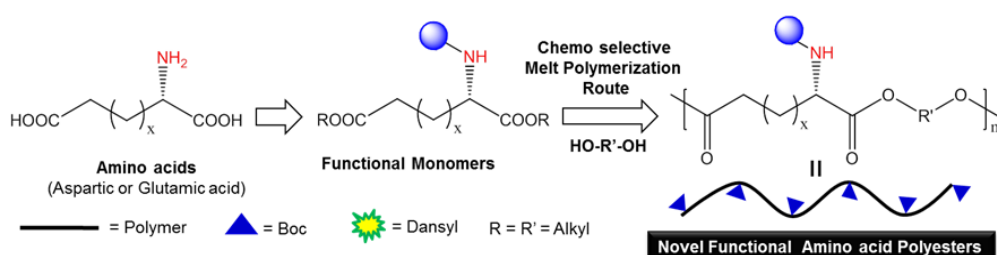
Figure 2.2. L-Amino acid based functional poly esters synthesized by melt poly condensation polymerization process (adopted from Anantharaj et al. *Biomacromolecules,* **2015**, *16,* 1009 – 1020).

Regardless of the above examples envisage the importance of non-peptide polymers; the full potential of L-amino acid resources are still un-tapped for biomaterial research especially in the area of drug delivery in cancer therapy. L-Tyrosine is very unique amino acid having phenolic functionality in addition to amine and carboxylic units at the α-carbon. Kohn and co-workers had designed L-tyrosine diphenolic monomers and these monomers were subjected to phosgene-assisted solution condensation to make unique classes of L-tyrosine based polycarbonates.[30-34] These polycarbonates exhibited excellent biocompatibility for cell adhesion and migration,[35] bone repair[36] and also soft tissue fillers in breast cancer surgery.[37] Efforts were also taken to make enzyme-induced hydrogels of poly(L-phosphotyrosine),[38] optically active polyurethanes[39-40] and poly(ester-urea)[41], etc.
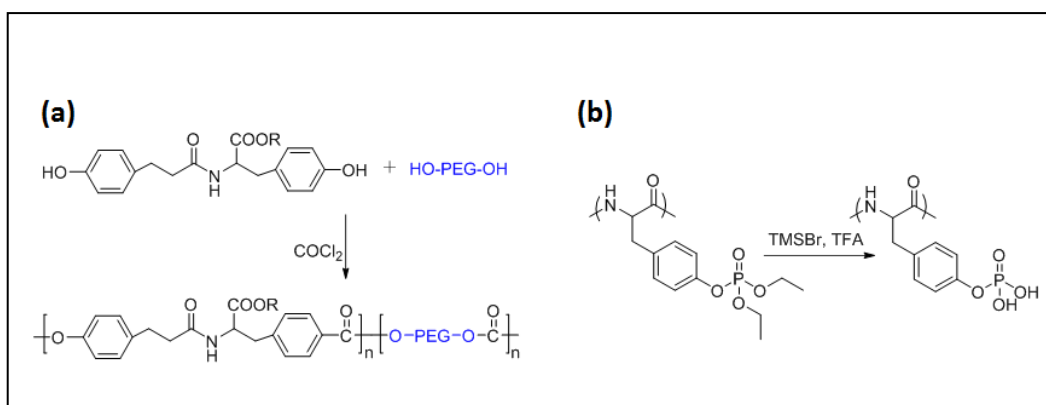
Figure 2.3. L-Tyrosine based poly carbonates (a) and poly(L-phosphotyrosine) (adopted from Magno et al. *J. Mater. Chem.* **2010**, *20*, 8885-8893 and Sun et al. *ACS Macro Lett.* **2015**, *4*, 1000-1003).

However, there is no attempt has been taken until the present on L-tyrosine based polymer nano-carriers for drug delivery applications. This is partially associated with the lack of unavailability of suitable synthetic methodologies to make L-tyrosine based amphiphilic polymer structures with appropriate biodegradation to deliver the drugs at the intracellular level. L-Tyrosine is very important biological resource; thus, the development of new synthetic approaches to make biodegradable polymer nano-scaffolds would open up new avenue of drug/gene delivery opportunities. To accomplish this goal, here we developed new classes of L-tyrosine based biodegradable amphiphilic poly(ester-urethanes)s via solvent free melt polycondensation process and employed their self-assembled nanoparticles as enzyme-responsive nano-carriers for multiple drug delivery to cancer cells. This new L-tyrosine polymer drug delivery strategy is shown in figure 2.4.

This chapter is emphasized to design and develop enzyme-biodegradable L-tyrosine based poly(ester-urethane)s by solvent free melt polycondensation process and explore their application for intracellular delivery of multiple anticancer drugs such as camptothecin (CPT) and doxorubicin (DOX) to cancer cells. For this purpose, the L-tyrosine resource was suitably modified as follows (see figure 2.4): (i) the amine and carboxylic acid groups were converted into urethane (or carbamate) and carboxylic ester, respectively, (ii) these ester-urethane monomers were polycondensed with hydrophilic poly ethylene glycols to produce poly
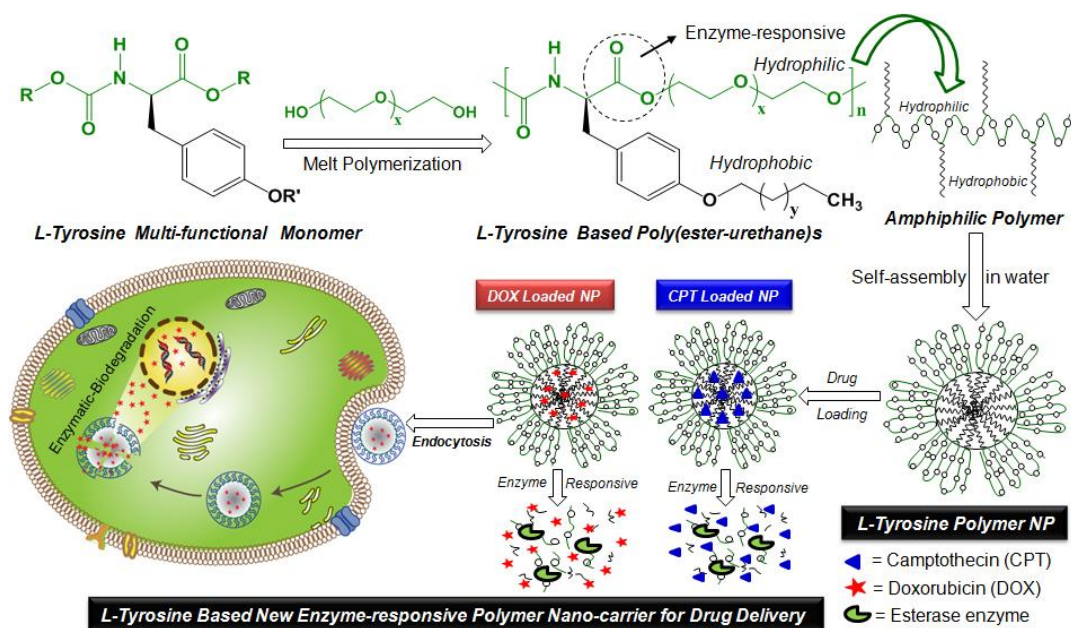
Figure 2.4. *Designing of new classes of L-tyrosine based amphiphilic poly(ester-urethane)s and employ their enzyme-responsive self-assembled nanoparticles as multiple anticancer drugs in cancer cells.*

(ester-urethane)s, (iii) the phenolic units was anchored with variable hydrophobic polymethylene units to bring appropriate self-assembly in the polymer geometry for producing stable aqueous nanoparticles, and (iv) the polymer design consists aliphatic ester and urethane (or carbamate) linkages in the polymer backbone that are readily susceptible for lysosomal enzymatic cleavage at the intracellular environment. The topology of the polymer structure was found to play significant role on the semi-crystalline, melt rheology and structure-property relationships. The amphiphilic polymers were self-assembled as stable nano-particles in aqueous media and showed excellent capability to load multiple anticancer drugs like doxorubicin (DOX) and camptothecin (CPT). *In vitro* studies exhibited that the self-assembled nanoparticles were found to be capable of loading multiple anticancer drugs and deliver the drugs through enzymatic-biodegradation under physiological conditions. Cytotoxicity of the L-tyrosine nano-carriers were studied in cervical cancer cells (HeLa) and Wild-type mouse embryonic fibroblasts (WT-MEF) cell lines. Confocal microscopy and flow cytometry analysis confirmed the cellular uptake of the drugs and internalization of drugs.

2.2. Experimental Section

2.2.1. Material and methods: L-Tyrosine, triethylene glycol, PEG-400, PEG-600, butyl bromide, 1-bromo hexadecane, titanium tetrabutoxide ($Ti(OBu)_4$), hydrochloride salt of doxorubicin, camptothecin and horse liver esterase enzyme were purchased from Aldrich chemicals and used without further purification. Methyl chloroformate, thionylchloride, and other solvents were purchased locally and purified prior to use.

2.2.2. General procedure: ^1H and ^{13}C-NMR spectra were recorded with 400-MHz JEOL NMR spectrophotometer in CDCl3, TMS used as a internal standard. GPC molecular weights were determined by using Viscotek VE 1122 pump equipped with Viscotek VE 3580 RI detector and Viscotek VE 3210 UV/VIS detector. Thermal stability of the monomers and polymers were investigated with Perkin Elmer thermal analyzer STA6000 model at the heating rate of 10 $^{°}C/min$. Thermal analysis of the polymers were carried by using TA Q20 instrument at heating rate of 10 $^{°}C/min$. Rheology measurements has carried out in Anton paar MCR 302 instrument by using 15 mm diameter parallel plate, measurements has carried out in melt state at 50 $^{°}C$. Polarized light microscope images have taken with LIECA DM 2500 P instrument. Absorbance and fluorescence spectra were recorded with Perkin-Elmer Lambda 45 UV-Visible spectrophotometer and SPEX FLUOROLOG HORIBA JOBIN VYON fluorescence spectrophotometer. DLS studies have carried out in Nano ZS-90 Malvern instrument, 633 nm red laser (90$^{°}$ angle) has used. FE-SEM and AFM images have taken with Zeiss Ultra Plus scanning electron microscope and Veeco Nanoscope IV atomic force microscope, AFM images has taken in tapping mode. Fluorescence microscopy imaging was done by using Carl Zeiss Axiovert 200 microscope. LSM 710 laser scanning microscope has used for confocal imaging. Flow cytometry analysis has carried out with BD LSRFortessa SORP cell analyzer.

Determination of critical micellar concentration (CMC): Critical micellar concentration was determined by fluorescence method, pyrene used as a probe. 0.6 μm pyrene solution in acetone has prepared and 1 mL of this solution has pippeted in to a glass vial. After evaporating all acetone, polymer solutions with different concentrations ranging from 0.1 mg/mL to 0.0005mg/mL was added to this vials

under N_2 atmosphere and equilibrated for 3 hours before recording their fluorescence spectra. Fluorescence spectra of these solutions were recorded by exciting the samples at 337 nm, fluorescence intensity ratio of pyrene I_1, I_3 bands at 375 nm and 386 nm respectively has determined and plotted against logarithmic concentrations of polymer, the slope of the plot gives the CMC of polymer.

Encapsulation of anticancer drugs in the polymer nanoparticles: Anticancer drugs such as doxorubicin and camptothecin were loaded into nanoparticles by dialysis method.[29] DOX.HCl was neutralized with triethyl amine and that was loaded in the polymer nanoparticles. For this purpose, 5.0 mg of polymer and 0.5 mg of drug were taken in DMSO (2.0 mL). Milli-Q water (3.0 mL) was added to the above solution dropwise and stirred for 4 hours in dark. The solution was transferred to dialysis semi-permeable membrane of MWCO 1KD and dialyzed for 48 h against milli-Q water to remove the un-encapsulated drug and DMSO. Fresh milli-Q water was replenished periodically. The dialyzed polymer nano-aggregates was filtered, lyophilized and stored in dark condition at 4 °C. The drug loading content (DLC) and drug loading efficiencies (DLE) were determined by absorption spectroscopy. The DOX absorbance at 510 nm and CPT absorbance at 366 nm were measured to determine the DLC and DLE. The amount of DOX and CPT loaded in to the polymer nanoparticles were calculated by using the molar extinction coefficients 11500 L mol^{-1} cm^{-1} and 11250 L mol^{-1} cm^{-1}, respectively.[42] DLC and DLE were calculated by using the following formulae.[42]

DLE (%) = {weight of drug in NPs / weight of drug in feed} X 100

DLC (%) = {weight of drug in NPs / weight of polymer taken} X 100

In vitro drug release studies: The release profiles of DOX and CPT were studied by dialysis method and the drug release monitored using absorption spectroscopy. Drug loaded polymer nanoparticles (1.0 mg/mL) were dispersed in PBS (pH = 7.4) at 37°C (1.0 mL) in a semi-permeable membrane dialysis tube with MWCO 1000. The dialysis tube was immersed in PBS (3.0 mL) and it was incubated at 37 °C. At specific time intervals 2.0 mL of PBS solution withdrawn to measure the absorbance and the solution was poured back in to reservoir after the measurements. This ensured the concentration of the reservoir maintained same. Drug release studies in

FBS has carried out by dispersing nanoparticles (1.0 mg/mL) in FBS at 37 °C in a dialysis tube (MWCO 1KD) as described above. For the esterase enzymatic drug release studies; a similar protocol was followed in PBS (pH = 7.4) at 37 °C in the presence of esterase enzyme (5.0 mg/mL). The cumulative drug release was calculated using the following equation:[43]

Cumulative drug release = {[Amount of drug released at time 't'] / [Total amount of drug in nanoparticles taken in dialysis tube] } X 100

Cell viability assay (MTT assay): The cytotoxicity of drug loaded polymer nanoparticles and nascent nanoparticles was studied in HeLa and WT-MEF cell lines using the tetrazolium salt, 3-(4,5-dimethylthiazol-2-yl)-2,5-diphenyltetrazolium bromide (MTT).[29,48] In a 96-well plate (Corning, USA), 1000 cells were seeded per well in 100 µL of DMEM with 10% FBS (fetal bovine serum) and allowed to adhere for 16 h. Prior to drug treatment, media from the cells was aspirated and various concentrations of DOX and drug loaded polymer nanoparticles were added as feed. A blank control, DMEM with FBS in the absence of cells and an untreated control, cells with DMEM containing FBS without nanoparticles, were used in each experiment. All control and treated experiment wells were in triplicate. Cells were incubated for 72 h without a change in medium and after 72 h the drug containing medium was aspirated. A freshly prepared stock solution of MTT in sterile PBS (5 mg/mL) was diluted to 50 µg/mL in DMEM. 100 µL of this solution was added to each well and incubated for 4 h at 37 °C. MTT solution was then aspirated from the wells and the purple formazan crystals that formed as a result of reduction of MTT by mitochondrial dehydrogenase enzyme from the cells were dissolved in 100 µL of DMSO (added per well). The absorbance from the formazan crystals was immediately measured using a micro plate reader at 570 nm (Varioskan Flash) which represents the number of viable cells per well. Values from triplicate run for each control and treated set were noted and their mean value was used for calculations. (Cell viability assay has done with the help of our lab mate Dr. Bapu rao surnar).

Cellular uptake studies using confocal microscopy: HeLa cells were seeded at a density of 1×10^5 cells on flame dried cover slips coated placed in 6 well plates containing DMEM medium with 10 % FBS. The cells were incubated at 37 °C for 16

hours and then exposed to the required concentrations of free DOX and DOX loaded polymer nanoparticles for 9 h in a CO_2 incubator at 37 °C.[29,42,48] After incubation, drug-containing medium was aspirated from each well, and cells were washed twice with PBS (1 mL per wash) and fixed with 4 % paraformaldehyde solution in PBS for 10 minutes at room temperature. The cells were washed twice with PBS (1 mL per wash) and stained with DAPI and incubated for 2 min at room temperature. This incubation was performed in the dark and excess of dye was washed from the cells with PBS. The cover slips were mounted on slides using Fluoromount-G mounting medium (Southern Biotech). Slides were then dried overnight at room temperature in the dark. The cells were imaged using a LSM 710 confocal microscope with the λ 405 nm (blue channel) and λ 560 nm (red channel) lasers. Images thus obtained were analyzed using Image J analysis software and the image for each channel was separated. (Confocal microscopy imaging has done with the help of our lab mate Mehak Malhotra and sonashree).

Flow Cytometry Measurements: The cellular uptake of free DOX and DOX-loaded polymer nanoparticles in cervical cancer cells was assessed using flow Cytometry cell analyzer.[45] HeLa cells were seeded in 6-well plate at a density of 10^5 cells containing DMEM media and incubated for 16 h at 37 °C. Cells were treated with desired concentration (1 μg/mL) of free DOX and DOX-loaded nanoparticles. After 9 h incubation, the drug containing media was aspirated and cells washed with PBS (1 x 1mL). Further cells were digested using 500 μL trypsin followed by 1 min incubation. The suspension in media was centrifuged at 10,000 rpm for 5 min and re-suspended the pellet in 1 mL PBS. Flow Cytometry studies were carried out by employing the BD LSRFortessa SORP cell analyzer that is equipped with five lasers and can detect 18 colours simultaneously. The 561 nm laser was used for the excitation of DOX and the band pass filter was chosen as 610 ± 10 nm. The fluorescence histograms were recorded from a population of 10, 000 cells. (Flow cytometry analysis has done with the help of our lab mate Mehak malhotra).

2.2.3. Synthesis of monomers

Synthesis of C-methyl ester N-methyl carbamate of tyrosine (1): To a suspension of L- tyrosine (10.0 g, 55.0 mmoL) in methanol (80 mL), thionylchloride (7.96 mL, 110.4 mmoL) was added drop wise at 0 $^\circ$C. The reaction mixture was refluxed for 12 h. The methanol and excess thionylchloride was removed by vacuum distillation to get a white solid residue. The solid mass was dissolved in sodium carbonate solution (15 wt%, 70 mL) by constant stirring. Methyl chloroformate (5.6 mL, 74.0 mmoL) in dichloromethane (70 ML) was added drop wise to this reaction mixture at 0 ºC. The solution was warmed to 25 °C and the reaction was continued for 12 h. The reaction mixture was extracted twice in to dichloromethane, dried over anhydrous Na_2SO_4. The solvent was evaporated by rotaevaporator to get white solid as product. The solid product was further purified by column chromatography using chloroform+methanol (9:1 v/v) as eluent. Yield = 14.0 g (90 %). ^{1}H-NMR (400 MHz, $CDCl_3$) δ ppm: 3.00-3.04 (m, 2H, $-C_6H_5CH_2$), 3.67 (S, 3H, $-NH-COOCH_3$), 3.73 (S, 3H, $-COOCH_3$), 4.60 (S, 1H, $C_6H_5CH_2CH$), 5.25 (S, 1H, N**H**) 6.81-6.83 (m, 2H, C_6H_5), 7.01-7.03 (m, 2H, C_6H_5). ^{13}C-NMR (100 MHZ, $CDCl_3$) δ ppm: 172, 156, 155, 130, 127, 115, 54, 52, 37. FT-IR (cm^{-1}): 642, 741, 825, 985, 1058, 1107, 1216, 1357, 1444, 1515, 1609, 1688, 1737, 2953, 3011, 3299, 3345, 3632, 3684, 3737, 3895, 3932. HRMS (ESI+): m/z calcd. for $C_{12}H_{15}NO_5$ [M+Na]$^+$: 276.0847; found= 276.0857.

Synthesis of O-butyl tyrosine ester-urethane (2): Typical procedure for O-substitution of tyrosine was described for C_4-substituted compound **2**. To a suspension of compound **1** (2.0 g, 7.9 mmoL) in dry acetonitrile (50 mL), K_2CO_3 (3.4 g, 25.2 mmoL) was added under nitrogen atmosphere. The mixture was refluxed for 30 minutes under nitrogen atmosphere. 1-Bromobutane (0.93 mL, 8.6 mmoL) was added drop wise and reaction was refluxed for 24 h under the nitrogen atmosphere. After completion of the reaction, it was filtered through sintered funnel and the solvent was evaporated by rotaevaporator to get a white solid product. The solid product was further purified by column chromatography using petether+ethylacetate (6:1 v/v) as eluent. Yield : 2.1 g (86 %). ^{1}H-NMR (400 MHz, $CDCl_3$) δ ppm: 0.96-0.99 (t, 3H, $-CH_2-CH_3$), 1.48 (t, 3H, $-CH_2-CH_2-CH_3$), 1.76 (t, 3H, $-CH_2-CH_2-CH_3$), 3.00-3.04 (m, 2H, $-C_6H_5CH_2$), 3.67 (S, 3H, $-NH-COOCH_3$), 3.72 (S, 3H, $-COOCH_3$), 3.91-3.95 (t, 2H, $C_6H_5-O-CH_2CH_2-$), 4.61 (S, 1H, $C_6H_5CH_2CH$), 5.14 (S, 1H, N**H**),

6.81-6.83 (m, 2H, C$_6$**H$_5$**), 7.01-7.03 (m, 2H, C$_6$**H$_5$**). ^{13}C-NMR (100 MHZ, CDCl$_3$) δ ppm: 172, 158, 156, 130, 127, 114, 67, 54, 52, 37, 31, 19, 13. FT-IR (cm^{-1}): 738, 821, 982, 1054, 1175, 1244, 1359, 1397, 1440, 1512, 1612, 1691, 1752, 2866, 2933, 3337, 3431, 3742. HRMS (ESI+): m/z calcd. for C$_{16}$H$_{23}$NO$_5$ [M+H]$^+$: 310.1654, found = 310.1653.

Synthesis of O-hexadecyl tyrosine ester-urethane (3): Compound **1** (1.0 g, 3.9 mmoL), 1-bromohexadecane (1.32 mL, 4.3 mmoL), K$_2$CO$_3$ (1.72 g, 12.5 mmoL) in acetonitrile (30 mL) were reacted and the isolation procedure was followed as described for **2**. Yield : 1.6 g, (89 %). ^{1}H-NMR (400 MHz, CDCl$_3$) δ ppm: 0.87-0.90 (t, 3H, -CH$_2$-**CH$_3$**), 1.27-1.31 (m, 24H, -CH$_2$-**CH$_2$**-**CH$_2$**-CH$_3$) 1.45 (m, 2H, -CH2-**CH$_2$**-CH$_2$-CH$_3$), 1.75 (m, 2H, -CH$_2$-**CH$_2$**-CH$_2$-CH$_2$-CH$_3$), 3.00-3.04 (m, 2H, -C$_6$H$_5$**CH$_2$**), 3.67 (S, 3H, -NH-COO**CH$_3$**), 3.73 (S, 3H, -COO**CH$_3$**), 3.93 (t, 2H, C6H5-O-**CH$_2$**CH$_2$-), 4.58 (S, 1H, C$_6$H$_5$CH$_2$**CH**), 5.11 (S, 1H, N**H**), 6.81-6.83 (m, 2H, C$_6$**H$_5$**), 7.01-7.03 (m, 2H, C$_6$**H$_5$**). ^{13}C-NMR (100 MHZ, CDCl$_3$) δ ppm: 171, 157, 155, 129, 126, 114, 67, 54, 51, 37, 31, 29, 28, 25, 22, 13 FT-IR (cm^{-1}): 672, 721, 817, 910, 988, 1053, 1155, 1242, 1351, 1372, 1440, 1514, 1691, 1748, 2850, 2915, 3329, 3480, 3633, 3739, 3847, 3894, 3932. HRMS (ESI+): m/z calcd. for C$_{28}$H$_{47}$NO$_5$ [M+H]$^+$: 478.3532. Found = 478.3538.

2.2.4. Synthesis of Polymers

P-6: Tyrosine monomer **3** (0.3 g, 0.6 mmoL), PEG-600 (0.25 g, 0.6 mmoL) were taken in a test tube shaped polymerization apparatus and melted by placing the tube in oil bath at 100 ºC under constant N$_2$ flow. The reaction mixture was evacuated with nitrogen and vacuum alternatively under constant stirring Titanium tetrabutoxide (0.003 g, 0.01 mmoL, 1 mole %) was added and the degassing was repeated at least twice. The polymerization was continued by immersing the polymerization tube at 150 ºC and stirring the melt for 4 h under constant nitrogen purge. During this stage, the methanol was removed along with purge gas and the polymerization mixture became viscous. The viscous melt was further subjected to condensation at high vacuum (0.01 mbar) at 150 ºC for 2 h. At the end of the polycondensation, the polymer was obtained as white solid. It was purified by dissolving in tetrahydrofuran, filtered and precipitated in to methanol. Yield : 0.51 g (98 %). ^{1}H NMR (400 MHz,

CDCl$_3$) δ ppm: 0.89 (t, 3H, -CH$_2$-**CH$_3$**), 1.26 (bs, 22 H, -**CH$_2$**-**CH$_2$**-CH$_2$), 1.44 (bs, 2H, -CH$_2$-**CH$_2$**-CH$_3$), 1.76 (q, 2H, -**CH$_2$**-CH$_2$-CH$_3$), 1.91 (bs, 4H, -**CH$_2$**-**CH$_2$**-CH$_2$), 3.00-3.04 (m, 2H, -C$_6$H$_5$**CH$_2$**), 3.67 (m, 34H, -NH-COOC**H$_3$** and -O-C**H$_2$**-C**H$_2$**-O-), 3.80 (S, 0.34H, -COOC**H$_3$**), 3.91 (t, 2H, C$_6$H$_5$-O-C**H$_2$**CH$_2$-), 4.22 (m, 2H, -NHCOOC**H$_2$**-), 4.28 (m, 2H, -COOC**H$_2$**), 4.61 (S, 1H, C$_6$H$_5$CH$_2$**CH**), 5.29 (S, 1H, N**H**), 6.79-6.81 (m, 2H, C$_6$**H$_5$**), 7.03-7.05 (m, 2H, C6**H$_5$**) . ^{13}C-NMR (100 MHZ, CDCl$_3$) δ ppm: 171, 157, 155, 129, 127, 114, 72, 70, 69, 68, 67, 63, 61, 54, 36, 31, 29, 25, 22, 13. FT-IR (cm^{-1}): 720, 837, 877, 946, 1057, 1187, 1215, 1319, 1397, 1434, 1546, 1609, 1657, 1719, 2857, 2920, 3511.

P-1: Tyrosine monomer 2 (0.2 g, 0.6 mmoL), Triethylene glycol (0.1 g, 0.6 mmoL), titaniumtetrabutoxide (0.003g, 0.01 mmoL, 1 mole %) were used and the reaction, purification were followed as described for **P-6** polymer. Yield : 0.23 g (92%). ^{1}H NMR (400 MHz, CDCl$_3$) δ ppm: 0.97 (t, 3H, -CH$_2$-**CH$_3$**), 1.47 (bs, 2H, -CH$_2$-**CH$_2$**-CH$_3$), 1.75 (q, 2H, -**CH$_2$**-CH$_2$-CH$_3$), 3.00-3.04 (m, 2H, -C6H5**CH$_2$**), 3.62-3.68 (m, 32H, -NH-COOC**H$_3$** and -O-C**H$_2$**-C**H$_2$**-O-), 3.73 (S, 0.28H, -COOC**H$_3$**), 3.93 (t, 2H, C6H5-O-C**H$_2$**CH$_2$-), 4.20 (m, 1.8H, -NHCOOC**H$_2$**-), 4.27 (m, 1.8H, -COOC**H$_2$**), 4.59 (S, 1H, C$_6$H$_5$CH$_2$**CH**), 5.37 (S, 1H, N**H**), 6.81-6.83 (m, 2H, C$_6$**H$_5$**), 7.01-7.03 (m, 2H, C$_6$**H$_5$**) . ^{13}C-NMR (100 MHZ, CDCl$_3$) δ ppm: 171, 158, 130, 127, 114, 70, 68, 67, 64, 54, 52, 37, 31, 19, 13. FT-IR (cm^{-1}) : 653, 719, 821, 877, 982, 1057, 1187, 1215, 1329, 1393, 1464, 1524, 1612, 1671, 1710, 2182, 2314, 2850, 2915, 3320, 3626, 3672, 3739, 3862, 3930.

P-2: Tyrosine monomer 2 (0.15 g, 0.4 mmoL), PEG-400 (0.19 g, 0.4 mmoL), titaniumtetrabutoxide (0.003g, 0.01 mmoL, 1 mole %) were used and the reaction, purification were followed as described for **P-6** polymer. Yield : 0.30 g (96%). ^{1}H NMR (400 MHz, CDCl$_3$) δ ppm: 0.97 (t, 3H, -CH$_2$-**CH$_3$**), 1.49 (bs, 2H, -CH$_2$-**CH$_2$**-CH$_3$), 1.75 (q, 2H, -C**H$_2$**-CH$_2$-CH$_3$), 3.00-3.04 (m, 2H, -C$_6$H$_5$**CH$_2$**), 3.67 (m, 30H, -NH-COOC**H$_3$** and -O-C**H$_2$**-C**H$_2$**-O-), 3.72 (S, 0.17H, -COOC**H$_3$**), 3.91 (t, 2H, C6H5-O-C**H$_2$**CH$_2$-), 4.20 (m, 1.95H, -NHCOOC**H$_2$**-), 4.26 (m, 1.95H, -COOC**H$_2$**), 4.62 (S, 1H, C$_6$H$_5$CH$_2$**CH**), 5.31 (S, 1H, N**H**), 6.81-6.83 (m, 2H, C$_6$**H$_5$**), 7.01-7.05 (m, 2H, C$_6$**H$_5$**) . ^{13}C-NMR (100 MHZ, CDCl$_3$) δ ppm: 171, 158, 130, 127, 114, 70, 68, 67, 64,

54, 37, 31, 19, 13. FT-IR (cm^{-1}): 721, 833, 877, 982, 1057, 1187, 1215, 1329, 1393, 1464, 1524, 1614, 1671, 1720, 2856, 2920, 3318.

P-3: Tyrosine monomer 2 (0.3 g, 0.9 mmoL), PEG-600 (0.6 g, 0.9 mmoL), titaniumtetrabutoxide (0.003g, 0.01 mmoL, 1 mole %) were used and the reaction, purification were followed as described for **P-6** polymer. Yield : 0.89 g (98%). ^{1}H NMR (400 MHz, CDCl$_3$) δ ppm: 0.97 (t, 3H, -CH$_2$-C**H$_3$**), 1.47 (bs, 2H, -CH$_2$-C**H$_2$**-CH$_3$), 1.73 (q, 2H, -C**H$_2$**-CH$_2$-CH$_3$), 3.00-3.04 (m, 2H, -C$_6$H$_5$C**H$_2$**), 3.67 (m, 50H, -NH-COOC**H$_3$** and -O-C**H$_2$**-C**H$_2$**-O-), 3.72 (S, 0.1H, -COOC**H$_3$**), 3.92 (t, 2H, C$_6$H$_5$-O-C**H$_2$**CH$_2$-), 4.21 (m, 2H, -NHCOOC**H$_2$**-), 4.26 (m, 2H, -COOC**H$_2$**), 4.59 (S, 1H, C$_6$H$_5$CH$_2$C**H**), 5.27 (S, 1H, N**H**), 6.79-6.81 (m, 2H, C$_6$**H$_5$**), 7.03-7.05 (m, 2H, C$_6$**H$_5$**) . ^{13}C-NMR (100 MHZ, CDCl$_3$) δ ppm: 171, 158, 155, 130, 127, 114, 72, 70, 68, 67, 63, 61, 54, 36, 31, 29, 19, 13. FT-IR (cm^{-1}): 720, 837, 877, 946, 1057, 1187, 1215, 1319, 1397, 1434, 1546, 1609, 1657, 1719, 2857, 2920, 3511.

P-4: Tyrosine monomer 3 (0.5 g, 1.0 mmoL), Triethylene glycol (0.1 g, 1.0 mmoL), titaniumtetrabutoxide (0.003g, 0.01 mmoL, 1 mole %) were used and the reaction, purification were followed as described for **P-6** polymer. Yield : 0.54 g (91%). ^{1}H NMR (400 MHz, CDCl$_3$) δ ppm: 0.89 (t, 3H, -CH$_2$-CH$_3$), 1.26 (bs, 24 H, -C**H$_2$**-C**H$_2$**-CH), 1.44 (bs, 2H, -CH$_2$-C**H$_2$**-CH$_3$), 1.76 (q, 2H, -C**H$_2$**-CH$_2$-CH$_3$), 3.00-3.04 (m, 2H, -C$_6$H$_5$C**H$_2$**), 3.67 (S, 0.54H, -NH-COOC**H$_3$**), 3.73 (S, 0.38H, -COOC**H$_3$**), 3.93 (t, 2H, C$_6$H$_5$-O-C**H$_2$**CH$_2$-), 4.02 (m, 2H, -NHCOOC**H$_2$**-), 4.04 (m, 2H, -COOC**H$_2$**), 4.61 (S, 1H, C$_6$H$_5$CH$_2$C**H**), 5.11 (S, 1H, N**H**), 6.81-6.83 (m, 2H, C$_6$**H$_5$**), 7.01-7.03 (m, 2H, C$_6$**H$_5$**) . ^{13}C-NMR (100 MHZ, CDCl$_3$) δ ppm: 171, 158, 156, 155, 130, 127, 114, 70, 69, 67, 64, 54, 52, 37, 31, 29, 26, 22, 13. FT-IR (cm^{-1}) : 653, 719, 821, 877, 982, 1057, 1187, 1215, 1329, 1393, 1464, 1524, 1612, 1671, 1710, 2182, 2314, 2850, 2915, 3320, 3626, 3672, 3739, 3862, 3930.

P-5: Tyrosine monomer 3 (0.3 g, 0.6 mmoL), PEG-400 (0.25 g, 0.6 mmoL), titaniumtetrabutoxide (0.003g, 0.01 mmoL, 1 mole %) were used and the reaction, purification were followed as described for **P-6** polymer. Yield : 0.51 g (98%). ^{1}H NMR (400 MHz, CDCl$_3$) δ ppm: 0.89 (t, 3H, -CH$_2$-C**H$_3$**), 1.26 (bs, 24 H, -C**H$_2$**-C**H$_2$**-CH$_2$), 1.44 (bs, 2H, -CH$_2$-C**H$_2$**-CH$_3$), 1.76 (q, 2H, -C**H$_2$**-CH$_2$-CH$_3$), 2.01 (bs, 4H, -

CH₂-**CH₂**-CH₂), 3.00-3.04 (m, 2H, -C₆H₅**CH₂**), 3.67 (m, 32H, -NH-COOC**H₃** and -O-**CH₂**-**CH₂**-O-), 3.80 (S, 0.17H, -COOC**H₃**), 3.91 (t, 2H, C₆H₅-O-C**H₂**CH₂-), 4.20 (m, 2H, -NHCOOC**H₂**-), 4.26 (m, 2H, -COOC**H₂**), 4.58 (S, 1H, C₆H₅CH₂C**H**), 5.36 (S, 1H, N**H**), 6.81-6.83 (m, 2H, C₆**H₅**), 7.01-7.05 (m, 2H, C₆**H₅**) . ¹³C-NMR (100 MHZ, CDCl₃) δ ppm: 171, 158, 155, 130, 127, 114, 70, 68, 67, 64, 54, 37, 31, 29, 26, 22, 14. FT-IR (cm⁻¹): 721, 833, 877, 982, 1057, 1187, 1215, 1329, 1393, 1464, 1524, 1614, 1671, 1720, 2856, 2920, 3318.

2.3. Results and Discussion

2.3.1. *Synthesis of Tyrosine Based Poly(ester-urethane)s*

L-Tyrosine is tri-functional natural L-amino acid and the acid and amine groups in L-Tyrosine resource were converted into their corresponding methyl ester and methyl urethane (or carbamate), respectively (compound **1**, in Scheme 2.1.). The phenolic group was anchored with two different types of alkyl chains C_4 and C_{16} by reacting their respective alkyl bromides. The monomers **2** and **3** were characterized by ^{1}H, ^{13}C NMR, and HR-MS and the details are given in the supporting information. The thermal stability of the monomers were tested for their suitability to high temperature melt polymerization. Thermogravimetric analysis (TGA) plots showed that these newly designed L-tyrosine monomers were thermally stable up to 180 °C for melt polycondensation.
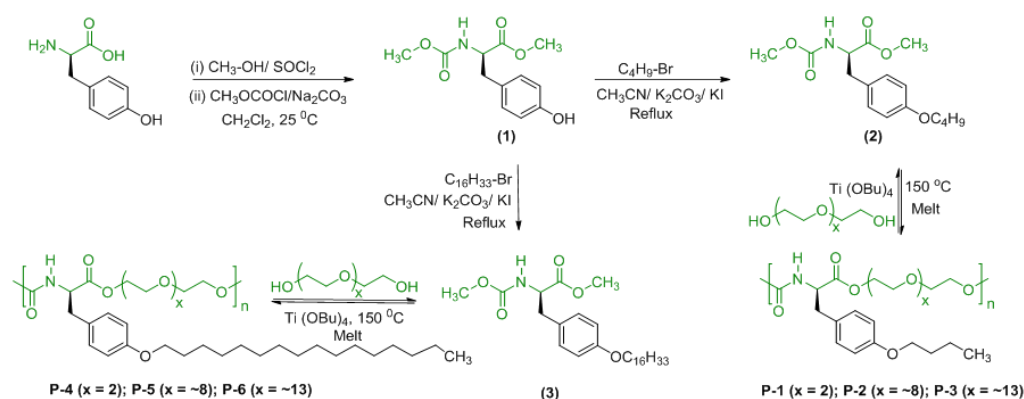
Scheme 2.1. Synthesis of L-tyrosine monomers and new classes of amphiphilic poly(ester-urethane)s.

Polyethylene glycols of MW= 400 and 600, and triethylene glycol were chosen for the melt polycondensation with L-tyrosine monomers using $Ti(OBu)_4$ catalyst (1 mol %) at 150 °C to produce linear amphiphilic poly(ester-urethane)s **P-1** to **P-6** (see Scheme 2.1.). L-Tyrosine monomers and PEG diols were taken in 1:1 mole ratio and subjected to melt polymerization. In this melt process, both the carboxylic ester and urethane underwent dual ester-urethane polycondensation with diols to produce high molecular weight polymers.[24] The polymerization was carried out in one-pot and two stages: (i) polymerization at 150 °C for 4 hours under

continuous N_2 purge to produce oligomers and (ii) further polycondensed under vacuum (0.01 mbar) for 2 h to get highly viscous polymer.
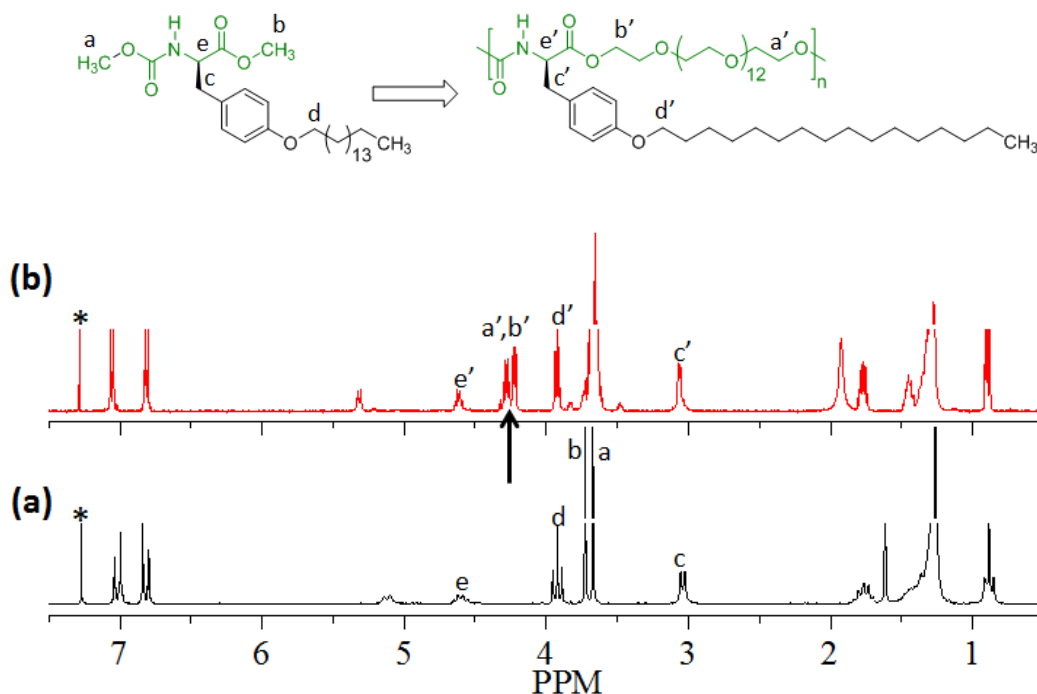
Figure 2.5. (a) ^{1}H-NMR spectra of monomer 3 and (b) polymer P-6 in CDCl$_3$. The peaks for different protons in the chemical structure are assigned by alphabets and the solvent peak is indicated by asterisks (*).

The occurrence of the melt polycondensation process was confirmed by NMR spectroscopic studies and representative spectra for P-6 are shown in figure 2.5. ^{1}H-NMR spectrum of monomer 2b showed peaks at 3.68 ppm and 3.72 ppm corresponding to methoxy protons in -NHCOOC**H$_3$** and -COOC**H$_3$**, respectively (see Figure 2.5.a). The disappearance of these peaks and appearance of new peaks at 4.02 ppm and 4.10 ppm corresponding to new urethane –NHCOOC**H$_2$** and new ester-linkages–COOC**H$_2$** in the polymer spectrum (see Figure 2.5.b) confirmed the occurrence of dual ester-urethane melt polycondensation in the L-tyrosine monomers.
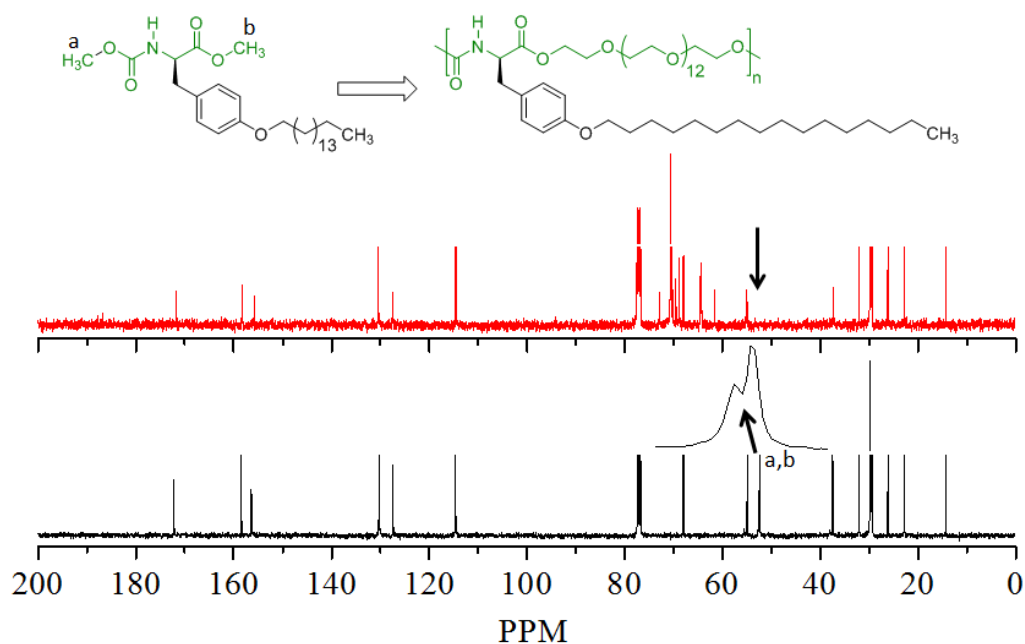
Figure 2.6. (a) ^{13}C-NMR spectra of monomer 3 and (b) polymer P-6 in CDCl$_3$. The peaks for different protons in the chemical structure are assigned by alphabets and the solvent peak is indicated by asterisks (*).

The occurrence of polymerization reaction was further confirmed by ^{13}C-NMR spectroscopy in figures 2.6.c and 2.6.d. The carbon peaks corresponding to –NHCOOC**H$_3$** and –COOC**H$_3$** at 51.94 and 51.96 ppm in the monomer were completely disappeared and new peaks corresponding to –NHCOOCH$_2$- and –COOCH$_2$- were appeared at 65.31 and 65.54 ppm (See Figures 2c and 2d). The number of repeating units (n) [or degree of polymerization , X_n] was determined from ^{1}H-NMR spectra by comparing the integration of end groups at (3.68 ppm and 3.72 ppm) with newly appeared protons in -NHCOOC**H$_2$** and –COOC**H$_2$** (4.02 ppm and 4.10 ppm). Based on the ^{1}H-NMR analysis, the degree of polymerization was determined to be > 20 units with respect to > 95 % percent conversion.
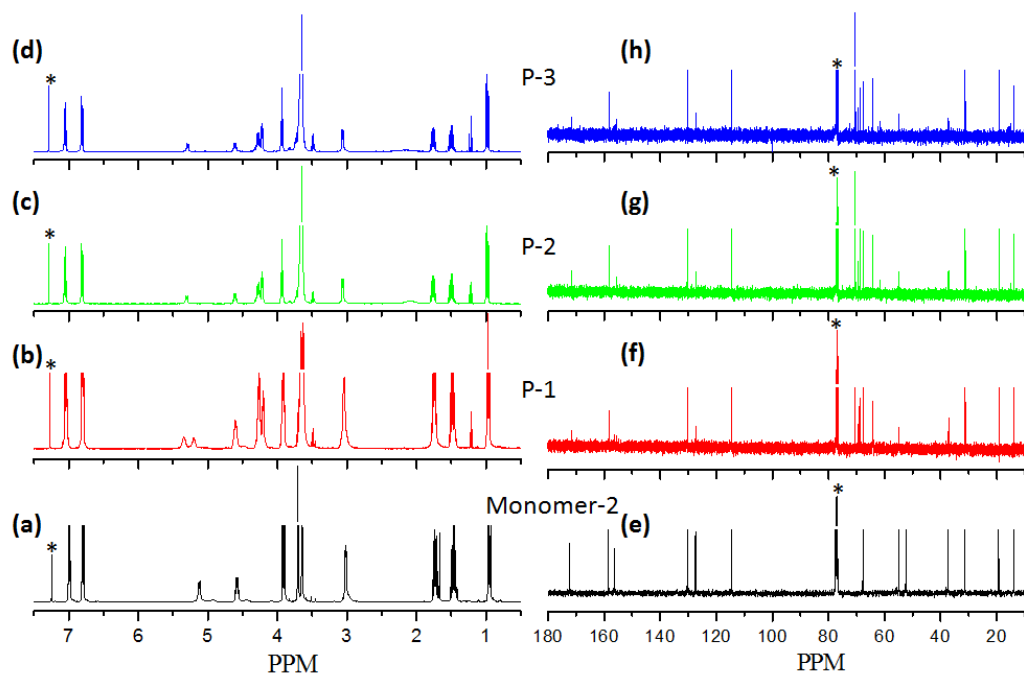
Figure 2.7. (a) ^{1}H-NMR spectra of monomer 2 and (b) polymer P-1, (c) polymer P-2, (d) polymer P-3 and ^{13}C-NMR spectra of monomer 2 (b) polymer P-1, (c) polymer P-2, (d) polymer P-3 in CDCl$_3$. The solvent peak is indicated by asterisks (*).
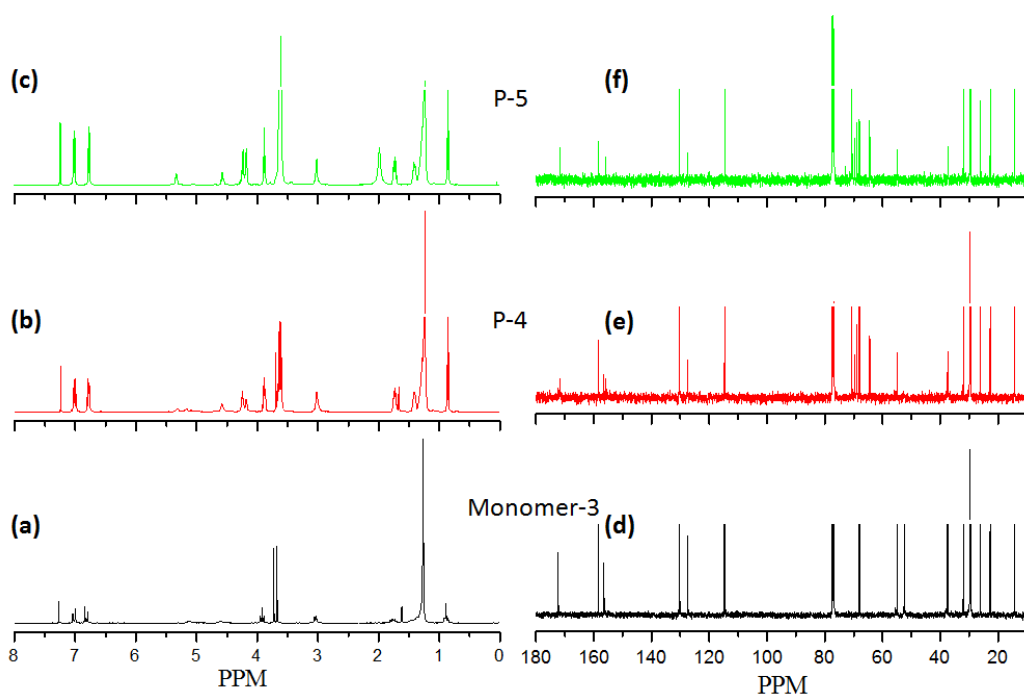
Figure 2.8. . (a) ^{1}H-NMR spectra of monomer 3 and (b) polymer P-4, (c) polymer P-5, and ^{13}C-NMR spectra of monomer 2 (d) polymer P-4, (e) polymer P-5, (f) in CDCl$_3$.

69

The molecular weights of the poly(ester-urethane)s were determined by gel permeation chromatography using polystyrene standards in THF. The GPC chromatograms in Figure 3a showed mono-modal distribution with respect to the formation of uniform molecular weights. The molecular weights of the polymers were obtained in the range of M_n = 4.0 to 13.0 × 10^3 g/mol, and M_w = 9.0 to 27.0 ×10^3 g/mol with PDI 1.9 to 2.2 (see table 1). The comparison of molecular weights of triethylene glycol to PEG-diol polymers revealed that longer PEG chains (PEG-400 and PEG-600) were found to be higher in molecular weights.
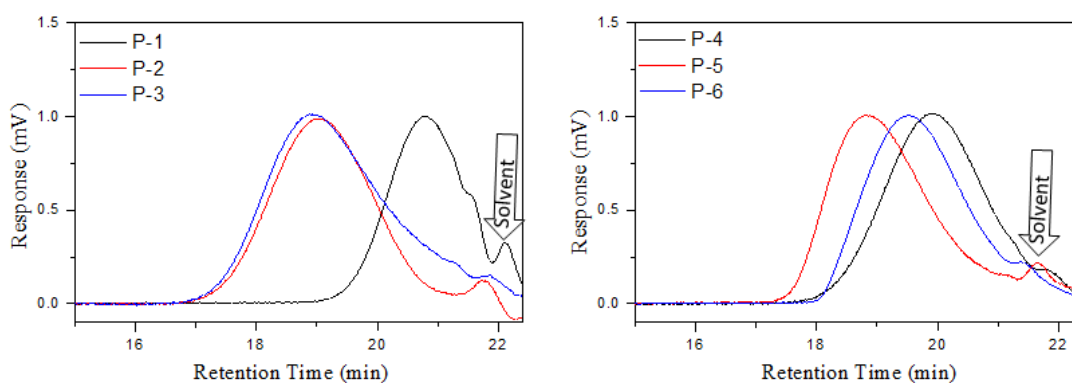
Figure 2.9. (a) GPC chromatograms of polymers in THF at 25 °C.

Further, the polymer P-6 was also made by three independent experiments to check the reproducibility of the polymer molecular weight in the new process. It was found that the molecular weights of polymer P-6 was obtained reproducible within experimental error limit. Based on the NMR analysis and GPC molecular weight determination, it may be concluded that the dual ester-urethane polycondensation approach is very good synthetic methodology for making moderate to high molecular weight poly(ester-urethane)s from L-tyrosine resources. For higher molecular weight diol such as PEG-1000, the molecular weight build was found to be very difficult. This is attributed to the availability of low concentration of hydroxyl functional group per unit volume in the melt which in turn produced low molecular weight polymers in melt polycondensation.[44]
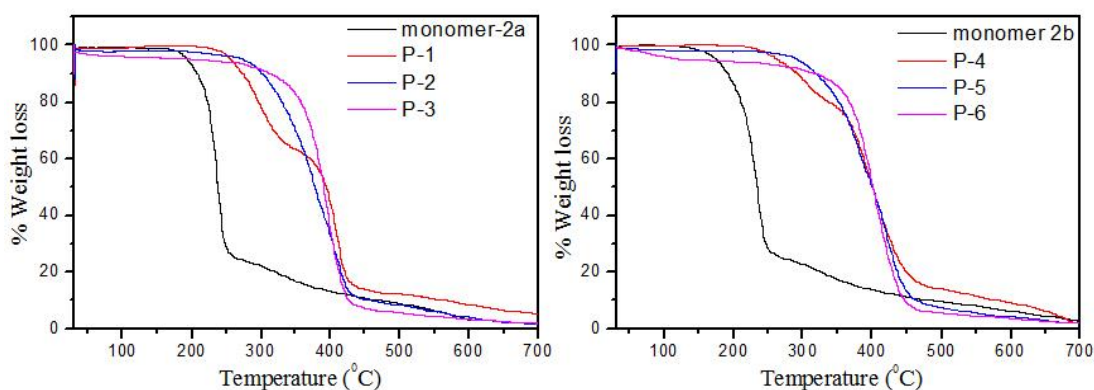
Figure 2.10. Thermal gravimetric analysis of monomers and polymers heated at 10 °C/min, under N_2 flow.

Thermal properties of the newly developed L-tyrosine poly(ester-urethane)s were studied by TGA and differential scanning calorimeter (DSC). TGA plots revealed that these polymers were thermally stable up to 300 °C (see Figure 2.10.). DSC thermograms of the polymers in the heating and cooling cycles are shown in Figure 2.11. (see table-1). From the DSC thermograms, it is clear that the crystalline and amorphous nature of the poly(ester-urethane)s were highly dependent on C_n substitution of the phenolic units rather than the length of the PEGs employed in the polymerization reaction. For example, the polymers with shorter C_4 side chain (**P-1** to **P-3)** were found to be amorphous whereas the polymers having longer C_{16} substitution (**P-4** to **P-6)** were semi-crystalline. The glass transition temperatures in **P-1** to **P-6** and melting transitions in **P-4** to **P-6** were decreased gradually with increasing the length of the PEG diols. Interestingly, the polymers with shorter PEGs have high enthalpy of melting and crystallization transitions with respect to enhanced polymer chain packing (see table-1). To visualize the crystallization process, the polymer **P-4** was subjected to polarizing light microscopy (PLM), the polymer sample was melted and cooled at a rate of 10 °/min on a hot stage as described earlier.[45] As can be seen in figure 2.11.c, the P-4 exhibited the nucleation of spherulites and then rapidly grown into larger fan-shaped crystallites at the end of the crystallization process. Although the polymers P-5 and P-6 are semi-crystalline in nature; their crystallization process could not be visualized due to their crystallization temperature in the sub-ambient region.

71

Table 1. Molecular weights and thermal properties of L-tyrosine based poly(ester-urethane)s.

Polymer	$M_n{}^a$ (g/mol)	$M_w{}^a$ (g/mol)	$M_w/M_n{}^a$	$T_d{}^b$ (°C)	$T_g{}^c$ (°C)	$T_m{}^c$ (°C)	$\Delta H_m{}^c$ (kJ/mol)	$T_c{}^c$ (°C)	$\Delta H_c{}^c$ (kJ/mol)
P-1	4000	8500	2.1	250	-5	-	-	-	-
P-2	10800	17700	1.7	280	-30	-	-	-	-
P-3	11300	20000	1.9	300	-20	-	-	-	-
P-4	4000	9000	2.1	260	-	41.5	31.9	33.5	33.4
P-5	13000	27000	2.1	286	-	11.3	12.9	6.4	11.5
P-6	8600	16200	1.9	240	-20	1.5	14.3	-3.8	13.4

[a]Molecular weights are determined by GPC in THF at 25 °C. [b]Decomposition temperature was estimated from TGA plots at 5 % decomposition under nitrogen atmosphere at 10 °/min heating rate. [c]DSC thermograms are recorded under nitrogen atmospheres at 10°/min heating/cooling cycles.
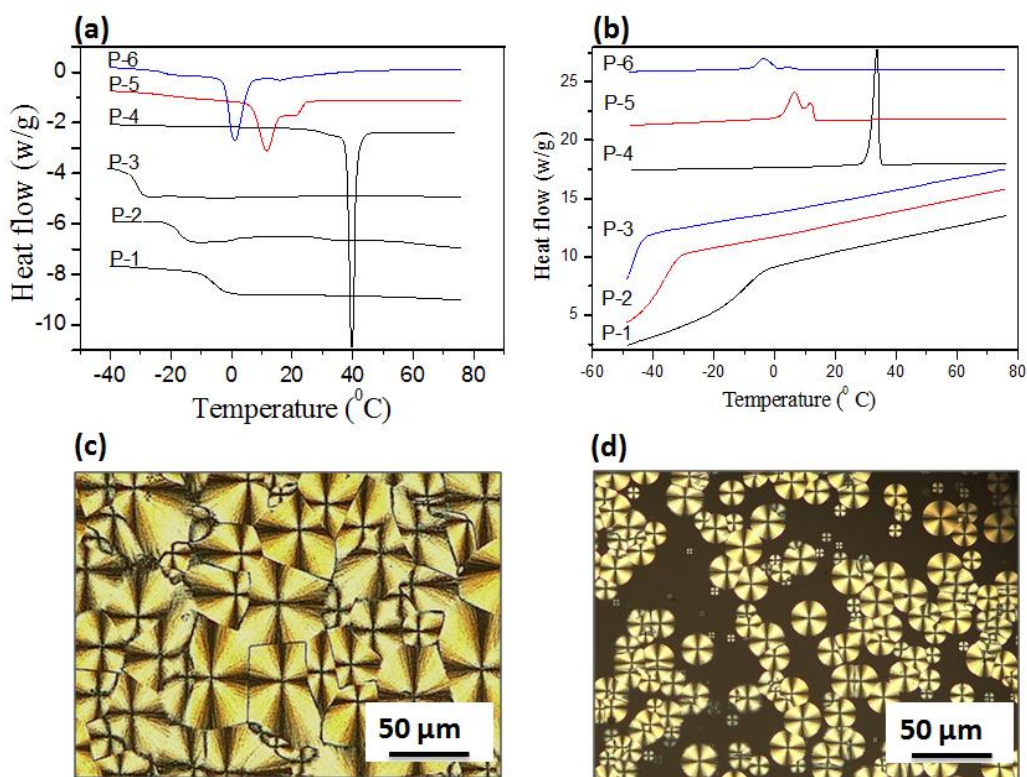
Figure 2.11. (a) DSC thermograms of polymers in the heating cycle and (b) cooling cycle at 10 °C/min under nitrogen atmosphere. (c) PLM images of polymer P-4 at 39 °C while crystallizing from melt.

Mechanical properties of the polymers were investigated by rheology measurements of storage modulus (G') and loss modulus (G'') at 50 °C above their melting temperatures. All polymers exhibited linear visco-elastic regime up to 1 % strain in figures 2.12. and 2.12. and therefore, the frequency sweep experiments were carried out at a constant strain of 0.1% which is well below the deformation limit (1 %). The polymers with triethylene glycol main chains (P-1 and P-4) were behaving as visco-elastic materials up to 5 % of strain. At larger strain the G'' became higher than the G' with respect to the viscous solid (see Figure 2.12). On the other hand, the polymers with longer PEG segments in the backbone exhibited viscous solid nature still at lower strain in Figure 2.12. As expected, the moduli of the C_4 chain polymers were found to be much higher than that of polymers with C_{16} side chains due to steric hindrance in the latter case.
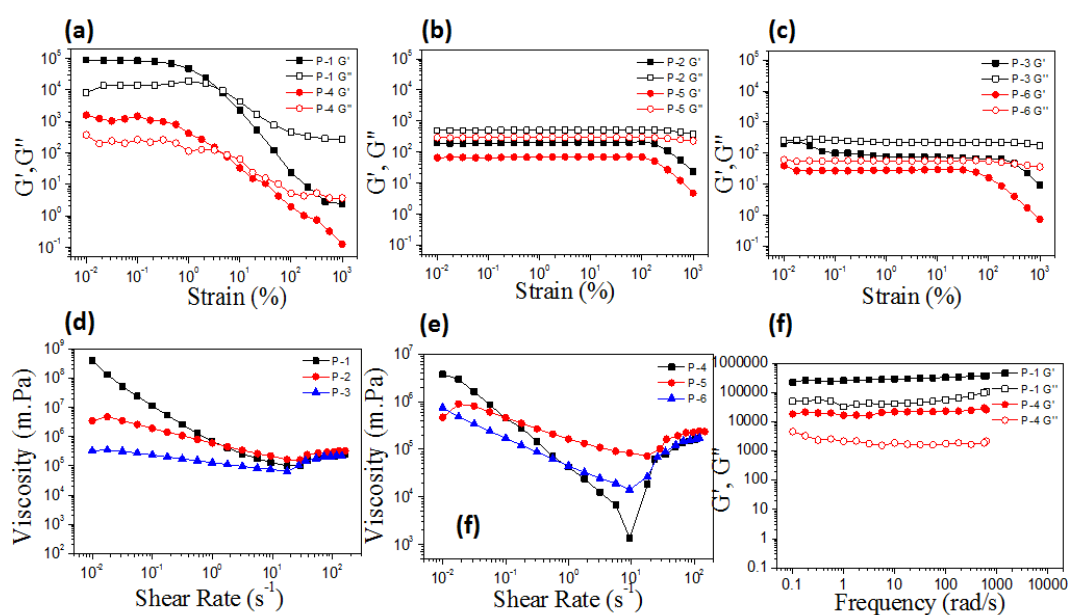
Figure 2.12. (a) Moduli versus strain sweep curves of polymers P-1 and P-4. (b) P-2 and P-5, (c) P-3 and P-6. (d) Viscosity versus shear rate curves of polymers P-1 to P-3, (e) P-4 to P-6. (f)) Moduli versus strain sweep curves of polymers P-1 and P-4.

In general, the increase in shear rate expected to decrease the viscosity of the material. As expected, the newly developed L-tyrosine poly(ester-urethane)s P-1 to P-6 have showed a gradual decrease in the melt viscosity with the increase in the shear rate up to 10 s^{-1} (see figure 2.12.f). Interestingly, at higher shear rate (> 10 s^{-1}) there is

a sudden enhancement in the viscosity observed in all polymers. The increase in the viscosity up on increase in shear rate is attributed to the shear thickening or dilatant which is a very important characteristic of polymeric materials for applications in body armour materials and automobiles etc. Based on these analysis, it may be concluded that the newly designed L-tyrosine poly(ester-urethane)s are excellent thermoplastics with tune-able thermal and mechanical properties.

2.3.2. Self-assembly and Loading Capabilities

The new classes of L-tyrosine based poly(ester-urethane)s were build with hydrophilic PEG -$(CH_2CH_2O)_x$- units (x= 3 to 15) in the backbone and short (C_4) and longer (C_{16}) hydrophobic alkyl chains as pendants. This design resembles the comb-type amphiphilic polymer structures as shown in figure 4a. The suitability of these amphiphilic poly(ester-urethane)s for drug delivery was tested by two methods: (i) the ability to produce stable and self-assembled nano-objects in the aqueous medium, and (ii) the encapsulation capability of the nano-assemblies for clinically important anticancer drugs. For this purpose, the polymer was dissolved in DMSO + water mixture and subjected to dialysis method, fresh water was replenished and the dialysis was continued for 48 h. The polymers having triethylene glycol spacer P-1 and P-4 were found to be completely insoluble and they precipitated from the aqueous medium during the dialysis. On the other hand, the long PEG-400 and PEG-600 containing amphiphilic polymers P-2, P-3, P-5 and P-6 produced stable aqueous nano-assemblies (see figure 2.13 and 2.14). The loading capacities of P-2, P-3, P-5 and P-6 nanoparticles were tested for hydrophobic anticancer drugs such as doxorubicin (DOX, topoisomerase inhibitor I and DNA intercalating agent) and camptothecin (CPT, topoisomerase inhibitor I). For this purpose, the polymer and drug were dissolved in water + DMSO and dialyzed against milli-Q water using a semi-permeable membrane for 48 h.
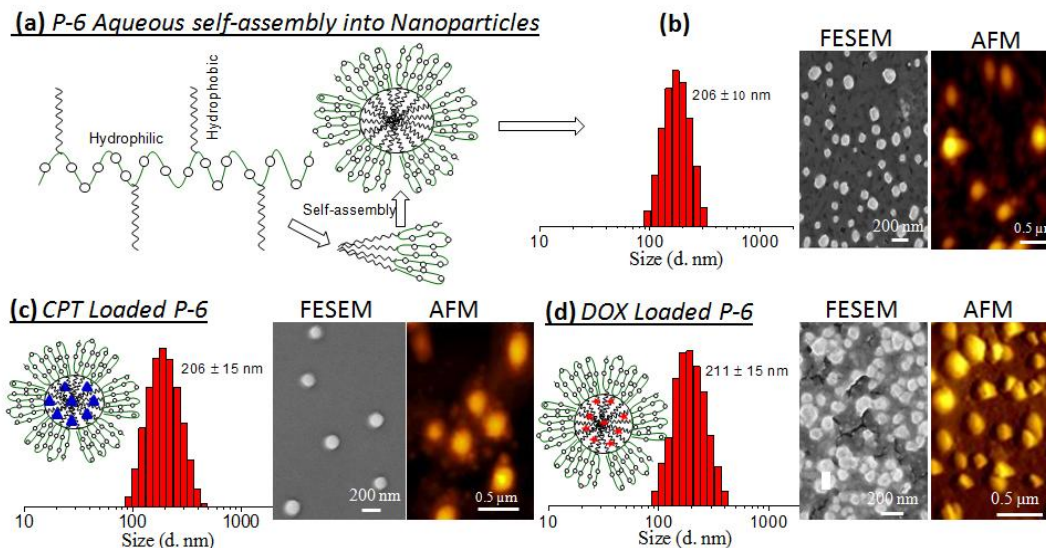
Figure 2.13. (a) Plausible mechanism for polymer self-assembly. (b) DLS histogram, FE-SEM and AFM images of aqueous self-assembly of P-6 polymer. (c) DLS histogram, FE-SEM and AFM images of CPT loaded P-6 nanoparticles. (d) DLS histogram, FE-SEM and AFM images of DOX loaded P-6 nanoparticles. Concentration of samples = 0.1 mg/mL.

Amongst all these polymers, only the polymer **P-6** having PEG-600 spacer and long C_{16} chains in the pendent found to produce stable encapsulation of DOX and CPT. These studies suggest that the polymer topology played a significant role on the formation of stable aqueous nano-assemblies of L-tyrosine polymer as well as the encapsulation of drugs. In the present design, a longer pendant alkyl chain is essential for producing stable nanoparticle assemblies in the L-tyrosine based poly(ester-urethane)s. A self-assembly model for the aqueous self-assembly of these comb-type polymers is shown in figure 4a. The hydrophobic tails in the pendant segregated together via like-like interactions to yield hydrophobic bundles and the hydrophilic backbone folded as hair-pin like arrangements as to produce tiny polymer aggregates. The self-assembly of these polymer aggregates subsequently produced micellar nanoparticles. The critical aggregation concentration of the **P-6** polymer was determined to be 5.0 µg/mL using pyrene as probe by fluorescence method[46]. Based on the self-assembly studies, theP-6 aqueous nanoparticle and its CPT and DOX loaded nanoparticles were chosen for further studies.
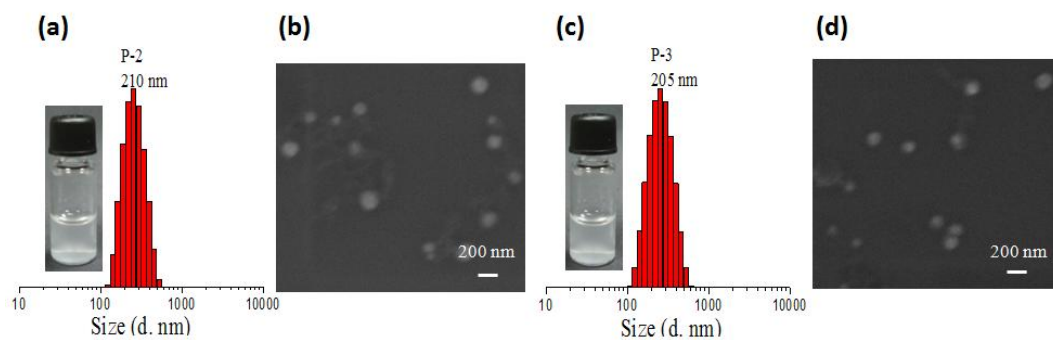
Figure 2.14. (a) DLS histogram, (b) FE-SEM image of P-2 polymer aqueous nano particles, (c) DLS histogram, (d) FE-SEM image of P-3 polymer aqueous nano particles.

The drug loading efficiency (DLE) for the P-6 nanoparticles were determined by absorption spectroscopy as 49 % and 15 % for DOX and CPT, respectively. The drug loading content (DLC) was obtained as 4.9 % and 1.5 % for DOX and CPT, respectively. These drug loaded nanoparticles are named as P-6-CPT and P-6-DOX. Dynamic light scattering (DLS) studies of P-6 aqueous polymer sample showed mono-modal distribution with respect to the formation of homogeneous nano-aggregates of 200 ± 10 nm in size (see Figure 2.13). To visualize the size and shape of the aqueous nano-aggregates, they were subjected to electron microscope (FE-SEM) and atomic force microscope (AFM) imaging. In figure 2.13, the FE-SEM image showed the formation of spherical nano-particles of size 200 ±10 nm. AFM images of the P-6 sample also confirmed the existence of spherical nano-particles of 200±10 nm. The hydrodynamic diameter of dispersed polymer nano-aggregates at low concentration 0.1 mg/mL in the aqueous medium was matching with the sizes of the nanoparticles in FE-SEM and AFM images[42,43,46]. This further confirmed that the amphiphilic polymers were pre-assembled in the solution as nanoparticles via hydrophilic and hydrophobic interactions as proposed in Figure 4a. This emphasized the need for appropriate PEG chain length and hydrophobic pendant for producing robust self-assembled structures based on L-tyrosine resources. The CPT drug loaded P-6 nanoparticles (named as P-6-CPT) showed the formation of stable nano-aggregate of 210 ± 15 nm (see Figures 2.13.c). FE-SEM image and AFM image confirmed the existence of spherical nano-particle morphology (see Figures 2.13.c). Similarly, the DOX loaded nanoparticles (named as P-6-DOX) was also found to retain the size and shape of the nanoparticles as 210 ± 15 nm in size (see Figure 2.13.d).

Both CPT and DOX are fluorescent anticancer drugs; thus the drug loaded nanoparticles were subjected to detail photo physical studies by absorption and emission spectroscopy (see Figure 2.15.). The photographs of the CPT and DOX loaded samples in the vials shown in figure 5a and 5b also confirmed the strong blue and red fluorescence. The absorption spectra showed maxima at 257 nm with respect to the polymer backbone and also broad peaks at 364 nm and 510 nm in P-6-CPT and P-6-DOX with respect to the absorption of CPT and DOX, respectively (see figures 2.15.c to 2.15.f). The emission spectra of the drug loaded nanoparticles showed emission maxima at 450 nm and 560 nm for CPT and DOX loaded P-6 nanoparticles, respectively. The photo physical characteristics of the drugs in the P-6 nanoparticles were found to be identical to that of their free form confirming that their luminescent characteristic were preserved without any change. Fluorescent microscopic images of the CPT and DOX loaded nanoparticles exhibited bright blue and red emission with respect to their chromophore nature (see Figures 2.15.a and 2.15.b). From the above detailed self-assembly studies accomplished by DLS, FE-SEM, AFM and also photophysical studies; it may be concluded that the newly designed amphiphilic poly(ester-urethane) nanoparticles from L-tyrosine resources are unique classes of nano-carriers for loading multiple anticancer drugs.
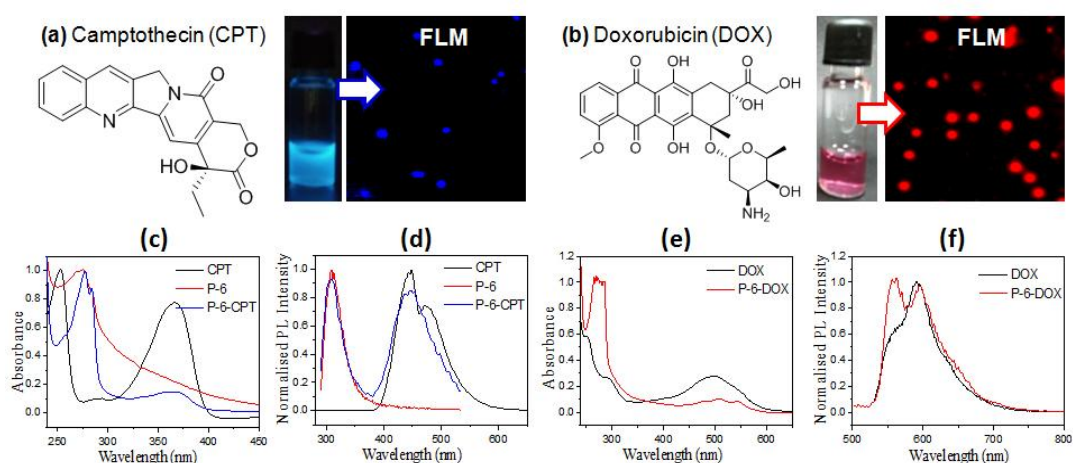
Figure 2.15. (a) CPT loaded P-6 nanoparticles in vial and its fluorescent microscope image (FLM). (b) DOX loaded P-6 nanoparticles in vial and its FLM image. (c) Absorbance spectra of P-6, free CPT and CPT loaded P-6 nanoparticles. (d) Emission spectra of P-6, free CPT and CPT loaded P-6 nanoparticles (λex=340 nm). (e) Absorbance spectra of free DOX and DOX loaded P-6 nanoparticles. (f) Emission spectra of free DOX and DOX loaded P-6 nanoparticles (λex = 484 nm).

2.3.3. Enzymatic-biodegradation and *in vitro* Drug Release

The L-tyrosine polymers were constituted by aliphatic ester and urethane chemical linkages in their back bone. It is well known that aliphatic polyester linkages are readily susceptible for enzymatic-degradation under physiological conditions.[42-43] In the present case, upon endocytosis by the drug loaded nanoparticles, the aliphatic ester part in the poly(ester-urethane)s can be readily biodegraded by the enzymes in the lysosomal compartments at the intracellular level in the cancer cells. Horse liver esterase is routinely employed in the drug delivery area to study the enzymatic-biodegradation of the aliphatic ester linkages and polyesters (Craig et al *J. Am. Chem. Soc.*, 1958, *80*,1574-1579). The enzyme active site seems to be almost identical in most of the esterase enzymes obtained from various sources. The activity of the horse liver esterase enzyme almost resembles the lysosomal esterase enzyme (Stoops et al *Can. J. Biochem*, 1975, *53*,565-573). Sonashree et al from our group have recently studied the enzymatic degradation of aliphatic polyesters based on L-aspartic resource, and it was reported that more than 5 different types of enzymes namely, horse liver esterase, chymotrypsin, trypsin, pappain and GSH and it was found that they were capable of degrading the nanoparticles in vitro. Among these enzymes horse liver esterase was found to be superior in degrading the aliphatic polyesters. (Sonashree and Jayakannan, *Biomacromolecule*, 2017,*18*, 2594-2609). Thus, the choice of the horse liver esterase enzyme is appropriate for the *in vitro* analysis in the present investigation. To investigate the effect of esterase enzyme on polymer structure, in vitro drug releasing studies were done in the presence of horse liver esterase enzyme using dialysis method in PBS (pH = 7.4) at 37 °C. The drug release-kinetics was studied using absorption spectroscopy. The plots of cumulative drug release in absence and presence of esterase enzyme for P-6-CPT nanoparticle is shown in Figure 6a. In the absence of esterase enzyme, the polymer nano-scaffolds showed less than 30 % leaching and exhibited very good stability in PBS at 37 °C for more than 48 h identical to that of extracellular conditions. On the other hand, in the presence of esterase enzyme more than 90 % of the CPT was released in 12 h. The DOX loaded nanoparticles exhibited very good stability (< 15 % leaching) at pH = 7.4 (in PBS) and selectively cleaved to release the DOX in the presence of the esterase enzymes (see Figure 2.16.b). To study the stability of polymer nanoparticles in blood

plasma, the CPT loaded nanoparticle was incubated in FBS at 37° C and the release profiles were monitored by absorbance spectroscopy (see Figure 2.17.b). It was found that the drug loaded nanoparticles were stable and only < 40 % drugs were released. This study confirmed that the polymer nanoparticles are stable against the enzymes in PBS or FBS in the presence of other biological species like proteins. They preserved more than 60 % of drugs in the nano-carrier that exclusively ruptured by the lysosomal-esterase enzymes at intracellular level to release in the cytoplasm. Our earlier studies based on the computational docking studies confirmed that the enzyme pocket is appropriate for the degradation of aliphatic esters. The hydrolytic degradation is very slow in the polyesters which is an added advantage for the enhanced stability of the polymer nanoparticles under circulation conditions.
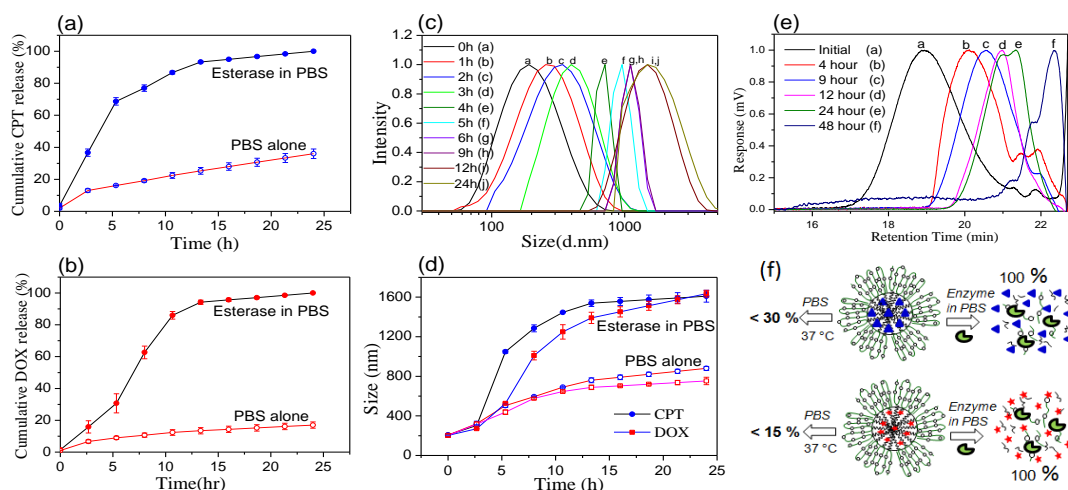
Figure 2.16. Cumulative drug release profiles of CPT (a) and (b) DOX. (c) DLS histograms of CPT loaded nano-particles in presence of esterase in pH =7.4 at 37 °C at different time intervals. (d) Plot of nanoparticle size for P-6-CPT and P-6-DOX in absence and presence of esterase enzyme (5 mg) in pH =7.4 at 37 °C at different time intervals. (e) GPC histograms of P-6 polymer treated with enzyme in pH =7.4 at 37 °C at different time intervals. (f) Schematic presentation for CPT and DOX releasing from nano-particles upon enzymatic action.
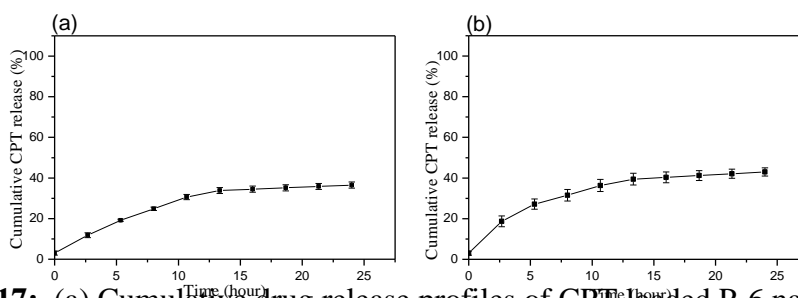
Figure 2.17: (a) Cumulative drug release profiles of CPT loaded P-6 nanoparticles in pH 4 buffer at 37 °C. (b) Cumulative drug release profiles of CPT loaded P-6 nanoparticles in Fetal Bovine Serum at 37 °C.

79

The degradation behaviour of the drugs loaded polymers in presence of esterase enzyme was also studied by using DLS.[47-48] DLS histograms for the P-6-CPT nanoparticles in the presence of esterase enzymes are shown in figure 6c. The initial DLS histograms showed mono-modal distribution with average size of 200 ± 15 nm. With an increase in time, the esterase enzyme cleaved the polymer backbone in the nanoparticles. During the enzymatic degradation, the nanoparticle loses its hydrophilic and hydrophobic balance; as a result, the hydrophobic bearing chains tend to phase separated from the aqueous medium which produces larger size aggregates (see Figure 2.16.c). In a controlled experiment in pH 7.4 PBS at 37 °C without esterase enzyme, these polymer nano-scaffolds are showing good stability and there is no appreciable change in the size of the self-assembled structures even after 48 h of incubation. The P-6-DOX nanoparticle also exhibited same trend in their DLS histograms in the absence and presence of esterase enzymes (see Figure 2.18.). The DLS size of the nanoparticles are plotted for both P-6-CPT and P-6-DOX systems and showed in Figure 2.16.d. This plot reflected similar trend as observed in the cumulative drug release profiles by absorption spectroscopy (see Figure 2.16.a and 2.16.b) and supports the cleavage of polymer nanoparticles selectively in the presence of esterase enzyme. Thus, two independent studies (DLS and absorbance) were done to confirm the enzymatic-biodegradation of P-6 nanoparticles and delivery of anticancer drugs under physiological conditions.
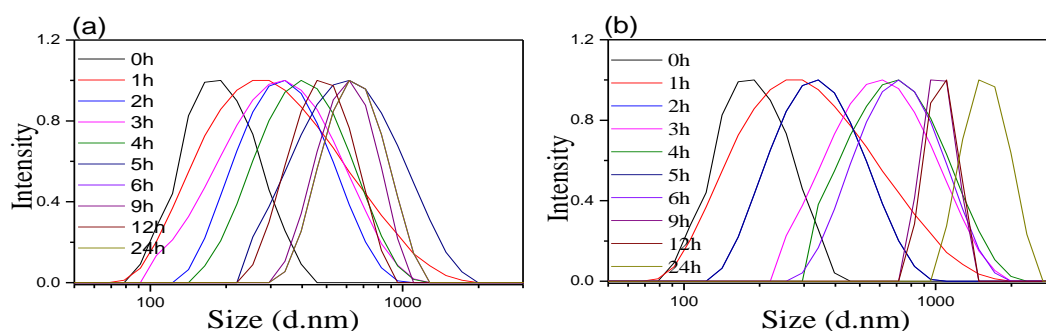
Figure 2.18. DLS histograms of DOX loaded P-6 polymer nano particles in pH 7.4 PBS without esterase enzyme (a), in pH 7.4 PBS with esterase enzyme (b).
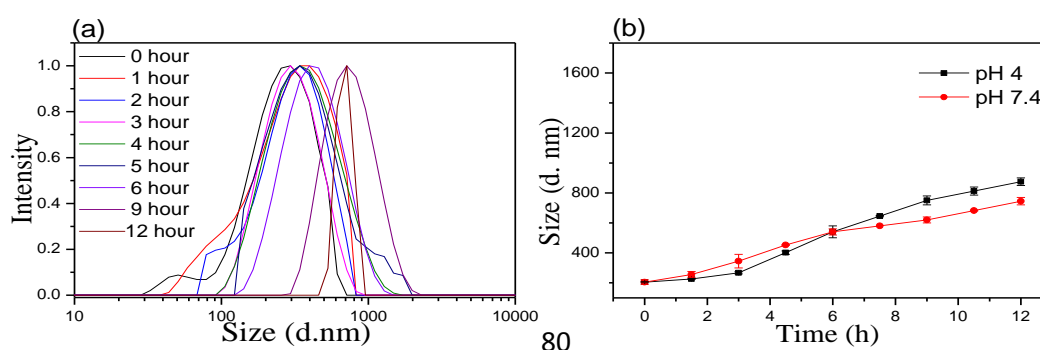
Figure 2.19. (a) DLS histograms of CPT loaded P-6 nano particles in pH 4 PBS at 37 °C without esterase enzyme. (b) Time Vs size plot for CPT loaded P-6 nanoparticles in pH 4 buffer at 37 °C without esterase enzyme.

Further, to study the influence of pH on the stability of the nanoparticles, the CPT loaded sample was subjected to DLS at pH=4.0 and pH = 7.4 at 37 °C (see Figure 2.19.). This sample was also subjected to release studies using absorbance spectroscopy at pH=4.0 at 37 °C (see Figure 2.19.b.). These data revealed that the nanoparticles were stable at pH= 4.0 indicating that the polymer structure is less susceptible for acidic conditions. To further support the enzymatic-biodegradation, the P-6 polymer was subjected to GPC studies before and after treatment with esterase enzymes for 48 h at 37°C in PBS (see figure 2.16.e). The GPC chromatograms at 4 to 24 h clearly indicate the biodegradation of the long polymers chains into low molecular weight species. At 48 h all the polymer chains were completely degraded into dimer or monomeric species and the chromatogram appeared along with solvent peak. This data clearly supports that the enzymatic-biodegradation of the polymer nanoparticles and release of the drugs exclusively at the conditions identical to that of intracellular environment. Based on the above *in vitro* drug release kinetics, the mechanism of the drug release is proposed in figure 6f for the biodegradation of P-6 scaffold in the presence of lysosomal esterase enzyme. Hence, it may be concluded that the newly designed L-tyrosine amphiphilic nanoparticles were stable at the extracellular conditions and exhibited enzymatic-biodegradation exclusively at the intracellular compartments to deliver the anticancer drugs.

2.3.4. Cytotoxicity and Cellular Uptake

The cytotoxicity of the newly designed poly(ester-urethane) and their corresponding drug loaded nano-particles were investigated in wild-type mouse embryonic fibroblasts (WT-MEFs) cell line and cervical cancer (HeLa) cell line by MTT assay method as described earlier.[29,46] Both the cell lines were exposed to various concentrations of polymer (P-6) ranging from 1 µg/mL to 60 µg/mL and their respective histograms are shown in figures 7a and 7b. The newly designed poly(ester-urethane) was found to be less cytotoxic at these concentrations and the polymer

showing more than 60% cell viability even at high concentration of 60 μg/mL. The cytotoxicity of free CPT and DOX and their corresponding drug loaded nanoparticles were studied in WT-MEFs and HeLa cell lines by varying the drug concentrations from 0.1 to 1.0 μg/mL (see figure 2.12.c, d, e, and f). In case of normal WT-MEFs, both free CPT and DOX exhibited higher cytotoxicity compared to their drug loaded P-6 nanoparticles (see figures 2.20.c and 2.20.e). Interestingly, in cervical cancer cell line (HeLa), the free CPT and DOX became less effective and the drug loaded P-6 nanoparticles exhibited much superior cell killing (see figures 2.20.d and 2.20.f). This observation is particular interesting since the drug load nanoparticles relatively less toxic to normal cells and in the same time they could able to accomplish better cell growth inhibition in cancer cells. These results revealed that the newly designed tyrosine poly(ester-urethane)s are very good new nano-carriers for drug delivery to tumor cell lines. The in vitro cytotoxicity analysis in 2D cell experiment is employed to establish the ability of the nano-carriers to transport the drugs across the cell membrane and accomplishing cell killing. The enhanced permeability and retention effect of polymer nano-carriers would become predominant only at the cancer tissue level under in vivo experiments. Hence, the current in vitro study only proved the
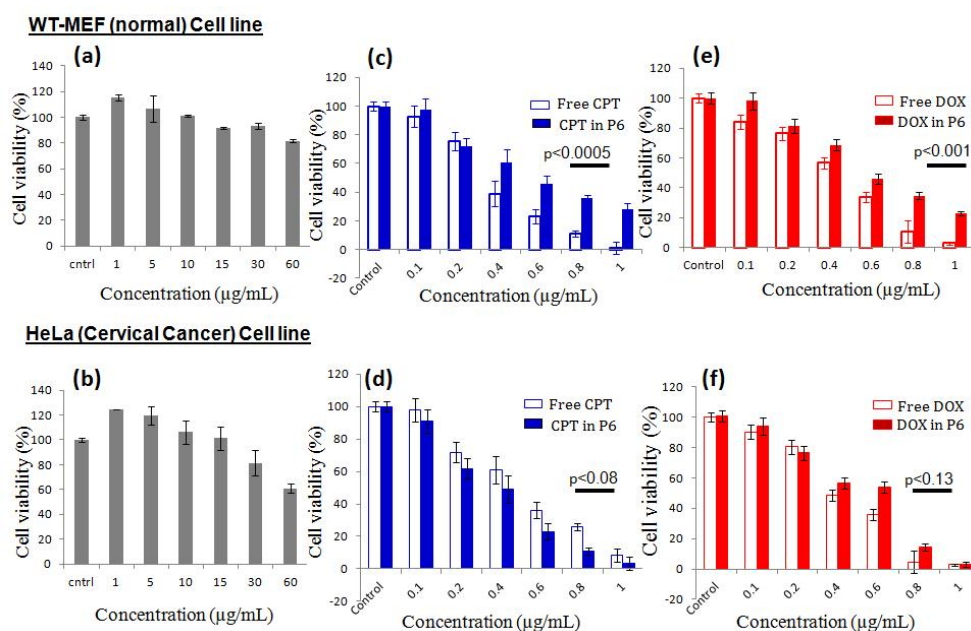
drug delivering capabilities of newly designed L-tyrosine polymer nanoparticles and establishes the proof-of-concept. Further, in vivo studies are required to see the difference among cell killing ability of free drugs and drug loaded nanoparticles.

Figure 2.20. (a) Cytotoxicity of **P-6** nascent nanoparticles in WT-MEF Cells. (b) Cytotoxicity of **P-6** nascent nanoparticles in HeLa cells. (c) Cytotoxicity of CPT loaded **P-6** loaded and free CPT in WT-MEF cells. (d) Cytotoxicity of CPT loaded **P-6** and free CPT in HeLa cells. (e) Cytotoxicity of DOX loaded **P-6** and free DOX in WT-MEF cells. (f) Cytotoxicity of DOX loaded **P-6** and free DOX in HeLa cells. (Incubation time = 72 h).
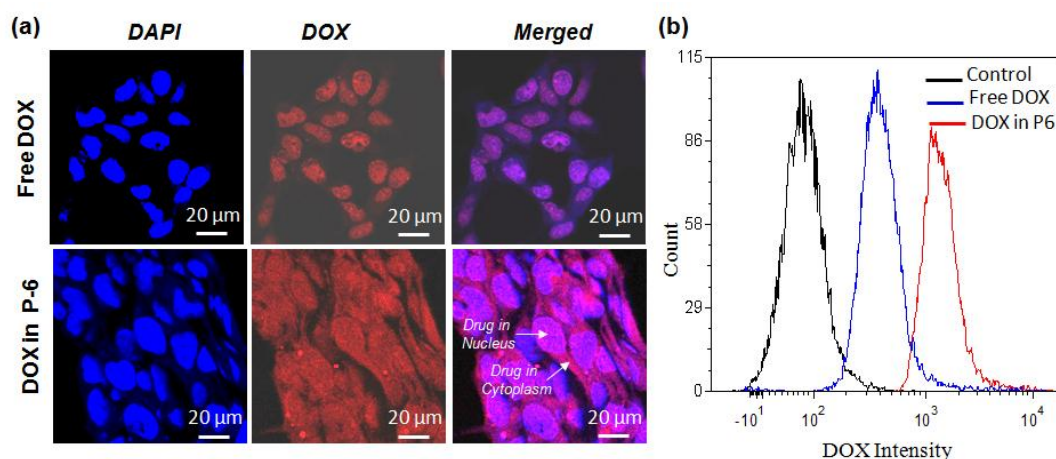
Figure 2.21. (a) CLSM images of free DOX and DOX loaded **P-6** incubated in HeLa cells. (b) Flow cytometry plots for control, free DOX, DOX loaded **P-6** nano particles in HeLa cell lines (9 h incubation, DOX concentration = 1 μg/mL and 10,000 cells were counted).

To visualize the cellular internalization of these polymer nanoparticles, HeLa and WT-MEFs treated with P-6 loaded with CPT and DOX respectively (keeping concentration of fluorescent drugs at 1 μg/mL), were subjected to confocal laser scanning microscopy (CLSM). For DOX loaded polymer samples, the cells were excited at 560 nm and images were visualized at red channel and nucleus of the cells were stained with DAPI (λ = 420 nm) and visualized at blue channel.[29] The CLSM images for free DOX and DOX loaded nanoparticles in HeLa cell line have been shown in figure 2.21. The image corresponding to the free DOX showed drugs predominantly occupied in the nucleus of the cells. This was further evident from the merged images showing magenta colour. In the case of drug loaded polymer nanoparticles, the DOX accumulated both in the cytoplasm as well as in the nuclei. This indirectly support that the nanoparticles were cleaved in the cytoplasm and subsequently delivered to nuclei.[48] This indicates the intake of P-6 nanoparticles in the cytoplasm of the cells accompanied with uptake of the DOX by nucleus. For CPT loaded polymer samples the nucleus was not stained with DAPI to avoid interference

with signals originating from CPT. The cells were excited at λ = 420 nm and visualized at blue channel.[42] The CPT loaded nanoparticle was also tested in HeLa cells. It was found that more CPT was taken by the cells while delivering them from nanoparticles than the free. The uptake of the nanoparticles loaded with anticancer drugs was further supported by flow cytometry analysis as shown in figure 8b. The plots showed maxima at 200-300 DOX relative intensity for free drug; however, the DOX loaded nanoparticles exhibited maxima at 2000-3000 DOX intensity. This revealed DOX was taken up by the cell almost 8-10 times better while delivering them form the L-tyrosine polymer nanoparticles. Comparing the cytotoxicity data in figure 7, the CSLM images in figure 8 with flow cytometry data; it can be concluded that the P-6 nanoparticles are capable of delivery the anticancer drugs into the cancer cells with high efficacy compared to their free drugs. The present investigation demonstrates one of the first examples of L-tyrosine amino acid based poly(ester-urethane)s by unique melt polycondensation route in the literature. Further, the amphiphilic poly(ester-urethane)s was explored to demonstrate their applications as efficient nano-carrier for delivering DOX and CPT in cancer treatment. Both the polymer design and synthetic methodology are highly novel; and the choice of the anticancer drugs and cancer cell lines are also not restricted to few examples demonstrated here. Currently efforts are taken to expand this synthetic methodology for wide range of other structures based on L-tyrosine for studying their structure-property relationship and exploring wide ranges of biomedical application.

2.4. Conclusion

In summarize, new classes of enzyme-responsive poly(ester-urethane)s were developed from the natural L-tyrosine amino acid by solvent free melt polycondensation process and the polymer topology was appropriately optimized to bring correct amphiphilicity to self-assemble them into aqueous nanoparticles for encapsulating and delivering multiple anticancer drugs in cancer therapy. L-Tyrosine was suitably modified into carboxylic ester and urethane monomer and subjected to dual ester-urethane melt polycondensation with commercial polyethylene glycols to yield amphiphilic poly(ester-urethane)s. The thermal properties, visco-elastic rheological properties and aqueous self-assembly of these new classes of poly(ester-urethane)s were highly specific to the polymer topology. The length of the alkyl side chain substitution in the phenolic unit and the number of hydrophilic PEG units in the

backbone played a crucial role on the aqueous self-assembly of the polymers. The polymer with long C_{16} alkyl side chain and PEG-600 segments in the main backbone was found to produce stable nanoparticles of 200 nm in size and provide appropriate geometry for encapsulation of anticancer drugs. The polymers have in-built with aliphatic ester chemical linkages in the backbone for lysosomal enzymatic biodegradation. Clinically important anticancer drugs such as DOX and CPT were loaded in these L-tyrosine nanoparticles and these drug loaded nanoparticles were stable at extracellular conditions. Exclusively, in the presence of esterase enzyme, the L-tyrosine nanoparticles underwent biodegradation to release the anticancer drugs at the intracellular compartments under physiological conditions. The cytotoxicity studies of the nascent polymers has revealed the biocompatibility of these newly designed poly(ester- urethane)s. The DOX and CPT drug loaded polymer nanoparticles showed more selectivity towards cancer cell lines in accomplishing > 95 % cell killing compared to free drugs. Confocal microscopy images and flow cytometry analysis confirmed the better uptake and cellular internalization of the drugs while delivering them form the L-tyrosine polymer nano-carriers. The present investigation opens new platform of poly(ester-urethane) polymeric materials from L-tyrosine amino acid resources for drug delivery and thermoplastic applications which are new entries in the literature.

References

1. Deming, T. Synthetic poly peptides for biomedical applications. J. *Prog. Polym. Sci.* **2007**, *32*, 858-875.

2. Zhang, P.; Cheetham, A. G.; Lin Y-a.; Cui, H. Self-Assembled Tat nanofibers as effective drug carrier and transporter. *ACS Nano,* **2013**, *7*, 5965-5977.

3. Shah, R. N.; Shah, N. A.; Lim, M. M. D. R.; Hsieh, C.; Nuber G.; S. I., Stupp. Supramolecular design of self-assembling nanofibers for cartilage regeneration. *Proc. Natl. Acad. Sci. USA,* **2010***, 107,* 3293-3298.

4. Cha. J. N.; Stucky, G. D.; Morse, D. E.; Deming, T. J. Biomimetic synthesis of ordered silica structures mediated by block copolypeptides. *Nature*, **2000**, *403*, 289-292.

5. Deming, T. J. Methodologies for preparation of synthetic block copolypeptides: materials with future promise in drug delivery. *Adv. Drug Delivery. Rev*. **2002**, *54*, 1145-1155.

6. Cai, C.; Wang, L.; Lin, J. Self-assembly of polypeptide-based copolymers into diverse aggregates. *Chem. Commun.* **2011**, *47*, 11189-11203.

7. Carlsen, A.; Lecommandoux, S. Self-assembly of polypeptide-based block copolymer amphiphiles. *Curr. Opin. Colloid Interface Sci.,* **2009**, *14*, 329-339.

8. He, C.; Zhuang, X.; Tang, Z.; Tian, H.; Chen, X. Stimuli-sensitive synthetic polypeptide-based materials for drug and gene delivery. *Adv. Healthcare Mater.* **2012**, *1*, 48-78.

9. Osada, K.; Kataoka, K. Drug and gene delivery based on supramolecular assembly of PEG-polypeptide hybrid block copolymers. *Adv. Polym. Sci.* **2006**, *202*, 113-153.

10. Bauri, K.; De, P. Polyisobutylene-based helical block copolymers with PH-responsive cationic side-chain amino acid moieties by tandem living polymerisation. *Macromolecules*, **2013**, *46*, 5861-5870.

11. Bauri, K.; Pant, S.; Roy, S. G.; De, P. Dual PH and temperature responsive helical copolymer libraries with pendant chiral leucine moieties. *Polym. Chem.* **2013**, *4*, 4052-4060.

12. Kumar, S.; Acharya, R.; Chatterji, U.; De, p. Side-chain amino-acid-based PH-Responsive sele-assembled block copolymers for drig delivery and gene transfer. *Langmuir*, **2013**, *29*, 15375-15385.

13. Mori, H.; Endo, T. Amino-acid-based block copolymer by RAFT polymerization. *Macromol. Rapid Commun.* **2012**, *33*, 1090-1107.

14. Sun, H.; Meng, F.; Dias, A. A.; Hendricks, M.; Feijen, J.; Zhong, Z. α-Amino acid containing degradable polymers as functional biomaterials: Rational design, synthetic pathway, and biomedical applications. *Biomacromolecules*, **2011**, *12*, 1937-1955.

15. Sun, H.; Cheng, R.; Deng, C.; Meng, F.; Dias, A. A.; Hendriks, M.; Feijen, J.; Zhong, Z. Enzymatically and reductively degradable α-amino acid-based poly(ester amide)s: Synthesis, cell compatibility, and intra cellular drug delivery. *Biomacromolecules*, **2015**, *16*, 597-605.

16. Deng, M.; Wu, J.; Reinhart-King, C. A.; Chu, C. C. Synthesis and characterization of biodegradable poly(ester amide)s with pendant amine functional groups and In Vitro cellular response. *Biomacromolecules*, **2009**, *10*, 3037-3047.

17. Lu, W.; Wang, X.; Cheng, R.; Deng, C.; Meng, F.; Zhong, Z. Biocompatible and bioreducible micelles fabricated from novel α-amino acid-based poly(disulfide urethane)s: Design, synthesis and triggered Doxorubicin release. *Polym. Chem.* **2015**, *6*, 6001-6010.

18. Kihara, N.; Kushida, Y.; Endo, T. Optically active poly(hydroxy urethane)s derived from cyclic carbonate and L-Lysine derivatives. *J. Polym. Sci., Part A: Polym. Chem.* **1996**, *34*, 2173-2179.

19. Cutlar, L.; Zhou, D.; Gao, Y.; Zhao, T.; Greiser, U.; Wang, W.; Wang, W. Highly branched poly(β-Amino esters): Synthesis and application in gene delivery. *Biomacromolecules*, **2015**, *16*, 26098-2617.

20. Yu, J.; Lin, F.; Gao, Y.; Becker, M. L. Phenylalanine-based poly(ester urea): Synthesis, characterization, and *in vitro* degradation. *Macromolecules*, **2013**, *47*, 121-129.

21. He, M.; Potuck, A.; Kohn, J. C.; Fung, K.; Reinhart-King, C. A.; Chu, C. C. Self-assembled cationic biodegradable nanoparticles from pH-Responsive amino acid based poly(ester urea urethane)s and their application as a drug delivery vehicle. *Biomacromolecules*, **2016**, *17*, 523-537.

22. Huang, F.; Cheng, R.; Meng, F.; Deng, C.; Zhong, Z. Micelles based on acid degradable poly(acetal urethane): Preparation, pH-Sensitivity, and triggered intracellular drug release. *Biomacromolecules*, **2015**, *16*, 2228-2236.

23. Wu, J.; Zhao, L.; Xu, X.; Bertrand, N.; Choi, W.; Yameen, B.; Shi, J.; Shah, V.; Mulvale, M.; MacLean, J. L.; Farokhzad, O. C. Hydrophobic Cysteine Poly(disulfide)-based Redox-Hypersensitive nanoparticle platform for cancer theranostics. *Angew. Chem. Int. Ed*. **2015**, *54*, 9218-9223.

24. Anantharaj S.; Jayakannan, M. Polymers from Amino acids: Development of ester-urethane melt condensation approach and mechanistic aspects. *Biomacromolecules,* **2012**, *13*, 2446-2455.

25. Anantharaj S.; Jayakannan, M. Amyloid-like hierarchical helical fibrils and conformational reversibility in functional polyesters based on L-amino acids. *Biomacromolecules,* **2015**, *16*, 1009-1020.

26. Anantharaj S.; Jayakannan, M. Catalyst and temperature driven melt polycondensation reaction for helical poly(ester-urethane)s based on natural L-amino acids. *J. Polym. Sci., Polym Chem.* **2016**, *54*, 1065-1077.

27. Anantharaj S.; Jayakannan, M. Melt polycondensation approach for reduction degradable helical polyester based on L- Cystine. *J. Polym. Sci., Polym Chem.* **2016**, *54*, 2864-2875.

28. Aluri, R.; and Jayakannan, M. One-pot two polymers: ABB' melt polycondensation for linear polyesters and hyperbranched poly(ester-urethane)s based on natural L-amino acids. *Polym. Chem*. 2015, **6,** 4641-4649.

29. Saxena, S.; Jayakannan, Enzyme and pH dual responsive L-Amino acid based biodegradable polymer nanocarrier for multi drug delivery to cancer cells. M. *J. Polym. Sci., Polym Chem.* **2016**, *54*, 3279-3293.

30. Magno, M. H. R.; Kim, J.; Srinivasan, A.; McBride, S.; Bolikal, D.; Darr, A.; Hollinger, J, O.; Kohn, J. Synthesis, degradation and biocompatibility of tyrosine-derived polycarbonate scaffolds. *J. Mater. Chem.* **2010**, *20*, 8885-8893.

31. Tangpasuthadol, V.; Shefer, A.; Hooper, K. A.; Kohn, J. Thermal properties and physical ageing behaviour of tyrosine-derived polycarbonates. *Biomaterials*, **1996**, *17*, 463-468.

32. Yu, C.; Kohn, J. Tyrosine-PEG-derived poly(ether carbonate)a as new biomaterials Part 1: Synthesis and evaluation. *Biomaterials*, **1999**, *20*, 253-264.

33. Sheihet, L.; Piotrowska, K.; Dubin, R. A.; Kohn, J.; Devore, D. Effect of tyrosine-derived triblocks copolymer compositions on nanosphere self-assembly and drug delivery. *Biomacromolecules*, **2007**, *8*, 998-1003.

34. Aamer, K. A.; Genson, K. A.; Kohn, J.; Becker, M. L. Impact of polymer-bound Iodine on Fibronectin adsorption and Osteoblast cell morphology in radiopaque medical polymers: Tyrosine-derived polycarbonate blends as a model system. *Biomacromolecules*, **2009**, *10*, 2418-2426.

35. Tziampazis, E.; Kohn, J.; Moghe, P. V. PEG-variant biomaterials as selectively adhesive protein templates:model surfaces for controlled cell adhesion and migration. *Biomaterials*, **2000**, *21*, 511-520.

36. James, K.; Levene, H.; Parsons, J. R.; Kohn, J. Small changes in polymer chemistry have a large impact on the bone-implant interface: evaluation of a series of degradable tyrosine derived polycarbonates in bone defects. *Biomaterials*, **1999**, *20*, 2203-2212.

37. Shpaisman, N.; Sheihet, L.; Bushman, J.; Winters, J.; Kohn, J. One-step synthesis of biodegradable Curcumin-derived hydrogels as potential soft tissue fillers after breast cancer surgery. *Biomacromolecules*, **2012**, *13*, 2279-2286.

38. Sun, Y.; Hou, Y.; Zhou, X.; Yuan, J.; Wang, J.; Lu, H. Controlled synthesis and enzyme-induced hydrogelation of poly(L-phosphotyrosine)s via ring-opening polymerization of α-amino acid N-carboxyanhydride. *ACS Macro. Lett*. **2015**, *4*, 1000-1003.

39. Yang, Y.; Zhou, Y.; Ge, J.; Wang, Y.; Chen, X. Synthesis, characterization and infrared emissivity property of optically active polyurethane derived from tyrosine. *Polymer*, **2011**, *52*, 3745-3751.

40. Nagai, A.; Ishikawa, J.; Kudo, H.; Endo, T. Synthesis of optically active polyurethanes by self-polyaddition of tyrosine-based monomers. *J. Polym. Sci., Polym Chem.* **2004**, *42*, 1143-1153.

41. Lin, F.; Yu, J.; Tang, W.; Zheng, J.; Xie, S.; Becker, M. L. Postelectrospinning "click" modification of degradable amino acid-based poly(ester urea) nanofibers. *Macromolecules*, **2013**, *46*, 9515-9525.

42. Pramod, P. S.; Takamura, K.; Chaphekar, S.; Balasubramanian, N.; Jayakannan, M. Dextran Vesicular Carriers for Dual Encapsulation of Hydrophilic and Hydrophobic Molecules and Delivery into Cells. *Biomacromolecules* **2012**, *13* , 3627–3640.

43. Pramod, P. S.; Shah, R.; Chaphekar, S.; Balasubramanian, N.; Jayakannan, M. Polysaccharide Nano-vesicular Multidrug Carrier for Synergistic Killing of Cancer Cells. *Nanoscale* **2014**, *6*, 11841-11855.

44. Jayakannan, M.; Ramakrishnan, S. Segmented polyethylene oxides: A new class of polyethers prepared via melt transetherification. *J. Polym. Sci., Polym Chem.* **2001**, *39*, 1615-1628.

45. Malhotra, M.; Surnar, B.; Jayakannan, M. Polymer Topology Driven Enzymatic-Biodegradation in Polycaprolactone Block and Random Copolymer Architectures for Drug Delivery to Cancer Cells, *Macromolecules*, **2016**, *49*, 8098-8112.

46. Kashyap, S.; Singh, N.; Surnar, B. Jayakannan, M. Enzyme and Thermal Dual Responsive Amphiphilic Polymer Core-shell Nanoparticle for Doxorubicin Delivery to Cancer Cells. *Biomacromolecules,* **2016**, *1*, 384-398.

47. Kulkarni, B.; Surnar, B.; Jayakannan, M. Dual Functional Nanocarrier for Cellular Imaging and Drug Delivery in Cancer Cells Based on π-

Conjugated Core and Biodegradable Polymer Arms. *Biomacromolecules,* **2016**, *17*, 1004-1016.

48. Surnar, B.; Jayakannan, M. Structural Engineering of Biodegradable PCL Block Copolymer Nano-assemblies for Enzyme-Controlled Drug Delivery in Cancer Cells. *ACS Biomater. Sci. Eng.,* **2016**, *2*, 1926-1941.

Chapter 3

Enzyme and Thermal Dual Responsive L-Tyrosine Poly(ester-urethane) Nanocarriers for drug delivery to Cancer Cells

Abstract

Thermo and enzyme-responsive poly(ester-urethane)s from L-tyrosine amino acid were developed and their aqueous self-assembled nanostructures were employed as multiple-drug nano-carriers to cancer cells. L-Tyrosine amino acid was tailor-made into multifunctional monomer by carefully substituting long PEG-chain at the phenolic position and converting the amine and carboxylic acid functional groups into urethane and carboxylic esters, respectively. The monomer was subjected to melt dual ester-urethane polycondensation with different linear and cyclic aliphatic diols to yield hydrophilic PEG side chain substituted poly(ester-urethane)s. The amphiphilic polymer design with appropriate hydrophilic-hydrophobic balance was self-assembled into 100 ± 10 nm nanoparticles in the aqueous medium. Interestingly, these polymers were completely soluble or dispersible in water at ambient temperature and they turned into turbid solution at higher temperature with respect to lower critical solution temperature (LCST) behaviours. This thermo-responsive LCST phase transition of the poly(ester-urethane)s were extensively investigated by variable temperature transmittance, DLS and ^{1}H-NMR studies. Polymers with C_{12} main chain in the backbone and PEG-350 side chain showed LCST at 44 °C which was very near to cancer tissue temperature for drug delivery applications. The self-assembled polymer nanoparticles were found to be capable of encapsulating wide ranges of anticancer drugs such as DOX and CPT. *In vitro* drug release studies revealed that the polymer nanoparticles were stable at physiological conditions and they underwent to disassembly at temperature near to cancer tissue temperature. Further, the polyester-urethane linkages in the polymer nanoparticles were found to be responsive to biodegrade in the presence of lysosomal esterase enzyme at the intracellular level. Cytotoxicity of these poly(ester-urethane)s were investigated in tumor tissue (MCF 7 and HeLa) and normal cell lines (WT-MEFs). Drug loaded polymer nanoparticles showed better cytotoxic effects than their free drugs. Confocal images and Flow cytometry confirmed the cellular internalisation of the drug loaded nanoparticles.

3.1. Introduction:

During the past decade increasing attention has been paid to the development of stimuli responsive polymers, also called "intelligent" or "smart" polymers, which can show obvious and abrupt changes in response to small variations in environmental conditions. Environmentally responsive polymers are capable of exhibiting fast and reversible changes in physical properties and/or chemical structures by inducing small change in external environment. Various types of stimuli such as pH[1-4], temperature[5-7], light irradiation[8], redox potential, ionic strength, etc., have been employed to induce conformational or phase changes of polymeric materials. Among the various stimuli, thermoresponsive polymers with the ability to respond to changes in temperature have led to the development of vast number of applications in areas spanning biotechnology, biomedicine, and nanotechnology for many potential applications including biomimetic actuators, immobilized biocatalyst, smart surfaces, bioseparation, and drug delivery systems[9-11]. Tumor tissue possess a unique physicochemical properties including vascular abnormalities[12-13], weak acidity[14-15], abnormal temperature gradients[16-18], over expressed proteins and enzymes[19-20] etc. on the other hand, upon cellular uptake of nanoparticles within tumor tissues, the nanoparticles exposed to a drastically different intracellular microenvironments such as acidic pH inside endosomes, and lysosmes[21], over expression of enzymes in lysosmes and oxidative microenvironment in mitochondria[22-24].
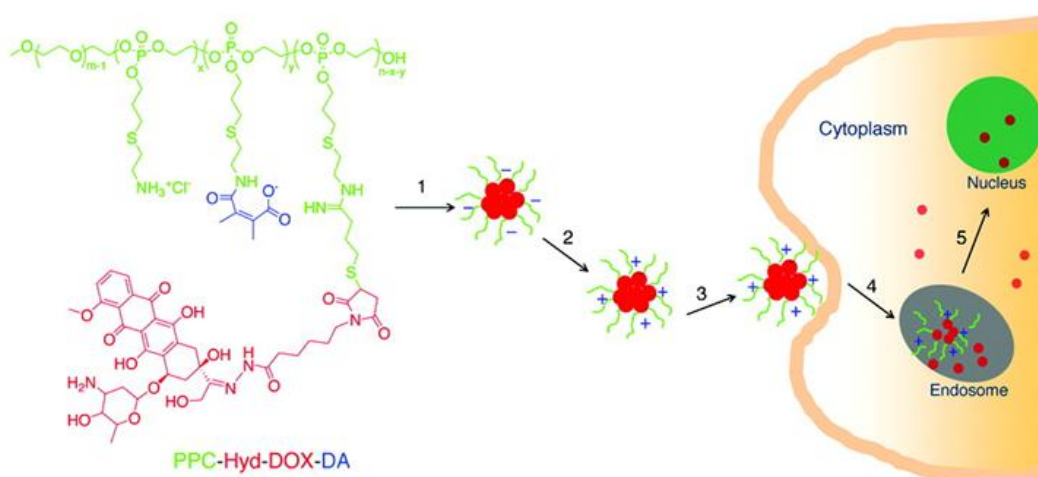
Figure 3.1. pH-Responsive polymer-doxorubicin conjugate and its pH triggered intracellular drug release (adopted from Jin-Zhi et al. *J. Am. Chem. Soc*, **2011**, *133*, 17560-17563).

For exploitation of this unusual cancer tissue environment researchers have developed a variety of stimuli responsive nanocarriers include pH responsive[25-29], enzyme responsive[30], reductive environment responsive[31-32] and temperature responsive nanocarriers[33-35]. Among these, temperature responsive polymers have been studied extensively because of their potential in vivo applications and also it is easy to control the temperature both in in-vitro and in-vivo. One of the most intensively studied thermo responsive polymer is PNIPAAM, which shows a temperature induced collapse from an extended coil to globular structure in water upon heating above 32 °C[36-37]. However the use of PNIPAAM in biomedical applications is problematic because they are toxic and non-biodegradable. To overcome this, researchers has developed alternative polymers with
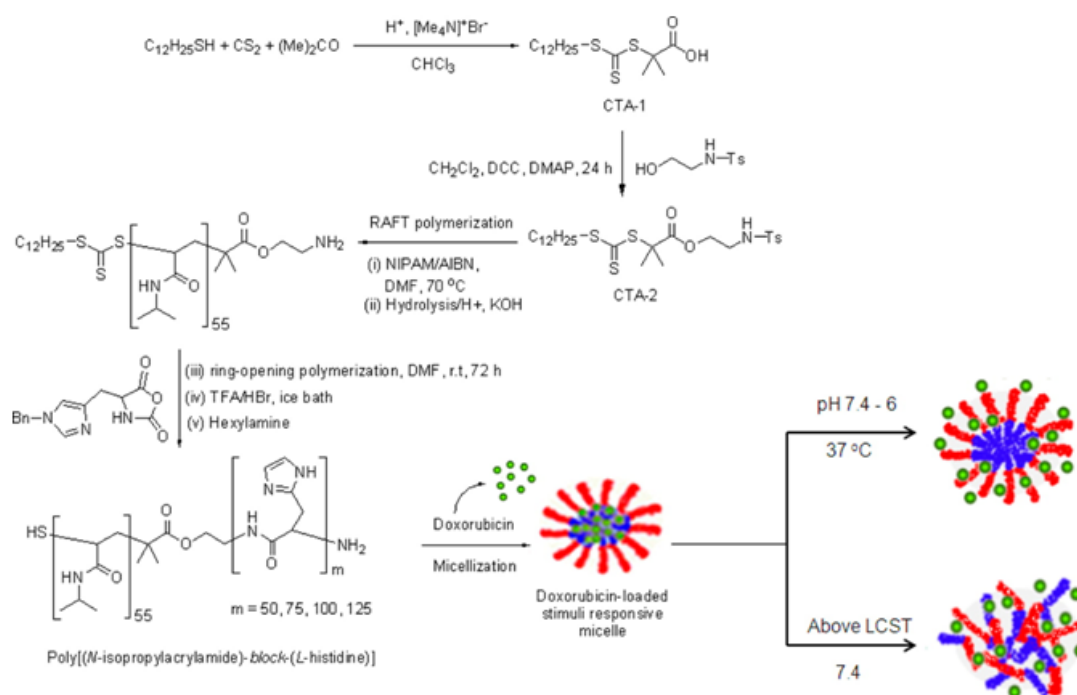
Figure 3.2. Temperature and pH-Responsive Poly(N-isopropyl acrylamide)-b-poly(L-histidine) block copolymers for the controlled delivery of doxorubicin into liver carcinoma (adopted from Renjith et al. *Biomacromolecules* **2013**, *14*, 1434-1443).

polyethylene glycols substituted with acrylates/methacrylates[38-39], PEG being a non-cytotoxic, aqueous soluble, and inexpensive material has extensively used in delivery of various bioactive compounds. PNIPAAM copolymerized with PEG[38-39], poly lactide[40], poly methyl methacrylate[41], poly styrene[42], poly vinyl methacrylate, poly (lactide-co-glycolide)[41] were some of the thermoresponsive polymers developed with varying LCST values. PNIPAMM also copolymerized with histidine and elastine like poly peptide to bring biocompatible nature in the polymer[43]. Side chain amino acid based PNIPAAM polymers were synthesized to achieve fluorescent labeled thermoresponsive nanoparticles. From our research group Kashyap et al. has reported enzyme and thermal dual responsive polymer nanocarriers based on acrylated 3-pentadecyl phenol copolymerised with acrylated oligoethylene glycol. And their anti cancer drug loaded nanoparticles were administered to cancer cells[44].

Recently Hoogenboom et.al, has reviewed supramolecular control over thermoresponsive polypeptides, polypeptoids, poly(2-oxazoline)s, and discussed their applications[45]. Amino acids are playing a vital role in all biological functions especially L-tyrosine amino acid is one of the most versatile amino acids because of the physicochemical character and the chemical reactivity of its side chain phenolic moiety. Since tyrosine side chain can be involved in hydrogen bonding, π- π interactions and cation-π interactions, tyrosine residues are widely used in the molecular recognition site of antibodies. Tyrosine residues also provide attractive targets for protein modifications, as these hydrophobic residues are present with intermediate frequency on protein surfaces, and the reactivity of the phenolic group is orthogonal to that of cysteine, lysine, and carboxylate containing residues. Incorporation of the L-Tyrosine amino acid in to the synthetic polymers benefits polymeric nano-materials interms of providing much higher complexity due to their amphoteric nature, chiral recognition, response to stimuli, as well as their viability to self-assemble in to secondary and high-order hierarchical structures[46].

In recent years extensive research has focused on the development of biodegradable/biocompatible stimuli responsive nanocarriers that can solubilise, stabilise against physiological conditions and release the loaded drug molecules at targeted site. Biodegradable and thermoresponsive materials based on renewable resources with well defined structures are more desirable for Drugdelivery applications. Stefan and co-workers recently reported the fine tuned thermoresponsive

functional poly(ε-caprolactone)s by ring opening polymerisation and showed loading and releasing abilities for a hydrophobic anti cancer drug doxorubicin[47-51]. other than this there are no thermo responsive and biodegradable polymeric systems were reported for anticancer drug delivery in the literature. To address this challenge in this chapter we have developed a biodegradable, non-toxic, well defined poly(ester-urethane)s from naturally available L-tyrosine amino acid by solvent free melt polycondensation polymerisation. The biodegradability of these amino acid based poly(ester-urethane)s potentiate themselves as a more promising drug delivery candidate material than the PNIPAM based polymers. Moreover due to the flexibility and feasibility of chemical modifications of these amino acid polymers the properties of their nanoparticles can be tailored to optimize delivery efficacy and maximize the therapeutic effect. Due to their combined thermoresponsive and biodegradable properties this family of polymers constitutes a new direction in synthetic polymeric nanocarriers for controlled drug delivery applications.
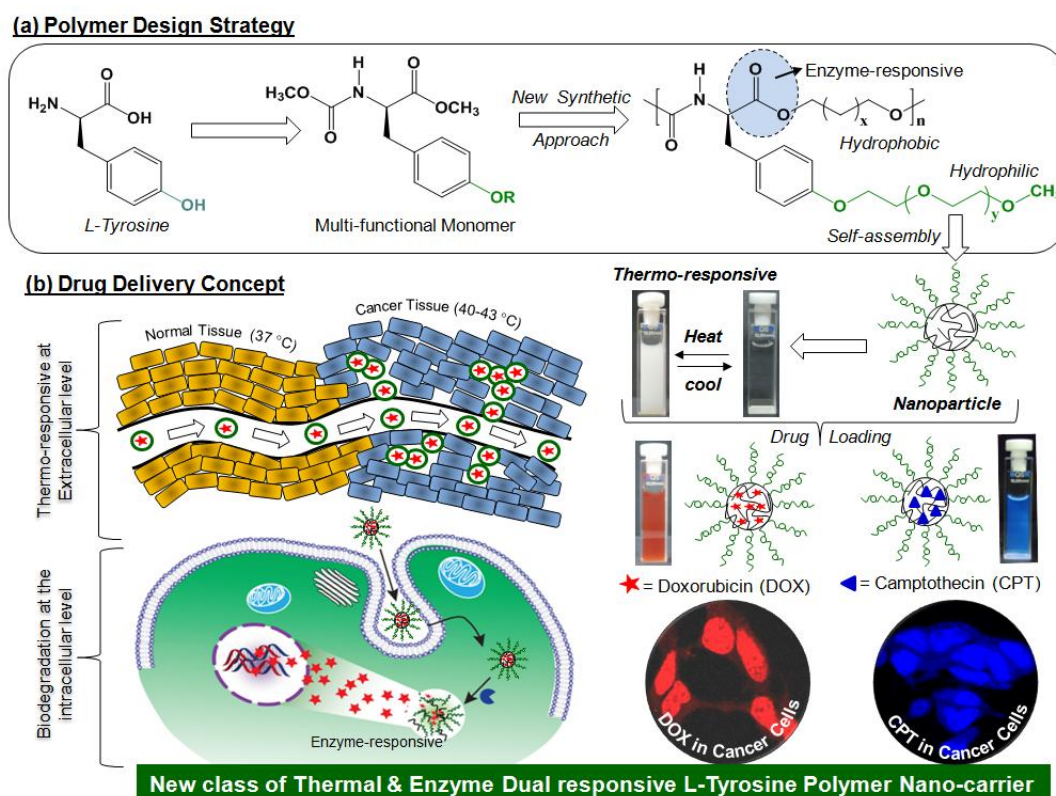
Figure 3.3. Designing of thermo and enzyme dual responsive of L-tyrosine based amphiphilic poly(ester-urethane)s and elucidation of their anti cancer drug delivery abilities

In this chapter, new classes of thermal and enzyme-responsive L-tyrosine amino acid based poly(ester-urethane)s were prepared and their anticancer drug delivery abilities were established. This polymer design strategy and drug delivery concept is shown in the figure 3.1. Anticancer drugs doxorubicin and camptothecin has incorporated with good loading efficiencies. In-vitro studies have confirmed that these polymeric nanoparticles are responsive to both esterase enzyme and temperature, drug release patterns has evident that polymer nanoparticles are stable at physiological conditions (PH 7.4 PBS, 37 °C) and they undergo bio-degradation in the presence of esterase enzyme (stimuli-1) and thermoresponsive drug release studies has confirmed that at 37 °C (healthy tissue temperature) polymeric nano particles are highly stable and they undergo selective degradation at 42 °C (cancer tissue temperature, stimuli-2)   Cytotoxicity studies and cellular internalization studies has carried out in normal wild type mouse embryonic fibroblast cell lines (WT-MEFs) and human breast cancer cell lines (MCF 7). Results are revealing that the drug loaded polymeric nano particles are showing excellent cytotoxicity towards the cancer cells compared to free drugs and cellular internalization by confocal and flowcytometry confirms the better delivery of drugs by polymer nanoparticles compared to their free form.

3.2. Experimental procedure:

3.2.1 Materials: L-Tyrosine, PEG-mono methyl ether-350, 1,6 hexane diol, 1,8 octane diol, 1,10-decane diol, 1,12 dodecane diol, 1,4 cyclohexane dimethanol, tosyl chloride, titanium tetrabutoxide (Ti(OBu)$_4$), DOX.HCl, Camptothecin and horse liver esterase enzyme were purchased from Aldrich chemicals and used without further purification. Other reagents and solvents were purchased locally and purified prior to use.

3.2.2. General procedure: All NMR spectra were recorded using 400-MHz JEOL NMR spectrophotometer in CDCl$_3$ containing TMS as internal standard. Molecular weights of the polymers were determined by Gel permeation chromatography (GPC) using Viscotek VE 1122 pump, Viscotek VE 3580 RI detector and Viscotek VE 3210 UV/Vis detector. Tetrahydrofuran (THF) used as mobile phase and instrument has calibrated with polystyrene standards. Thermal stability of the polymers and monomers were analyzed with Perkin Elmer thermal analyzer STA 6000 model at a heating rate of 10 ℃/min under nitrogen atmosphere. Thermal analysis of the polymers was performed using TA Q20 Differential scanning calorimeter. Polymers were heated and cooled at 10 ℃/min under nitrogen atmosphere and their thermograms were recorded. Rheological measurements has carried out in Anton paar MCR 302 instrument by using 15 mm diameter parallel plate, measurements has carried out in molten state. Absorption spectra were recorded by Perkin-Elmer Lambda 45 UV-Visible spectrophotometer and steady-state emission studies were done by a SPEX Fluorolog HORIBA JOBIN VYON fluorescence spectrophotometer. Dynamic light scattering (DLS) studies has carried out by using Nano ZS-90 apparatus equipped with 633 nm red laser (At 90º angle) from Malvern instruments, in LCST measurements histograms were recorded by heating and cooling the samples from 30 °C to 80 °C. Microscopy images has recorded with Zeiss ultra plus scanning electron microscope (FE-SEM), Veeco Nanoscope IV instrument (AFM), Carl Zeiss Axiovert 200 microscope (fluorescence microscope) and LSM 710 instrument (confocal microscope), AFM images has recorded in tapping mode.

3.2.3. Synthesis of Monomers

Synthesis of C-methyl ester N-methyl carbamate of tyrosine (1): To a suspension of L- tyrosine (10.0 g, 55.0 mmoL) in methanol (80 mL); thionylchloride (7.96 mL, 110.4 mmoL) was added drop wise at 0 $^{\circ}$C. The reaction mixture was refluxed for 12 hours under the nitrogen atmosphere. The solvent and excess thionylchloride was removed by distillation. The residue was dried under vacuum to get the product as white solid. The solid mass was stirred in sodium carbonate solution (15 wt%, 70 mL) at 0 ºC. To this ice cold solution, methyl chloroformate (5.6 mL, 74.0 mmoL) in dichloromethane (70 ML) was added drop wise and the reaction was continued for 12 h at 25 °C. The reaction mixture was extracted in to dichloromethane and the organic layer was dried over anhydrous Na_2SO_4. The solid product was further purified by passing through silica gel column using chloroform, methanol (9:1 v/v) as eluent. Yield = 14.0 g (90 %). ^{1}H-NMR (400 MHz, CDCl$_3$) δ ppm: 3.00-3.04 (m, 2H, -C$_6$H$_5$C**H$_2$**), 3.67 (S, 3H, -NH-COOC**H$_3$**), 3.73 (S, 3H, -COOC**H$_3$**), 4.60 (S, 1H, C$_6$H$_5$CH$_2$C**H**), 5.25 (S, 1H, N**H**) 6.81-6.83 (m, 2H, C$_6$**H$_5$**), 7.01-7.03 (m, 2H, C$_6$**H$_5$**). ^{13}C-NMR (100 MHZ, CDCl$_3$) δ ppm: 172, 156, 155, 130, 127, 115, 54, 52, 37. FT-IR (cm^{-1}): 642, 741, 825, 985, 1058, 1107, 1216, 1357, 1444, 1515, 1609, 1688, 1737, 2953, 3011, 3299, 3345, 3632, 3684, 3737, 3895, 3932. HRMS (ESI+): m/z calcd. for C$_{12}$H$_{15}$NO$_5$ [M+Na]$^+$: 276.0847; found= 276.0857.

Synthesis of Polyethylene glycol monomethyl ether-tosylate (2): Typical procedure for tosylation of glycols was described for polyethylene glycol monomethyl ether (PEG-350). To a solution of PEG-350 (15g, 42.8 mmoL) in dichloromethane (50 mL), triethyl amine (18 mL, 128.0 mmoL) was added and stirred for 10 minutes, tosyl chloride (16.28 g, 85.7 mmoL) in dichloromethane (50 mL) was added drop by drop at ice cold condition to the reaction mixture, reaction continued for 12 hours at 25 ˚C. Solvent was evaporated by rota evaporator and the crude product was purified by column chromatography, 10 % chloroform-methanol as mobile phase and purified product was dried by vacuum oven. Yield: 18.2 g (87 %). ^{1}H-NMR (400 MHz, CDCl$_3$) δ ppm: 2.44 (s, 3H, -C$_6$H$_5$-C**H$_3$**), 3.37 (s, 3H, -O-CH$_2$-CH$_2$-O-C**H$_3$**), 3.58-3.68 (m, 26H, -O-C**H$_2$**-C**H$_2$**-O-), 4.15 (t, 2H, -CH$_2$-C**H$_2$**-O-SO$_2$-C$_6$H$_5$-), 7.78-7.80 (d, 2H, -

C$_6$**H$_5$**-), 7.33-7.35 (d, 2H, -C$_6$**H$_5$**-). ^{13}C-NMR (400 MHz, CDCl$_3$) δ ppm: 144, 132, 129, 127, 71, 70, 69, 68, 58, 21.

Synthesis of O-PEG tyrosine monomer (3): Typical procedure for O-substitution of tyrosine was described for PEG-350 substituted monomer. To a suspension of tyrosine monomer (1) (8.25 g, 32.6 mmoL), in dry acetonitrile (80 mL), K$_2$CO$_3$ (14.39 g, 104.3 mmoL) was added and nitrogen gas was purged for 15 minutes and refluxed for 30 minutes, to this PEG-350 tosylate (13.68 g, 27.1 mmoL) in dry acetonitrile (20 mL) was added drop wise and reaction was refluxed for 48 hours under the nitrogen atmosphere. Progress of the reaction was monitored by thin layer chromatography after the completion of reaction it was filtered through sintered funnel, solvent was evaporated by rota evaporator, the crude product was purified by column chromatography in 20 % methanol-chloroform system and the purified product was dried under vacuum to get a white solid product. Yield: 9.0 g (94 %). ^{1}H-NMR (400 MHz, CDCl$_3$) δ ppm: 3.00-3.04 (m, 2H, -C6H5C**H$_2$**), 3.37 (S, 3H, -OC**H$_3$**), 3.53-3.56 (t, 2H, O-C**H$_2$**-CH$_3$), 3.67 (S, 3H, -NH-COOC**H$_3$**), 3.71 (S, 3H, -COOC**H$_3$**), 3.66 (t, 2H, O-C**H$_2$**-CH$_2$-O-), 3.68 (t, 2H, O-C**H$_2$**-CH$_2$-O-), 3.73 (t, 2H, O-C**H$_2$**-CH$_2$-O-), 3.84 (t, 2H, O-CH$_2$-C**H$_2$**-O-), 4.08-4.10 (t, 2H, O-C**H$_2$**-CH$_2$-O-), 4.60 (S, 1H, C$_6$H$_5$CH$_2$C**H**), 5.14 (S, 1H, N**H**), 6.81-6.83 (m, 2H, C$_6$**H$_5$**), 7.01-7.03 (m, 2H, C6**H$_5$**). ^{13}C-NMR (100 MHZ, CDCl$_3$) δ ppm: 172, 157, 156, 130, 127, 114, 71, 70, 69, 67, 58, 54, 52, 37.

3.2.3. Synthesis of Polymers

Synthesis of L-tyrosine poly(ester-urethane)s (P-12): L-Tyrosine poly(ester-urethane)s were synthesized by using the similar procedure as reported earlier. Tyrosine monomer (**3**) (0.5 g, 0.86 mmoL), 1,12-dodecane diol (0.17 g, 0.86 mmoL), titanium tetrabutoxide (0.003 g, 0.008 mmoL). Yield: 0.59 g (97 %). ^{1}H NMR (400 MHz, CDCl$_3$) δ ppm: 1.27 (bs, 18H, -C**H$_2$**-C**H$_2$**-), 1.60 (m, 4H, -C**H$_2$**-C**H$_2$**-), 1.83 (m, 4H, -C**H$_2$**-C**H$_2$**-), 3.00-3.04 (m, 2H, -C$_6$H5C**H$_2$**), 3.38 (s, 3H, -OC**H$_3$**), 3.56 (m, 2H, -OC**H$_2$**CH$_2$O-), 3.60-3.67 (m, 24H, -OC**H$_2$**C**H$_2$**O-), 3.70-3.74 (m, 2H, -OC**H$_2$**CH$_2$O-), 3.84 (m, 2H, -OC**H$_2$**CH$_2$-), 4.08-4.13 (m, 6H, -OC**H$_2$**CH$_2$-, –COOC**H$_2$-,** and **-NHCOOC**H$_2$**-**), 4.56 (S, 1H, C$_6$H$_5$CH$_2$C**H-**), 5.12 (S, 1H, N**H-**), 6.81-6.83 (m, 4H,

C$_6$**H$_5$-**), 7.01-7.03 (m, 4H, C6**H$_5$-**). ^{13}C-NMR (100 MHZ, CDCl$_3$) δ ppm: 171, 157, 155, 130, 127, 114, 71, 70, 69, 67, 65, 58, 54, 37, 32, 29, 25.

P-6: Tyrosine monomer (**3**) (0.226 g, 0.38 mmoL), 1,6 hexane diol (0.045 g, 0.38 mmoL), titaniumtetrabutoxide (0.001 g, 0.003 mmoL, 1 mole %). Yield : 0.22 g (92%). ^{1}H NMR (400 MHz, CDCl$_3$) δ ppm: 1.35 (bs, 2H, -CH$_2$-**CH$_2$**-), 1.60 (bs, 2H, -CH$_2$-**CH$_2$**-), 1.99 (bs, 4H, -CH$_2$-**CH$_2$**-), 3.00-3.04 (m, 2H, -C6H5C**H$_2$**), 3.38 (S, 3H, -OC**H$_3$**), 3.55 (m, 2H, -OC**H$_2$**C**H$_2$**O-), 3.65-3.67 (m, 24H, -OC**H$_2$**C**H$_2$**O-), 3.70-3.74 (m, 2H, -OC**H$_2$**C**H$_2$**O-), 3.84 (m, 2H, -OC**H$_2$**CH$_2$-), 4.08 (m, 6H, -OC**H$_2$**CH$_2$-, − COOC**H$_2$-,** and **-**NHCOOC**H$_2$-**), 4.56 (S, 1H, C$_6$H$_5$CH$_2$C**H-**), 5.12 (S, 1H, N**H-**), 6.81-6.84 (m, 2H, C$_6$**H$_5$-**), 7.01-7.02 (m, 2H, C6**H$_5$-**). ^{13}C-NMR (100 MHZ, CDCl$_3$) δ ppm: 172, 157, 156, 155, 130, 127, 114, 71, 70, 69, 67, 65, 58, 54, 52, 37, 28, 25.

P-8: Tyrosine monomer (**3**) (0.21 g, 0.35 mmoL), 1,8 Octane diol (0.052 g, 0.35 mmoL), titaniumtetrabutoxide (0.001 g, 0.003 mmoL, 1 mole %). Yield : 0.22 g (94%). ^{1}H NMR (400 MHz, CDCl$_3$) δ ppm: 1.31 (bs, 6H, -**CH$_2$**-**CH$_2$**-), 1.60 (m, 4H, -**CH$_2$**-**CH$_2$**-), 2.06 (m, 2H, -**CH$_2$**-**CH$_2$**-), 3.00-3.03 (m, 2H, -C6H5C**H$_2$-**), 3.38 (s, 3H, -OC**H$_3$**), 3.56 (m, 2H, -OC**H$_2$**C**H$_2$**O-), 3.60-3.67 (m, 24H, -OC**H$_2$**C**H$_2$**O-), 3.70-3.74 (m, 2H, -OC**H$_2$**C**H$_2$**O-), 3.84 (m, 2H, -OC**H$_2$**CH$_2$-), 4.06-4.10 (m, 6H, -OC**H$_2$**CH$_2$-, − COOC**H$_2$-,** and **-**NHCOOC**H$_2$-**), 4.56 (S, 1H, C$_6$H$_5$CH$_2$C**H-**), 5.12 (S, 1H, N**H-**), 6.81-6.84 (m, 4H, C$_6$**H$_5$-**), 7.01-7.03 (m, 4H, C6**H$_5$-**). ^{13}C-NMR (100 MHZ, CDCl$_3$) δ ppm: 171, 157, 155, 130, 127, 114, 71, 70, 69, 67, 65, 58, 54, 37, 32, 29, 25.

P-10: Tyrosine monomer (**3**) (0.203 g, 0.34 mmoL), 1,10 decane diol (0.06 g, 0.34 mmoL), titaniumtetrabutoxide (0.001 g, 0.003 mmoL, 1 mole %). Yield : 0.22 g (96%). ^{1}H NMR (400 MHz, CDCl$_3$) δ ppm: 1.28 (bs, 10H, -**CH$_2$**-**CH$_2$**-), 1.60 (m, 4H, -**CH$_2$**-**CH$_2$**-), 1.93 (m, 2H, -**CH$_2$**-**CH$_2$**-), 3.00-3.04 (m, 2H, -C6H5C**H$_2$**), 3.38 (s, 3H, -OC**H$_3$**), 3.56 (m, 2H, -OC**H$_2$**C**H$_2$**O-), 3.60-3.67 (m, 24H, -OC**H$_2$**C**H$_2$**O-), 3.70-3.74 (m, 2H, -OC**H$_2$**C**H$_2$**O-), 3.84 (m, 2H, -OC**H$_2$**CH$_2$-), 4.08-4.13 (m, 6H, -OC**H$_2$**CH$_2$-, − COOC**H$_2$-,** and **-**NHCOOC**H$_2$-**), 4.58 (S, 1H, C$_6$H$_5$CH$_2$C**H-**), 5.13 (S, 1H, N**H-**), 6.81-6.83 (m, 4H, C$_6$**H$_5$-**), 7.01-7.03 (m, 4H, C6**H$_5$-**). ^{13}C-NMR (100 MHZ, CDCl$_3$) δ ppm: 171, 157, 155, 130, 127, 114, 71, 70, 69, 67, 65, 58, 54, 37, 32, 29, 25.

P-CHDM: Tyrosine monomer (**3**) (0.215 g, 0.36 mmoL), CHDM (0.052 g, 0.36 mmoL), titaniumtetrabutoxide (0.001g, 0.003 mmoL, 1 mole %). Yield: 0.21g (93%). ^{1}H NMR (400 MHz, CDCl$_3$) δ ppm: 0.96 (bs, 2H, -C$_6$**H$_{12}$**-), 1.49 (bs, 4H, -C$_6$**H$_{12}$**-), 1.78 (bs, 2H, -C$_6$**H$_{12}$**-), 2.09 (bs, 2H, -C$_6$**H$_{12}$**-), 3.02-3.04 (m, 2H, -C6H5C**H$_2$**), 3.38 (s, 3H, -OC**H$_3$**), 3.54 (m, 2H, -OC**H$_2$CH$_2$**O-), 3.60-3.67 (m, 24H, -OC**H$_2$CH$_2$**O-), 3.70-3.74 (m, 2H, -OC**H$_2$CH$_2$**O-), 3.84 (m, 2H, -OC**H$_2$**CH$_2$-), 4.09-4.13 (m, 6H, -OC**H$_2$**CH$_2$-, **–COOCH$_2$-,** and **-NHCOOCH$_2$-**), 4.58 (S, 1H, C$_6$H$_5$CH$_2$C**H-**), 5.13 (S, 1H, N**H-**), 6.81-6.84 (m, 4H, C$_6$**H$_5$-**), 7.01-7.03 (m, 4H, C6**H$_5$-**). ^{13}C-NMR (100 MHZ, CDCl$_3$) δ ppm: 172, 171, 157, 156, 130, 127, 114, 71, 70, 69, 67, 58, 54, 52, 37, 36, 28, 25.

Optical transmittance measurement:

Optical transmittance of all the polymer aqueous solutions was measured using PerkinElmer Lambda 45 UV-visible spectrophotometer equipped with temperature controlled peltier system. In LCST measurement concentration of the polymer maintained as 3 mg/mL. Heating and cooling cycles were recorded by continuously heating and cooling the samples from 30 °C to 80 °C.

Encapsulation of anticancer drugs in the polymer nanoparticles: Loading of anticancer drugs (DOX and CPT) has done by dialysis method. For this purpose, 5.0 mg of polymer and 0.5 mg of drug were taken in DMSO (2.0 mL). Milli-Q water (3.0 mL) was added to the above solution dropwise and stirred for 4 hours in dark, prior to this DOX.HCl was neutralized with try ethyl amine. The solution was transferred to semi-permeable membrane of MWCO 1KD and dialyzed for 48 h against large amount of milli-Q water to remove the un-encapsulated drug and DMSO. Fresh milli-Q water was replenished periodically. The dialyzed transparent aqueous solution was filtered, lyophilized and stored in dark condition at 4 °C. The drug loading content (DLC) and drug loading efficiencies (DLE) were determined by absorption spectroscopy using the molar extinction coefficients of 11500 L mol^{-1} cm^{-1} and 11250 L mol^{-1} cm^{-1}, for DOX and CPT respectively. DLC and DLE were calculated by using the following formulae[52].

DLE (%) = {weight of drug in NPs / weight of drug in feed} X 100

DLC (%) = {weight of drug in NPs / weight of polymer taken} X 100

In vitro drug release studies: The drug release profiles of drug loaded polymer nanoparticles were studied by dialysis method using absorbance spectroscopy. Drug loaded polymer nanoparticles (1.0 mg/mL) were dispersed in PBS (pH = 7.4) at 37°C (1.0 mL) in a semi-permeable membrane with MWCO 1000D. The dialysis tube was immersed in PBS (3.0 mL) and it was incubated at 37 °C. At specific time intervals 2.0 mL of PBS solution withdrawn to measure the absorbance and the solution was poured back in to reservoir after the measurements. This ensured the concentration of the reservoir maintained same. Esterase enzyme responsive drug release studies have carried out using same protocol in the presence of esterase enzyme (5 mg/mL). For the thermoresponsive drug release the concentration of the polymer has maintained as 3 mg/mL since the minimum concentration required to show thermo responsiveness is 2 mg/ml. Thermoresponsive drug release studies has carried out at 44 °C. The cumulative drug release was calculated using the following equation[53].

Cumulative drug release = {[Amount of drug released at time 't'] / [Total amount of drug in nanoparticles taken in dialysis tube] } X 100.

Cell viability assay (MTT assay): The cytotoxicity of nascent polymer nanoparticles and drug loaded polymer nanoparticles was studied in MCF 7, HeLa and WT-MEF cell lines by using MTT assay method. In a 96-well plate (Corning, USA), 1000 cells per well were allowed to adhered for 16 h in 100 μL of DMEM with 10% FBS (fetal bovine serum). Prior to drug treatment, media from the cells was aspirated and various concentrations of free drug and drug loaded polymer nanoparticles were added as feed. A blank control, DMEM with FBS in the absence of cells and an untreated control, cells with DMEM containing FBS without drug and nanoparticles, were used in each experiment. All control and treated experiment wells were in triplicate. Cells were incubated for 72 h without a change in medium and after 72 h the drug containing medium was aspirated. A freshly prepared stock solution of MTT in sterile PBS (5 mg/mL) was diluted to 50 μg/mL in DMEM. 100 μL of this solution was added to each well and incubated for 4 h at 37 °C. MTT solution was then aspirated from the wells and the purple formazan crystals that formed as a result of reduction of MTT by mitochondrial dehydrogenase enzyme from the cells were dissolved in 100 μL of DMSO (added per well). The absorbance from the formazan

crystals was immediately measured using a micro plate reader at 570 nm (Varioskan Flash) which represents the number of viable cells per well. Values from triplicate run for each control and treated set were noted and their mean value was used for calculations. (Cell viability assay has been done with the help of our lab mate Dr. Bapurao Surnar).

Cellular uptake studies using confocal microscopy: HeLa cells were seeded at a density of 1 x 10^5 cells on flame dried cover slips placed in 6 well plates containing DMEM medium with 10 % FBS. The cells were incubated at 37 ^{o}C for 16 hours and then exposed to the required concentrations of free drug and drug loaded polymer nanoparticles for 9 h in a CO_2 incubator at 37 ^{o}C. After incubation, drug-containing medium was aspirated from each well, and cells were washed twice with PBS (1 mL per wash) and fixed with 4 % paraformaldehyde solution in PBS for 10 minutes at room temperature. The cells were washed twice with PBS (1 mL per wash) and stained with DAPI and incubated for 2 min at room temperature. This incubation was performed in the dark and excess of dye was washed from the cells with PBS. The cover slips were mounted on slides using Fluoromount-G mounting medium (Southern Biotech). Slides were then dried overnight at room temperature in the dark. The cells were imaged using a LSM 710 confocal microscope with the λ 405 nm (blue channel) and λ 561 nm (red channel) lasers. Images thus obtained were analyzed using Image J analysis software and the image for each channel was separated. (Confocal microscopy imaging has been done with the help of our lab mate Mehak Malhotra and sonashree).

Flow Cytometry Measurements: The cellular uptake of free DOX and DOX-loaded polymer nanoparticles in MCF 7 and HeLa cells lines were assessed using Flow Cytometry cell analyzer. HeLa cells were seeded in 6-well plate at a density of 10^5 cells containing DMEM media and incubated for 16 h at 37 °C. Cells were treated with desired concentration (1 μg/mL) of free DOX and DOX-loaded nanoparticles. After 9 h incubation, the drug containing media was aspirated and cells were washed with PBS (1 x 1mL). Further cells were digested using 500 μL trypsin followed by 1 min incubation. The suspension in media was centrifuged at 10,000 rpm for 5 min and re-suspended the pellet in 1 mL PBS. Flow Cytometry studies were carried out by

employing the BD LSRFortessa SORP cell analyzer that is equipped with five lasers and can detect 18 colors simultaneously. The 561 nm laser was used for the excitation of DOX and the band pass filter was chosen as 610 ± 10 nm. The fluorescence histograms were recorded from a population of 10, 000 cells. (Flow cytometry analysis has been done with the help of our lab mate Mehak Malhotra).

3.3. Results and Discussion

3.3.1 Synthesis and structural characterisation of Poly(ester-urethane)s

Acid and amine functional groups in the L-Tyrosine amino acid were converted in to ester and urethane, polymerizable moieties respectively and the phenolic hydroxyl group was substituted with monomethyl ether of polyethylene glycol-350 to get L-Tyrosine monomer (**3**). This monomer was characterized by ^{1}H, ^{13}C- NMR and HRMS. Prior to the polymerization thermal stability of the monomer was investigated by thermal gravimetric analysis which shows the thermal stability up to 200 °C. L-Tyrosine monomer (3) was subjected to melt polymerization[54] with different aliphatic diols ranging from 1,6 hexane diol, 1,8 octane diol, 1,10 decane diol, 1,12 dodecane diol and CHDM at 150 °C using Ti(OBu)$_4$ as catalyst (1 mol %) to get poly(ester-urethane)s with variable hydrophilic to hydrophobic ratio. Polymers were named as P-6 for 1,6 hexane diol, P-8 for 1,8 octane diol, P-10 for 1,10 decane diol, P-12 for 1,12 dodecane diol and P-CHDM for CHDM respectively.
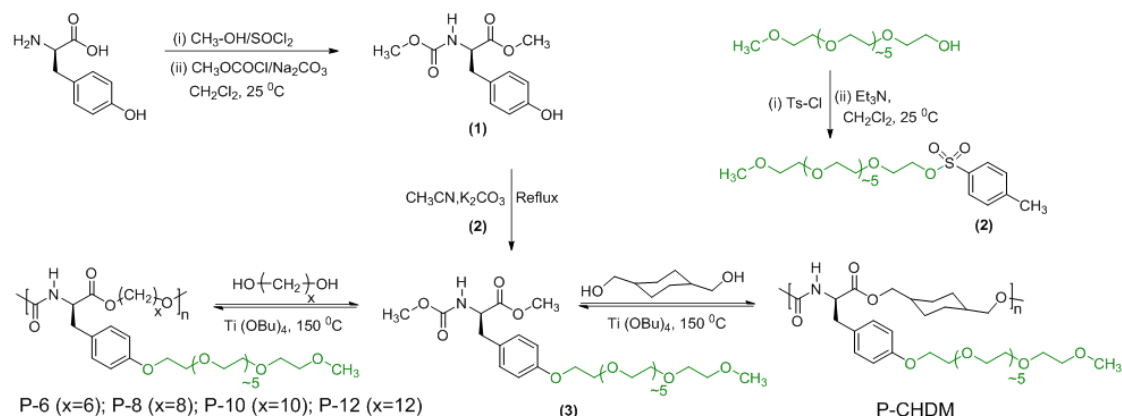
Scheme 3.1. Synthesis of L-tyrosine monomers and dual responsive amphiphilic poly(ester-urethane)s.

The occurrence of the melt polymerization and the formation of high molecular weight polymers were confirmed by NMR spectroscopy. Representative NMR spectra for P-12 polymer has shown in figure 3.4. The peaks at 3.66 ppm and 3.72 ppm in monomer ^{1}H-NMR spectrum corresponding to end group methoxy protons of urethane and ester (-NHCOOCH3, -COOCH3) respectively, were disappeared in the polymer spectrum. Two new peaks at 4.04 ppm and 4.10 ppm

appeared in the polymer spectrum which were corresponding to newly formed urethane and ester linkages respectively (-NHCOOCH2-, -COOCH2-). In the ^{13}C-NMR spectrum of the monomer, the peaks at 52.26 ppm and 52.27 ppm corresponding to methoxy carbons of urethane and ester (-NHCOOCH3, -COOCH3) respectively, were completely disappeared and two new peaks at 65.52 and 65.54 ppm corresponding to newly formed urethane and ester linkages (-NHCOOCH2-, -COOCH2-) were appeared in polymer. Both 1H-NMR and ^{13}C-NMR analysis confirmed the occurrence of the melt polymerization reaction.
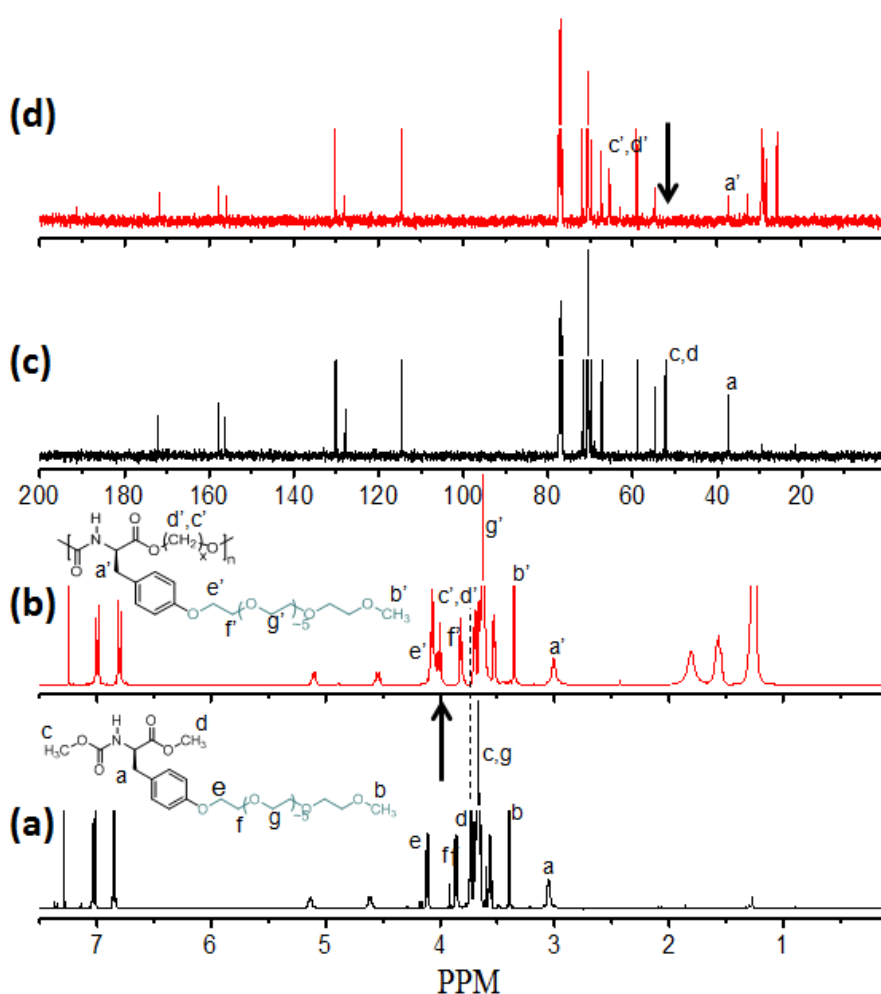

Figure 3.4. (a) ^{1}H-NMR spectra of monomer 3 and (b) polymer P-12 in CDCl₃. (c) ^{13}C-NMR spectra of monomer 3 and (d) polymer P-12 in CDCl₃. The peaks for different protons in the chemical structure are assigned by alphabets and the solvent peak is indicated by asterisks (*). (e) GPC chromatograms of polymers in THF at 25 °C. (f) GPC molecular weights.
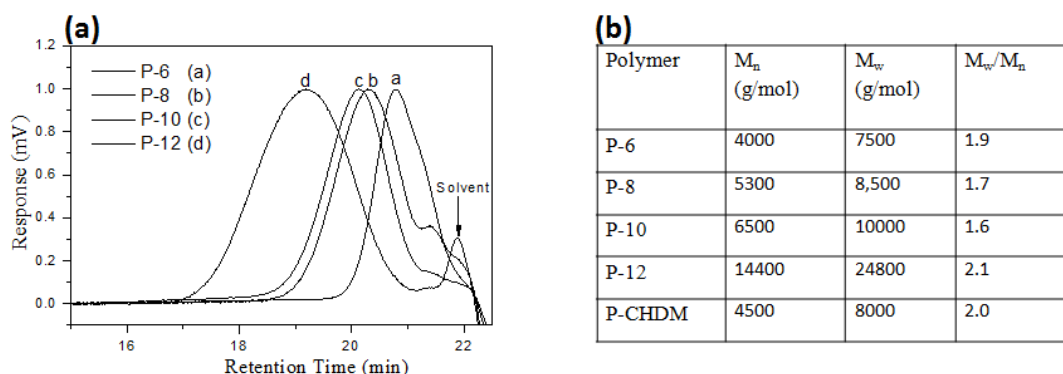
Figure 3.5. (a) GPC chromatograms of polymers in THF at 25 °C and (b) their molecular weights.

The molecular weights of the poly(ester-urethane)s were determined by gel permeation chromatography (GPC) in THF using polystyrene standards, the GPC chromatograms in the figure 2b showed mono model distributions at lower retention times shows the formation of pure moderate high molecular weight polymers. The GPC molecular weights were obtained in the range of $M_n = 4$ to 15×10^3 g/mol and $M_w = 7.5$ to 27×10^3 g/mol. It is observed that there is a linear increment in GPC molecular weights with increasing the carbon atoms in diol used in polymerization (figure 3.5.c), which shows the vulnerability of degree of polymerization on alcohol functional group, P-12 polymer with maximum number of diol carbon atoms (C_{12}) is obtained in high molecular weights.

Thermal properties of these poly(ester-urethane)s were studied by thermal gravimetric analysis and differential scanning calorimeter, TGA studies has showed that the polymers were stable up to 300 °C which shows a remarkable increase in the polymer thermal stability compare to monomer (200 °C). Differential scanning calorimetry studies have revealed that all the polymers are in amorphous nature and the glass transition temperature showed little increment with increase in the carbon atoms in diol (figure 3.6).
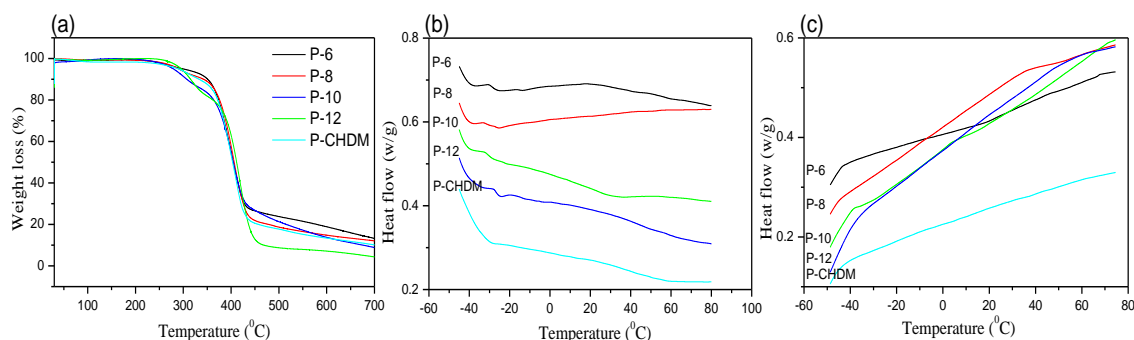
Figure 3.6. (a) GPC chromatograms of polymers in THF at 25 °C. (b) DSC thermograms of polymers in the heating cycle, and (c) cooling cycle at 10 °C/min under nitrogen atmosphere.
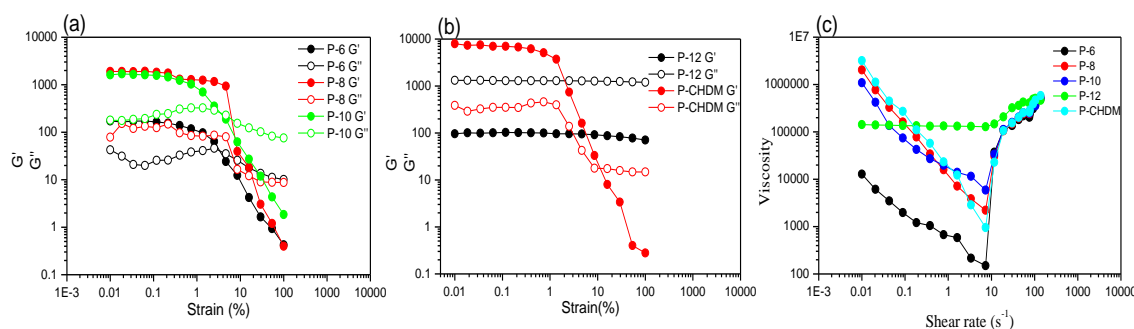
Figure 3.7. (a) Moduli versus strain sweep curves of polymers P-6, P-8 and P-10. (b) Moduli versus strain sweep curves of polymers P-12 and P-CHDM. (c) Viscosity versus shear rate curves of polymers P-6 to P-CHDM.

Mechanical properties of the polymers were investigated by rheological measurements, storage modulus (G'), and loss modulus (G'') was measured as a function of shear strain (see figure 3.7). All the polymers were having higher storage modulus than the loss modulus shows the elastic behavior of the polymers. Loss modulus is predominating at higher strain values (>5-10%) indicating that at higher strains polymers are in viscous nature and at lower strains they are behaving as a elastic materials. As increasing the shear rate viscosity of the polymers was decreasing up to 10 s^{-1} and there is abrupt increase in the viscosity was observed for all the polymers (see figure 3.7.c). This increase in viscosity with increase in shear rate is called shear thickening. Shear thickening is a important characteristic of the materials which used in automobiles and body armours etc.

3.3.2 Thermo-responsiveness of amphiphilic poly(ester-urethane)s

Thermoresponsiveness of these L-tyrosine poly(ester-urethane)s were investigated by transmittance studies using absorbance spectroscopy[44] (see figure 3.8). Prior to this all the polymers were dialyzed against milli-Q water. For this purpose 15 mg of the polymer was dissolved in DMSO (2 mL) and milli-Q water (3 mL) and stirred for 4 hours then transferred to a semi permeable membrane with MWCO = 1000 daltons, and dialyzed against large amount of milli-Q water with continuous replenishing of fresh water for 48 hours. The resulted solution was transparent at room temperature with 100% transmittance for all polymers (see figure 3.8). These aqueous solutions were subjected to transmittance studies to investigate the thermoresponsive behaviour. The % of transmittance was studied as a function of temperature and it was found that all the polymer aqueous solutions were converting from transparent to turbid solutions at temperatures 38 °C to 50 °C (see figure 3.8).
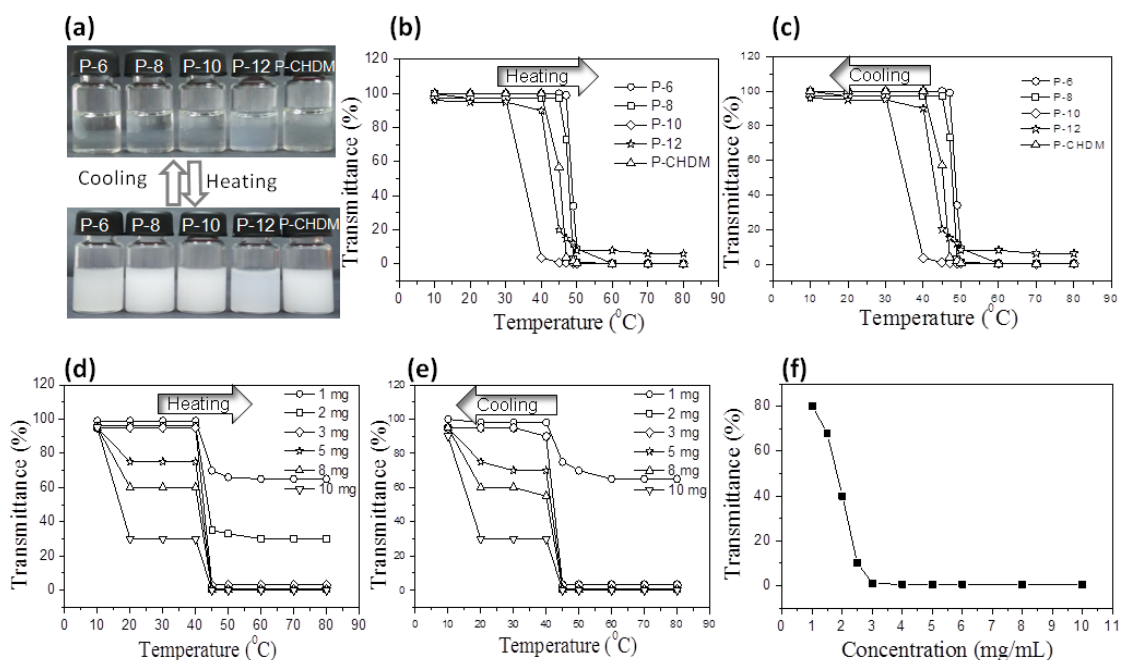
Figure 3.8. (a) Photographs of Dialysed aqueous solutions of polymers before and after LCST. (b) % Transmittance of polymer solutions at different temperatures heating cycle and (c) cooling cycle. (d) % Transmittance of P-12 polymer at different concentrations heating cycle and (e) cooling cycle. (c) Plot of % of transmittance Vs concentration for P-12 polymer.

The extent of turbidity for all the polymers is identical although the lower critical solution temperature (LCST) were varied. P-6 polymer with shorter diol

exhibited the phase transition behaviour at higher temperature (50 °C) compared to P-12 polymer with longer diol (42 °C). From these studies it was found that P-12 polymer with PEG-350 side chain and dodecane diol main chain showing the phase transition near to the cancer tissue temperature (42-43 °C) and this polymer was chosen for the future studies.
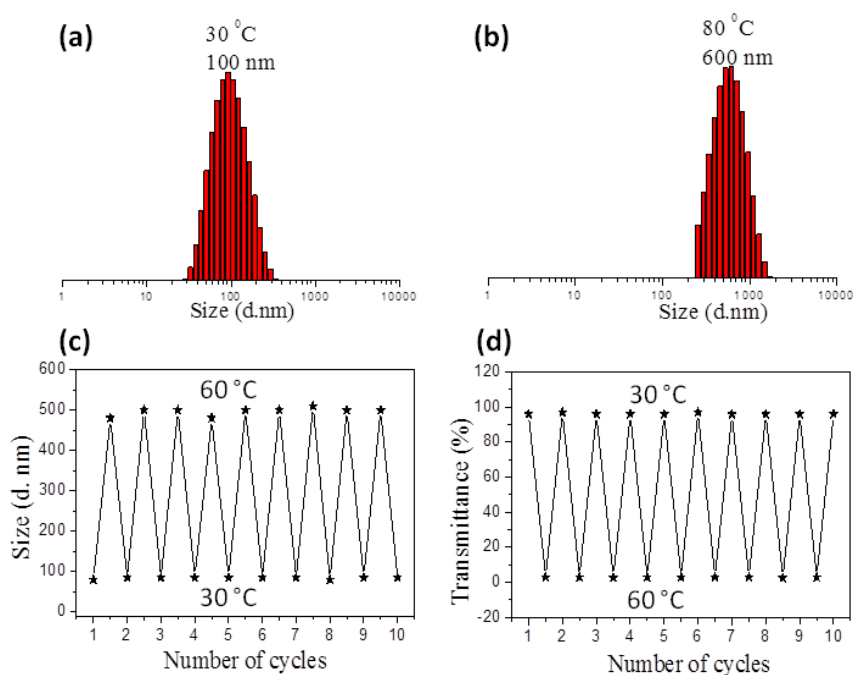
Figure 3.9. (a) DLS histograms of P-12 polymer at 30 °C and (b) 80 °C. (c) DLS size Vs no.of cycles at 30 °C and 60 °C. (d) % Transmittance Vs no.of cycles at 30 °C and 60 °C.

To shed more light on thermoresponsiveness of the polymers, aqueous nanoparticles sizes of these poly(ester-urethane)s were investigated by DLS studies. DLS histograms were recorded in the heating and cooling cycles as a function of temperature. At ambient temperature all the polymers self-assembled in to nanoparticles of the size 100 nm. Increasing the temperature above the lower critical solution temperature, there was a sudden increment in their size from 100 nm to 600 nm (see figure 3.9). This ttrend has observed in all polymer nanoparticles irrespective of the variation in their aliphatic chains in the backbone. The reversibility of this phase transition behaviour was examined by measuring the % of transmittance and size of the nano particles with DLS in 10 consecutive heating and cooling cycles. It

was found that the polymer retained the LCST behaviour even after 10 cycles (see figure 3.9). The change in the transmittance and (or) size is occurring at same temperature in both heating and cooling cycles i.e there is no hysteresis is observed in either transmittance or size of the nanoparticles. To investigate the minimum concentration of polymer required to exhibit the LCST behavior, concentration dependent transmittance studies were carried out. It was found that 2 mg/mL is the minimum concentration required to show phase transition (see figure 3.8).

3.3.3. Variable Temperature 1H-NMR Analysis

To study the structural changes of poly(ester-urethane)s from the transparent to turbid phase transition process, the P-12 polymer was subjected to variable temperature ^{1}H-NMR studies in D_2O (see figure 3.10). Polymer sample was heated from 30 °C to 80 °C at 10° intervals and then cooled back to 30 °C. In the hydrated form (below LCST), the protons corresponding to ethylene glycol side chains at 3.65 ppm showed broad peaks from 30 to 45 °C and no peaks were observed for hydrophobic aliphatic polymer chain backbone or phenyl protons. As the temperature increased above LCST, the signals of ethylene glycol units were sharpened at 3.65 ppm and the peaks for the aliphatic part in the hydrophobic and phenyl ring were also appeared at 1.0-2.0 ppm and above 7.00 ppm, respectively. This trend was attributed to the following arrangements of the polymer nanoparticles in the aqueous medium. Below LCST, the PEG units projected at the pheriphery of the nanoparticles which were interacted with D_2O solvent. At this condition, the hydrophobic chains at the core of the nanoparticles were not accessible by the solvent; thus, no signals were observed in the spectra. Above LCST, the polymer nanoparticles underwent more open-chain conformation in which both the PEGs and the hydrophobic backbone came in contact with D_2O solvent molecules. As a result, the signals were observed for both hydrophilic and hydrophobic parts of the polymers in the nanoparticles. The NMR signals were perfectly reversible in the heating and cooling cycles confirming their reversible self-assembly process.
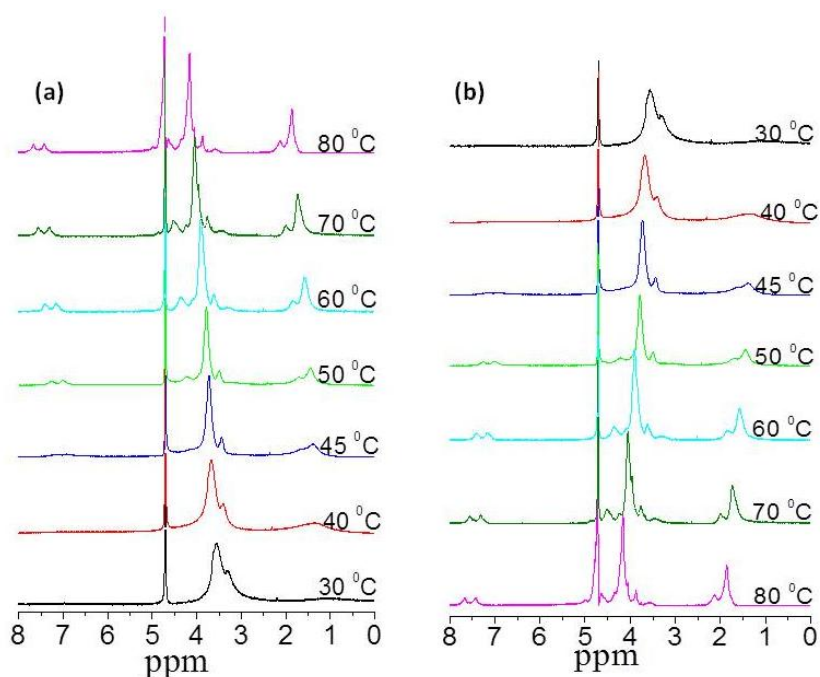
Figure 3.10. ¹H-NMR spectrum of P-12 polymer in D2O solvent, heating and cooling cycles temperature varied from 30 °C to 80 °C.
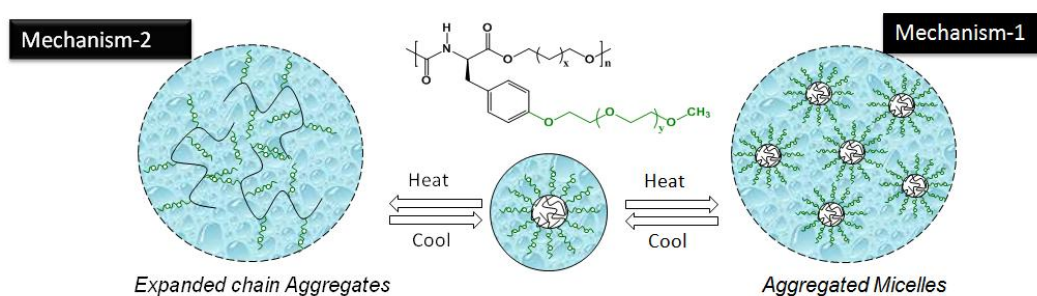
Figure 3.11. Plausible mechanism for the phase separation of the polymers above LCST

The plausible mechanism for this temperature dependent phase transition is shown in figure 5b. At ambient temperature, inter-molecular hydrogen bonding between the oxygen of ester and urethane carbonyl with water molecules are favourable. This makes the PEG part in the polymer chains at the highly hydrate state. PEG chains behaves as more hydrophilic in nature and the inter-molecular hydrogen bonding between water molecules and PEG chains facilitates the completely dispersion of the polymer chains in aqueous medium. Thus, below LCST the polymer chains adopted more globular conformation and existed as < 100 nm sized nanoparticles. At higher temperatures, the PEG chain water molecules interaction

became weak and which makes the polymer chains less hydrate. As a result, the polymer chains precipitate out in the aqueous medium. The increase in the NMR signals for the hydrophobic segments above LCST revealed that the polymer chains probably underwent disassembly from the globular nature to open-chain confirmation. The aggregation of these open-chain produced micrometer-sized polymer aggregates (as shown Path-1 in figure 3.11). Another possible aggregation mechanism could drown for the precipitation of tiny nanoparticles together above LCST to produce micrometer sized particles (path-2 in Figure 3.11). This process is ruled out in the present investigation since this process would not expose the hydrophobic part of the polymers chains to give signals in the NMR spectra above LCST. Thus, the variable NMR experiments revealed that the polymer chains expected to undergo globular to more open-chain conformation changes above LCST which in turn produced micrometer sized aggregates and account for the turbidity of the solution.
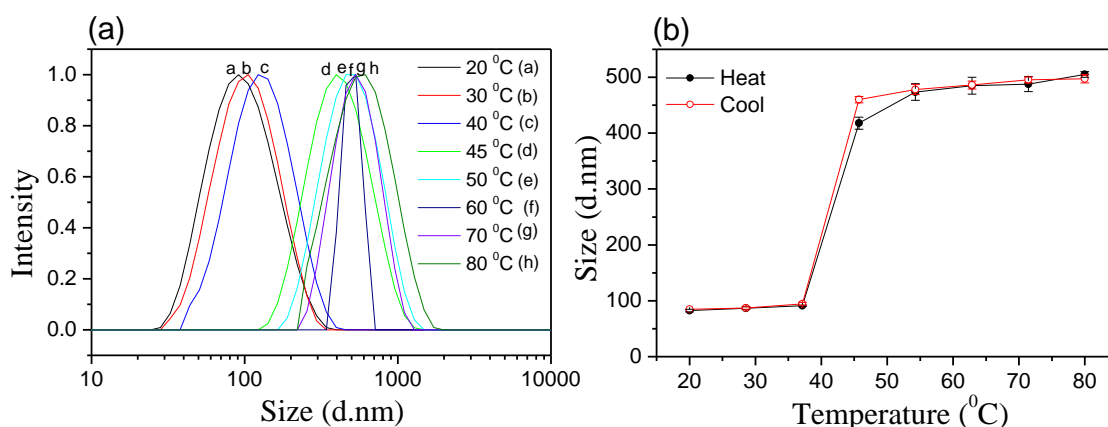
Figure 3.12. (a) DLS histogram, FE-SEM and AFM images of aqueous self-assembly of P-12 polymer.(b) DLS histograms of P-12 nanoparticles at variable temperatures. (c) DLS size Vs temperature plot of P-12 nanoparticles at variable temperatures.

To strengthen the above hypothesis variable temperature DLS studies[44] has carried out by sweeping the temperature from 30 °C to 80 °and cooled back to 30 °C. Data has shown in the figure 3.8 which confirms that at ambient temperature polymer is completely dispersed in the aqueous medium with the formation of nanoparticles of the size around 100 ± 10 nm. Upon heating the nanoparticles were undergoing to phase separation which results the formation of nano assemblies of around 600 ± 10 nm. This DLS data confirms that above LCST polymer chains are undergoing to intermolecular hydrogen bonding which leads to the formation of nano assemblies with larger size.

Self-assembly and Encapsulation of Anticancer Drugs in aqueous medium:

These L-tyrosine poly(ester-urethane)s were build with hydrophilic PEG units in the side chain and hydrophobic alkyl chains in the backbone. The capability of self-assembling in aqueous medium was investigated by dialysis method[30]. All the polymers were completely dispersed in the aqueous medium and forming nano self-assemblies. The size and shape of the nanoparticles were determined by DLS and microscopic techniques. DLS shows the formation of 100 ± 10 nm size nanoparticles, and the shape of nanoparticles were visualised by field emission
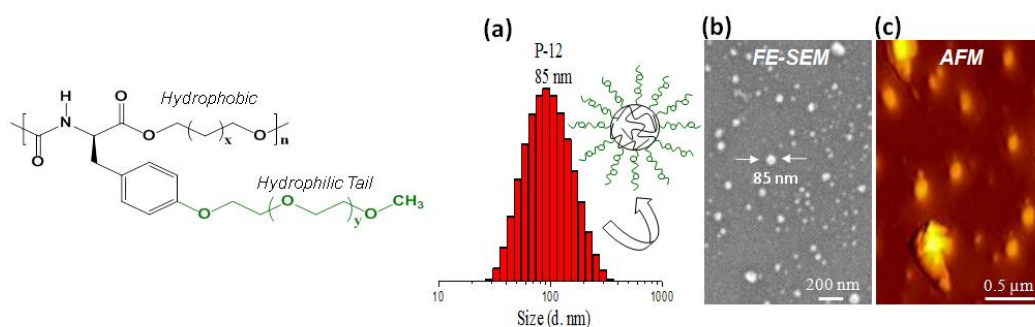
Figure 3.13. (a) DLS histogram, (b) FE-SEM and (c) AFM images of aqueous self-assembly of P-12 polymer.

scanning electron microscope (FE-SEM) and atomic force microscope (AFM) at 25 °C. FE-SEM images of P-12 polymers have given in figure 3.13. The FE-SEM images have showed the existence of spherical nanoparticles with size of 200 nm. The formation of these spherical particles was further confirmed by AFM images. AFM images of P-12 polymer have shown in figure 3.13, which shows the spherical nanoparticles with sizes of 200 nm.

Nanoparticles of these L-tyrosine poly(ester-urethane)s were capable of loading hydrophobic anticancer drugs such as doxorubicin (DOX) and camptothecin (CPT). Loading capabilities of these poly(ester-urethane)s were investigated by dialysis method. For this purpose 5 mg of the polymer and 0.5 mg of the drug were dissolved in DMSO (2mL) and milli-Q water (3 mL) and stirred for 4 hours at 25 °C in dark then it was transferred to a semi permeable membrane of the MWCO = 1000 daltons and dialyzed against large amount of milli-Q water. The resulted transparent

solution was subjected for absorbance spectroscopy to calculate the amount of drug encapsulated in the nanoparticles. It was found that all the polymer nanoparticles are callable of loading hydrophobic drugs. From this study, it was confirmed that the P-12 polymer with 1, 12-dodecane diol main chain is capable of encapsulating maximum amount of drug. The drug loading efficiency (DLE) for the P-12 nanoparticles were determined by absorbance spectroscopy as 50 % and 15% for DOX, and CPT respectively. The drug loading content (DLC) was obtained as 5.0 % and 1.5% for DOX and CPT respectively.

To investigate the thermoresponsive behaviour of the drug loaded P-12 polymer nanoparticles, P-12-DOX and P-12-CPT were recorded as the function of temperature in heating and cooling cycles (see figure 3.14.e). From the figure 3.14.e it was confirmed that both in heating and cooling cycles the transparent nanoparticle solution has becoming turbid at 42 °C. From this experiment it was confirmed that after encapsulating the anticancer drugs also the polymer scaffolds are retained their thermoresponsive behavior and no change in the lower critical solution temperature (42 °C) has observed. To investigate the size of the drug loaded polymer nanoparticles they were subjected for dynamic light scattering studies. DLS histogram of the DOX and CPT loaded P-12 polymer has shown in figure 3.14.a and b DLS histogram is showing a single histogram with size corresponding to 200 nm. From this DLS study it was confirmed that there is no change in the size of the nanoparticles was observed after encapsulating the anti cancer drugs. Size and shape of the drug loaded polymer nanoparticles were visualized by FE-SEM and AFM microscopic techniques. The SEM images has shown in the figure 3.14.a and b which shows the formation of spherical nanoparticles with size of 200 nm and the AFM images in the figure 3.14.a and balso confirm the formation of spherical nanoparticles with 200 nm size.
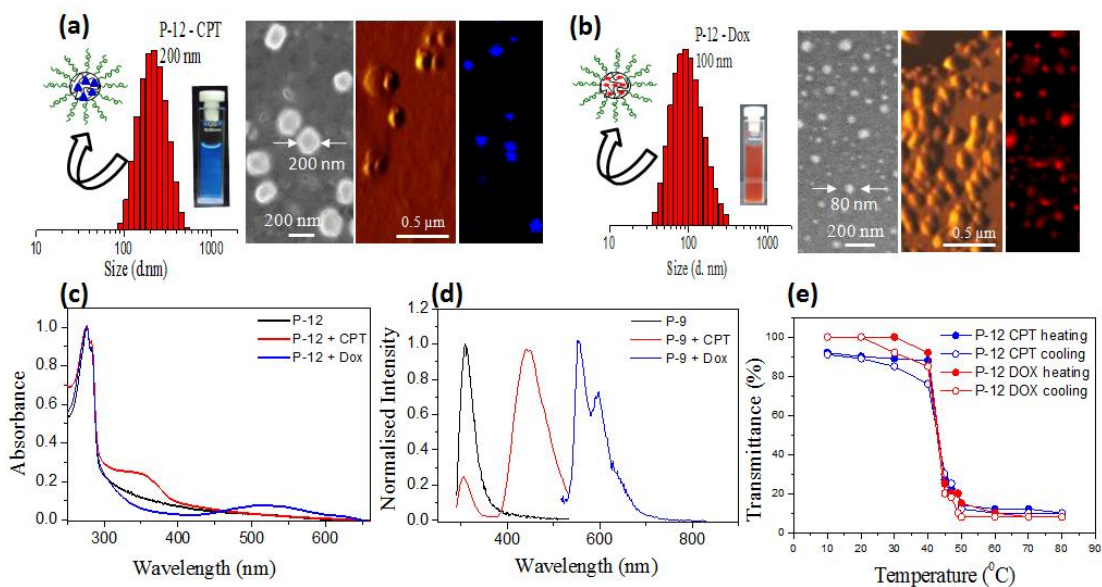
Figure 3.14. (a) DLS histogram, FE-SEM and AFM images of CPT loaded P-12 nanoparticles. (d) DLS histogram, FE-SEM and AFM images of DOX loaded P-12 nanoparticles. (c) Absorbance spectra of P-12 polymer and CPT, DOX loaded P-12 polymer. (d) Fluorescence spectra of P-12 polymer and CPT, DOX loaded P-12 polymer. (e) % Transmittance of CPT and DOX loaded P-12 polymer in heating and cooling cycles.

Both the anticancer drugs DOX and CPT used in the present investigation are fluorescence in nature, so the drug loaded polymer nanoparticles were subjected for detailed photophysical studies by absorption and emission spectroscopy (see figure 3.14.c and d). The photographs of the CPT and DOX loaded samples in the vials shown in figure 3.14.a shows the strong blue and red fluorescence confirmed the encapsulation of these fluorescent anticancer drugs. The absorption spectra in the figure 3.14.c showed peaks at 257 nm corresponding to polymer backbone and broad peaks at 364 and 510 nm in P-12-CPT and P-12-DOX corresponding to absorption of CPT and DOX respectively. The emission spectra of the P-12-CPT and P-12-DOX polymer nanoparticles have shown the emission maxima at 450 and 560 nm corresponding to CPT and DOX respectively. The photo physical characteristics of the drugs in the P-12 nanoparticles were found to be identical to that of their free form confirming their luminescent characteristics were preserved without any change. Fluorescent microscopic images (see figure 3.14 a and b) of the CPT and DOX loaded P-12 polymer scaffold shows the bright blue and red spherical nanoparticles which confirms the encapsulation of these anti cancer drugs. From the above detailed self-assembly studies accomplished by DLS, FE-SEM, AFM and photo physical studies it

may be concluded that these poly(ester-urethane)s synthesized from L-tyrosine amino acid are good candidates for loading the anti cancer drugs with thermoresponsive character.

Enzymatic and thermo-responsive drug Release

The L-tyrosine poly(ester-urethane)s were constituted by aliphatic polyester backbone and they were susceptible for enzymatic-biodegradation to release the drugs. To investigate the enzyme-responsive drug release of these polymer nanoparticles; in-vitro drug release studies has carried out in the presence of esterase enzyme (excreted from horse liver) in pH=7.4 PBS at 37 °C. The drug release kinetics was studied by using absorption spectroscopy monitoring the peaks at 364 and 510 nm for CPT and DOX respectively. The plots of cumulative drug release in the absence and presence of esterase enzyme has shown in figure 3.15.
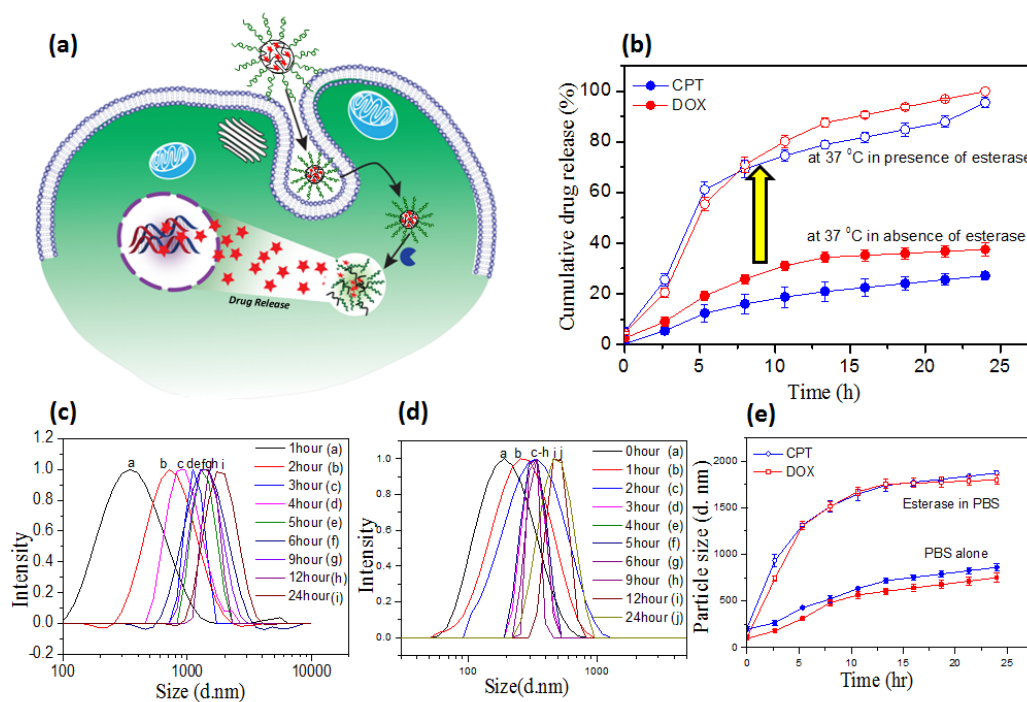
Figure 3.15. (a) schematic representation of cellular internalisation of nanoparticles. (b) Cumulative drug release profiles of CPT and DOX in pH 7.4 PBS in the presence and absence of esterase enzyme at 37 °C. (c) DLS histograms at various time intervals in presence of esterase and (d) absence of esterase. (e) DLS size of CPT and DOX loaded nanoparticles at various time intervals.

In the absence of esterase enzyme only 30 % of the CPT has leached out confirming the highly stable morphology of the nanoparticles in pH=7.4 PBS at 37 °C

for more than 48 hours identical to that of extracellular conditions. In other hand in the presence of esterase enzyme complete release of CPT has accomplished in 24 hours. DOX loaded nanoparticles also showing good stability in pH=7.4 PBS (~35% leached) and 100% DOX released in the presence of esterase enzyme. Degradation behavior of the drugs loaded polymer nanoparticles in the presence of esterase enzyme were also investigated by DLS studies[55-56]. DLS histograms of the drugs loaded P-12 nanoparticles were shown in figure 3.15 c and d The initial histograms showed monomodal distribution with average sizes of 200±15 nm. As the time progressing esterase enzyme reacted with ester bonds in these poly(ester-urethane)s and destroys the self-assembled nanoparticles as a result the hydrophobic bearing chains tend to phase separated from the aqueous medium which produces larger size aggregates. Where as in the absence of esterase enzyme in pH=7.4 PBS buffer even after 48 hours the nanoparticles retained their stable self-assembled structures with no appreciable changes in the sizes of the nanoparticles. DOX loaded polymer nanoparticles also showed the same trend in their DLS histograms in the presence of esterase enzyme nanoparticles size changed from nanometer to micrometer and in the absence of esterase enzyme there is no appreciable change has observed (see figure 3.15). The DLS size of the drug loaded polymer nanoparticles were plotted against time showed in figure 3.15e. This plot reflects similar trend as observed by cumulative drug release profiles by absorption spectroscopy and supports the cleavage of nanoparticles selectively in the presence of esterase enzyme. From the above both
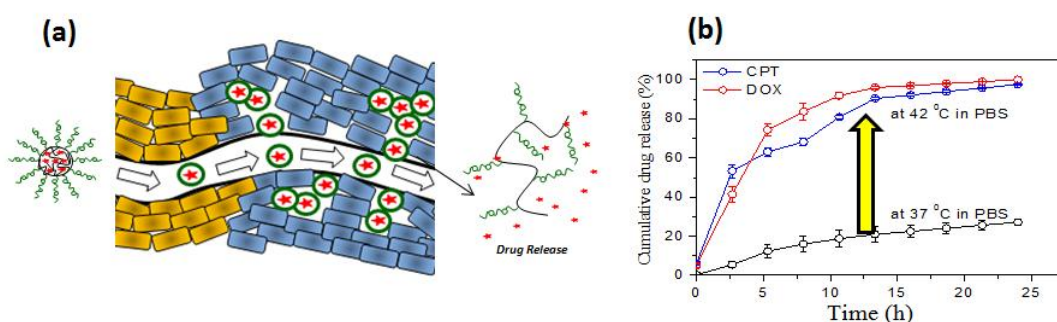

Figure 3.16. (a) schematic representation of more accumulation and release of drugs from nanoparticles at 42 C. (b)Cumulative drug release profiles of CPT and DOX in pH 7.4 PBS at 42 °C temperatures (Temperative responsive).

studies (DLS and absorbance) it can be conclude that these poly(ester-urethane) nano scaffolds are very stable at physiological conditions and selectively undergoes cleavage in the presence of esterase enzyme to release the loaded cargoes.
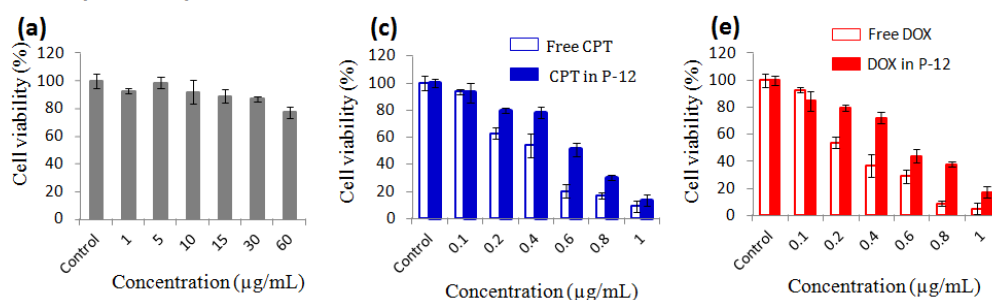
Further to study the thermoresponsive drug release, these drugs loaded polymer nanoparticles were incubated at two different temperatures (i) normal body temperature (37 °C) and (ii) temperature close to cancer tissue temperature (42 °C) in pH=7.4 PBS buffer. The cumulative drug release profiles of these drugs loaded polymer nanoscaffolds have shown in figure 3.16. From the figure 3.16 it was confirmed that at normal body temperature this polymer scaffolds are stable and releasing only 30% of the total CPT whereas at cancer tissue temperature (42 °C) 90% of the CPT has been released within 12 hours. DOX loaded P-12 nanoparticles has also shown similar trend as that of CPT at the body tissue temperature ~35% of the DOX has released and at cancer tissue temperature 100% drug has released within12 hours. From this experiment it was confirmed that these polymer nanoparticles synthesized from naturally available L-tyrosine amino acid are responsive to the temperature changes (LCST), undergoing to disassembly at higher temperature close to cancer tissue temperature and releasing the loaded drug molecules. The plausible mechanism for the temperature responsive drug release from the nanoparticles has schematically shown in the figure 3.16 at higher temperatures the intermolecular hydrogen bonding between oxygen atom of carbonyl group and proton of water molecules will turned in to intramolecular hydrogen bonding between oxygen atom of carbonyl carbon and proton of amide –NH group as a result the self-assembled structures will undergoes destruction and release the loaded drug molecules.

3.3.4. Cytotoxicity and cellular uptake

The cytotoxicity of these poly(ester-urethane) scaffolds was investigated in normal wild-type mouse embryonic fibroblasts (WT-MEFs) cell lines, breast cancer MCF 7 cell lines and cervical cancer cell lines (HeLa) by using MTT assay as described earlier. The cytotoxicity of the nascent polymer scaffold was investigated by treating the cell lines with different concentrations of polymer ranging from 1 µg/mL to 60 µg/mL and the data has been shown in the figure 3.17. From the figure 3.17 it was evidenced that these polymer nanoparticles are non-toxic to the cells, even

at very high concentration (60 µg/mL) 80% of the cell viability was observed in all the cell lines. It shows that the L-tyrosine poly(ester-urethane) nanoparticles are biocompatible to the cell lines. Further to investigate the drug internalization and cell killing ability of the drug loaded polymer nanoscaffolds, P-12-CPT and P-12-DOX polymer samples were administered to the cell lines. Drug concentrations were maintained as 0.1 µg/mL to 1 µg/mL and the MTT assay details has shown in figure…In the normal WT-MEF cell lines free drugs were showing much more killing effect than the drug loaded polymer nano scaffolds at all concentrations, interestingly where as in case of cancer cell lines (MCF 7 and HeLa) the free CPT and DOX became less effective and the drug loaded polymer scaffolds are accomplishing good cell killing (see figure..). From these results it may be concluded that in the *in vitro* 2D cell experiments the poly(ester-urethane) nano scaffolds are capable of delivering the anti cancer drugs selectively to the cancer tissue over the normal cell lines and leads to the selective killing of cancer cell lines.

Figure 3.17. (a) Cytotoxicity of **P-12** nascent nanoparticles in WT-MEF Cells. (b) Cytotoxicity of **P-12** nascent nanoparticles in MCF 7 cell lines. (c) Cytotoxicity of CPT loaded **P-12** and free CPT in WT-MEF cells. (d) Cytotoxicity of CPT loaded **P-12** and free CPT in MCF 7 cell lines. (e) Cytotoxicity of DOX loaded **P-12** and free DOX in WT-MEF cells. (f) Cytotoxicity of DOX loaded **P-12** and free DOX in MCF 7 cell lines. (Incubation time = 72 h).

Cellular internalization of these drugs loaded polymer nanoparticles were visualized by subjecting the P-12-CPT and P-12-DOX nanoparticles to cell lines and using confocal laser scanning microscope (CLSM) for imaging. For DOX loaded polymer samples, the cell lines were excited at 561 nm and visualized through red channel, nucleus of the cells were stained with DAPI (λ= 405 nm) and visualized through blue channel. The CLSM images for free DOX and DOX loaded polymer nanoparticles in MCF 7 cell lines were shown in figure 3.18.a. and 3.19. From the image it is confirmed that the free DOX is predominantly internalized to nucleus of the cells and it was further confirmed from magenta colour of the merged image. DOX loaded polymer nanoparticles are internalized throughout the cell, nucleus as well as cytoplasm of the cells which supports the cleavage of nanoparticles in the cytoplasm by enzymes and subsequent delivery of the DOX to the nuclei. From this study it was confirmed that P-12 polymer nanoparticles are successfully internalized by cells and DOX has released inside the cells. P-12-CPT administered cells were visualized by exciting at λ = 405 nm and visualized through blue channel and the nucleus was not stained with DAPI to avoid the interference with signals which is originating from CPT. Images have shown in figure…, images corresponding to free CPT and P-12-CPT were showing bright blue fluorescence which confirms the successful internalization of the CPT. The uptake of the drug loaded polymer nano particles were further confirmed by flow cytometry analysis. The plot in the figure 3.18b reveals that the free DOX administered cells were showing the DOX intensity of 200-300 where as the cells incubated with DOX in polymer scaffold were showing 1500-2000 DOX intensity. From this flow cytometry data it was confirmed that when DOX was administered by loading in polymer scaffold it shows 6-8 X more internalization compared to free form. From the above three independent experiment MTT assay, confocal microscope images and flow cytometry it may be concluded that these poly(ester-urethane) nano scaffolds synthesized from L-tyrosine amino acid are biocompatible to the cells and excellent vehicles for delivering the anti cancer drugs.
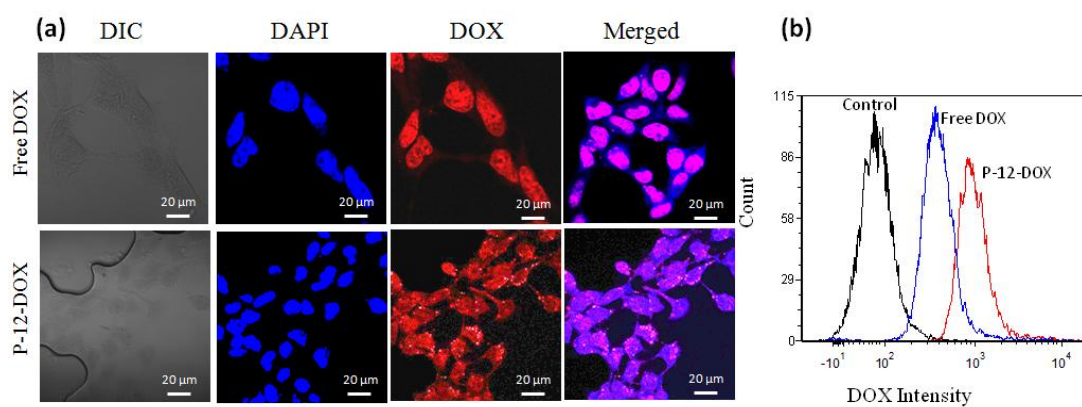
Figure 3.18. (a) CLSM images of free DOX and DOX loaded **P-12** incubated in MCF 7 cells. (b) Flow cytometry plots for control, free DOX, DOX loaded **P-6** nano particles in MCF 7 cell lines (9 h incubation, DOX concentration = 1 μg/mL and 10,000 cells were counted).
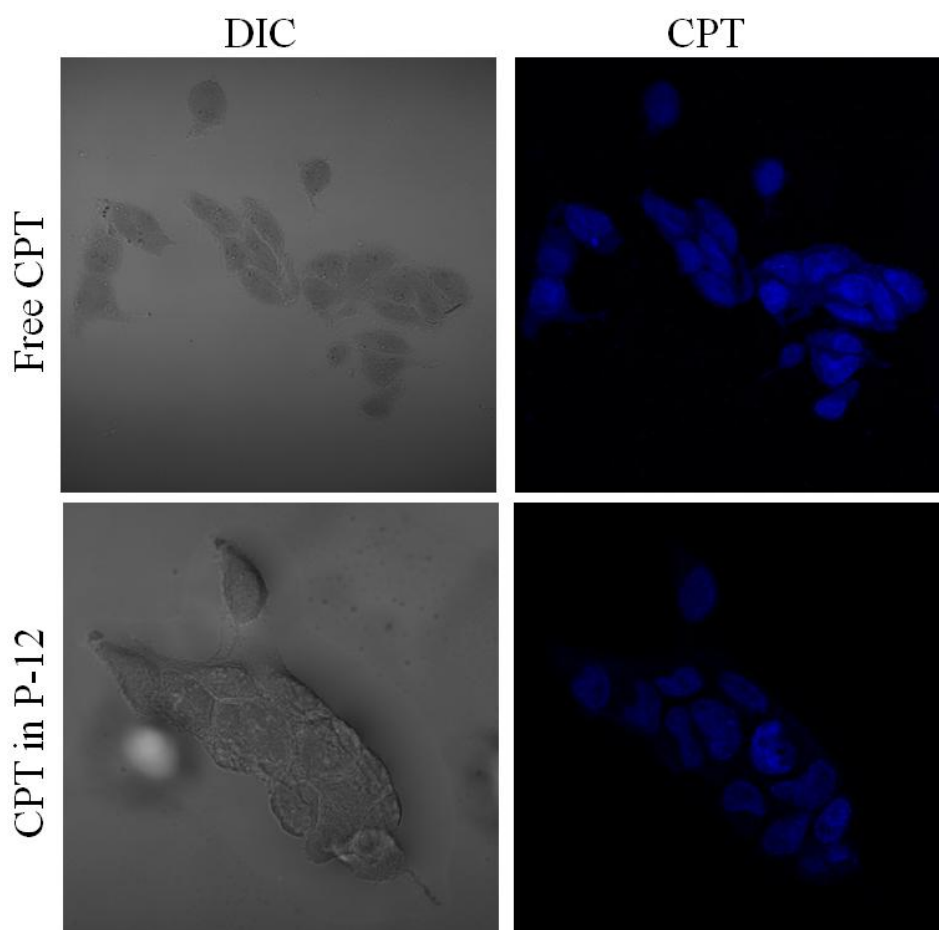
Figure 3.19. CLSM images of free CPT and CPT loaded **P-12** incubated in MCF 7 cells.

To further evaluate the temperature responsive drug release of polymer nano particles, cellular internalization studies were carried out at two different

temperatures. After administering the drug loaded nanoparticles cells were incubated at two different temperatures 37 °C (normal tissue temperature) and 42 °C (cancer tissue temperature) and the internalization of the drugs were visualized through confocal microscopy (figure 3.20), the results confirmed that at 42 °C more internalization of the anti cancer drugs has occurred compared to normal tissue temperature which confirms the temperature responsive drug delivery of polymer nanoparticles.
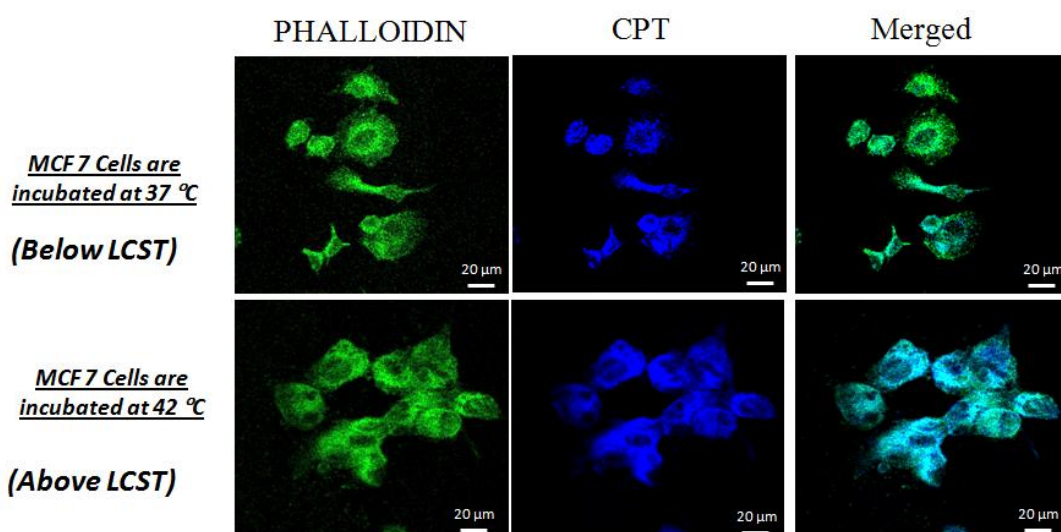
Figure 3.20. CLSM images of free CPT and CPT loaded **P-12** incubated in MCF 7 cells at two different temperatures (37 °C healthy tissue temperature, and 42 °C tumour tissue temperature).

3.3.5. Conclusions

In summary, enzyme and thermo-responsive poly(ester-urethane)s developed from L-tyrosine amino acid resources and their drug deliverying cabapilities were demonstrated in cancer cell lines. Polymers were synthesized by solvent free melt condensation polymerization and their structural and self-assembled structures were well characterized. In the aqueous medium these poly(ester-urethane)s were self-assembled into < 200 nm sized nanoparticles at ambient temperatures. These polymer nanopartciles exhibited temperature responsive phase transition and lower critical solution temperature (LCST) closer to cancer tissue temperature. This LCST behavior

of the polymers was studied extensively by using absorbance and DLS techniques. These poly(ester-urethane)s nanoparticles are capable of loading hydrophobic anticancer drugs such as DOX and CPT. Their in-vitro drug release studies has revealed that these polymer nanoparticles are very stable at normal physiological conditions (37 °C, pH = 7.4 PBS) and they can release the loaded drugs extensively at high temperature cancer tissue (thermoresponsive), or in the presence of lysosomal esterase enzymes (enzyme responsive). Cytotoxic studies of these poly(ester-urethane)s has carried out in normal cell lines as well as in cancer tissue which reveals the biocompatibility of these polymer nanoparticles even at high concentrations. And the drug loaded polymer nanoparticles were showing better cytotoxic effects than the free drugs, interestingly in the normal cell lines drug loaded polymer nanoparticles are exhibiting less cell killing whereas in tumor tissue they were showing more cell killing compared to the free drugs which shows selective tumor killing of drug loaded polymer nanoparticles over the normal tissue. Confocal microscopy images and flow cytometry analysis has revealed the better uptake of the polymer loaded nanoparticles over free drugs. In a overall conclusion the present investigation is one of the first report on thermo responsive and enzyme responsive drug delivery system developed from naturally available L-tyrosine amino acid and their thermoresponsiveness, esterase responsiveness and cytotoxic effects were thoroughly studied.

References

1. Chen, C.-Y.; Kim, T. H.; Wu, W.-C.; Huang, C.-M.; Wei, H.; Mount, C. W.; Tian, Y.; Jang, S.-H.; Pun, S. H.; Jen, A. K.-Y. *Biomaterials* **2013**, 34, 4501-4509.

2. Du, J.-Z.; Du, X.-J.; Mao C.-Q.; Wang, J. *J. Am. Chem. Soc*. **2011**, 133, 17560-17563.

3. Quan, C.-Y.; Chen, J.-X.; Wang, H.-Y.; Li, C.; Chang, C.; Zhang X.-Z.; Zhuo, R.-X. *ACS Nano* **2010**, 4, 4211-4219.

4. Surnar, B.; Jayakannan, M. *Biomacromolecules,* **2013**, 14, 4377-4387.

5. Ding, J.; Zhao, L.; Li, D.; Xiao, C.; Zhuang, X.; Chen, X. *Polym. Chem.* **2013**, 4, 3345-3356.

6. Abulateefeh, S. R.; Spain, S. G.; Thurecht, K. J.; Aylott, J. W.; Chan, W. C.; Garnett, M. C.; Alexander, C *Biomater. Sci.* **2013**, 1, 434-442.

7. Li, Y.; Li, J.; Chen, B.; Chen, Q.; Zhang, G.; Liu, S., Ge, Z. *Biomacromolecules* **2014**, 15, 2914-2923.

8. Roy, D.; Cambre, JN.; Sumerlin, BS. Prog Polym Sci, 2010, 35, 278-301.

9. Gil E.S,; Hudson S. M. *Prog Polym Sci* **2004,** 29, 1173e222.

10. Galaev IY, Mattiasson B. Smart polymers and what they could do in biotechnology and medicine. *Trends Biotech* **1999**, 17, 335e40.

11. Jeong B, Bae YH, Lee DS, Kim SW. Biodegradable block copolymers as injectable drug-delivery systems. *Nature,* **1997**, 388, 860-862.

12. Narang, A. S.; Varia, s.; *Adv. Drug Delivery Rev*. **2011**, 63, 640-658.

13. McDonald, D. M.; Thureton, G.; Baluk, P. *Microcirculation*, **1999**, 6, 7-22.

14. Volk, T.; Jahde, E.; Fortmeyer, H.P.; Glusenkamp, K. H.; Rajewsky, M. F.; Br. *J. Cancer,* **1993**, 68, 492-500.

15. Gerweek, L. E.; Seetharaman, K. *Cancer Res.*, **1996,** 56, 1194-1198.

16. Jayasundar. R.; Singh, V. P. *Neurol. India*, **2002**, 50, 436-439.

17. Issels, R. D.; Eur. *J. Cancer*, **2008**, 44, 2546-2554.

18. Yahara, T.; Koga. T.; Yoshida, S.; Nakagava. S.; Deguchi, H.; Sharouze, K. *Surg. Today*, **2003**, 33, 243-248.

19. De La Rica. R.; Aili, D.; Stedens, M. M. *Adv. Drug Delivery*, **2012,** 64, 967-978.

20. Adresen, T. L.; Thompson, D. H.; Kaasgaard, T. *Mol. Membr. Biol.,* **2010**, 27, 353-363.

21. Murphy, R. F.; Powers, S.; Contor, C. R. *J. Cell. Biol.,* **1984**, 98, 1757-1762.

22. Fang, J.; Seki, T.; Maeda, H.; *Adv. Drug Delivery*, **2009**, 61, 290-302.

23. Ishikawa, K.; Takenaga, K.; Akimoto, N.; Koshikawa, N.; Yamagechi, A.; Imanishi, H.; Nakada, K.; Honma,Y.; Hayashi, *J. Science*, **2008,** 320, 661-664.

24. Fruehauf, J. P.; Meyskens, F. L. *Clin. Cancer Res.*, **2007**, 13, 789-794.

25. Larson, N.; Ghandehari, H. **2012**, 24, 840-853.

26. Xu, X.; Flores, J. D.; McCormick, C. L. *Macromolecules* **2011**, 44, 1327-1334.

27. Kale A. A.; Torchilin, V. P. *Bioconjug. Chem.* **2007**, 18, 363-370.

28. Vijayakameswara, R. N.; Mane, S. R.; Kishore, A.; Sarma, J. D.; Shunmugam, R. *Biomacromolecules* **2012**, 13, 221-230.

29. Liu, R.; Zhang, Y.; Zhao, X.; Agarwal, A.; Muller, L. J.; Feng, P. *J. Am. Chem. Soc*. **2010**, 132, 1500-1501.

30. Aluri, R.; Jayakannan, M. *Biomacromolecules*, **2017**, *18*, 189-200.

31. Li, D.; Bu, Y.; Zhang, L.; Wang, X.; Yang, Y.; Zhuang, Y.; Yang, F.; Shen, H.; Wu, D. *Biomacromolecules*, **2016**, 17, 291-300.

32. Sun, H,; Deng, R.; Meng, F.; Dias, A.; Hendricks, M.; Feijen, J.; and Zhong, Z. *Biomacromolecules,* **2015**, 16, 597-605.

33. Chilkoti, A.; Dreher, M,; Meyer, Drazen Raucher, *Adv. Drug Delivery Rev*. **2002**, 54, 613-630.

34. Chen C.; Wang, Z.; Li, Z. *Biomacromolecules*, **2011**, 12, 2859, 2863.

35. Panja, S.; Dey, G.; Bharti, R.; Maiti, T. K.; Mandal, M.; Chattopadhyay, S. *ACS Appl. Mater. Interfaces* **2016**, 8, 12063-12074.

36. Schild, H. G.; *Prog. Polym. Sci.,* **2007**, 208, 245-253.

37. Maeda, Y.; Higuchi, T.; Ikeda, I. *Langmuir*, **2000**, 16, 7503-7509.

38. Kotsuchibashi, Y.; Narain, R. *Polym. Chem.*, **2014**, 5, 3061-3070.

39. Chenga , C.; Weia, H.; Shib, B.; Chenga, B.; Lia, C.; Guc, Z.; Chenga, S,; Zhanga, X.; Zhuoa, R, *Biomaterials*, **2008**, 29, 947-505.

40. Li, W,; Li, J.; Gao, J.; Li, B.; Xia, Y.; Meng, Y.; Yu, Y.; Chen, H.; Dai, J.; Wang, H.; Guo, Y. *Biomaterials,* **2011**, 32, 3832-3844.

41. S.Q. Liu, Y.W. Tong, Yi-Yan Yang. *Biomaterials*, **2005**, 26, 5064-5074.

42. Hua, W,; Cheng, S.; Zhang, X.; Zhuo, R. *Prog. Polym. Sci. 2009, 34, 893-910.*

43. Josnson, R. P.; Jeong, Y.; John, J. V.; Chung, C.; Kang, D. H.; Selvaraj, M.; Suh, H.; Kim, I. *Biomacromolecules,* **2013**, 14, 1434-1443.

44. Kashyap, S.; Singh, N.; Surnar, B. Jayakannan, M. *Biomacromolecules,* **2016**, *1*, 384-398.

45. Rosa, V. R.; Woisel, P.; Hoogenboom, R. *Mtaerials Today*, **2016**, 19, 491-502.

46. Wang, L.; Wu, L.; Liu, L.; Wang, X.; Yang, S.; Zhao, H. *RSC ADV.*, **2015**, 5, 30456-30463.

47. Cheng, Y.; Hao, J.; Lee, L. A.; Biewer, M. C.; Wang, Q.; Stefan, M. C. *Biomacromolecules* **2012**, 13, 2163-2173.

48. Rainbolt, E. R.; Miller, J. B.; Washington, K. E.; Senevirathne, S. A.; Biewer, M. C.; Siegwart, D. J.; Stefan, M. C. *J. Mater. Chem. B* **2015**, 3, 1779-1787.

49. Rainbolt, E. R.; Washington, K. E.; Biewer, M. C.; Stefan, M. C. *J. Mater. Chem. B* **2013**, 1, 6532-6537.

50. Rainbolt, E. R.; Washington, K. E.; Biewer, M. C.; Stefan, M. C.; *Polym. Chem.* **2015**, 6, 2369-2381.

51. Hao, J.; Cheng, Y,; Ratanatuga, U. R. J. K.; Senevirathne, S.; Biewer, M. C.; Nielsen, S. O.; Wang, Q,; Stefan, M. C. *Macromolecules* 2013, 46, 4829-4838.

52. Pramod, P. S.; Takamura, K.; Chaphekar, S.; Balasubramanian, N.; Jayakannan, M. *Biomacromolecules* **2012**, *13* , 3627–3640.

53. Pramod, P. S.; Shah, R.; Chaphekar, S.; Balasubramanian, N.; Jayakannan, M. *Nanoscale* **2014**, *6*, 11841-11855.

54. Anantharaj S.; Jayakannan, M. *Biomacromolecules,* **2012**, *13*, 2446-2455.

55. Kulkarni, B.; Surnar, B.; Jayakannan, M. *Biomacromolecules,* **2016**, *17*, 1004-1016.

56. Surnar, B.; Jayakannan, M. *ACS Biomater. Sci. Eng.,* **2016**, *2*, 1926-1941.

Chapter 4

One-pot Two Polymers: ABB' Melt Polycondensation for Linear Polyesters and Hyperbranched Poly(ester-urethane) Based on Natural L-Amino acids

Abstract

A novel one-pot ABB' synthetic route for linear polyester and hyperbranched poly(ester-urethane)s based on multi-functional L-amino acid monomers via temperature selective melt polycondensation approach has developed. L-Serine, D-serine and L-threonine amino acids were converted into multi functional ABB' monomers (A= hydroxyl, B= carboxylic ester and B' = urethane). At 120 °C, the ABB' monomer underwent thermo-selective transesterification polycondenstaion (A reacted with B) to produce linear polyesters with B' functionality as pendent in each repeating units. At 150 °C, the ABB' monomer underwent dual ester-urethane self-polycondensation to produce new classes of hyperbranched poly(ester-urethane)s (A reacted with B and B'). Interestingly, the secondary hydroxyl group in the L-threonine monomer did not react at 120 °C; however it became active at 150 °C to yield exclusively linear polyester. In the case of L-tyrosine the phenolic hydroxyl group is lethargic to react with either ester or urethane at 120 °C or 150 °C, but after derivatising this with aliphatic alcohol the primary hydroxyl in L-tyrosine monomer is able to produce linear polyester at 120 °C and hyperbranched poly(ester-urethane) at 150 °C. The temperature selective polycondenstaion process was confirmed by appropriate model reactions and ^{1}H and ^{13}C NMR spectroscopic analysis. The role of the macrocyclic formation in the polycondensation process was also investigated by MALDI-TOF MS. The amino acid based new polymers were found to exhibit diverse molecular self-assembly. The linear polyesters adopted β-sheet conformation which produced helical nano-fibrous morphology. The hyperbranched polymers underwent globular coil-like conformation for spherical nano-particular assemblies. Both the secondary structures formation as well as their morphological features were confirmed by Circular dichroism spectroscopy and electron and atomic microscopic analysis. The new one-pot synthetic pathway is versatile in making diverse linear and branched polymers based on natural L-amino acid with nano-fibrous or spherical morphology for futuristic application in biomedical and thermoplastic industry.

4.1. Introduction:

Hyperbranched polymers (HB) have recently attained significant importance due to their potential applications in drug delivery,[1-3] catalyst development[4-6] and self-assembled nanoscale materials.[7-8] HB polymers have thermal and visco-elastic properties that are completely different from linear, block and graft macromolecular architectures.[9] One-pot synthesis of high molecular weight polymer is an additional advantage associated with the hyperbranched structures.[7,8] In the past two decades, hyperbranched polymers based on polyesters,[9] polyurethanes,[10,11] polyethers,[12-14] polyketals,[15] polyamides and poly(ester-amide)s,[15] and conducting polymers[17] were reported. Amino acids are important building blocks for polypeptides and their sequence and chain length drove the function and enzymatic activity in biological system. AB_2 or A_2B monomers of L-lysine or L-aspartic acid (or L-glutamic acid) were polycondensed to make hyperbranched polyamides[18-19] and poly(ester-amides).[20-22]
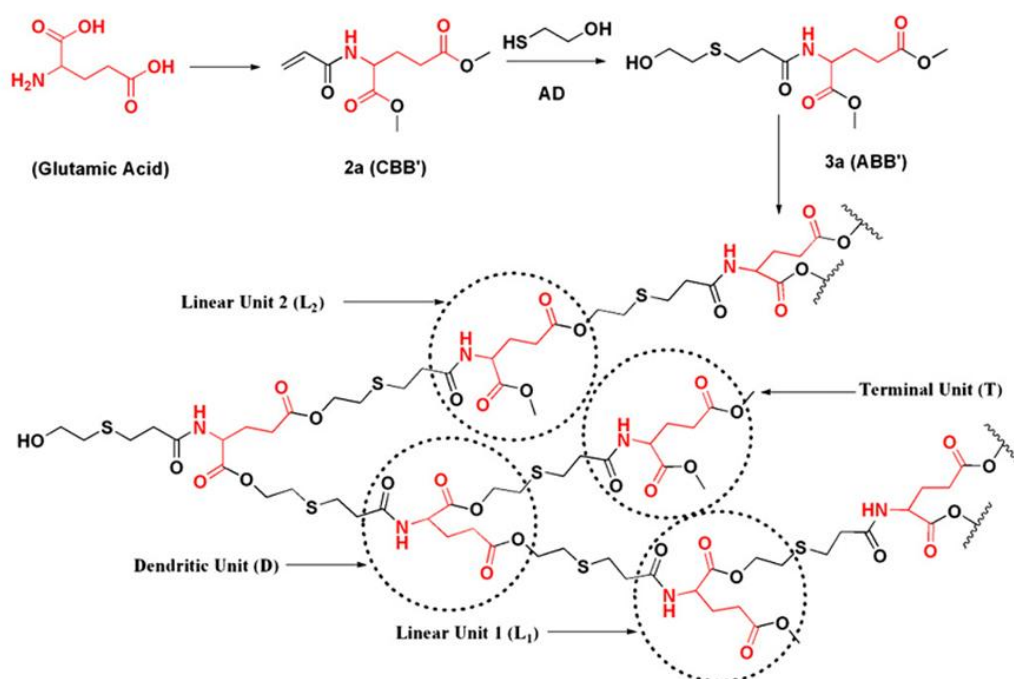

Figure 4.1 AD + CBB' strategy for synthesis of hyperbranched polymer based on L-glutamic acid (adopted from Bao et al. *Polymer*, **2012**, *53,* 145-152).

Till date, there is no synthetic route is reported in the literature to make linear polyesters and hyperbranched poly(ester-urethane)s under the identical process from

a single amino acid residue. This is partially associated with the non-availability of the synthetic methodologies that could simultaneously activate both carboxylic unit (as ester derivative) and amine unit (as urethane derivative) towards alcohol under the same reaction conditions. Recently, we have reported the development of dual ester-urethane melt condensation approach for linear poly(ester-urethane)s[23] and functional helical polyesters[24] based on natural L-amino acids under solvent free melt polymerization process. This methodology was developed by merging the well-known melt transesterification reaction with melt transurethane process[25-26] that was earlier developed in our laboratory. During the course of this methodology development; we identified that the carboxylic ester and urethane functionalities had very high selective reactivity towards alcohol (or diols) in melt condensation reaction. This unique finding here seeded for the development of temperature selective one-pot melt polycondensation approach that could produce both linear polyester and hyperbranched poly(ester-urethane) from single multifunctional amino acid source as shown in figure 1.
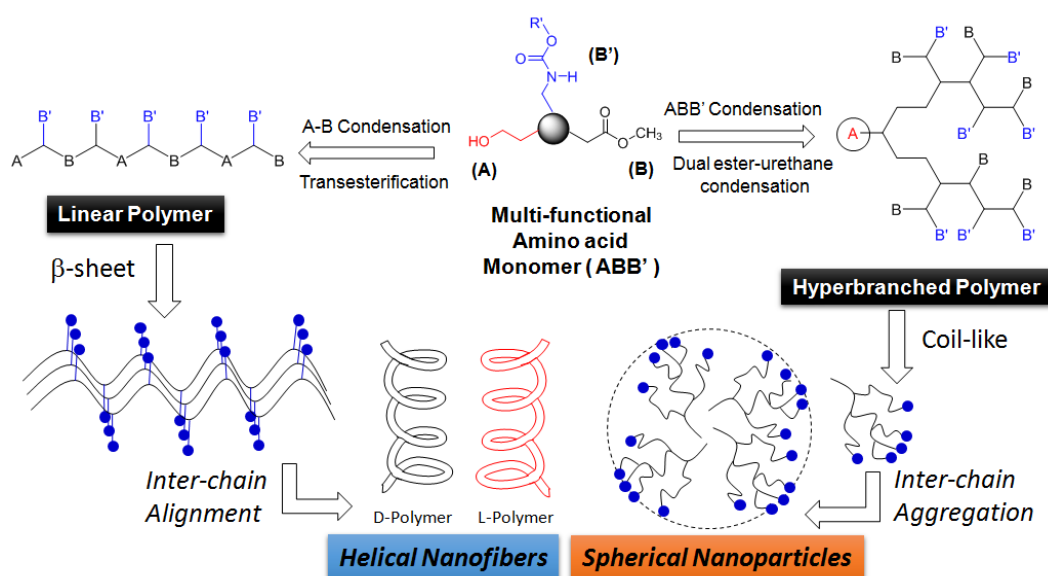

Figure-4.2. *A novel one-pot temperature selective polycondensation approach for linear and hyperbranched polymers based on L-amino acids and their self-assembled nano-structures.*

The present investigation reports one of the first melt polycondensation approaches for hyperbranched polymers based on natural L-amino acids. For this purpose two natural amino acids having carboxylic acid, amine and hydroxyl functional groups are selected. Both L (or) D-serine and L–threonine have fulfilled this requirement with primary and secondary hydroxyl functionality, respectively. These monomers were readily converted into their corresponding ABB' monomers, where A, B and B' represented the hydroxyl, carboxylic ester and urethane functional groups, respectively. Thermo-selective one-pot polycondensation of these monomers produced linear polyester and hyperbranched poly(ester-urethane)s (see figure 1). The reaction of A with B produced A-B linear polyester with B' anchored as pendent in each repeating unit. Simultaneous reaction of A towards B and B' produced hyperbranched poly(ester-urethane)s. Efforts were taken to study the role of cyclization versus linear polymer chain on the molecular weight of the polymers. Further, the ability of the linear and hyperbranched polymers to produce secondary structures was investigated by circular dichroism (CD), electron microscopes and atomic forces microscopes. The overall finding revealed that the linear polymers adopted β-sheet expanded conformation and produced helical nano-fibrous whereas the hyperbranched polymer produced spherical nano-particles through coil-like conformations.

4.2. Experimental Procedure

4.2.1. Materials: L-Serine, D-serine, L-threonine, octyl amine, palmitic acid, cyclohexanol and titanium tetrabutoxide (Ti (OBu) $_4$) were purchased from Aldrich chemicals and used without further purification. Methyl chloroformate, thionylchloride, and other solvents were purchased locally and purified prior to use.

4.2.2. General procedure: ^{1}H and ^{13}C-NMR were recorded using 400-MHz JEOL NMR spectrophotometer. All NMR spectra were recorded in CDCl$_3$ and DMSO-d$_6$ containing TMS as internal standard. Mass of the polymer was determined by using Applied Biosystems 4800 PLUS MALDI TOF/TOF Analyzer. The polymer samples were dissolved in Dichloromethane (DCM) at 10 mg/ml. Dihydroxy benzoic acid (DHB) was used as matrix. The matrix solution was prepared by dissolving 30mg in 1 ml. A 1-2 μL aliquot of the polymer/matrix mixture was deposited on top of maldi

plate and air-dried. High resolution mass spectra (HRMS) of monomers were obtained from micro mass ESI-TOF MS Spectrometer. Gel permeation chromatographic (GPC) analysis which was performed using Viscotek VE 1122 pump, Viscotek VE 3580 RI detector and Viscotek VE 3210 UV/Vis detector in dimethyl formamide (DMF) using polystyrene as standard. Thermal stability of the polymers was determined using Perkin Elmer thermal analyzer STA 6000 model at a heating rate of 10 ºC/min under nitrogen atmosphere. Thermal analysis of the polymers was performed using TA Q20 Differential scanning calorimeter. The instrument was calibrated using indium standards. All the polymers were heated to melt before recording their thermograms to remove their previous thermal history polymers were heated and cooled at 10 ºC/min under nitrogen atmosphere and their thermograms were recorded. Infrared spectra of the samples were recorded using Perkin Elmer FT-IR spectrophotometer. The absorption studies were done by a Perkin-Elmer Lambda 45 UV-Visible spectrophotometer in tetrahydrofuran solvent. Circular Dichroism (CD) analysis of the polymer samples was done using JASCO J-815 spectrometer at 20 $^\circ$C in THF. FE-SEM images were recorded using Zeiss ultra plus scanning electron microscope. For FE-SEM the samples were prepared by drop casting the polymer solution on silicon vapors and coated with gold. TEM images were recorded using a Technai-300 instrument by drop casting the sample on Formvar-coated copper grid. Atomic force microscope (AFM) images were recorded by drop casting the samples on freshly cleaved mica surface, using Veeco Nanoscope IV instrument. The experiment was done in tapping mode.

4.2.3 Synthesis of Monomers

Synthesis of L-Serine monomer (1): Typical procedure for carboxylic methyl ester methyl carbamate of amino acids was described for L-serine monomer. To a suspension of L-serine (10.0 g, 95.0 mmoL) in methanol (70 mL), thionylchloride (13.7 mL, 190.4 mmoL) was added drop wise at 0 $^\circ$C under nitrogen atmosphere. The reaction mixture was refluxed for 12 hours under the nitrogen atmosphere. The solvent and excess thionylchloride was removed by distillation. The residue was dried under vacuum to get the product as white solid. The solid mass was stirred in sodium carbonate solution (25 wt%, 54 mL) at 0 ºC. To this ice cold solution, methyl chloroformate (9.82 mL, 128.0 mmoL) was added drop wise and the reaction was continued for 12 h at 25 °C. The reaction mixture was extracted with dichloromethane

and the organic layer was dried over anhydrous Na_2SO_4. The liquid product was further purified by passing through silica gel column using ethyl acetate and pet ether (4:6 v/v) as eluent. Yield = 12.6 g (75 %). ^{1}H-NMR (400 MHz, $CDCl_3$) δ ppm: 5.87 (s, 1H, -N**H**), 4.41 (m, 1H, -C**H**), 3.96-3.88 (dd, 2H, -C**H$_2$**), 3.76 (S, 3H, COOC**H$_3$**), 3.68 (S, 3H, NHCOOC**H$_3$**). ^{13}C-NMR (100 MHZ, DMSO-d_6) δ ppm: 171.61, 156.91, 61.43, 56.79, 52.17, and 51.90. FT-IR (cm^{-1}): 3389, 2956, 1701, 1526, 1446, 1350, 1268, 1210, and 1066. HRMS (ESI+): m/z [M+Na$^+$] calcd. for $C_6H_{11}NO_5$ [M$^+$]: 200.0534; found: 200.0537.

Synthesis of L-Threonine Monomer (2): L-Threonine (10 g, 84 mmoL), $SOCl_2$ (12.21 mL, 168 mmoL) methanol (100 mL), methyl chloroformate (8.25 mL, 107 mmoL), Na_2CO_3 (11.42 g, 20 wt %) dichloro methane (70 mL) were used and the experimental procedure for the monomer 1 was followed. Yield: 13.0 g (81%). ^{1}H NMR (400 MHz, $CDCl_3$) δ ppm: 5.77 (s, 1H, -N**H**), 4.29-4.26 (m, 2H, -NH-C**H** and –C**H**-OH), 3.74 (s, 3H, -COOC**H$_3$**), 3.68 (s, 3H, NH-COOC**H$_3$**), 2.62 (s, 1H, O**H**), and 1.24-1.21 (d, 3H, OH-CH-C**H$_3$**). ^{13}C-NMR (100 MHZ, $CDCl_3$) δ ppm: 171.84, 157.40, 67.82, 59.15, 52.52 and 19.74. FT-IR (cm^{-1}): 3449, 2975, 2867, 2683, 2362, 2095, 1965, 1729, 1645, 1514, 1457, 1361, 1245, and 1206. HRMS (ESI+): m/z [M+Na$^+$] calcd. for $C_7H_{13}NO_5$: 214.0687; found: 214.0699.

Synthesis of D-Serine monomer (3): D-Serine (10 g, 95.0 mmoL), $SOCl_2$ (13.72Ml, 190.4 mmoL), methanol (70mL), methyl chloroformate (9.82 mL, 128mmoL), Na_2CO_3 (25 wt %, 54 mL) dichloro methane (70 mL) were used and the experimental procedure for the monomer 1 was followed. Yield: 13.31 g (79 %).^{1}H-NMR (400 MHz, $CDCl_3$) δ ppm: 5.86 (s, 1H, -N**H**), 4.42 (m, 1H, -C**H**), 3.96-3.90 (dd, 2H, -C**H$_2$**), 3.77 (S, 3H, COOC**H$_3$**), 3.69 (S, 3H, NHCOOC**H$_3$**). ^{13}C-NMR (100 MHZ, DMSO-d_6) δ ppm: 171.0, 156.71, 61.40, 56.75, 52.17, and 51.90. FT-IR (cm^{-1}): 3380, 2956, 1715, 1520, 1446, 1355, 1260, 1210, and 1066. HRMS (ESI+): m/z [M+Na$^+$] calcd. for $C_6H_{11}NO_5$ [M$^+$]: 200.0534; found: 200.0497.

Synthesis of L-Tyrosine Monomer (4): L-tyrosine (10 g, 84 mmoL),), $SOCl_2$ (11 mL, 165.4 mmoL), methanol (70mL), methyl chloroformate (7.45 mL, 105mmoL), Na_2CO_3 (25 wt %, 48 mL) dichloro methane (70 mL) were used and the experimental procedure for the monomer 1 was followed. Yield: 13.31 g (79 %).^{1}H-NMR (400 MHz, $CDCl_3$) δ ppm: 5.11 (s, 1H, -N**H**), 4.59 (m, 1H, -C**H**), 4.08-4.04 (m, 4H,

OCH$_2$) 3.93-3.86 (m, 8H, OCH2CH$_2$) 3.77 (S, 3H, COOCH$_3$), 3.69 (S, 3H, NHCOOCH$_3$). ^{13}C-NMR (100 MHZ, DMSO-d$_6$) δ ppm: 171.0, 155.71, 59.10, 56.75, 52.17, and 51.90.

Synthesis of Palmitic ester: Palmitic acid (5.0 g, 19.5 mmoL) was dissolved in MeOH (55 mL) and SOCl$_2$ (2.83 mL, 39 mmoL) was added slowly at ice cold condition and it was refluxed for 12 hours. The solvent was removed and it was poured into brine solution. It was extracted into ethylacetate then Na$_2$CO$_3$ solution was added to remove the unreacted acid. The product was purified by passing through silica gel column using 10 % ethylacetate in hexane (9: 1 v/v) as eluent. Yield: 4.8 g (91 %). ^{1}H-NMR (400 MHz, CDCl$_3$) δ ppm: 3.67 (s, 3H, -COO-C**H$_3$**), 2.31 (t, 2H, -CH$_2$-C**H$_2$**-COO-CH$_3$),1.61 (m, -C**H$_2$**-CH$_2$-COO-CH$_3$), 1.26 (s, 24H, -C**H$_2$**-C**H$_2$**), 0.88 (t, 3H, -CH$_2$-C**H$_3$**).

Synthesis of n-Octyl urethane; Octyl amine (2g, 15.5 mmoL) was dissolved in 10 wt % Na$_2$CO$_3$ (1.97 g, 18.6 mmoL) and methyl chloroformate (1.30 mL, 17 mmoL) in dichloromethane (20 mL) was added. The reaction was continued at 25 °C for 12 h. The solvent was removed and the crude product was purified by passing through silica gel column using 5 % ethyl acetate in hexane (10: 0.5 v/v) as eluent. Yield: 2.8 g (96 %). ^{1}H-NMR (400 MHz, CDCl$_3$) δ ppm: 4.68 (s, 1H, -N**H**), 3.66 (s, 3H, -NHCOOC**H$_3$**), 3.16 (s, 2H, -CH$_2$-C**H$_2$**-NH-), 1.48 (s, 2H, -CH$_2$-C**H$_2$**-CH$_2$-NH-), 1.28 (s, 10H, CH$_3$-C**H$_2$**-CH$_2$-), 0.88(s, 3H, -C**H$_3$**).

Model recation-1: Palmitic ester (0.5 g, 2.3 mmol) and cyclohexanol (0.26 g, 2.6 mmol) were taken in a test tube shaped polymerization apparatus. The polycondensation apparatus were made oxygen and moisture free by purging with nitrogen under constant stirring at 90 °C for about 10 minutes, titanium-tetrabutoxide (0.009g, 0.026 mmol) was added and again degassed for 20 minutes. Then the condensation reaction was carried out at 150 °C under nitrogen purge for 4h. Yield: 0.65g (90 %). ^{1}H NMR (400 MHz, CDCl$_3$) δ ppm: 4.76 (s, 1H, -CH$_2$-COO-C$_6$H$_{10}$-**H**), 2.31-2.34 (t, 2H, CH$_2$-C**H$_2$**-COO-C$_6$H$_5$), 1.82-1.61 (m, 10H, -C$_6$**H$_{10}$**), 1.26 (m, 26H, -C**H$_2$**-C**H$_2$**), 0.88 (t, 3H, -CH$_2$-C**H$_3$**). FT-IR (cm^{-1}): 3499, 2975, 2864, 2682, 2360, 2094, 1966, 1726, 1644, 1457, 1364, 1286, 1183.

Model recation-2: Octyl amine urethane (0.5 g, 2.6 mmol) and cyclohexanol (0.29 g, 2.9 mmol) were taken in a test tube shaped polymerization apparatus. The polycondensation apparatus made oxygen and moisture free by purging with nitrogen under constant stirring at 90 °C for about 10 minutes, titanium-tetrabutoxide (0.009g, 0.026 mmol) was added and again degassed for 20 minutes. Then the condensation reaction was carried out at 150 °C under nitrogen purge for 4h. Yield: 0.3g (30 %). ^{1}H-NMR (400 MHz, CDCl$_3$) δ ppm: 4.68 (s, 1H, -N**H**), 4.33 (s,1H, -NH-COO-C$_6$H$_{10}$-**H**), 3.66 (s, 3H, -NHCOOC**H$_3$**), 3.16 (s, 2H, -CH$_2$-C**H$_2$**-NH-), 1.48 (s, 2H, -CH$_2$-C**H$_2$**-CH$_2$-NH-), 1.28 (s, 10H, CH$_3$-C**H$_2$**-CH$_2$-), 0.88(s, 3H, -C**H$_3$**). FT-IR (cm^{-1}): 3502, 2977, 2856, 2682, 2361, 2094, 1965, 1724, 1645, 1457, 1364, 1242, 1183.

4.2.4 Synthesis of Polymers

Synthesis of L-Serine linear Polyester (L-SLP): Typical melt polymerization procedure was explained for L-serine. L-Serine monomer **1** (1.0 g, 5.6 mmoL) was taken in a test tube shaped polymerization apparatus and melted by placing the tube in oil bath at 80 °C with constant N$_2$ flow, then titaniumtetrabutoxide (0.019 g, 0.06 mmoL, 1 mole %) was added in to it. The reaction mixture was degassed by purging with nitrogen and subsequent evacuation by vacuum under constant stirring at 80 °C. The oil bath was preheated to 120 °C and the polycondensation was carried out at 120 °C for 4 h with constant stirring under nitrogen purge. During this stage, the methanol was removed along with purge gas and the polymerization mixture became viscous. The viscous melt was further subjected to condensation at high vacuum (0.01 mbar of Hg) at 120 °C for 2 h. At the end of the polycondensation, the linear polymer was obtained as solid. It was purified by dissolving in tetrahydrofuran, filtered and precipitated in to diethyl ether. Yield = 0.8 g (98 %). ^{1}H NMR (400 MHz, CDCl$_3$) δ ppm: 5.86 (s, 1H, -N**H**), 4.64-4.42 (m, 3H,-C**H$_2$** and -C**H**), 3.81 (s, 3H, -OC**H$_3$**), 3.72 (s, 3H, -NHCOOC**H$_3$**). ^{13}C-NMR (100 MHZ, DMSO-d$_6$) δ ppm: 156.58, 107.00, 105.82, 97.20, 66.61, 65.74, 51.80, 33.18, 29.14, 23.33, 23.84. FT-IR (cm^{-1}): 3313, 2956, 1690, 1528, 1449, 1351, 1248, 1205, 1161 and 1055.

Synthesis of L-Serine Hyperbranched Poly(ester-urethane) (L-SHPEU): Serine monomer **1** (1.30 g, 7.30 mmoL) and titanium-tetrabutoxide (0.024 g, 0.073 mmoL, 1

mole %) was polymerized at 150 °C for 4 h under nitrogen purge and 2h under vacuum (0.01 mbar) as described for **L-SLP**. Yield = 0.77 g (95 %). ^{1}H NMR (400 MHz, CDCl$_3$) δ ppm: 6.21-5.70 (m, 1H, N**H**), 4.63-4.3 (m, 3H, C**H**CH$_2$OH and CHC**H$_2$**OH), 3.80 (s, 3H, -OCH$_3$), 3.72(s, 3H, -NHCOOCH3). ^{13}C-NMR (100 MHZ, DMSO-d$_6$) δ ppm: 169.13, 156.39, 67.96, 64.92, 61.61, 53.06, 25.59, 14.47, 14.08. FT-IR (cm^{-1}): 3317, 2958, 1521, 1449, 1345, 1205 and 1082.

Synthesis of L-Threonine Linear Polyester (L-TLP): Threonine monomer (**2**) (1.0 g, 5.20 mmoL) and titanium-tetrabutoxide (0.017 g, 0.052 mmoL, 1 mole %) was polymerized at 150 °C for 4 h under nitrogen purge and 2h under vacuum as described for L-SLP. Yield = 0.80 g (96 %). ^{1}H-NMR (400 MHz, CDCl$_3$) δ ppm: 6.22 (s, 1H, -NH), 4.75 (q, 1H, -**CH**-O-CO-), 4.55 (q, 1H, -**CH**-O-CO-NH-), 4.02 (d, 1H, **CH**-CH-O-CO-), 3.96 (d, 1H, **CH**-CH-O-CO-NH-), 3.82 (s, 3H, -NHCOOC**H$_3$**),3.74 (s, 3H, -COOC**H$_3$**), 1.57 (d, 3H, **CH$_3$**-CH-O-CO), 1.34 (d, 3H, **CH$_3$**-CH-O-CO-NH). ^{13}C-NMR (100 MHZ, CDCl$_3$) δ ppm: 170.73, 159, 60.95, 53.62, 21.64. FT-IR (cm^{-1}): 3573, 3504, 3260, 2975, 2862, 2682, 2361, 1966, 1778, 1644, 1457, 1365, 1285 and 1184.

Synthesis of D-Serine linear poly ester (D-SLP): D-Serine monomer (3) (1.0 g, 5.6 mmoL) and titanium-tetrabutoxide (0.019 g, 0.06 mmoL, 1 mole %) was polymerized at 120 °C for 4 h under nitrogen purge and 2h under vacuum as described for L-SLP. Yield: 0.80 g (98 %). ^{1}H NMR (400 MHz, CDCl$_3$) δ ppm: 5.92 (s, 1H, -N**H**), 4.64-4.42 (m, 3H,-C**H$_2$** and -C**H**), 3.81 (s, 3H, -OC**H$_3$**), 3.72 (s, 3H, -NHCOOC**H$_3$**). ^{13}C-NMR (100 MHZ, DMSO-d$_6$) δ ppm: 170.42, 169.92, 168.91, 156.60, 66.0, 63.89, 61.19, 56.65, 52.76, 52.36, 51.82. FT-IR (cm^{-1}): 3313, 2956, 1690, 1528, 1449, 1351, 1248, 1205, 1161 and 1055.

Synthesis of D-Serine Hyperbranched poly(ester-urethane) (D-SHPEU): D-Serine monomer (3) (1 g, 5.6 mmoL)and titanium-tetrabutoxide (0.019g, 0.06 mmoL, 1 mole %) was polymerized at 150 °C for 4 h under nitrogen purge and 2h under vacuum as described for L-SHPEU. Yield: 0.79 g (97%). ^{1}H NMR (400 MHz, CDCl$_3$) δ ppm: 5.72 (m, 1H, N**H**), 4.66-4.45 (m, 3H, C**H**CH$_2$OH and CHC**H$_2$**OH),

3.80 (s, 3H, -OCH$_3$), 3.72(s, 3H, -NHCOOCH3). ^{13}C-NMR (100 MHZ, DMSO-d$_6$) δ ppm: 170.51, 170.00, 168.99, 158.63, 156.69, 66.02, 63.96, 61.25, 56.70, 52.87, 52.44, 51.90, 51.73. FT-IR (cm^{-1}): 3317, 2958, 1521, 1449, 1345, 1205 and 1082.

Synthesis of L-Tyrosine linear poly ester : L-tyrosine monomer (4) (1.0 g, 2.6 mmoL) and titanium-tetrabutoxide (0.025 g, 0.03 mmoL, 1 mole %) was polymerized at 120 °C for 4 h under nitrogen purge and 2h under vacuum as described for L-SLP. Yield: 0.65 g (88 %). ^{1}H-NMR (400 MHz, CDCl$_3$) δ ppm: 5.11 (s, 1H, -N**H**), 4.59 (m, 1H, -C**H**), 4.42-4.39 (m, 2H, COOC**H$_2$**) 4.08-4.04 (m, 4H, OC**H$_2$**) 3.93-3.86 (m, 8H, OCH2C**H$_2$**) 3.72 (S, 3H, COOC**H$_3$**), 3.69 (S, 3H, NHCOOC**H$_3$**). ^{13}C-NMR (100 MHZ, DMSO-d$_6$) δ ppm: 171.0, 155.71, 60.95, 59.10, 56.75, 52.17, and 51.90.

Synthesis of L-Tyrosine Hyperbranched poly(ester-urethane): L-tyrosine monomer (4) (1.0 g, 2.6 mmoL) and titanium-tetrabutoxide (0.03 g, 0.035 mmoL, 1 mole %) was polymerized at 150 °C for 4 h under nitrogen purge and 2h under vacuum as described for L-SHPEU. Yield: 0.72 g (93 %). ^{1}H-NMR (400 MHz, CDCl$_3$) δ ppm: 5.11 (s, 1H, -N**H**), 4.59 (m, 1H, -C**H**), 4.42-4.39 (m, 4H, COOC**H$_2$,** NHCOOC**H2**) 4.08-4.04 (m, 4H, OC**H$_2$**) 3.93-3.86 (m, 8H, OCH2C**H$_2$**) 3.72 (S, 3H, COOC**H$_3$**), 3.69 (S, 3H, NHCOOC**H$_3$**). ^{13}C-NMR (100 MHZ, DMSO-d$_6$) δ ppm: 171.0, 155.71, 61.45, 59.10,57.15, 56.75, 52.17, and 51.90.

4.3. Results and discussions

4.3.1. Serine Based Linear and HB Polymers

Ester-urethane monomers were synthesized starting from naturally available L-amino acids as shown in scheme 1. L-Serine was converted into its carboxylic acid chloride and subsequently reacted with methanol to yield methyl ester amine hydrochloride salt. The amine salt was converted into its free amine and further reacted with methyl chloroformate to make methyl urethane (or carbamate). The resultant molecule represented ABB' type monomer in which the hydroxyl (A) unit reacts with ester (B) and urethane (B') functionalities. A similar procedure was used to make monomers based on L-threonine (**2**) and D-serine (**3**). Thermogravimetric analysis (TGA) revealed that these monomers were stable up to 170 °C for melt polycondensation.
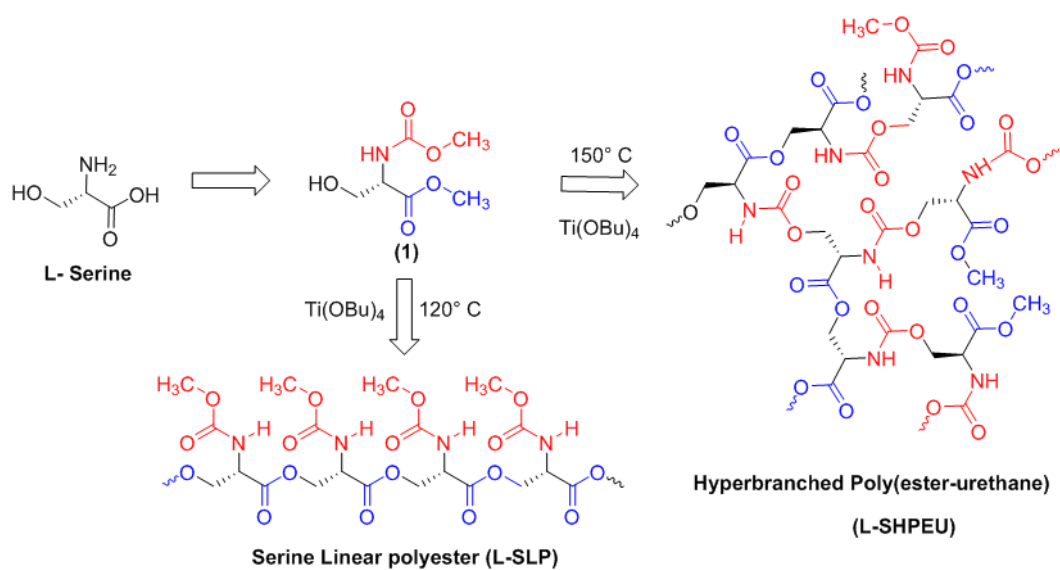
Scheme 4. 1. Synthesis of linear and hyperbranched polymers based on L-serine and L-threonine monomers.

The ABB' monomer was polycondensed using Ti(OBu)$_4$ as catalyst (1 mole %) at two different temperatures: (i) at 120 °C for selective transesterification of alcohol (A) with ester units (B) to produce linear polyester and (ii) at 150 °C for dual ester-urethane polycondensation of alcohol (A) with both ester (B) and urethane (B') to yield new classes of hyperbranched poly(ester-urethane). The structures of the linear and hyperbranched polymers are shown in scheme 4.1. Prior to the polymerization, the monomer and catalyst (in a cylindrical polymerization tube) were subjected to evacuation under vacuum and nitrogen purge to make it oxygen and moisture free. Subsequently, the polymerization was proceeded under nitrogen purge at the desired temperature (either 120 ℃ or 150 ℃) for 4 hours to make the oligomers. These oligomers were further polycondensed for 2 hours under vacuum (0.01 mbar). At the end of the polymerization, the polymers were obtained as white solid mass products.
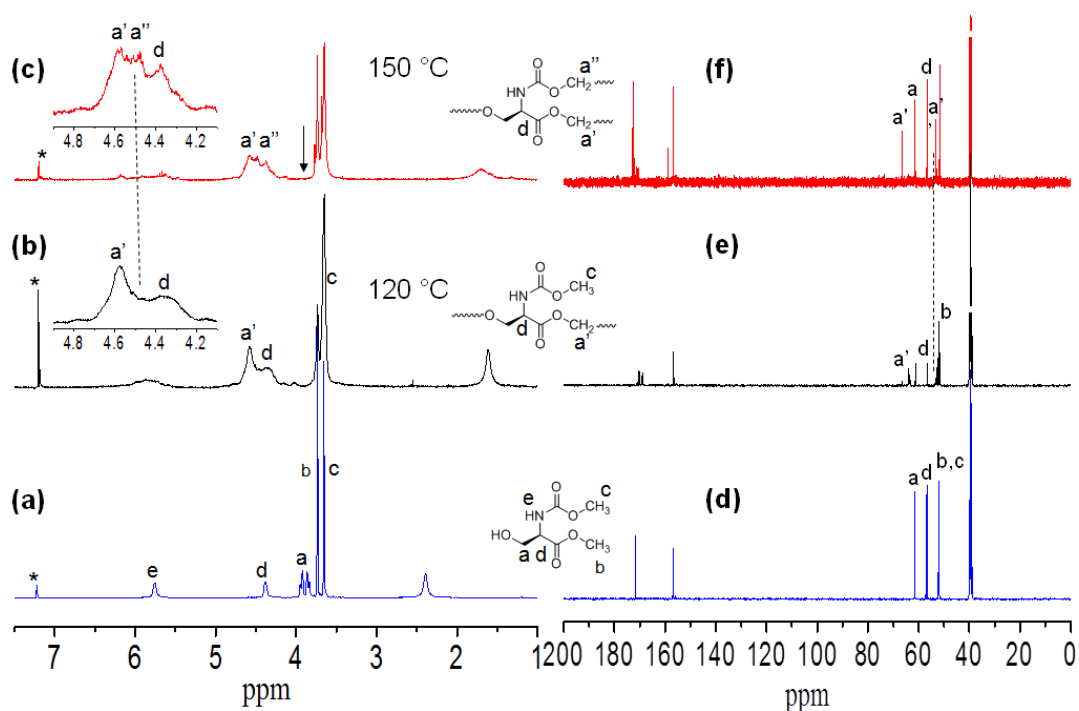

Figure 4.3. ^{1}H-NMR spectra of L-serine monomer 1 (a), its linear polyester(L-SLP) (b) and hyperbranched poly(ester-urethane) (c). All the spectra are recorded in CDCl$_3$. solvent peak is indicated by asterisks (*).

^{1}H NMR spectra of the L-serine monomer, linear polyester (L-SLP) and the HB polymer (L-SHPEU) are shown in figure 4.3. The different peaks in the spectra

are assigned with alphabets with respect to their protons in the chemical structures. At 120 °C, the -CH_2OH (proton-a) at 3.90 ppm was almost vanished and new carboxylic ester peak corresponding to –CH_2OOCCH- was appeared at 4.62 ppm (see Fig. 2b). The integration of the peak intensities confirmed the occurrence of the reaction up to 95 %. Thus, the number of the repeating unit in the linear polyester was theoretically estimated to be 15-20 units. Control polymerization was performed at 120 °C and aliquots were collected at regular interval. ^{1}H NMR spectra of their aliquots (see figure 4.4.) showed the vanishing of -CH_2OH protons and the appearance of new ester peak. During this process, the urethane methyl protons -$CHNHCOOCH_3$ was completely inert. Hence, at 120 °C in the ABB' monomer, only –CH_2OH (A) functional group reacted with carboxylic ester B and the urethane functional group B' was not disturbed. The self-condensation of ABB' monomer at 150 °C facilitated the simultaneous reaction of –CH_2OH (A) with carboxylic ester (B) and urethane (B') functional groups to produce hyperbranched polymer. In figure 4.3.c, the –CH_2OH protons completely vanished and new urethane peak appeared at 4.55 ppm (see peak-a'') along with the ester peak at 4.62 ppm (see proton-a').
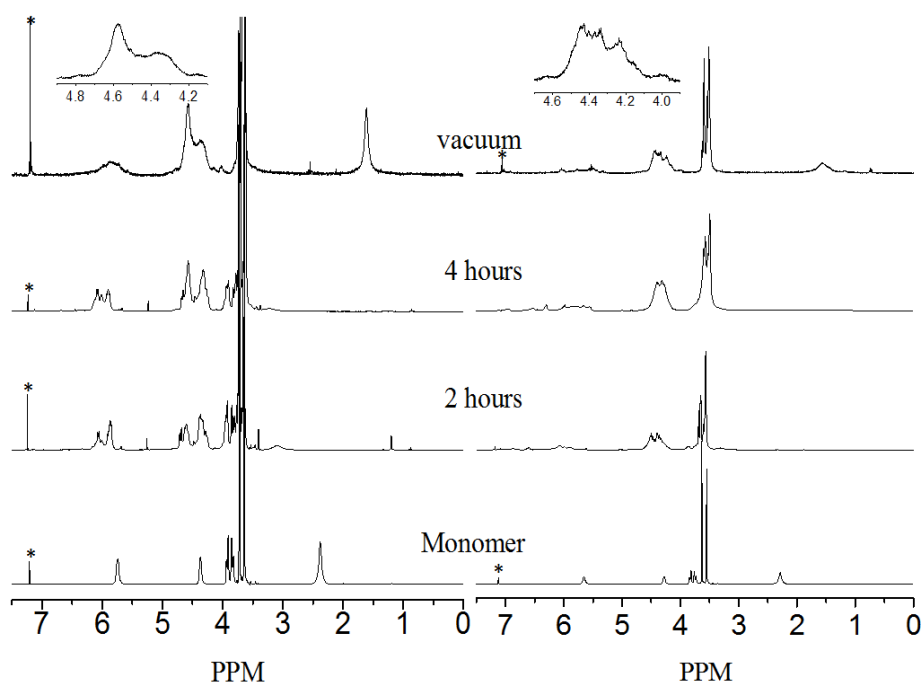

Figure 4.4. ^{1}H-NMR spectra of L-serine monomer and linear poly ester at different time intervals. All the spectra are recorded in CDCl$_3$. solvent peak is indicated by asterisks (*).

144

Further, the ^{1}H-NMR spectra of the hyperbranched polymer aliquots (see figure 4.5) were also supported the fast vanishing of the - CH_2OH protons and appearance of the new ester and urethane peaks seen as in figure 4.3.c. A similar investigation by ^{13}C-NMR further confirmed the temperature selective condensation of the ABB' monomer to produce linear polyester and hyperbranched poly(ester-urethane)s.

4.3.1. Degree of branching

The degree of branching (DB) of the HB polymer was determined using the expression DB = [D+T] / [D+T+L] or DB = [2T] / [D+T+L] or [2D] / [D+T+L] where D, L and T represent the dendritic, linear and terminal units, respectively.[12,27-28] The hyperbranched structures produced by AB_2 monomer has equal amount of end groups (B=B). It is also important to mention that in hyperbranched polymers, number of dendritic units are always equivalent to the number of terminal units (D = T). In the present case, B and B' have different in reactivity towards A; thus, the difference between B and B' peak integration values at the terminal units actually represent the amount of dendrite unit produced by B in reaction with A. Thus T = B, T+L = B' and L= D= B'- B in the present case. Upon forming the hyperbranched structure the dendritic and linear units appeared together for protons in the polymer-**CH_2OOCCH** and polymer-**CH_2-OOCNHCH** at 4.6 - 4.5 ppm (see NMR spectra in figure 4.6.). The terminal units from both ester and urethane units were appeared together at 3.72 and 3.81 ppm respectively. Based on the NMR integration values, the DB was estimated as 66 %. Earlier reports on HB polyesters and polyethers had reported DB ~ 60 %. Thus, the hyperbranched poly(ester-urethane) has DB as similar to literature examples.[9]

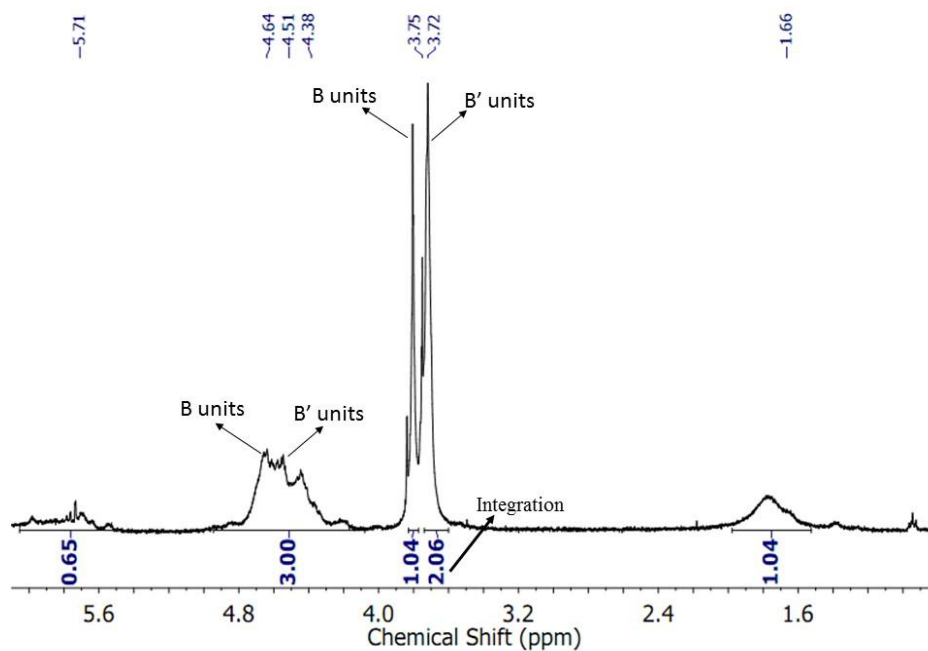**Figure 4.6.** Degree of branching calculated from ^{1}H-NMR spectrum of L-SHPEU.

Calculation Details:

Degree of Branching (DB) = [D+T]/D+T+L] or DB = [2D]/[D+T+L] or [2T]/[D+T+L] [12,27-28]

(D= Dendritic; L= Linear and T= terminal)

In the present case, T+L = B' and D = L = B'-B

Therefore, DB = 2 (B'-B) / [B' + B'-B]

By Substituting B' = 2.06 and B = 1.04 (based on NMR in SF-5) in the above equation we have calculated DB as 66% for the present system.

4.3.3. Molecular Weights and End Group Analysis

The molecular weight of the newly synthesized linear polyesters and hyperbranched poly(ester-urethane)s were determined by gel permeation chromatography in DMF at 25 °C. The GPC molecular weights are given in Table 1. The molecular weights of the polymers were obtained as M_n ~ 16,000 and M_w ~ 20,000 g/mol. The molecular weights of the aliquots of the polymer samples corresponding to the polymerization at 120 ° and 150 °C were also determined by GPC. These molecular weights are plotted against the polymerization time (see figure 4.7.). In the case of the linear polyester, the molecular weight increases with increase in the polymerization time and maximum was achieved toward the end of the

146

reaction. On the other hand, the molecular weights of hyperbranched polymers were enhanced rapidly at the initial stage of the reaction onwards. To further study the enantiomeric effect on the synthesis of the linear and hyperbranched polymers, D-serine monomer (**3**) was synthesized and polymerized at 120° and 150 °C . The molecular weights of these polymers were also obtained as similar to that of the L-serine counterpart (see table ST1 in ESI). Both natural L-serine monomer and un-natural D-serine monomer followed the thermo-selective polycondensation to produce high molecular weight linear polyester and hyperbranched poly(ester-urethane)s.

Table 1. Molecular weights and thermal properties of linear and hyperbranched polymers.

Polymer	Monomer	Polymerization Temperature (°C)	M_n^a (g/mol)	M_w^a (g/ml)	T_g^b (°C)	T_D^c (°C)
L-SLP	1a	120	15700	18300	4.3	185
D-SLP	3a	120	11700	20100	5.9	208
L-SHPEU	1a	150	16600	20100	55.0	211
D-SHPEU	3a	150	18300	24300	40.0	215
L-TLP	2a	150	8400	13300	-27.8	167

[a] Molecular weights are determined by GPC in dimethyl formamide at 25 °C using polystyrene standards. [b] Determined by DSC under nitrogen atmosphere at 10°/min heating rate. [c] Determined by TGA under nitrogen atmosphere.(T_D decomposition starting temperature).
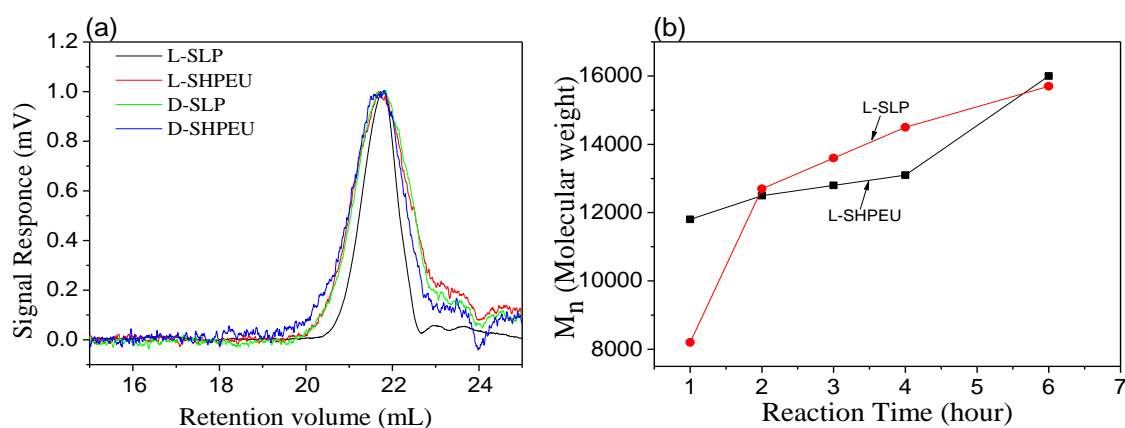

Figure 4.7. (a) GPC chromatograms of polymers, (b) plot of GPC number average molecular weight vs reaction time.

MALDI-TOF mass spectrometry provides direct information on the types of the end groups present in the polymer chains as well as the macrocyclic formation that occurred during the polymerization of ABB' monomer. MALDI-TOF spectra of the polyester and hyperbranched polymer are shown in figures 4.8.a and 4.8.b, respectively. The polymer showed two sets of intense peaks for every repeating unit with respect to the linear and cyclic units (as both Na+ and K+ ions). Each repeating unit mass was resolved for the repeating unit formula: $(145)_n+32+23$ for sodium ion peaks $[(145)_n+32+40$ for potassium ion peak]. In figure 4.8.a, the mass peaks are visible up to 12 repeating units. The intensity of the linear units became more abundant with increases in the molecular weight polymers at higher conversion.
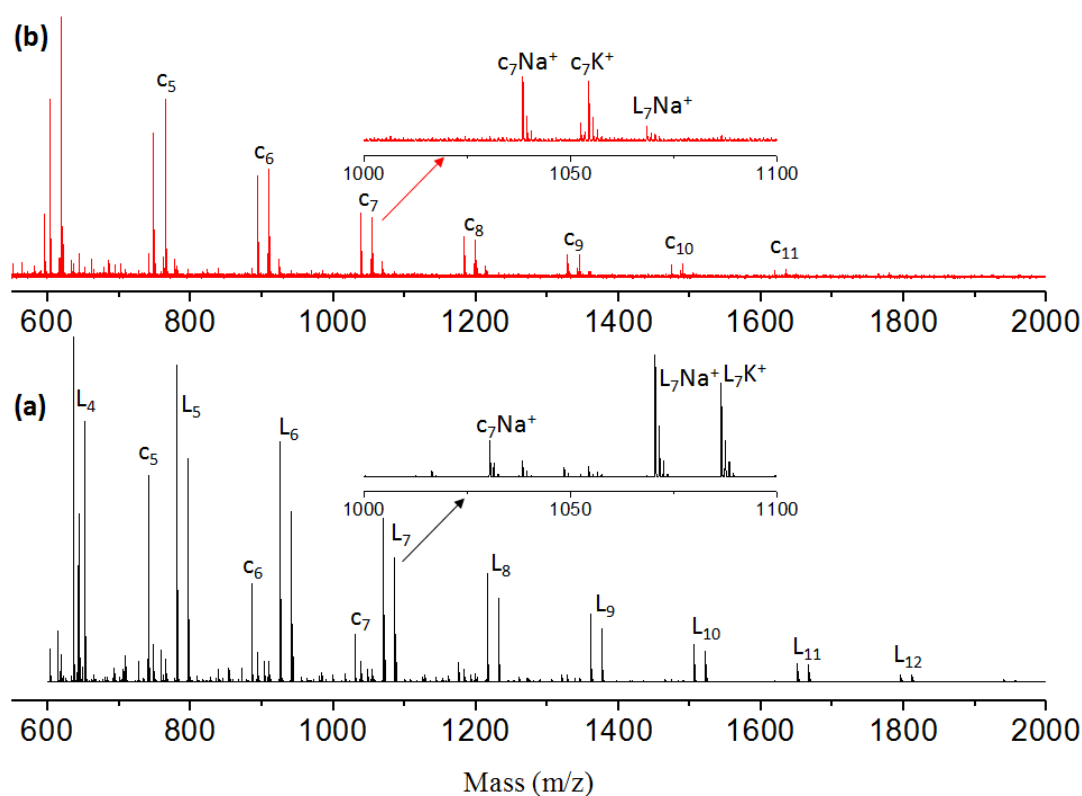

Figure 4.8. MALDI-TOF Mass spectra of L-SLP (a) and L-SHPEU (b)

The hyperbranched polymer (see figure 4.8.b) showed peaks up to 11 units. Interestingly, the hyperbranched structures predominantly showed mass peaks with respect to cyclic structures and the linear units are almost absent at higher conversion. A similar observation was earlier report in the synthesis of hyperbranched polyether[29]

and other hyperbranched polymers.[30] This indicated that the macrocyclic formation was one of the major obstacles in building the high molecular weight polymer in hyperbranched polymers. Further, the chain ends have active ester and urethane end groups confirming their thermo-stability towards the melt condensation approach.

4.3.4. L-Threonine Based Linear Polyesters

L-Threonine amino acid has secondary hydroxyl group unlike its L-serine counterpart. L-Threonine monomer was subjected to thermo-selective polymerization at 120° and 150 °C. At 120 °C, the monomer did not polymerize even after prolonged condensation for more than 10 h (it produced only oligomers of 1-3 units). At 150 °C, the self-condensation of the L-threonine occurred significantly to produce white solid polymer mass.
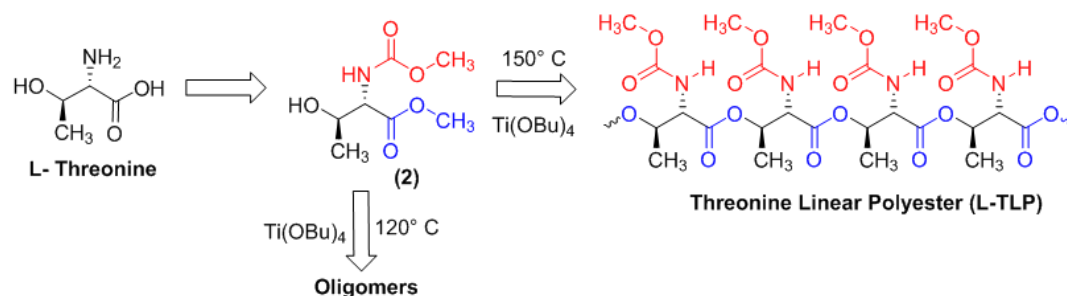
Scheme 4. 2. Synthesis of linear and hyperbranched polymers based on L-serine and L-threonine monomers.

^{1}H and ^{13}C NMR spectra of the L-threonine monomer and the polymer (produced at 150° C) are shown in figures 2d to 2g. The molecular weight of the L-threonine polymer was determined as M_n = 10,500 and M_w= 12,000 (see Table 1). To clarify the role of secondary hydroxyl group reactivity in L-threonine monomer towards ester and urethane in the condensation reaction; model reactions were carried out using cyclohexanol. Cyclohexanol was chosen because of its secondary hydroxyl group and its high boiling point suitable for melt process. n-Octyl urethane monomer and palmitic carboxylic ester were synthesized.
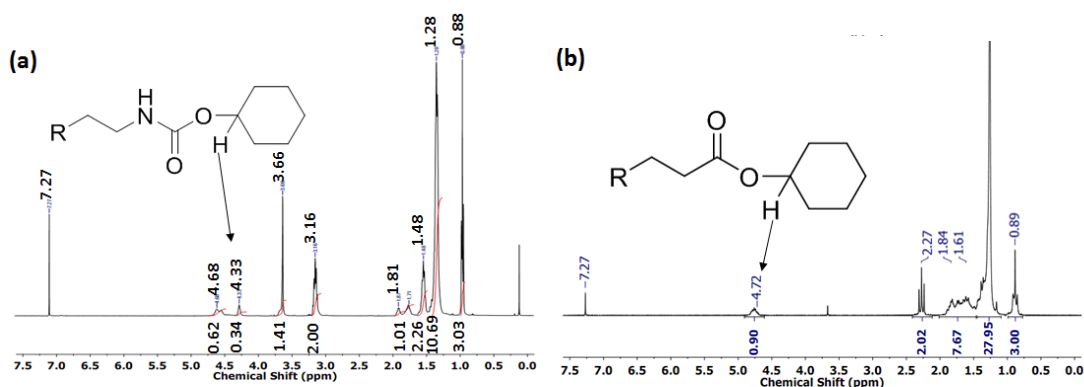
Figure 4.9. ^{1}H-NMR spectra of model reactions.

The reaction of palmitic ester with cyclohexanol produced new ester linkage R-COO**CH**-Cy (90 % yield) which appeared at 4.72 ppm. On the other hand, the n-octyl urethane monomer underwent slow reaction at 150 °C and the new urethane linkage R-HNCOO**CH**-Cy (30 % yield) was observed at 4.33 ppm. The comparison of the model reaction products with polymer spectrum (see figure 4.9. and figure 4.10) revealed that the only new ester linkage was formed in the L-threonine monomer self-condensation at 150 °C. This was further supported by the comparison of ^{13}C NMR spectra of the monomer and polymer in figure 4.10.c and 4.10.d. In figure 4.10.c, the carbon atom CH-**CH**(CH$_3$)-OH in the monomer completely disappeared at 67.82 ppm and new peak for ester carbon atom CH-**CH**(CH$_3$)-O-CO-R appeared at 75.0 ppm (near the solvent carbon).
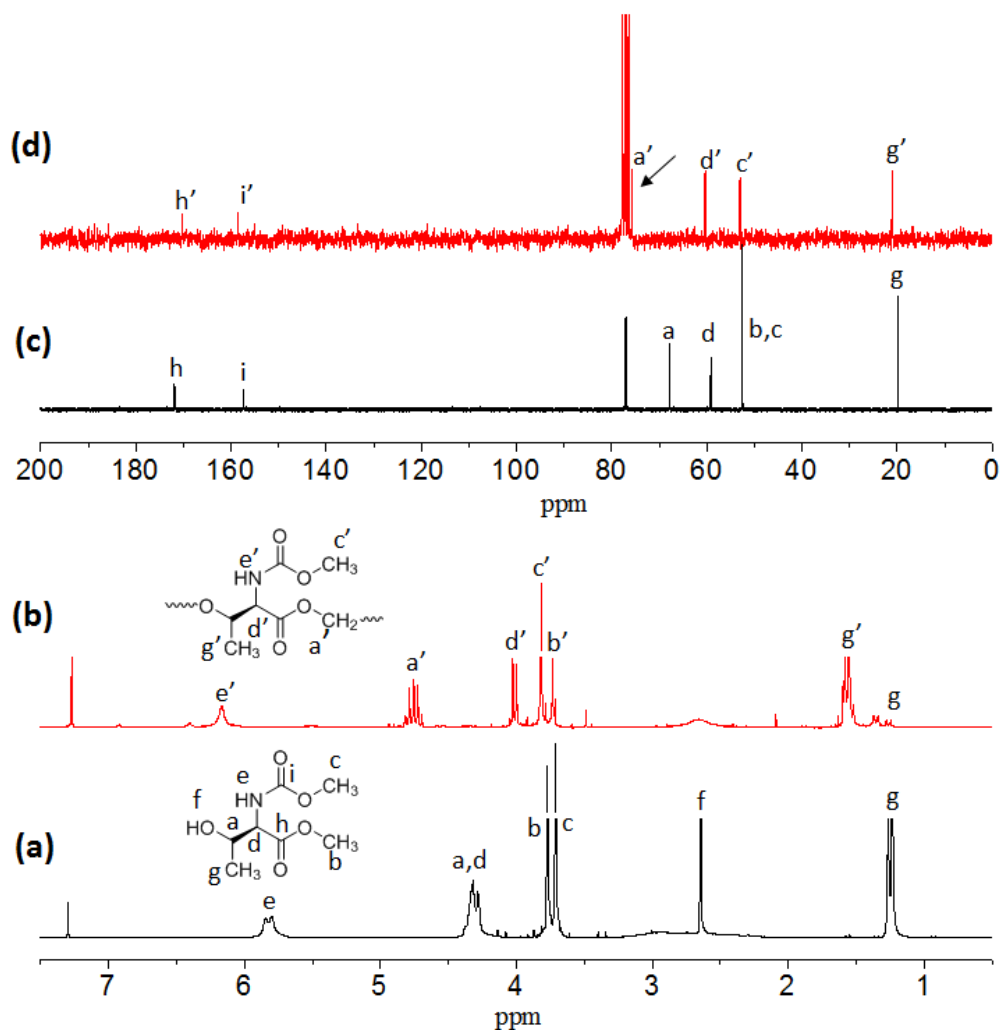
Figure 4.10. ^{1}H-NMR spectra of L-threonine monomer 2 (a), its linear polyester(L-TLP)(b) ^{13}C-NMR spectra of L-threonine monomer 2 (c), its linear polyester(L-TLP) (d). All the spectra are recorded in CDCl$_3$. solvent peak is indicated by asterisks (*).

Thus, at 150 °C, L-Threonine monomer produced exclusively linear polyester. The L-threonine linear polyester showed very low T$_g$ at -25 °C with respect to their steric hindered polymer backbone. The reason for this trend was attributed to the steric hindrance induced by the α-methyl unit in the L-threonine monomer.

The TGA-plots of the linear and HB polymers revealed that the newly designed polymers are stable up to 200 to 230 °C. Thermal properties of the polymers were studied by differential scanning calorimetry (DSC) at 10°/min heating and cooling rates. DSC thermograms of the linear polyesters showed glass transition (T$_g$)

151

temperature as 2 to 4 °C (see Table 1). The HB polymers showed higher T_g values at 40 to 55 °C (see Table 1). The higher T_g values in HB polymers are attributed to presence H-bonding end groups at the periphery of HB structure compared to that of linear polyesters.
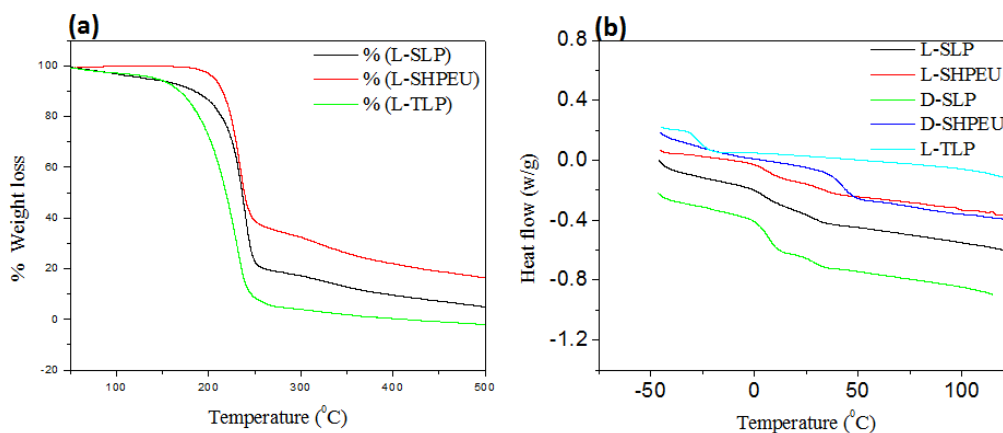

Figure 4.11. Thermal gravimetric analysis of monomers and polymers heated at 10 °C/min, under N_2 flow.

4.3.4. L-Tyrosine based polymers Polyesters

Unlike serine and threonine L-tyrosine is aromatic ring contained amino acid and it has phenolic hydroxyl group whose reactivity is comparatively lower than primary and secondarily hydroxyl groups in serine and threonine, attempt has made to synthesise linear and hyperbranched polymers at 120 °C and 150 °C respectively by self-polycondencing the phenolic hydroxyl with ester and urethane in the presence of $Ti(OBU)_4$ catalyst, but since the phenolic hydroxyl group is low in reactivity towards ester and urethane no polymer has obtained at neither 120 °C nor 150 °C.
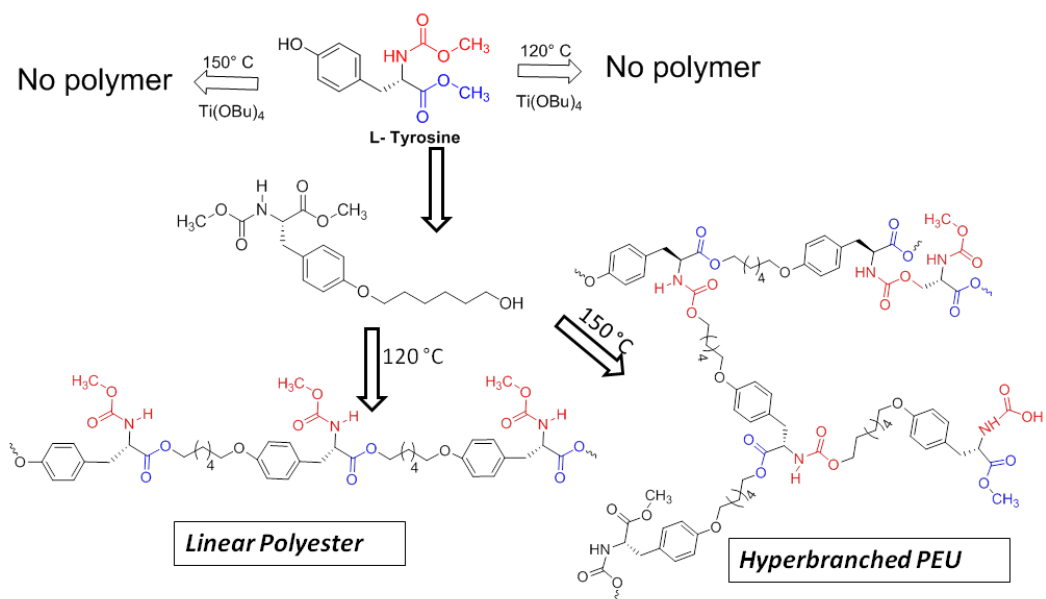
Scheme 4. 3. Synthesis of linear and hyperbranched polymers based on L-serine and L-threonine monomers.

In an another approach to make L-tyrosine based linear poly esters and hyperbranched poly(ester-urethane), the phenolic hydroxyl group was derivatised with 1,6 hexane diol which ends up with primary hydroxyl group then this monomer undergone to self-polycondensation at 120 C and 150 C in the presence of TI(OBU)4 to give linear poly ester and hyperbranched poly(ester-urethane) respectively. Occurrence of the polymerisation was confirmed by ^{1}H-NMR spectroscopy, at 120 °C the peak at 3.72 ppm corresponding to ester methyl protons in the monomer has disappeared and a new peak at 4.16 ppm has appeared which corresponds to new ester peak (see figure 4.12). And at 150 °C there is a decrease in the intensity of the peaks corresponding to both ester and urethane methyl protons at 3.72 and 3.67 ppm and two new peaks has appeared around 4.16 to 4.25 ppm (see figure 4.12) corresponding to new ester and urethane peaks by this way it was confirmed that after substituting the phenolic hydroxyl group with primary hydroxyl group, linear poly ester and hyperbranched poly(ester-urethane) has synthesised from the L-tyrosine monomer.

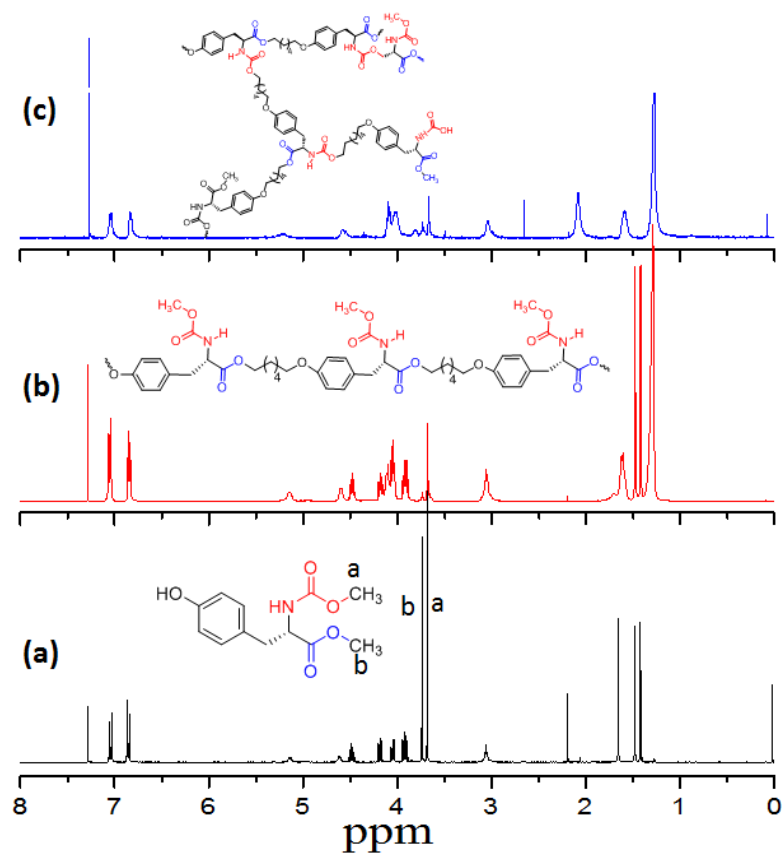**Figure 4.12.** ^{1}H-NMR spectra of L-tyrosine monomer 4 (a), its linear polyester(b), and hyperbranched poly(ester-urethane) (c). All the spectra are recorded in CDCl$_3$.
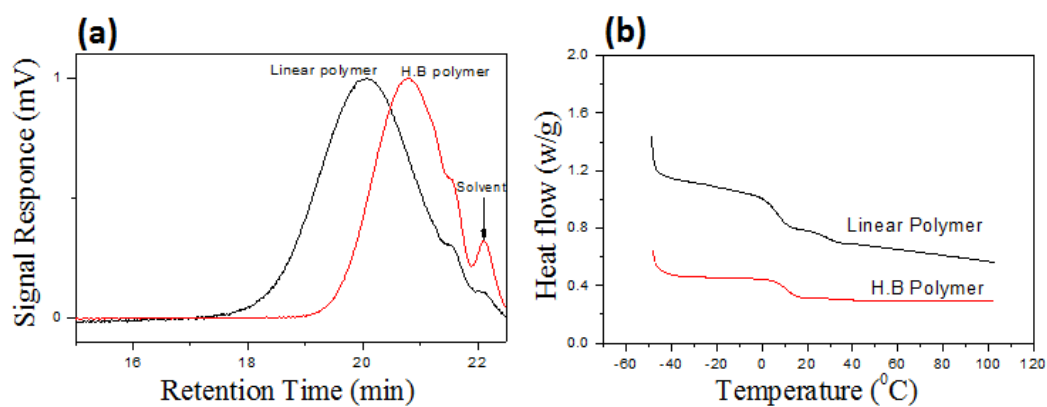

Figure 4.13. (a) GPC chromatograms of polymers in THF at 25 °C.

Further the molecular weights of the polymers were determined by gel permeation chromatography THF as eluent at 25 °C and it shows the formation of the polymers with moderate molecular weights (see figure 4.13). Differential scanning calorimetry shows that both the polymers were in amorphous in nature with glass transition temperatures around 10 °C.

4.3.5. Self-assembly and Morphology of Linear and HB Polymers

The newly synthesized polymers were derived from enantiomeric L-serine, D-serine and L-threonine monomers; thus, the circular dichroism (CD) spectroscopic analysis was carried out to investigate their secondary structures in solution. Typically, peptides showed a positive band at 192 nm and two negative bands at 208 and 222 nm with respect to α-helical conformation.[31] The β-sheet structure exhibited a positive CD band at 205 nm and a negative
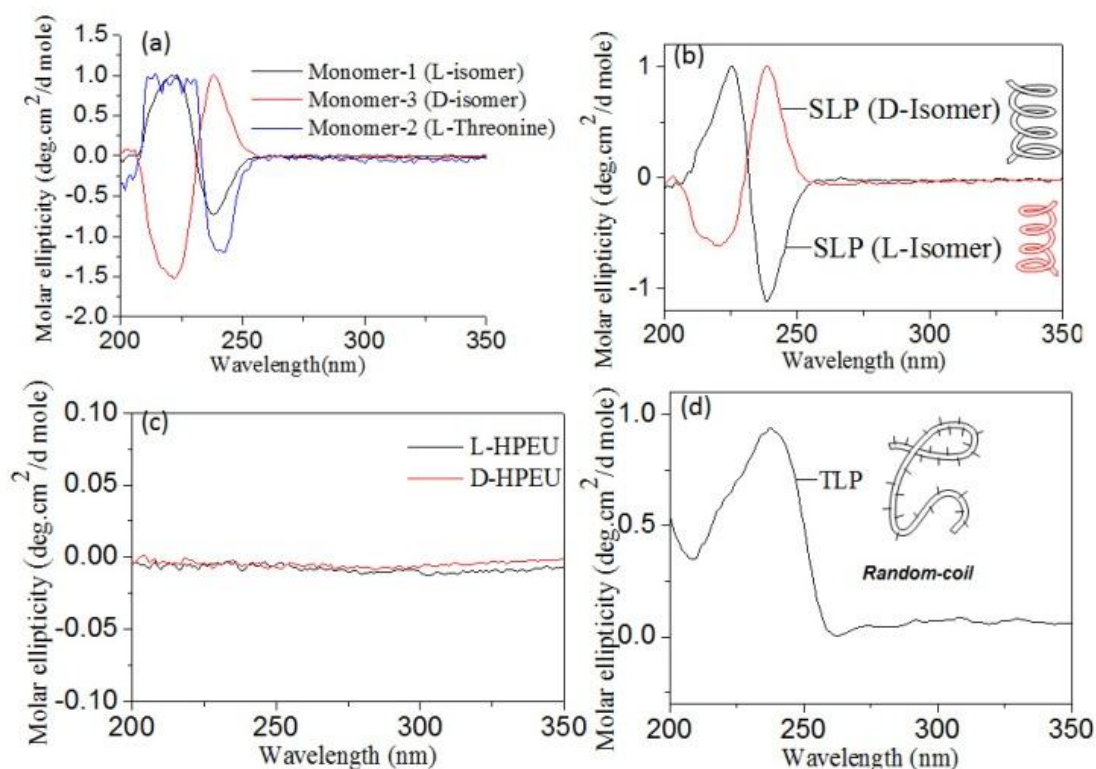

Figure 4.14. CD spectra of monomers 1, 2 and 3 (a). CD spectra of linear L and D-serine polyesters. (c) CD spectra of L and D-serine hyperbranched poly(ester-urethane)s (c). CD spectrum of linear L -Threonine polyesters (d).

CD band at 230 nm.Random coil structures are expected to show single negative CD band at 205 nm.[24] CD spectra of the L-serine and D-serine monomers (see figure 4.14.a) showed opposite Cotton signals with respect to their sterio-isomeric structures. Similarly, L-Threonine monomer was also showed expected CD signal. In figure 4b, the CD spectra of the linear polyester from the L-serine and D-serine monomers showed helicity with opposite CD bands. The L-serine linear polyester showed one positive CD band at 225 nm for $\pi-\pi^*$ and a negative CD band around 237 nm for $n-\pi^*$ transition.[24] These band signatures represent the secondary structures for the polymer chains in the β-sheet conformation.[24] Absorption spectra of the polymers were matched with that of the CD signal wavelength region. This proved that the high temperature condensation reaction did not disturb the optical activity of the monomers in the reaction and their optical property was preserved in the polymer structures as well. Surprisingly, the HB polymers (see figure 4.14.c) obtained from L-serine (or D-serine) did not show any CD signal. In figure 4d, the L-Threonine linear polyester (from secondary alcohol) showed positive CD signal with respect to the proline type II random coil structure. Thus, based on the above CD signals, it may be summarized that L (or D)-serine linear polyesters exhibited β-sheet conformation whereas random-coil was obtained for the steric hindered secondary alcohol based polyesters of L-Threonine. The highly branched structures did not allow the polymer chains to undergo self-organization in the hyperbranched structure; thus, they did not show CD signals (see figure 4.14.c).
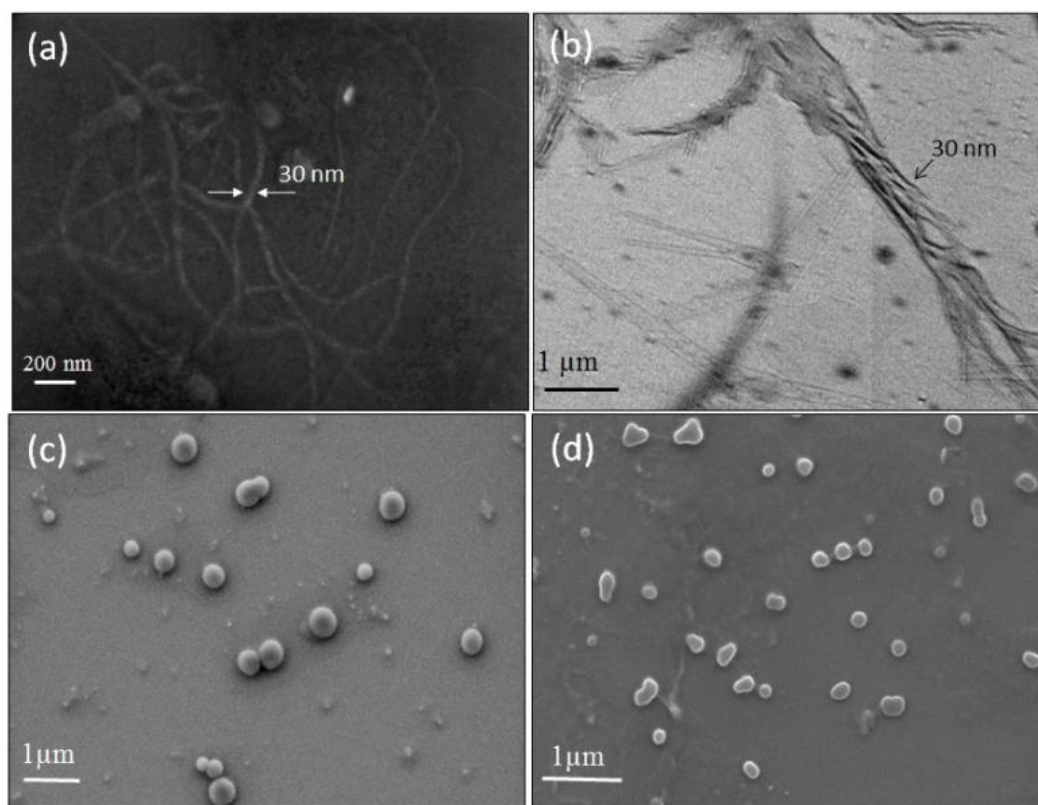
Figure 4.15. FE-SEM (a) and HR-TEM (b) images of linear L -serine polyesters. FE-SEM image of L-serine based HB poly(ester-urethane)s (c). L -Threonine linear polyester (d).

The polymer samples were subjected to electron microscope analysis (FE-SEM and HR-TEM) to visualize the size and shape of the self-assembled objects. FE-SEM images of the L-serine linear polyesters showed the formation of long twisted nano-fibrous morphology (see figure 4.15.a). This was further confirmed by the HR-TEM images in figure 4.15.b. The thickness and length of the nano-fibers were obtained as 30 nm and 2-3 μm, respectively. The formation of nanofiber was attributed to the β-sheet hydrogen bonding interactions facilitated by the pendent urethane attached in each repeating unit of linear polyester.[24] FE-SEM images of the hyperbranched polymer showed the formation of spherical nano-particle assemblies (see Fig 5c). This suggested that the branched macromolecular architectures adapted the globular coil-like conformation and thus produced spherical particles. The larger size of the HB nano-particles indicated that they were produced by the aggregation of more than one hyperbranched polymer chains together in the spherical shape as

shown in figure 1. The L-threonine polyester showed the CD signal for coil-like proline type-II self-assembly that produced spherical particles (see figure 4.15.d). FT-IR spectra of all the above three polymers were recorded to trace their morphological differences. All, three polymers showed the existence of hydrogen bonding interactions with respect to N-H stretching vibrational band at 3350 cm^{-1} and C=O band at 1722 cm^{-1}.[24] Thus, the difference in the morphological features are not due to the variation in their hydrogen bonding ability and it is mainly due to the difference in their topology of the polymer structure. Linear polyester with urethane hydrogen bonding pendent at each repeating units self-assembled to produce expanded nano-fibrous morphology. Though, the hydrogen bonding interactions present in the hyperbranched structures in the urethane units; the branched network disturbed their chain alignment. In the case of the L-threonine polymer, the proline type-II did not allow the chain to adopt expanded conformation.

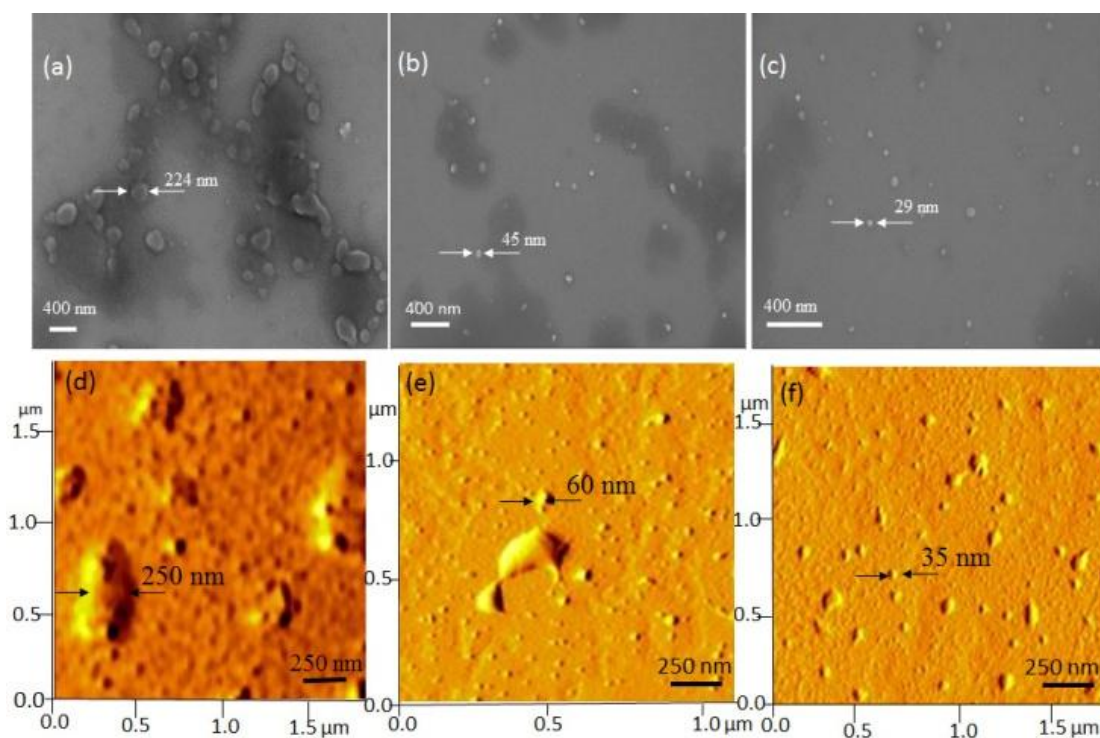**Figure 4.16.** FE-SEM images of HB aliquots having molecular weights: M_n = 10,000 g/mol (a), 12,000 g/mol (b) and 16,000 g/mol (c). ATM images of HB aliquots having molecular weights: M_n = 10,000 g/mol (a), 12,000 g/mol (b) and 16,000 g/mol (c).

Recently, Lederer and co-workers reported the molecular self-assembly of dendtronized glycopolymers based on maltose shell having lysine amino acid residues. It was found that the molecular weight of the polymers (dendron generation) and pH played vital roles in aggregation phenomena of these big molecules and transforming them from helical fibres to globular structures. In the present investigation, the newly designed hyperbranched polymers (resembled the dendritic architectures) underwent coil-like conformational changes to produce globular particles. In order to investigate the role of the molecular weights on the globular particle formation by the HB polymers, more than 10 aliquots of the HB samples were collected starting from 30 minutes of the polymerization till the end of the process at 6h. These samples were subjected to FE-SEM and atomic force microscopy and their images are given in figure 4.16. It is very clear from the FE-SEM images that the low molecular weight polymers collected at the initial stage of the polymerization showed larger aggregates of 250 nm (see figure 4.16.a to 4.16.c). With the increase in the molecular weights, the HB polymers produced smaller aggregates of < 40 nm. AFM images (see figure 4.16.d to 4.16.f) of the aliquots also confirmed the spherical shape of the nano-aggregates as well as their sizes with that of SEM images.
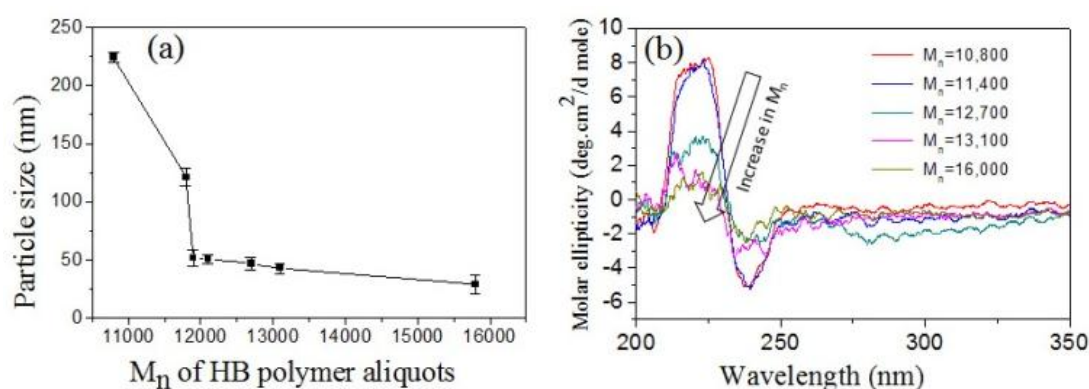

Figure 4.17. (a) Plot of nanoparticle size versus the M_n of the HB polymer aliquots. (b) CD spectra for various molecular weight HB polymer aliquots.

To further analyze the role of the HB polymers, the size of the nano-particles was plotted against M_n of the HB polymers and shown in figure 4.17.a. At low molecular weight sample, the HB polymer chains showed larger size aggregate

formation. The size of the particle became < 40 nm beyond M_n = 12,000 g/mol. CD signals of these HB polymer aliquots were also recorded and their spectra are shown in figure 4.17.b. The CD signals were relatively visible at low molecular weight samples; however, they gradually disappeared with increase in molecular weights. The appearance of CD signal at low molecular weight sample was attributed to the loosely packed HB chains which in turn facilitated the partial alignment of the chains to become CD active. This observation was supported by the larger particles size in FE-SEM and AFM images in figures 4.16.a and 4.16.d. The higher molecular weight HB samples produced tightly packed nano-particle; thus, the samples became CD inactive. Hence, as observed by Lederer and co-workers in dendronized polymers; in the present case, the HB polymers based on natural L-amino acids attained globular spherical conformation at higher molecular weights. It may be concluded that the molecular weights of the hyperbranched structures of amino acid residues are very crucial factor in determining the globular nature of the structures. Higher molecular HB polymers adopted the globular structures as in the case of dendrite macromolecules. In the present investigation, for the first time, the roles of the polymer topology on the molecular self-assemblies of the amino acid based polymers were resolved. This was accomplished with help of linear and hyperbranched polymers produced from identical starting materials. Though, the present approach here demonstrated only for L-serine and L-threonine based polymers; this approach is not restricted only to these examples and it may be expanded to other multifunctional amino acid monomers or other monomeric resources for making diverse polymer structures with appropriate molecular self-assembly. Further, the present investigation opens up new synthetic pathways for linear or hyperbranched polymers based on multi-functional amino acids.

4.3.6. Conclusion

In conclusion, a new temperature selective polycondenstaion approach has been successfully developed to make new classes of linear polyester and hyperbranched poly(ester-urethane)s based on natural L-amino acid monomers. L-Serine (also D-serine) and L-threonine provided exact structural requirement with hydroxyl, carboxylic acid and amine functionalities that facilitated the synthesis of new ABB' monomers (A= hydroxyl, B= ester and C= urethane). The ABB' monomer underwent temperature selective polycondenstaion reaction among A and B at 120 °C

to produce linear polyesters. In this linear polyester, the un-reacted functional group B' kept as pendent in the each unit. At 150 °C, the hydroxyl (A) reacted equally with both B and B' under the dual ester-urethane melt condensation approach to yield novel hyperbranched poly(ester-urethanes). These optically active polymers showed diverse CD signals with respect to their polymer topology. The linear polyester produced by the L-serine and D-serine showed expanded chain conformation through hydrogen bonding interactions that resulted in the self-assembly of nano-fibrous morphology. Hyperbranched polymers did not show any CD signal and produced spherical morphologies. The branched structures did not allow the chain to pack; thus, they favored coil-like conformation (no CD signal) that assembled the polymer chains as the globular spherical nano-particles. L-Threonine based polymer adapted random-coil proline type II structures that also produced spherical nano-particle assemblies. The globular nano-particle nature The HB polymers were found to be driven by the molecular weights of the samples. Both the vanishing of the CD signal and formation of tightly packed nano-particle formation were found to be maxima at higher molecular weight HB samples. The present investigation provides first time insight into the molecular self-assemblies of linear and hyperbranched polymers based on L-amino acids from single starting materials. Both the synthetic methodology and the linear and hyperbranched structures are new entities in the literature and they may be very useful for applications in biomedical and thermoplastic industries.

References

1. H. Jin, W. Huang, X. Zhu, Y. Zhou, and D. Yan, *Chem. Soc. Rev.,*2012, **41***,* 5986-5997.

2. A. Sousa-Herves, S. Wedepohl, and M. Calderon, C*hem. Commun.*, 2015, **DOI:** 10.1039/C5CC00644A.

3. J. Chen, C. Wu, D. Oupicky, *Biomacromolecules*, 2009, **10**, 2921-2927.

4. L. Xu, and Z. Ye, C*hem. Commun.*, 2013, **49**, 8800-8802.

5. J. Sebastian, and D. Srinivas, C*hem. Commun.*, 2011, **47**, 10449-10451.

6. S. V. de Vyver, J. Gebboers, S. Helsen, F. Yu, J. Thomas, M. Smet, W. Dehaen and B. F. Sels, *Chem. Commun.*, 2012, **48**, 3497-3499.

7. Y. Zhou, and D. Yan, *Chem. Commun.*, 2009, 1172-1188.

8. A. Zill, A. L. Rutz, R. E. Kohman, A. M. Alkilany, C. J. Murphy, H. Kong, and S. C. Zimmerman, *Chem. Commun.*, 2011, **47**, 1279-1281.

9. C. Gao, D. Yan, *Prog. Polym. Sci.* 2004, **29**, 183-275.

10. S. P. Rannard, N. J.Davis, and I. Herbert, *Macromolecules*, 2004, **37**, 9418-9430.

11. T. Ranganathan, C. Ramesh, and A. Kumar, *Chem. Commun.*, 2004, 154-155.

12. M. Jayakannan, S.Ramakrishnan, *Chem. Commun.*, 2000, **19**, 1967-1968.

13. M. Jayakannan, S. Ramakrishnan, *Macromol. Rapid Commun.* 2001, **22**, 1463-1473.

14. A.Saha, S. Ramakrishnan, *Macromolecules*, 2009, **42**, 4956-4959.

15. S. Chatterjee, S. Ramakrishnan, *Macromolecules***,** 2011,**44**, 4658-4664.

16. M. Scholl, Z. Kadlecova, and H. A. Klok, *Prog. Polym. Sci.* 2009, **34**, 24-61.

17. C. R. Yates, W. Hayes, *Eur Polym J,* 2004, **40**, 1257-1281.

18. M. Scholl, T. Q. Nguyen, B. Bruchmann, and H. A. Klok, *Macromolecules*, 2007, **40**, 5726-5734.

19. M. Scholl, T. Q. Nguyen, B. Bruchmann, and H. A. Klok, *J. Polym. Sci. Part A: Polym. Chem.*2007, **45**, 5494-5508.

20. M. Scholl, T. Q.Nguyen,B.Bruchmann, and H. A. Klok, *Macromolecules*, 2007, **40**, 5726-5734

21. Y. Bao,; J. He,; and Y. Li, *Polymer*, 2012, **53**, 145-152.

22. Y. M. Bao, X. H. Liu, X. L. Tang, and Y. S. Li, *J. Polym. Sci. Part A: Polym. Chem.*2010**, 48**, 5364-5374.

23. S. Anantharaj and M. Jayakannan, M. *Biomacromolecules*, 2012, **13**, 2446-2455.

24. S. Anantharaj, M. Jayakannan, *Biomacromolecules*, 2015, asap DOI: 10.1021/bm501903t

25. P. Deepa, M. Jayakannan, *J. Polym. Sci., Part A: Polym. Chem.*2007**, 45***, 2351-2366.

26. P. Deepa, M. Jayakannan, *J. Polym. Sci., Part A: Polym. Chem.*2008, **46***, 2445-2458.

27. C. J. Hawker, R. Lee, J. M. J. Frechet, *J. Am. Chem. Soc.,* 1991, **113,** 4583-4588.

28. D. Holter, A. Burgath, H. Frey, *Acta Polym.*, 1997, **48**, 30-35.

29. M. Jayakannan, J. L. J. V. Dongen, G. CH. Behera, S. Ramakrishnan, *J. Polym. Sci., Part A: Polym. Chem.*2002**, 40***,4463-4476.

30. H. R. Kricheldorf, s. Bohme, G. Schwarz, and C. L. Schultz, *Macromolecules*, 2004, **37**, 1742-1748.

31. Sinaga, A.; Hatton, T. A.; and Tam, K. C. *Biomacromolecules*, 2007, **8**, 2801-2808.

32. S. Boye, D. Appelhans, V. Boyko, S. Zschoche, H. Komber, P. Friedel, P. Formanek, A. Janke, B.I. Voit, and A. Lederer, *Biomacromoleules*, 2012, **13**, 4222-4235.

Summary and Future directions

The thesis entitled ***L-Tyrosine Based Polymers for Drug delivery in Cancer Therapy*** accords with L-Amino acid based synthetic polymers and their biomaterial applications in tissue engineering, bone repair, biomineralization, drug and gene delivery. The thesis is aimed to develop unique classes of amphiphilic poly(ester-urethane)s from L-tyrosine amino acid resources under solvent free melt polycondensation approach and employ them as enzyme and thermo-responsive nanocarriers for intracellular delivery of multiple anticancer drugs such as camptothecin (CPT) and doxorubicin (DOX) in cancer treatment. L-tyrosine is very distinguished amino acid having phenolic functionality in addition to amine and carboxylic units at the α-carbon. It is an important biological resource for the development of biodegradable polymer nanoscaffolds which opens up new route for drug/gene delivery applications. Further, the synthetic methodology is expanded to developed linear polyester and hyperbranched poly (ester-urethane) from a single amino acid monomer in one pot by adjusting the temperature of the polymerization reaction.

A unique class of enzyme-responsive poly(ester-urethane)s were developed from the natural L-tyrosine amino acid through solvent free melt polycondensation approach. In this method, L-Tyrosine was appropriately modified into carboxylic ester and urethane monomer and further subjected to dual ester-urethane melt polycondensation process with commercial polyethylene glycols to yield amphiphilic poly(ester-urethane)s. The topology of the polymer were play a specific role to the thermal properties, viscoelastic rheological properties and aqueous self-assembly of poly(ester-urethane). The self-assembly of the polymers acquired by the substitution of alkyl side chain in the phenolic unit and the number of hydrophilic PEG units in the backbone. Further, long C16 alkyl side chain and PEG-600 segments in the main backbone of the polymer formed stable nanoparticles of 200nm in size that provides an appropriate geometry for encapsulation of anticancer drugs. Exclusively, these L-tyrosine nanoparticles were loaded with clinically important anticancer drugs such as DOX and CPT which were stable at extracellular conditions. Likewise, it undergoes biodegradation in the presence of esterase enzyme to release these anticancer drugs at the intracellular compartments under physiological conditions. The CPT and DOX loaded polymer nanoparticles illustrates >95% cell killing towards cancer cell lines as compared to free drugs. Flow cytometry analysis and confocal microscopy images

approved the better uptake and cellular internalization of the drug-loaded nanoparticles.

The enzyme and thermos-responsive poly(ester-urethane)s were synthesized from naturally available L-Tyrosine amino acid in order to identify their aspect in anticancer drug delivery. In this process, L-Tyrosine aminoacid was tailored into trans ester-urethane polymerizable monomeric entity and melt polycondensed with different linear and cyclic aliphatic diols to get poly(ester-urethane)s with variable hydrophobic content. These polymeric entities self-assembled into a 200 nm sized nanoparticles in the aqueous medium at ambient temperatures. Further, it exhibits LCST (lower critical solution temperature) behaviour means the polymer solution is transparent at ambient temperature and becomes turbid when the temperature raises to 38-50^{0}C and it starts precipitating out from the aqueous medium. This LCST property has been extensively studied through absorbance and DLS methods. In vitro drug release studies conceded that these polymer nanoparticles are stable at normal physiological conditions (37 °C, pH = 7.4 PBS) and it can release the loaded drugs such as DOX and CPT at high temperature cancer tissue (thermos responsive), or in the presence of lysosomal esterase enzymes (enzyme responsive). Cytotoxicity studies in the cancer and normal cell lines reports that the nascent L-tyrosine nanoparticles were non toxic, whereas the drug loaded polymer nanoparticles shown excellent cell killing in cancer cells.

The synthetic approach is also widened to other amino acids such as L-serine and L-threonine to develop new classes of linear and hyperbranched poly(ester-urethanes)s based on multifunctional L-amino acid monomers via a temperature selective melt polycondensation method. These amino acids (L-Serine, D-Serine and L-Threonine) expedite the synthesis of new ABB' monomers while providing exact structural requirements with hydroxyl, carboxyl acid and amine functionalities (A= hydroxyl, B=ester and B'= urethane). At 120^{0}C, the ABB' monomer undergo temperature selective polycondensation reaction to yield linear polyesters while at 150^{0}C, equally reacted with both B and B' to produce novel hyperbranched poly(ester-urethane)s under the dual melt polycondensation approach. Circular dichroism (CD) analysis explains that linear polyesters showed expanded chain conformation through hydrogen bonding interactions resulted in a helical nano-fibrous morphology while hyperbranched polymers produced spherical nanoparticles

through coil-like conformations. These linear and hyperbranched structural entities are very beneficial for biomedical and thermoplastic industries.

Future Directions

This thesis is mainly focused on the synthesis of amino acid based polymers by using a novel melt polycondensation method and utilising their aqueous polymer nanoparticles for anticancer drug delivery applications. In this thesis we have extended the dual (ester-urethane) melt condensation process to multi functional amino acids such as serine, threonine, and tyrosine. Various types of polymer architectures has constructed such as linear polyester and hyperbranched poly(ester-urethane)s and their self-assembly characteristics, anticancer drug loading abilities has evaluated. Lower drug loading efficiencies and leaching of the loaded cargoes before reaching the target site are some of the limiting factors for many of the drug delivery vehicles, with the knowledge of the work done in this thesis we can develop hydrogel based polymer nanoparticles from multifunctional amino acids like tyrosine. Hydrogels are three dimensional cross-linked networks of water soluble polymers, they can effectively improve the drug loading efficiencies of the polymer nanoparticles and also will protect the drug molecules in the blood stream and by triggering any stimuli such as Ph, temperature, enzymatic action, or redox potential we can selectively deliver the drugs at target site from the hydrogels.
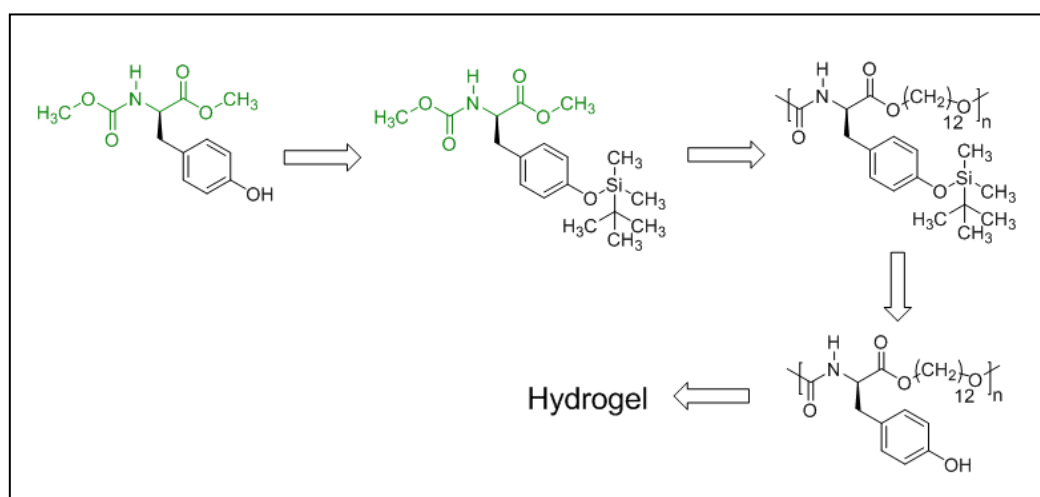

Figure 5.1: Future direction of thesis work schematic representation for the synthesis of hydrogels from L-tyrosine amino acid.

There has been considerable progress in recent years for the development of tagged nanoparticles for tumor cell targeting, imaging and diagnosis. By our melt condensation approach from L-amino acids we can synthesise clickable polymers to which any fluorescent moity or receptor directing moity can be attached for targeted drug delivery and for imaging purposes.
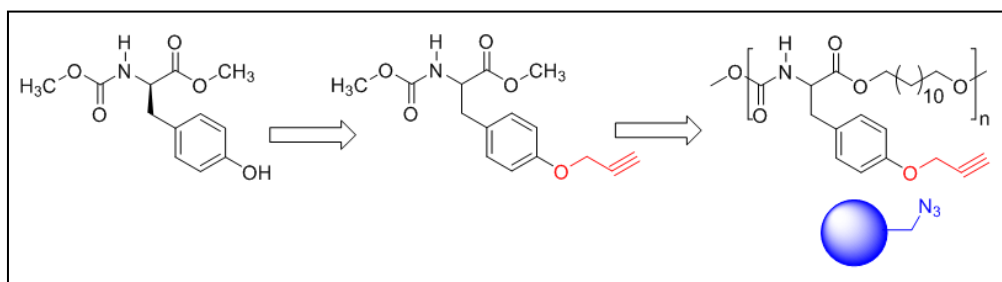

Figure 5.2n   **:** Future direction of thesis work schematic representation for the development of clickable L-tyrosine polymers.

Therefore ongoing projects concentrated on the synthesis of hydrogels and clickable poly(ester-urethane)s from natural amino acids for drug delivery applications.

List of publications

List of Publications from Thesis work

1. Aluri, R.; Jayakannan, M. Development of L-Tyrosine Based Enzyme-responsive Amphiphilic Poly(ester-urethane) Nano-carriers for Multiple Drug Delivery to Cancer Cells. *Biomacromolecules*, **2017**, *18*, 189-200.

2. Aluri, R.; Jayakannan, M. One-pot Two Polymers: ABB' Melt Polycondensation for Linear Polyesters and Hyperbranched Poly(ester-urethane) Based on Natural L-Amino acids. *Polym. Chem*., **2015**, *6*, 4641-4649.

3. Aluri, R.; Jayakannan, M. Enzyme and Thermal Dual Responsive L-Tyrosine Poly(ester-urethane)s Nanocarriers for drug delivery to Cancer Cells, **Submitted to** *Biomacromolecules*.

Publications in International Conference Proceedings:

1. Aluri, R.; Jayakannan, M. Thermal and enzyme dual stimuli sensitive polymer nanocarriers for anticancer drug delivery applications, *ICONSAT-2016*, IISER PUNE, March 2016.

2. Aluri, R.; Jayakannan, M. Synthesis of L-tyrosine based poly(ester-urethane)s and their drug delivery applications, *"7th peptide Engineering meeting",* IISER PUNE, Dec-2015.

3. Aluri, R.; Jayakannan, M. Synthesis of Linear and hyperbranched polymers from natural L-amino acids. *MACRO-2015,* IACS Kolkata, Jan-2015.

4. Aluri, R.; Jayakannan, M. Development of melt polycondensation approach for multifunctional L-amino acids. *"International meet on Advances in Polymer Science",* NCL Pune, Oct-2014.